AD NUMBER
AD506331
CLASSIFICATION CHANGES
TO: unclassified
FROM: confidential
LIMITATION CHANGES
TO: Approved for public release, distribution unlimited
FROM: Distribution authorized to U.S. Gov't. agencies and their contractors; Critical Technology; DEC 1969. Other requests shall be referred to Air Force Rocket Propulsion Lab., Edwards AFB, CA 93523.
AUTHORITY
31 Dec 1981, DoDD 5200.10, Group-4; AFRPL ltr, 5 Feb 1986

AD 506 331

AUTHORITY: AFRPL ltr. 5 Feb 86

GENERAL DECLASSIFICATION SCHEDULE

IN ACCORDANCE WITH

DOD 5200.1-R & EXECUTIVE ORDER 11652

SECURITY MARKING

The classified or limited status of this report applies to each page, unless otherwise marked.
Separate page printouts MUST be marked accordingly.

AFRPL-TR-69-164

(Unclassified Title)

INVESTIGATION OF NON-TUBULAR WALL REGENERATIVELY COOLED THRUST CHAMBER CONCEPTS

FINAL REPORT

D. L. Fulton

Rocketdyne Advanced Systems, Large Engines

December 1969

Group 4
Downgraded at 3-Year Intervals
Declassified After 12 Years

In addition to security requirements which must be met, this document is subject to special export controls and each transmittal to foreign governments or foreign nationals may be made only with prior approval of AFRPL (RPPR-STINFO), Edwards, California 93523

Air Force Rocket Propulsion Laboratory
Edwards, California
Air Force Systems Command
United States Air Force

CONFIDENTIAL

"When U.S. Government drawings, specifications, or other data are used for any purpose other than a definitely related Government procurement operation, the Government thereby incurs no responsibility nor any obligation whatsoever, and the fact that the Government may have formulated, furnished, or in any way supplied the said drawings, specifications, or other data, is not to be regarded by implication or otherwise, or in any manner licensing the holder or any person or corporation, or conveying any rights or permission to manufacture, use, or sell any patented invention that may in any way be related thereto."

CONFIDENTIAL
(This page is unclassified)

Best
Available
Copy

CONFIDENTIAL

AFRPL-TR-69-164

(Unclassified Title)

INVESTIGATION OF NON-TUBULAR WALL
REGENERATIVELY COOLED THRUST CHAMBER CONCEPTS

FINAL REPORT

D. L. Fulton
Liquid Rocket Division

Rocketdyne, A Division of North American Rockwell Corp.
6633 Canoga Ave., Canoga Park, California

TECHNICAL REPORT AFRPL-TR-69-164

December 1969

Group 4
Downgraded at 3-Year Intervals
Declassified After 12 Years

THIS MATERIAL CONTAINS INFORMATION AFFECTING THE NATIONAL DEFENSE OF THE UNITED STATES WITHIN THE MEANING OF THE ESPIONAGE LAWS, TITLE 18 U. S. C., SECTIONS 793 AND 794. ITS TRANSMISSION OR THE REVELATION OF ITS CONTENTS IN ANY MANNER TO AN UNAUTHORIZED PERSON IS PROHIBITED BY LAW.

In addition to security requirements which must be met, this document is subject to special export controls and each transmittal to foreign governments or foreign nationals may be made only with prior approval of AFRPL (RPPR-STINFO), Edwards, California 93523

Air Force Rocket Propulsion Laboratory
Edwards, California
Air Force Systems Command
United States Air Force

CONFIDENTIAL

FOREWORD

This report describes the results of an experimental program conducted by Rocketdyne, a Division of North American Rockwell Corp. and entitled "Investigation of Non-Tubular Regeneratively Cooled Thrust Chamber Concepts". This program, conducted during the period of 1 April 1968 to 2 July 1969 was authorized by the U.S. Air Force Rocket Propulsion Laboratory under

Contract Number	--	F04611-68-C-0061
Project Number	--	3058
Task	--	305803

The confidential data presented in pages 44, 45, 46, 47, 56, 57, 58, 97, 98, 99, 152, 158, 181, 182, 184, 189, 193, 204, 205, 211, 245 and A-11 of this report were taken from Contract F04611-67-C-0116 and that on page 33 from Report AFRPL TR-67-275.

The contributions of numerous Rocketdyne personnel and of Battelle Memorial Institute of Columbus, Ohio, who contributed to this report are appreciated.

This publication was prepared by Rocketdyne, a Division of North American Rockwell Corporation, as Report R-7910.

The Air Force Project Engineer was Mr. C. D. Penn, RPRRE.

This technical report has been reviewed and is approved.

C. D. Penn
Project Engineer - Liquid Rocket Division
Air Force Rocket Propulsion Laboratory
Edwards, California

ABSTRACT

The objective of the "Investigation of Non-Tubular Wall Regeneratively Cooled Thrust Chamber Concepts" program (F04611-68-C-0061) was to investigate advanced fabrication techniques applicable to non-tubular regeneratively-cooled thrust chambers and to demonstrate the lower cost and improved performance that could be achieved through their use. Propellants of interest were CPF/Amine and F_2/H_2, considering both bell and annular thrust chambers.

During Phase I, parametric analyses, materials evaluation and thrust chamber ranking studies provided the basis for the selection of three fabrication concepts for experimental evaluation.

In Phase II test panels and full-size chambers of the three concepts were fabricated and laboratory tested to establish process parameters, structural limits, dimensional repeatability and non-destructive inspection techniques for subsequent hot firing hardware.

In Phase III thrust chambers representing each of the three concepts were successfully fabricated and hot fire tested demonstrating the structural integrity and thermal performance of the three fabrication concepts when exposed to the combustion environment.

(Unclassified Abstract)

TABLE OF CONTENTS

Page

Page

ILLUSTRATIONS

Figure		Page
19	Available Coolant Flowrate and Outlet Bulk Temperature for CPF/N_2H_4 Aerospike Configurations . .	49
20	Coolant Pressure Loss for CPF/N_2H_4 Aerospike Design	50
21	Flow Schematic for Oxidizer Heat Exchange Concept . .	52
22	Backup Panel Cooling Channel /d vs Enthalpy Ratio .	55
23	Typical Isotherm Profiles in a F_2/H_2 Double Panel Cooling Design	58
24	Coating Temperature Drop vs Heat Flux	59
25	Cooland Channel Geometries	60
26	Structural Limits for Nickel 200 Channel Walls . . .	63
27	Structural Limits for Beryllium Copper 10C, and 50C Channel Walls	64
28	Structural Limits for Hastelloy-C and INCO 625 . . .	65
29	Minimum Thickness Requirements of Cast Aluminum, Inconel 718 and Nickel (Electroformed or Sintered) Backup Structure for Bell Chambers	67
30	terial Yield Strength at Elevated Temperatures . .	69
31	pical Segmented Annular Chamber Structure	85
32	Design Criteria for Powder Metal Nickel Bell Chamber.	97
33	Design Criteria for Spun Bell Chamber	98
34	Design Criteria - Cast BeCu Segment	99/100
35	Solid Wall Powder Metal Cylinder	104
36	Elevated Temperature Thermal Conductivity Tests . . .	105
37	Thermal Conductivity of Pure Nickel	106
38	Short Time Tensile Properties of Powder Metal Nickel.	108
39	Internally Cored Powder Metal Cylinder with Various Core Configurations	110
40	Internally Cored Powder Metal Cylinder with Various Sizes of Rectangular Cores.	112
41	Typical Cerrolow-136 Cores	114
42	Solid Wall Sintered Nickel Bell Chamber Fabricated by the Powder Metal Process	116

Figure		Page

TABLES

NOMENCLATURE

A_s = Thrust chamber heated surface area (in^2)

A_F = Coolant passage flow area (in^2)

b = Spacing between hydrogen and oxidizer panels (in)

C_p = Specific heat at constant pressure (Btu/lb_m-F

C_H = Stanton number

d = Cooling passage hydraulic diameter, A_F/P_W (in)

f = Coolant friction factor

g = Gravitational constant (in/sec^2)

G_c = Coolant mass flux (lb_m/in^2-sec)

h_g = Hot gas film coefficient (Btu/in^2-sec-F)

h = Channel depth (in)

h_c = Coolant film coefficient (Btu/in^2-sec-F)

H_s = Hot gas stagnation enthalpy (Btu/lb_m)

H_W = Hot gas enthalpy at the wall (Btu/lb_m)

H_{AW} = Adiabatic wall hot gas enthalpy (Btu/lb_m)

K_F = Turbulence pressure loss coefficients

L_P = Cooling passage length (in)

M* = Mach Number function

MR = Propellant mixture ratio

N = Number of channels

P_r = Hot gas Prandtl Number

C* = Characteristics velocity

ΔP_f	=	Frictional coolant pressure loss (psi)
ΔP_T	=	Total coolant static pressure drop (psi)
P_c	=	Combustion chamber stagnation pressure (psia)
q	=	Heat flux (Btu/in^2-sec)
q^*	=	Throat heat flux (Btu/in^2-sec)
q_{BO}	=	Coolant "Burnout" heat flux (Btu/in^2-sec)
R	=	Thrust chamber radius (in)
R^*	=	Thrust chamber throat radius (in)
$R_{e\phi}$	=	Hot gas Reynolds Number
S	=	Contour wall length (axial direction) (in)
T_B	=	Coolant bulk temperature (R)
T_{wc}	=	Wall temperature at cooling surface (F)
T_{wg}	=	Wall temperature at heated surface (F)
T_{AW}	=	Hot gas adiabatic wall temperature (F)
T_{sat}	=	Coolant vapor saturation temperature (F)
U_s	=	Hot gas free stream velocity (in/sec)
V_c	=	Coolant velocity (ft/sec)
$\dot{W}_c$	=	Coolant flowrate (lb_m/sec)
W	=	Channel width (in)
L	=	Land width (in)
X_w	=	Wall thickness (in)
F	=	Thrust (lb_f)

P_c = Chamber Pressure, psia

h = Channel height, in.

C_F = Thrust coefficient

D_E = Exit Diameter

Greek Symbols

ϵ	=	Relative roughness
μ	=	Viscosity (lb_m/in-sec)
ρ	=	Density (lb_m/in^3)
ϕ	=	Momentum thickness (in)
η	=	Efficiency

Subscripts

r	=	Recovery condition
s	=	Free stream conditions

INTRODUCTION

(U) Most regeneratively cooled thrust chambers are presently made from formed and tapered tubes, brazed together and reinforced against the chamber pressure induced loads by steel bands, filament winding, or a bolted on backup structure. Demands for increased rocket engine performance and flexibility achieved through the use of new propellants, high chamber pressures, annular combustor configurations and throttling require smaller diameter and thinner wall tubes. The use of such tubes inhibits the ruggedness of thrust chambers and increases the fabrication complexity and cost.

(U) Conversely, the use of non-tubular regeneratively cooled thrust chambers provides techniques for reducing the fabrication cost of such combustion chambers and of improving their performance (regenerative cooling capability).

(U) A tube wall chamber has a higher exposed area for heat transfer due to the scallop effect of brazed tubes. The use of a smooth wall as is achieved with the non-tubular fabrication techniques results in approximately a 15 to 25 percent reduction in the overall heat input and coolant bulk temperature; particularly important for low thrust engine applications. A significant fin-cooling effect can also be obtained under certain conditions with channel type construction. The actual magnitude of the fin effect depends greatly on the panel material, the local heat flux level, the coolant temperature and the coolant channel geometry.

(U) Conventional tubular wall thrust chambers require a relatively large number of small diameter tubes which are tapered and die formed to produce the chamber contour and to provide the required circuit flow area

for the coolant. These tubes are then brazed together to form the chamber contour and coolant circuit. These steps result in relatively high fabrication costs and are somewhat restrictive in that material selection is limited to available tubing that can be formed and reliably brazed together. Conversely, the use of advanced construction techniques for fabricating non-tubular thrust chambers reduce these time consuming steps thus offering the potential of reduced fabrication cost in production.

(U) In addition non-tubular construction techniques allow for more flexibility in the choice of materials or material combinations; extending the potential range of application of regeneratively cooled thrust chambers. Also non-tubular construction techniques allow for independent variation of wall thickness and coolant geometry; producing more flexibility and greater control of the coolant flow area.

(U) In April 1968, Rocketdyne was awarded an Exploratory Development Program by the Air Force Rocket Propulsion Laboratory, for the "Investigation of Non-Tubular Wall Regeneratively Cooled Thrust Chamber Concepts" (F04611-68-C-0061). The objective of this program was to investigate advanced fabrication techniques applicable to non-tubular wall regeneratively-cooled thrust chambers and demonstrate the lower cost and improved performance which can be achieved through their use.

SUMMARY

(U) This report presents the results of an Exploratory Development Program contracted with the Air Force Rocket Propulsion Laboratory at Edwards Air Force Base. The program, entitled "Investigation of Non-Tubular Wall Regeneratively Cooled Thrust Chamber Concepts" (F04611-68-C-0061) had as its objective the evaluation of advanced fabrication techniques applicable to regeneratively cooled thrust chambers and the definition of the lower cost and improved performance, as compared to tubular wall chambers, that could be achieved through their use.

(U) The program was divided into three phases:

- Phase I - Design and Fabrication Limits Study
  - Task I - Parametric Design and Limits Study
  - Task II - Materials Study
  - Task III - Fabrication Study
- Phase II - Fabrication Process Evaluation
- Phase III - Design and Performance Evaluation

PHASE I - RESULTS

(U) During Phase I, Task I, parametric heat transfer analyses were conducted to determine the limits of regeneratively cooling of non-tubular wall thrust chambers. The analyses considered the effects of materials, coatings, coolant limitations (i.e., bulk temperature rise), and fabrication limits (i.e., minimum channel size and wall thickness).

(U) This parametric study defined the limits of regenerative cooling of annular and bell chambers using either hydrogen, fluorine, amine (N_2H_4), CPF or decomposed hydrazine as the coolant. Also considered were

combinations of the above, such as fuel-cooled chamber and oxidizer cooled nozzle or multiple layers of coolant passages, where the fuel is used as the primary (chamber) coolant and the oxidizer is used to absorb heat from, and thereby extend, the coolant capability of the fuel.

(U) The parametric stress analyses effort of Phase I Task I established coolant circuit geometry limits for a number of candidate materials. Also investigated were the external structure requirements to withstand the imposed hoop loads of bell chambers.

(U) In Phase I, Task II, literature and industry surveys were completed to collect and summarize the physical, thermal, and environmental compatibility data of candidate materials for use in the analytical and experimental efforts of this program. Materials considered included high-conductivity and high-temperature alloys, refractory alloys, non-metallic, and high-strength lower temperature alloys for use as backup structures in both bell and annular chambers. Evaluation criteria for the candidate materials included: (1) compatibility, (2) mechanical properties (strength, thermal conductivity, and ductility), (3) material and processing cost, and (4) fabricability (ease of fabrication, and fabrication limits such as duty cycle, material property changes, and achievable tolerances). Data for this task was made available by Battelle Memorial Institute of Columbus, Ohio, through a subcontract on this program, as well as various divisions of North American Rockwell Corporation.

(U) The objective of the Phase I, Task III Fabrication Study was to define and establish thrust chamber fabrication concepts to be further evaluated using the results of the Task I and Task II studies. This was accomplished through the use of a fabrication concept ranking system which considered Development Risk, Range of Application, and Production Costs.

(U) The Phase I study culminated in the recommendation by Rocketdyne of six of the more promising advanced thrust chamber concepts for experimental evaluation in the subsequent phases of the program. Subsequently, three of the fabrication concepts were selected for experimental evaluation in Phase II:

Concept No. 1 - Powder Metal Nickel Bell Chamber

Concept No. 2 - Spun Hastelloy or INCO 625 Bell Chamber Liner with Machined Slots, Electroformed Nickel Closeout and Integrally Cast Aluminum Structure

Concept No. 3 - Cast Beryllium Copper Segment of an Annular Chamber with Electroformed Nickel Closeout and Oxidizer Heat Exchange Panel on One Side

PHASE II - RESULTS

(U) In Phase II test panels and full-size chambers and segments were fabricated and laboratory tested to establish process parameters, explore fabrication limits, establish design criteria and in-process controls and inspection techniques for use in the Phase III hot firing hardware. Results on each concept were as follows.

Powder Metal Bell Chamber

(U) The fabrication process for this concept (Fig. 1) is:

Initially, nickel powder is packed and pressed around a hard steel mandrel which forms the internal diameter of the chamber. The outer surface of this as-pressed liner is then machined to the required hot gas wall thickness. Soft tooling which forms the coolant passages is then stacked around this liner, additional powder is packed to form

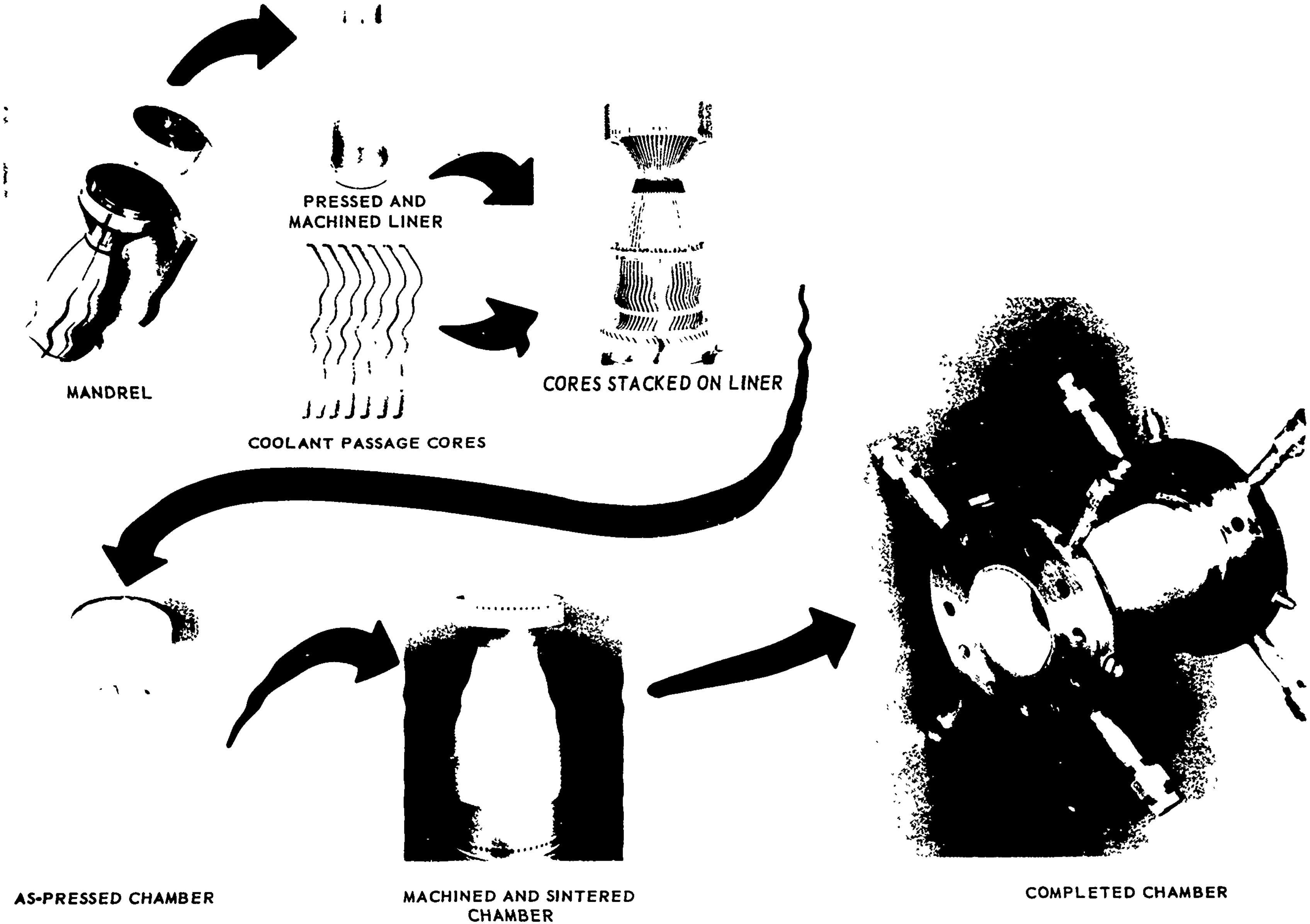

Figure 1. Fabrication Sequence - Powder Metal Bell Chamber (U)

the lands and coolant circuit closure and the entire unit pressed at a higher pressure. The as-pressed chamber is then machined on the outer surface to design dimensions, the hard mandrel removed, the coolant passage tooling flushed out with hot water and the entire unit sintered as a free standing part in the furnace. Subsequently, nickel 200 flanges are electron beam welded onto the sintered body, completing the chamber.

(U) The structural integrity and dimensional repeatability of the process were demonstrated through the fabrication, pressure testing and sectioning of internally cored cylinders and full-size bell chambers. Pressure test results showed excellent structural integrity of sintered nickel hardware. Full-size chambers were pressure tested to greater than 5000 psig with cylinders and sections of chambers pressure tested to over 20,000 psig. Dimensional results were also quite good reflecting tolerances in the range of $\pm$ 0.003 in the critical regions. Average density measurements showed values as high as 96.3 percent of theoretical. Sintered nickel properties were obtained through elevated temperature tensile testing of ASTM tensile bars machined from solid wall cylinders. Results showed tensile properties quite similar to wrought and annealed nickel 200. Experimental determination of the thermal conductivity of sintered nickel gave results equivalent to measured values of nickel 200 and to the National Bureau of Standards values of 99.94 per ent pure nickel.

<u>Spun Bell Chamber with Machined Passages and Electroformed Nickel Closure</u>

(U) The fabrication sequence of this concept (Fig. 2) is:

Initially, a flat plate is spun into the chamber shape to form the liner. After annealing, the inner and outer surfaces of the liner are machined to the prescribed thickness. Sixty constant width

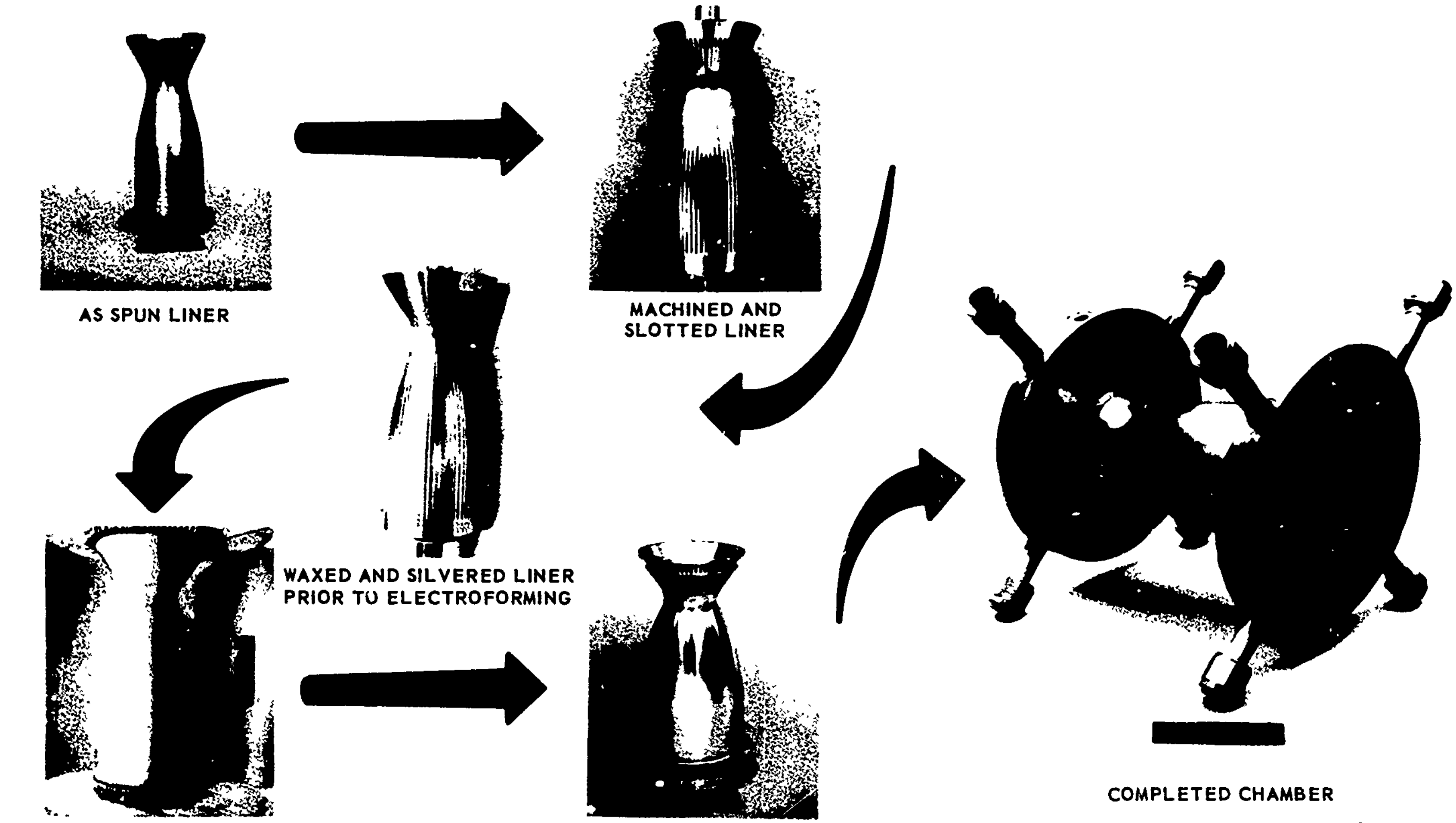

Figure 2. Spun Liner with Electroformed Nickel Closure (U)

variable depth coolant passages are machined into the outer surface of the spinning, and nickel is electroformed onto the outer surface to close off the coolant circuit and provide necessary structure to withstand chamber pressure loads. Subsequently, flanges and manifolds are electron beam welded in place.

(U) Fabrication development tasks successfully completed in support of this concept included (1) spinning of INCO 625 liners, (2) passage machining in Spun INCO 625, and (3) electroforming nickel onto INCO 625. Structural integrity of the electroformed nickel to INCO 625 bond was demonstrated to $\sim$ 20,000 psig on test panels and verified on regeneratively cooled chambers where pressure tests to 14,800 psig were completed. Dimensional repeatability of the hot gas wall thickness and coolant passage cross sections were demonstrated with tolerances of $\pm$ 0.003 in the critical regions.

Cast Segment with Electroformed Nickel Closure and Oxidizer Heat Exchange Panel

(U) This fabrication concept (Fig. 3) incorporates an investment cast beryllium copper segment liner (hot gas wall and coolant passage lands) followed by successive layers of electroformed nickel, to closeout the primary coolant passages and form the heat exchange panel and coolant manifolds. Subsequently, coolant transfer tubes and injector attach flange are welded in place and the workhorse backup structure is bolted on.

(U) Fabrication development tasks successfully completed on this concept included (1) investment casting of beryllium copper segment liners, (2) electroforming nickel onto cast beryllium copper and onto itself, (3) machining of heat exchange panel passages and, (4) experimental determination of beryllium copper tensile properties and thermal conductivity.

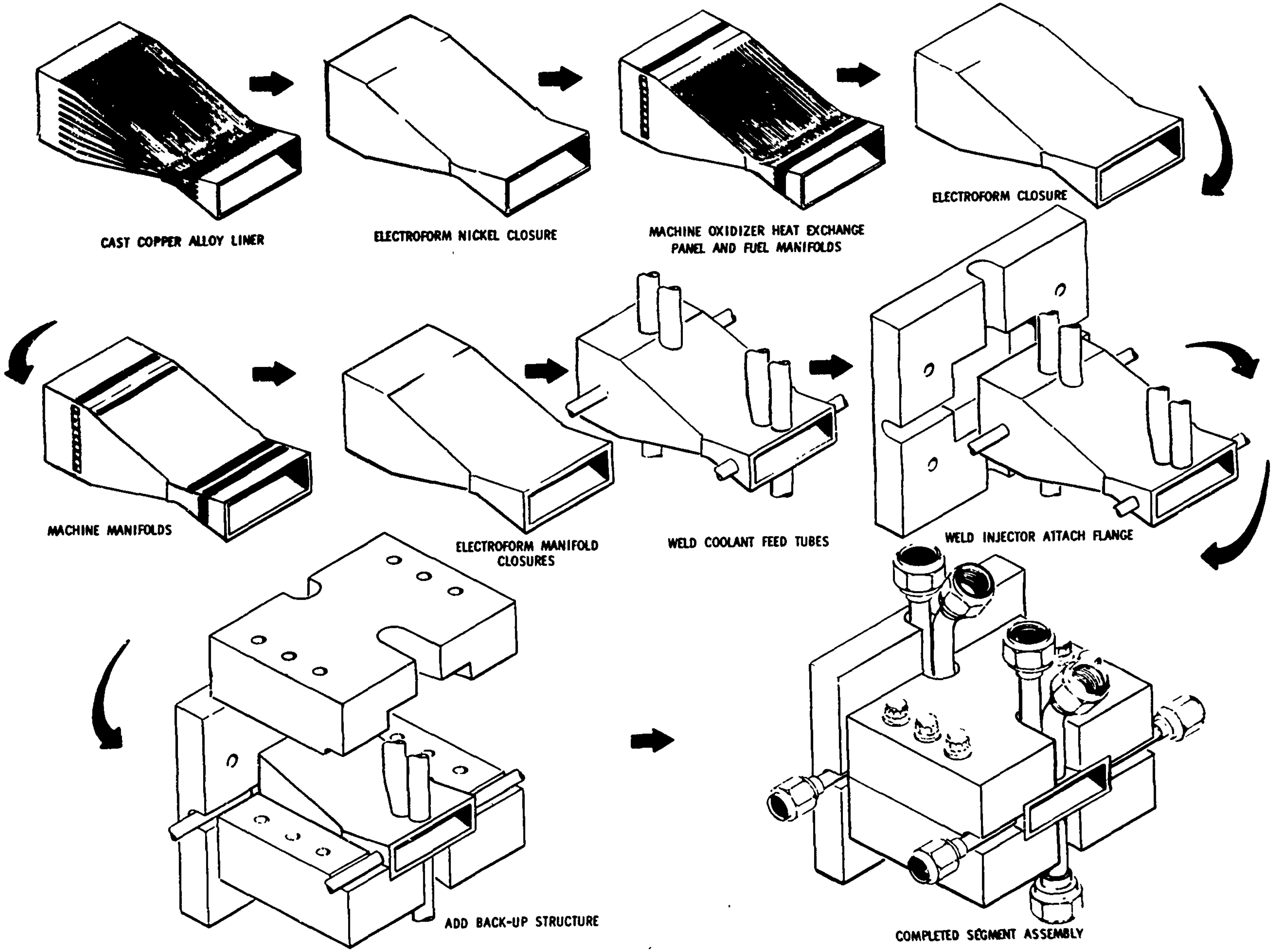

Figure 3. Cast Segment with Electroformed Nickel Closure and Oxidizer Heat Exchange Panel. (U)

(U) The investment casting process was demonstrated to be an economical technique for producing segments of annular chambers, through the successful casting of segment liners with good material properties and dimensional repeatability. Results learned here are applicable to larger size segments and to other configurations such as bell chambers.

(U) Material property evaluation (tensile, ductility and thermal conductivity) showed the feasibility of using the selected beryllium copper alloys (BeCu-10C and -50C) in regeneratively cooled thrust chambers and provided the necessary data to indicate the range of application of the materials.

(U) The bond strength between electroformed nickel and cast beryllium copper was demonstrated by pressure testing segments to values in excess of 10,000 psig. These same pressure tests verified the feasibility of using electroformed nickel to closeout the heat exchange panel and the coolant manifolds.

(U) Conventional shop practices and techniques were shown to be practical for machining the heat exchange coolant passages into the electroformed nickel.

PHASE III - RESULTS

(U) In Phase III the powder metal nickel bell chamber, the Spun INCO 625 bell chamber and the investment cast beryllium copper segment were successfully hot fired and demonstrated structural integrity and thermal performance of the selected fabrication concepts. All tests were conducted with a LF_2/GH_2 combustion environment. The chamber coolant bypassed the injector so that coolant and/or injector flow could be varied as required to subject the chambers to various structural and thermal conditions.

(U) The powder metal nickel bell chamber was GH_2 cooled in all tests. The INCO 625 bell chamber was tested with water as the coolant (simulating the N_2H_4 amine type fuel used in the Phase I studies). The primary coolant of the segments was GH_2. The heat exchange panel, located on one side of the segment, used LN_2 and subsequently LF_2 coolant to demonstrate the heat exchange capability.

Powder Metal Nickel Bell Chamber

(C) A total of seven tests were completed on the powder metal nickel bell chamber over a chamber pressure range of 296 to 528 psia with a mixture ratio excursion of 11.2 to 12.3. Accumulated test duration was 41.6 seconds including a 10.6 second demonstration test at 528 psia chamber pressure.

(C) Calculated hot gas wall temperatures ranged between 1100 and 1670 F including 26.2 seconds at a wall temperature of 1570 to 1670 F (design hot gas wall temperature was 1600 F). Coolant inlet pressures ranged from 1600 to 2000 psig. These tests demonstrated the structural integrity and thermal performance of the concept under conditions equal to or more severe than those planned for an actual production chamber.

Spun Bell Chamber

(C) Four hot firing tests were completed on the spun INCO 625 bell chamber over a chamber pressure range of 308 to 382 psia and a mixture ratio excursion of 11.7 to 14.4. Accumulated test duration was 19 seconds including a demonstration test of 13.5 seconds at 377 psia chamber pressure. The potential application for this fabrication concept was in a

regeneratively cooled CPF/N_2H_4 engine system which required operation at a hot gas wall temperature of 2000 F to extend the range of application. A chamber pressure of 480 psia with a F_2/H_2 combustion environment (as was used in the Phase III tests) gives a heat flux equivalent to operation at 750 psia with CPF/N_2H_4 propellant.

(C) The bulk temperature limited amine fuel (N_2H_4) was simulated on these tests by using water as the coolant. Results of these tests which demonstrated the structural integrity and thermal performance of the fabrication concept under more adverse conditions than would be experienced in actual application (calculated hot gas wall temperatures ranged between 1900 and 2300 F) have shown the feasibility of utilizing this fabrication concept on potential advanced amine fuel regeneratively cooled thrust chambers.

Cast Beryllium Copper Segment

(C) Four hot firing tests were completed on the cast beryllium copper segment over a chamber pressure range of 406 to 460 psia and a mixture ratio excursion of 12.1 to 1[illegible] . Accumulated test duration was 13.4 seconds with gaseous hydrogen as the primary coolant on all tests. The first three tests used LN_2 as the coolant in the heat exchange panel to provide data for evaluation of the heat exchange benefit to be gained from multiple layers of coolant panels. The last test used LF_2 as the coolant in the heat exchange panel and was a demonstration of the capability of this fabrication concept with the propellants of interest.

(C) Calculated maximum hot gas wall temperatures attained on these tests ranged between 900 and 1000 F demonstrating the design value of 1000 F. On one test the LN_2 coolant in the heat exchange panel was shut off during the test; the resulting bulk temperature increase in the primary GH_2 coolant of approximately 33 percent demonstrated the beneficial effect of the heat exchange principle.

(C) These tests have demonstrated the structural integrity and thermal performance of the fabrication concept under conditions quite similar to those of a system in an actual application. These parameters (hot gas wall temperature of $\sim$ 1000 F, GH_2 coolant pressures to 2400 psig and LF_2 in the heat exchange panel) have shown the feasibility of incorporating this fabrication concept on current and future annular or bell chambers to reduce fabrication cost and extend their range of application.

PHASE I - DESIGN AND FABRICATION LIMITS STUDY

(U) Phase I was a parametric design and analytical investigation of advanced construction techniques applicable to non-tubular regeneratively cooled thrust chambers. Propellants of interest included advanced storable (CPF/amines) and cryogenic (F_2/H_2) propellants and encompassed both annular and bell thrust chambers. The effort was divided into three tasks:

Task I: Parametric Design and Limits Study
Task II: Materials Study
Task III: Fabrication Study

(U) Task I was a parametric heat transfer and stress analysis study to determine regenerative cooling and structural limits of thrust chambers employing advanced construction techniques.

(U) Task II was a literature and industry survey to determine the mechanical properties and compatibility of materials selected for investigation in the Task I and III studies.

(U) Task III identified and evaluated candidate fabrication concepts and culminated in the recommendation of six of these to the AFRPL from which three were subsequently selected for experimental evaluation in Phases II and III.

(U) The results of the Phase I study, which were presented in detail in the Phase I report (Ref. 1) are summarized in the following paragraphs.

TASK I - PARAMETRIC DESIGN AND LIMITS STUDY

(U) Task I was a parametric heat transfer and stress analysis study to determine the limits of regenerative cooling of thrust chambers employing advanced construction techniques. Coolant techniques considered were: (1) fuel coolant, (2) oxidizer coolant, (3) simultaneous use of fuel and for the amine fuel as a gas, formed by decomposing the fuel, and (5) multiple layers of coolant passages. Materials of interest included: high conductivity, refractory and high thermal resistance. The design cases used in the study were:

Thrust, pounds	Propellant	Chamber Configuration	Throttling Range
1,000	CPF/Amine and LF_2/LH_2	Bell	0
10,000	CPF/Amine	Bell	0 and 10:1
10,000	LF_2/LH_2	Bell and Annular	0
100,000	CPF/Amine	Bell and Annular	0
100,000	CPF/Amine	Bell	10:1
100,000	LF_2/LH_2	Bell and Annular	0 and 10:1

(U) Additional ground rules considered that (1) the mixture ratio was uniform across the injector with no film cooling elements, (2) η_{C*} was 98 percent, (3) the mixture ratios for CPF/Amine and LF_2/LH_2 were 2.7 and 12, respectively, and (4) the coolant circuit pressure drop did not exceed chamber pressure or 1000 psia, whichever is less. The propellant selected to represent the "amine" fuel for these studies was hydrazine, N_2H_4.

Parametric Heat Transfer Analysis

(U) General Approach. The analysis of heat transferred at each point in a regenerative cooled thrust chamber may logically be divided into three regions of primary interest: (1) the hot gas boundary layer, (2) chamber wall, and (3) the coolant film. The heat transferred across these conductances is absorbed by the coolant resulting in a rise in bulk temperature as the coolant progresses through the circuit.

(U) The Integral Method, Ref. 9, was utilized to calculate the hot gas film coefficient distribution along the heated surface, assuming the usual 1/7 power law for the turbulent flow velocity profile. This film coefficient compares favorably with experimental data. The point of maximum heating is located near the geometric throat. Hence, the throat heat flux determines most of the cooling characteristics in thrust chamber design. The maximum heat flux is obtained from the film coefficient and convective heating relation

$$\dot{q}'' = h_g (T_{aw} - T_{wg})$$

(U) Graphs of the throat heat flux as a function of chamber pressure are given in Figs. 4 and 5, for the annular and bell geometries with F_2/H_2 and CPF/N_2H_4 propellants. The F_2/H_2 propellant combination results in a heat flux level that is 40 percent higher than CPF/N_2H_4. The maximum heat flux determines the peak mass flux requirement for the coolant, and the minimum channel size.

(U) Materials. A brief discussion of the materials evaluated in Task II is presented here to point out the requirements of a material insofar as heat transfer and stress considerations are concerned.

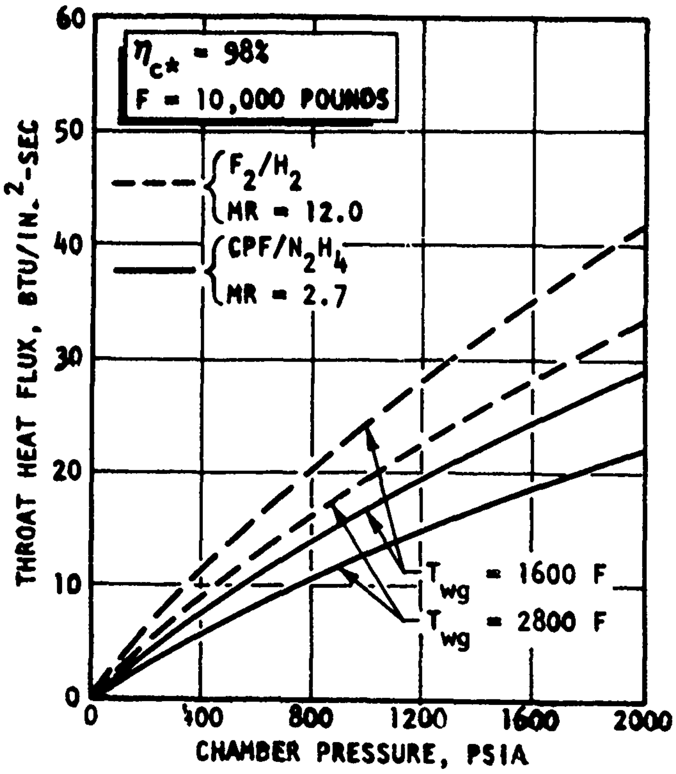

Figure 4. Bell Heat Flux as a Function of Combustion Chamber Pressure (U)

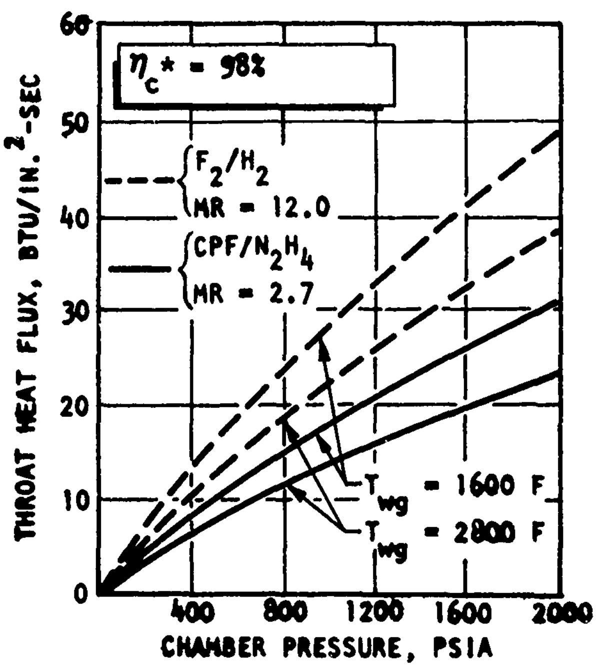

Figure 5. Aerospike Heat Flux as a Function of Combustion Chamber Pressure (U)

(U) Nickel was selected for the parametric study as representative of the conventional materials. In addition, it is compatible with the propellants and exhibits acceptable yield strength.

(U) A high thermal conductivity is desirable for high chamber pressure designs where the coolant surface is cooled by forced convection (H_2, F_2, or CPF) rather than nucleate boiling (N_2H_4). The use of Ni or Cu with H_2 cooling will result in lower cooling requirements than 347 stainless steel or INCO 625, since materials with higher conductivities allow the coolant wall temperature to increase at equivalent thicknesses. In the case of N_2H_4 cooling, the coolant wall temperature is fixed at the saturation temperature by the nucleate boiling process, and the chamber pressure is determined only by the thermal conductivity and hot gas wall temperature. A material of low thermal conductivity may actually be desirable for low to moderate chamber pressure designs with N_2H_4 cooling to eliminate excessive wall thickness and weight.

(U) The allowable wall thickness was determined from the conduction equation

$$\dot{q}'' = \frac{K}{X_w} (T_{wg} - T_{wc})$$

(U) The conduction equation is also utilized to fix the coolant surface temperature in the regenerative cooling computer program used for this study.

(U) The cooling correlations for both fuels and oxidizers were discussed in detail in Ref. 1. It is these correlations and the coolant convection equation that determine the coolant mass flux requirements at a given set of heat flux, coolant bulk temperature, and cooling surface temperature conditions. The coolant convective equation is given by

$$\dot{q}'' = h_c (T_{wc} - T_B)$$

(U) The integrated heat flux over the thrust chamber along with the heat absorption capability of the coolant determine the coolant bulk temperature at every location, where

$$\dot{q}'' \, d \, A_s = \dot{W}_c \, C_p \, d \, T_B$$

(U) These procedures are incorporated in the regenerative cooling computer program, along with the particular thrust chamber geometrical relationships.

(C) Limiting Criteria. Based on fabrication and stress considerations of non-tubular thrust chambers, a minimum wall thickness of 0.020 inch was established for this study. Minimum coolant passage dimensions of 0.040 by 0.040 inch were initially established as a lower limit to determine where coolant passage size was the predominant factor in establishing the regenerative cooling limits of the cases under investigation. This lower limit was relaxed in specific cases using smaller cross section passages and/or rectangular rather than square passages in the throat region to determine the possible extension of the regenerative cooling limits. The maximum allowable coolant bulk temperature for hydrazine was taken as 350 F, based on the Amine Propellant Selection discussion, Ref. 1. In the case of hydrogen and fluorine, there is no coolant temperature limit except, of course, that it must not exceed the allowable temperature of the wall material. In the case of the CPF a maximum coolant temperature limit of 200 F was necessary because of its low saturation temperature. The maximum allowable coolant pressure drop was taken as equal to chamber pressure or 1000 psia, whichever was less. This pressure drop was applied to the coolant circuit only and did not include the injector drop.

(U) <u>Cooling Method</u>. Initially both the fuel and the ozidizer were considered as primary coolants for the systems of interest. Results indicated the value of using the oxidizer is significant only as augmentation where needed, since the fuels considered in this study are significantly superior to the oxidizers in terms of cooling capability. Using the oxidizer as augmentation to the fuel can be achieved in either of two ways: (1) direct use as a nozzle coolant, or (2) in a heat exchanger mode with the fuel to reduce the fuel bulk temperature rise. This latter approach may be achieved by various design techniques (such as multi-layer passages) as discussed in the following sections.

(U) <u>Bell Thrust Chamber</u>. The parametric study of the limits of regenerative cooling of conventional bell chambers considered hydrogen, fluorine, hydrazine, CPF, and decomposed hydrazine as the coolant.

(U) <u>H_2 Regenerative Cooling</u>. A parametric study was conducted for the conventional chambers using fluorine/hydrogen propellants. Hydrogen is an excellent coolant so that the range of application is much broader than for the CPF/amine chambers.

(U) The primary advantage of hydrogen is that it is not bulk temperature limited except that it must not exceed the temperature of the chamber wall and structural materials. For the range of thrust levels of interest in this study, it was determined that no bulk temperature problem was involved. The maximum exit bulk temperature encountered was about 860 R (for an inlet temperature of 70 R) at an area ratio of 100 (maximum value considered), a thrust of 1000 pounds, and a chamber pressure of 3000 psia; a temperature well within the capability of conventional materials.

(U) The high mixture ratio (MR = 12) associated with F_2/H_2 propellants results in rather limited amount of coolant available. An analysis was completed to determine if minimum channel size criterion would impose a system limit.

(U) For a single pass coolant circuit the 1K design was limited to about 980 psia chamber pressure. At F = 10K, the P_c limit is about 3000 psia and increases greatly as thrust is increased. The channel size limitation for the small-thrust case can be circumvented by considering a double-pass design allowing the 1K chamber pressure limit based on channel size to be increased to about 1600 psia. However, a double-pass design has a higher pressure drop, because of the increased length of the cooling circuit.

(U) The remaining feasibility limit to be determined was that associated with coolant jacket pressure drop. A single up-pass (counterflow) coolant circuit was selected for the thrust levels of 10K and 100K with two-pass circuit selected for the 1K thrust design. The coolant curvature enhancement factor (ϕ_c) was taken as 1.5 in the throat region. This factor is readily achieved by proper design of the nozzle radius of curvature in the throat. A channel surface roughness of 50 microinches rms was assumed (the effect of varying this roughness is considered later). The chambers were considered to be fabricated of nickel 200 with a minimum hot gas wall thickness of 0.020 inch and a maximum gas side wall temperature of 1600 F.

(U) Results showed that the 10K and 100K designs can be regeneratively cooled up to pressures of about 2800 psia and 3200 psia, respectively. Variation in area ratio does not appreciably affect the higher thrust cases since the nominal coolant bulk temperatures are quite reasonable. The

low thrust level case benefited in decreasing area ratio from 100 to 60. This results from a more optimum hydrogen temperature in the throat on the second (counterflow) pass. The limiting criterion for the lower area ratio case was found to be the minimum channel size constraint.

(U) The final feasibility line incorporating the various limiting criteria is presented in Fig. 6 and clearly indicates the wide operational limits achievable with F_2/H_2 bell chambers using conventional materials.

(U) The use of advanced refractory materials and coatings was also considered briefly for the F_2/H_2 bell chambers. It was quickly apparent that the use of such materials extends the limit of regenerative cooling well above a 3000 psia chamber pressure. Since these high chamber pressures are not of paramount importance at the present time, this area of the study was not pursued in detail.

(U) The throttling limit for a hydrogen-cooled system is determined on the basis of maximum wall temperature considerations. As the chamber is throttled, the bulk temperature and coolant-side wall temperature increase in a nearly parallel manner. (The difference between coolant-side wall and bulk remains relatively constant because the coolant film resistance increases as the heat flux decreases.) The decreasing heat flux level results in a decreased temperature differential across the wall (constant thermal resistance) so that the combustion-side wall temperature initially decreases during throttling. As the throttling requirement deepens, the bulk temperature rise becomes excessive and the combustion side temperature begins to increase until the original value is reached. Results using these criteria showed throttling capability well in excess of 10:1.

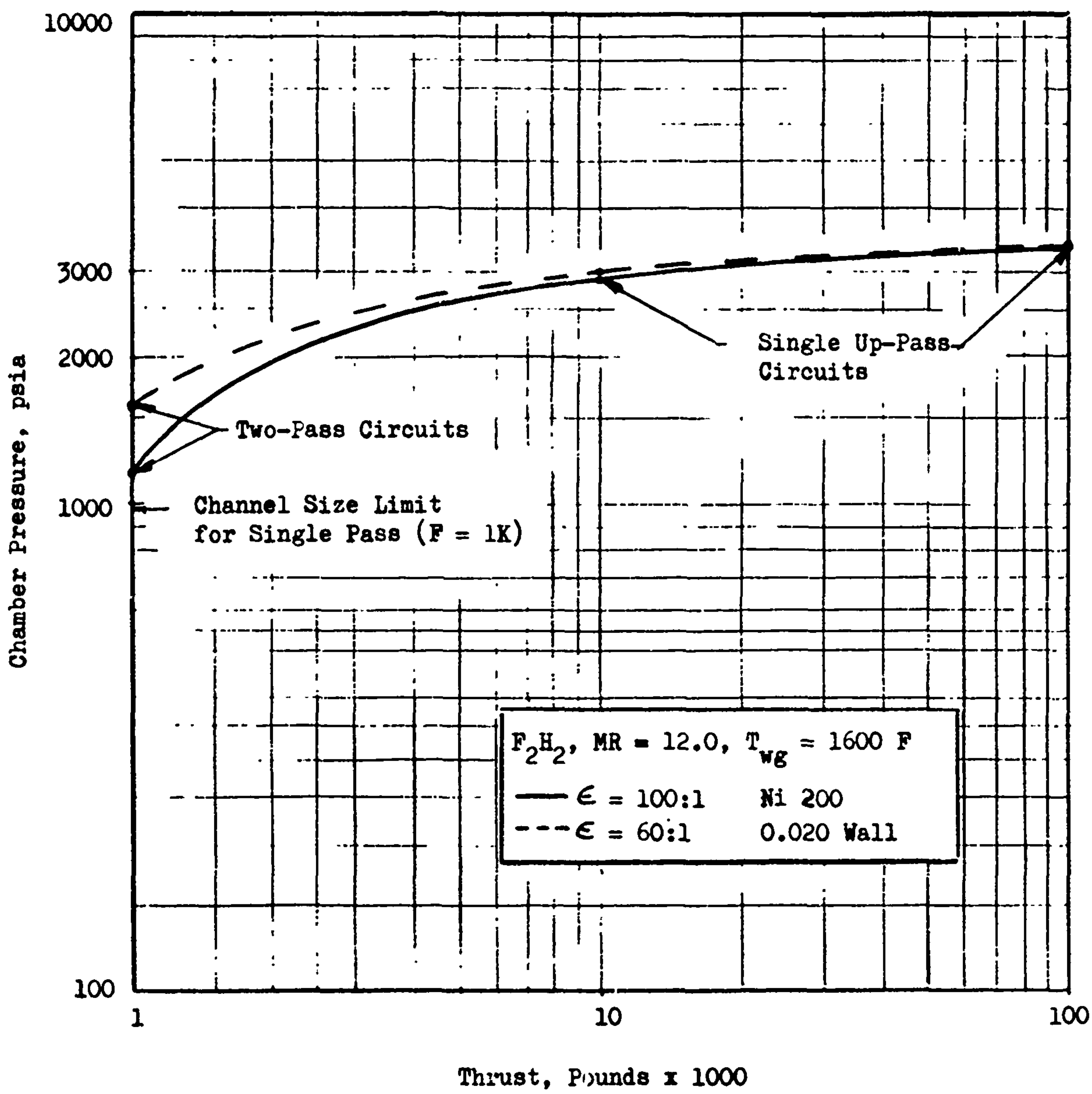

Figure 6. Regenerative Cooling Feasibility Limits for Conventional Chambers (U)

(U) In summary, the F_2/H_2 bell chambers utilizing the hydrogen as the coolant can be regeneratively cooled over an extremely wide range of operating conditions including deep throttling. Augmentation cooling with the oxidizer is unnecessary except, perhaps, at very extreme conditions. Oxidizer cooling of the nozzle may be advantageous from other considerations pertaining to injector performance (i.e., vaporization of the oxidizer to achieve gas-gas injection). This is discussed in a later section.

(C) $\underline{F_2}$ Regenerative Cooling. Fluorine cooling was also evaluated for conventional bell thrust chambers for comparison to hydrogen. Cooling circuits as shown in Fig. 7 below.were selected to yield the maximum chamber pressure limits, and do not necessarily represe convenient design arrangements. The circuit chosen for low chamber pressure designs ($<$ 500 psia) is set up to gasify the F_2 prior to reaching the throat,

$P_c <$ 500 psia - Coolant Subcritical

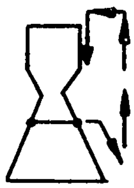

Coolant Gasified
Prior to Entering
the Throat

$P_c \geq$ 500 psia - Coolant Supercritical

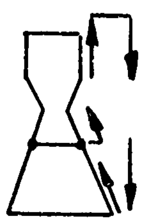

Coolant Bulk Temperature
Minimized at Throat

Figure 7. Cooling Circuit Schematics - F_2 Coolant (U)

in order to avoid exposing the two phase flow regime to the throat heat flux. In contrast, the bulk temperature is minimized at the throat when the coolant is at supercritical pressure (P_c > 500 psia), by cooling the upper portion of the nozzle prior to cooling the throat. It is necessary to heat the F_2 above the critical temperature in the upper portion of the nozzle of the high pressure designs, since the film coefficient is low in that temperature region.

(C) Analysis showed that coolant circuit pressure losses exceeded chamber pressure for all cases except thrust levels of 100,000 pounds with chamber pressures less than 300 psia. If the coolant passage and pressure drop limitations are relaxed, the chamber pressure limits become:

F (Klb_f)	ΔP (psi)	P_c Limit (psia)
1	700	100
10	1000	750
100	1000	1000

(U) N_2H_4 Regenerative Cooling. Regenerative cooling limitations of conventional thrust chambers with N_2H_4* were investigated on the basis of minimum channel dimensions, bulk temperature limitations and coolant pressure drop.

* Throughout the report all references to N_2H_4 actually consider N_2H_4 with an additive of 10 percent ethylenediamine (EDA) as discussed in Ref. 1 .

(U) The effect of minimum channel dimensions on operating limits was investigated using throat heat flux curves discussed previously in conjunction with the hydrazine cooling capability curves of Ref. 4. These established required coolant velocities as a function of thrust and chamber pressure for comparison to the maximum available velocity as a function of thrust and chamber pressure for minimum channel dimensions of 0.035 by 0.035 inch and 0.040 by 0.040 inch. (The land width was taken as equal to the channel width.) The point at which the required velocity exceeded the available velocity determined an operational limit.

(U) Results show that at lower thrust levels ($<$ 10K) a definite restriction on the allowable chamber pressure is encountered. This is to be expected because of the very low coolant flow available. At a thrust of 1000 pounds, for example, the maximum chamber pressure is limited to about 300 psia for a conventional material such as nickel (T_{wg} = 1600 F). The use of a higher temperature (2800 F), as would result from a coating or a refractory material, allows a maximum chamber pressure of 560 psia. At higher thrust levels ($>$ 10K), the minimum channel size criterion imposes no limit on the system. For these cases, other criteria will limit the system. In actuality, even at low thrust levels the channel size is not the most critical criterion, as will be shown presently.

(U) A primary limitation on the hydrazine coolant is the maximum allowable bulk temperature of about 350 F. This limitation becomes particularly critical at low thrust levels because of the increased heat input per pound of coolant flow. Equating the imposed heat input (Σ Q/F) with the allowable value for the hydrazine coolant allows a cross determination of thrust, chamber pressure, and nozzle area ratio limits.

(U) The results of the integrated heat input comparison showed that at a thrust level of 1000 pounds, it is barely possible to cool the throat and combustion zone using conventional materials (T_{wg} $\sim$1600 F). The 100 Klb_f-thrust level, however is capable of regenerative cooling to an area ratio of slightly more than 100. The use of a high surface temperature design (as would be achieved by a coating or a refractory material) results in a marked extension in the allowable cooling range. The area ratio limit on the F = 1K chamber can be extended to a reasonable value of about 20 for chamber pressures of less than 1000 psia. The higher thrust levels (F = 10K and 100K) are capable of being cooled to area ratios in excess of 100.

(U) For the higher-thrust cases, the coolant pressure drop becomes the limiting factor of interest. Using the Rocketdyne Regenerative Cooling digital computer program, the coolant pressure drops were obtained for various cases with single downpass fuel cooling circuits. Applying the criterion that pressure drop not exceed chamber pressure or 1000 psi (whichever is less), the limiting chamber pressures were obtained for the 10K and 100K cases using a conventional material (nickel). The $1Klb_f$ thrust level case assumed that the coolant was used primarily in the throat region. The maximum chamber pressures were about 1700 and 2200 psia for the 10K and 100K chambers, respectively. Increasing the gas-side operating temperature to 2800 F (coolant side temperature remains relatively constant) allowed extension of the above chamber pressure limits to about 2400 and 3100 psia. However, materials capable of withstanding temperatures of 2800 F generally possess high thermal conductivity and thus become quite thick to raise the surface temperature to 2800 F.

(U) The various controlling limits were then incorporated into a single feasibility line for each thrust level of interest, as shown in Fig. 8; indicating areas of feasible operation for a selected system.

(U) Summarizing, for conventional materials, the 1K thrust design is bulk temperature limited, whereas the 10K design is bulk temperature limited at lower pressures and channel size and pressure drop limited at higher chamber pressures. The 100K design limit is affected only by pressure drop considerations. Increased gas-side wall temperatures produce changes in pressure drop limits for the 10K and 100K designs. The 1K design operating limit is still determined primarily by bulk temperature considerations.

(U) Throttling of chambers using amine-type coolants is a rather severe requirement because of the increased bulk temperature rises. In general, as an engine is throttled, the heat input drops off as the 0.8 power of the chamber pressure, whereas the coolant flow drops off linearly. The resulting relation for the bulk temperature rise is

$$T_{bulk} \sim \left(\frac{1}{F}\right)^{0.2}$$

(U) For example, with a 10:1 throttling requirement imposed on the chamber, the bulk temperature rise is increased by about 58 percent.

(U) Consequently for a bulk temperature-limited coolant the throttling requirement must be known in advance since it will govern the nominal operating limits of the chamber. Considering the case of a 10:1 throttling requirement on a hydrazine-cooled chamber and assuming a

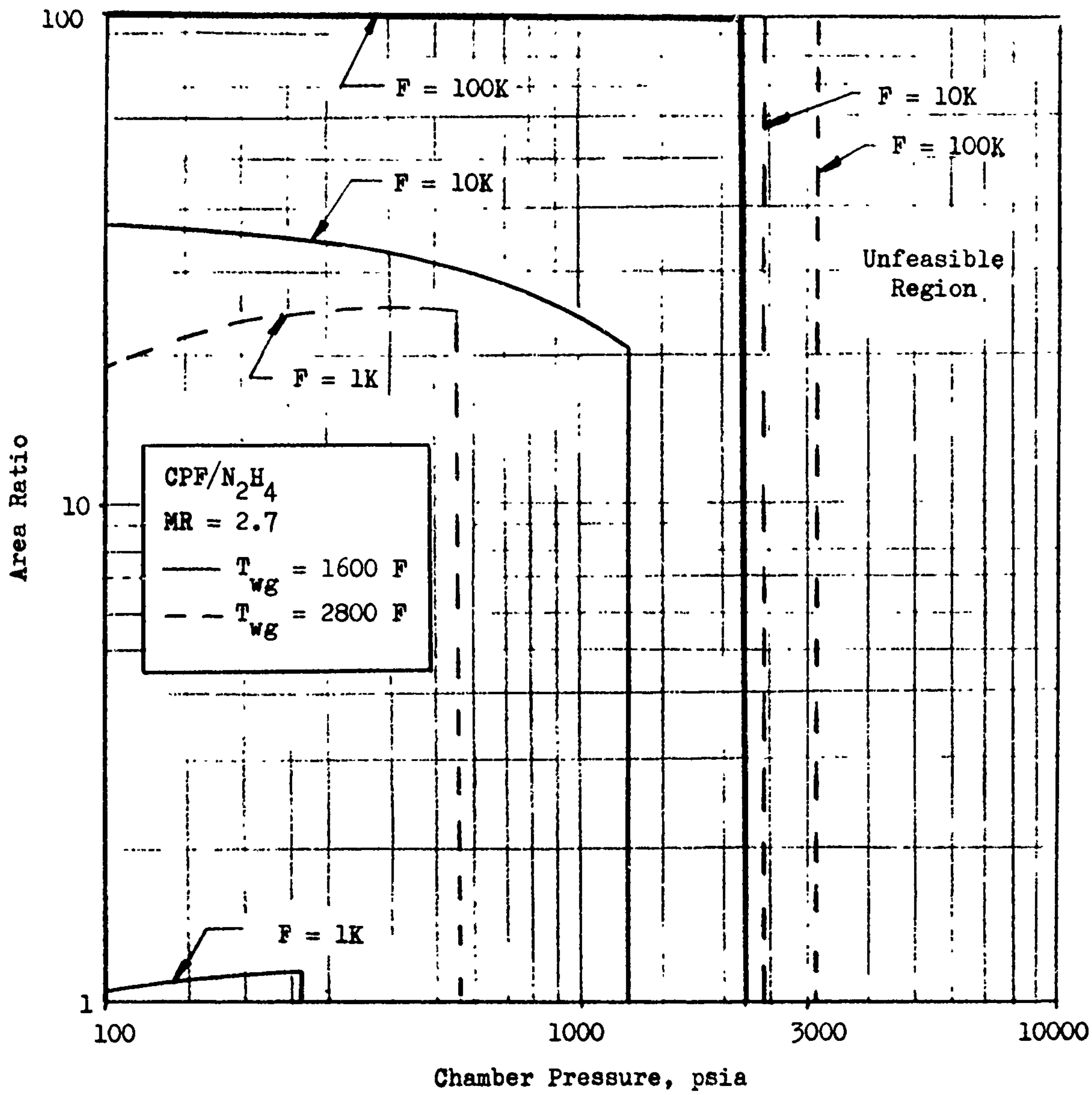

Figure 8. Regenerative Cooling Feasibility Combined Limits for Bell Chambers. (U)

maximum allowable bulk temperature of 350 F at throttled conditions, requires that at nominal full-thrust conditions, the hydrazine exit temperature must not exceed approximately 247 F. (This assumes an inlet temperature of 70 F with a 58-percent increase in ΔT_B during throttling.) The net effect of the throttling requirement is to reduce the allowable heat-absorption capability of the hydrazine at full-thrust conditions.

(U) Typical design cases of 10K, 30K* and 100K with a 10:1 throttling requirement were evaluated to determine feasibility limits of operation (Fig. 9). Additional 30K design points were estimated to indicate the effects of changing wall temperature and throttle ratio. It may be noted from the data shown that decreasing the required throttling range of a 30K thrust chamber (P_c = 750 psia and T_{wg} = 1600) from 10:1 to 5:1 permits a nozzle area ratio increase from 10 to 30. The maximum area ratio for regenerative cooling of a 100K design is limited to about 27 for conventional materials. An increased wall temperature will extend the limiting area ratio to about 75. This compares with a feasible area ratio greater than 100 for the nonthrottled requirement. Clearly, a throttling requirement has a significant effect upon the nominal chamber design conditions.

(U) An additional factor to be considered during throttling is the decrease in the hydrazine coolant saturation temperature with pressure. To prevent bulk boiling of the hydrazine, it is necessary that the coolant

---

* The 30K thrust chamber was included since this was the thrust level selected for the Task III point design.

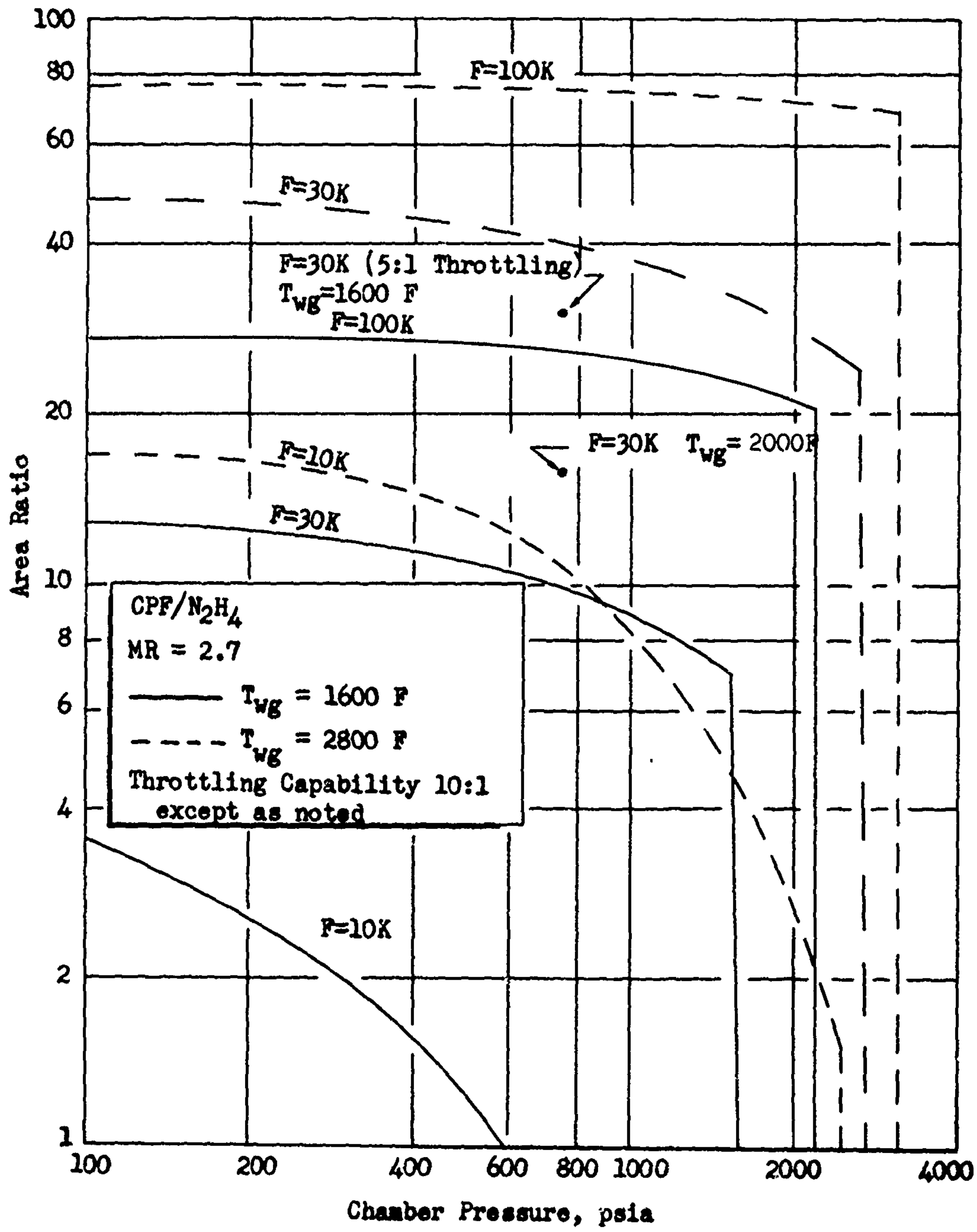

Fig. 9 . Regenerative Cooling Feasibility Limits for Bell Chambers With a Throttling Requirement Using N_2H_4 Coolant. (U)

bulk temperature remain below the saturation temperature at all times. This meams that at low coolant pressures ($p < 90$ psia), the maximum allowable exit temperature will drop lower than the 350 F limit imposed previously. The effect upon the nominal design is to decrease the allowable area ratio even further.

(C) CPF Regenerative Cooling. Regenerative cooling with CPF as the primary coolant was analyzed for bell thrust chambers to compare its capability to that of N_2H_4. The CPF cooling correlations taken from Ref. 6. were used to predict the requirements for this portion of the study. Downpass cooling circuits were used to reduce the coolant bulk temperature at the throat, which is the critical location. The coolant was assumed to be at supercritical pressure for chamber pressures in excess of 500 psia, and in subcritical nucleate boiling regime at lower pressures.

(C) Coolant bulk temperature at the throat is variable with the thrust level. The coolant is in the liquid-gas phase at thrust levels under 10 Klb_f and is completely gasified at the 1 Klb_f value. There is very little subcooling available until the thrust level is increased to 100 Klb_f, indicating that this is the minimum thrust to consider for CPF cooling. In addition; only low nozzle area ratios may be used with CPF, since the bulk temperature at the throat is only 80 F below the coolant saturation temperature.

(C) Analysis showed that the pressure drop equal to chamber pressure limit is exceeded everywhere, because the coolant pressure must be elevated to 500 psia to maintain a reasonable coolant wall temperature ($\sim$saturation temperature). The pressure drop limit of 1000 psi is reached at 350 psia chamber pressure.

(C) These results showed the CPF to be inferior as compared to N_2H_4 for use as the primary thrust chamber coolant and should be considered only as an auxiliary cooling technique (heat exchanger or nozzle cooling).

(U) <u>Decomposed N_2H_4 Regenerative Cooling</u>. The feasibility of regenerative cooling of a thrust chamber with N_2H_4 decomposition products becomes dependent upon selection of the wall material, the coolant pressure, and the chamber pressure level.

(U) A decomposed hydrazine (98 percent) exhaust temperature for 0 percent secondary reaction is theoretically 2480 F for a complete primary reaction (Ref. 1). In practice with catalytic and thermal reactors the secondary reaction can be driven to an 80 percent completion point with a resulting temperature of 1340 F. The utilization of this high temperature decomposed fuel for cooling a regenerative thrust chamber precludes the use of nearly all conventional materials, and a refractory metal (Mo-50 Re) was chosen to evaluate its cooling feasibility. A conventional thrust chamber geometry was selected for the evaluation at constant throat area and variable chamber pressure and thrust level. The resulting coolant pressure loss is shown in Fig. 10.

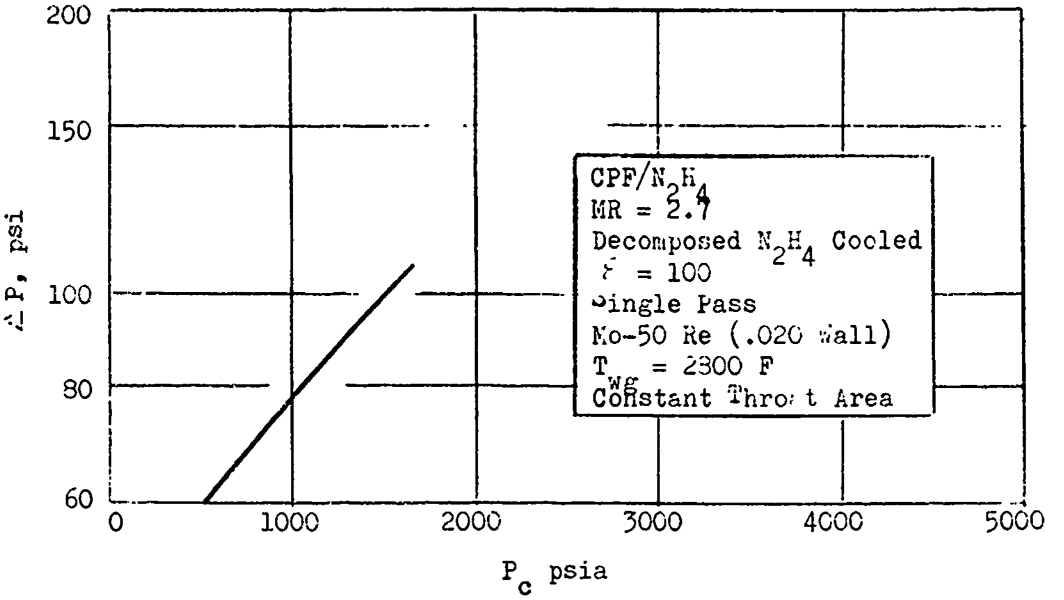

Figure 10. Jacket Pressure Drop for Decomposed N_2H_4 Cooling.

(U) Regenerative cooling with decomposed N_2H_4 is feasible; however, a major problem appears to be the design of a reactor for the N_2H_4 decomposition. A thermal reactor presently appears to be the most attractive method, since a catalytic type would be extremely large for the coolant flowrates under investigation. It was not the intent of this study to evaluate potential reactors for decomposing the N_2H_4 but to evaluate the regenerative cooling limitations of the decomposed N_2H_4. A complete systems analysis is required to establish the overall advantages and limitations of this regenerative cooling technique.

(U) Annular Thrust Chamber. The parametric study of the limit of regenerative cooling of annular thrust chamber was limited to hydrogen and hydrazine since the parametric study on the bell chambers had established the superiority of the fuel as compared to the oxidizers for primary coolant.

(U) H_2 Regenerative Cooling. The goal of any parametric study is to develop a set of curves that yield the information necessary to select any design point over the range of independent variables of interest. Selection of a typical design point for an annular chamber constitutes fixing the engine thrust level, chamber pressure, and engine diameter. Determination of coolant pressure drop is arrived at parametrically by allowing the chamber pressure to vary after the engine diameter and thrust level are chosen.

(U) Study is necessary to utilize the maximum engine diameter possible, to obtain high area ratio and performance and yet still provide adequate cooling. Large engine diameter/thrust ratios result in high coolant bulk temperatures and increased cooling requirements. Elevated chamber pressure designs also exhibit high performance and relatively severe cooling requirements. A design point can be selected from a parametric array at the largest possible engine diameter and chamber pressure within the limits of regenerative cooling, performance, and weight.

(U) The variation in required hydrogen mass flux, presented as a function of coolant bulk temperature and heat flux in Ref. 7 was used to predict cooling requirements parametrically with chamber pressure and thrust per unit circumference as independent parameters. Bulk temperatures and available coolant flow for hydrogen appear in Figs. 11 and 12. For multiple pass coolant circuits the bulk temperature increase per pass is obtainable by dividing the value of Fig. 11 and 12 by the number of passes.

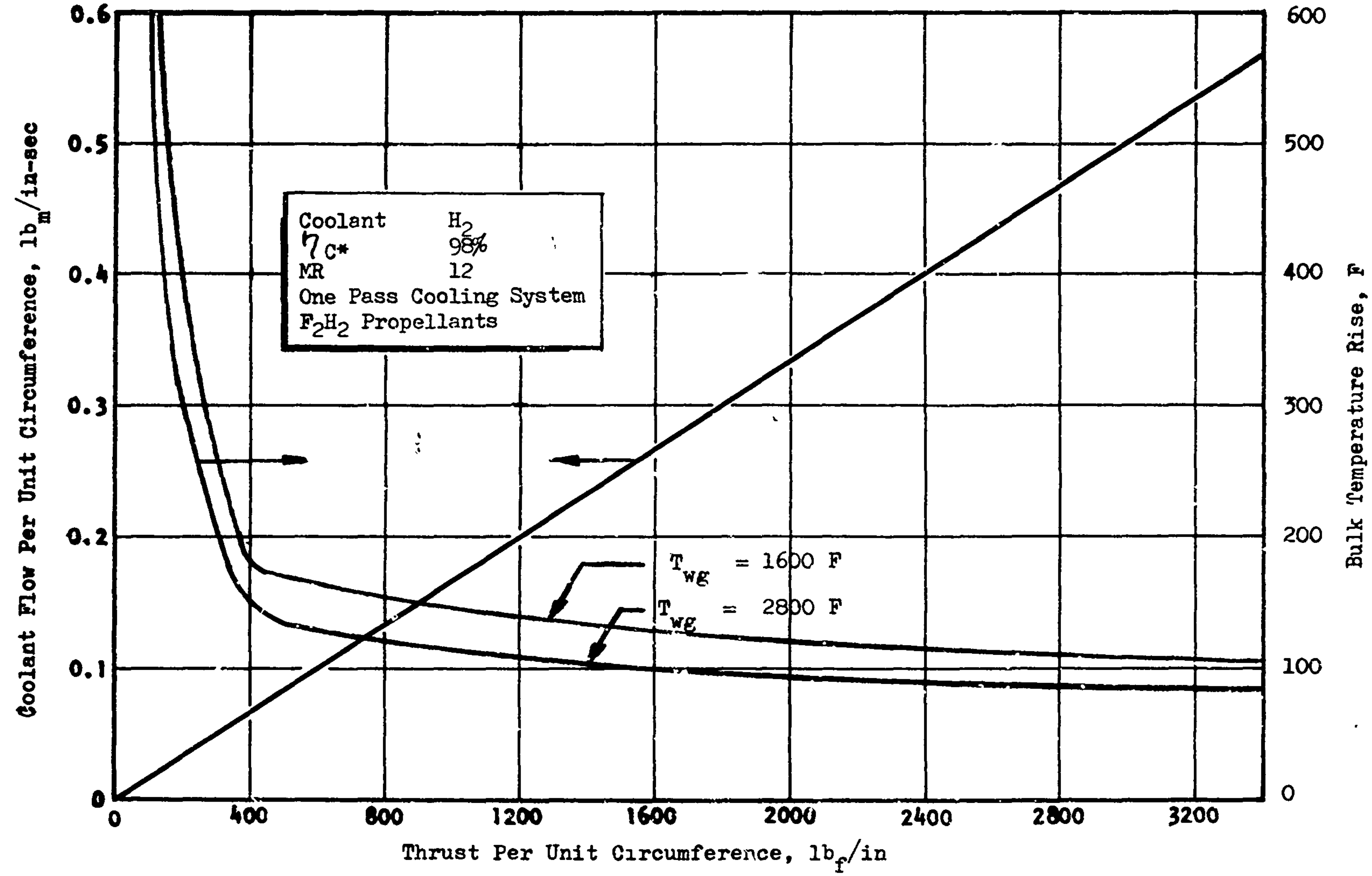

Figure 11. Available Coolant Flowrate for F_2/H_2 and Combustion Chamber Bulk Temperature Rises for Aerospike Configurations. (U)

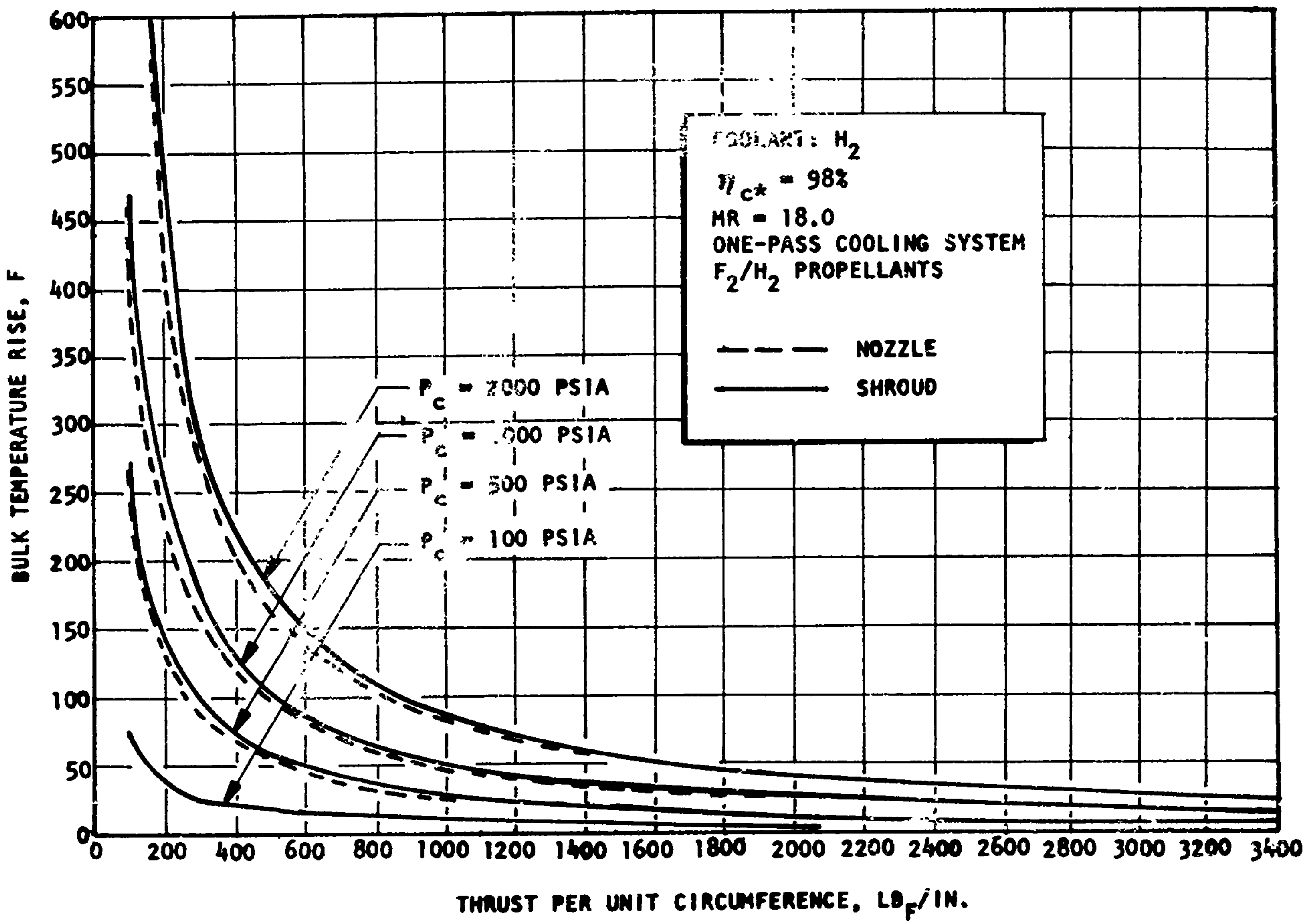

Figure 12. Upper Nozzle and Shroud Coolant Bulk Temperature Rise for Aerospike Configurations (Uncoated) (U)

(U) Determination of the coolant bulk temperatures provides for the computation of the annular throat coolant mass flux at any given chamber pressure. The throat cooling requirement is of particular interest because it is the point of maximum heating and determines the minimum channel width. These calculations were performed with the equations provided by the discussion devoted to cooling considerations. The resulting channel width is plotted in Fig. 13 as a function of the relative availability of coolant, for a variety of wall thicknesses. The number of channels is defined in Fig. 14 for various wall thicknesses of Nickel 200.

(U) Geometric considerations that must be accounted for during a parametric study of aerospike thrust chambers include throat gap, engine area ratio, and combustion chamber contraction ratio. Figure 15 presents throat gap as a function of thrust per inch and Fig. 16 reflects area ratio as a function of throat gap and engine diameter.

(U) Hydrogen does not have any specific coolant bulk temperature limit; however, it is usually restricted to a coolant Mach number of 0.5 to define a reasonable pressure drop limit. A further increase in chamber pressure will demand an increase in coolant mass flux with a rapid drop in density, which will result in excessive coolant pressure drops. The coolant mass flux requirement and allowable mass flux ($M = 0.5$) are both functions of bulk temperature, which implies that the chamber pressure limits are a function of thrust per unit circumference as presented in Fig. 17. The last pass of the cooling system exhibits the highest throat bulk temperature, and the Mach 0.5 limit is reached at that point before any other location in the thrust chamber.

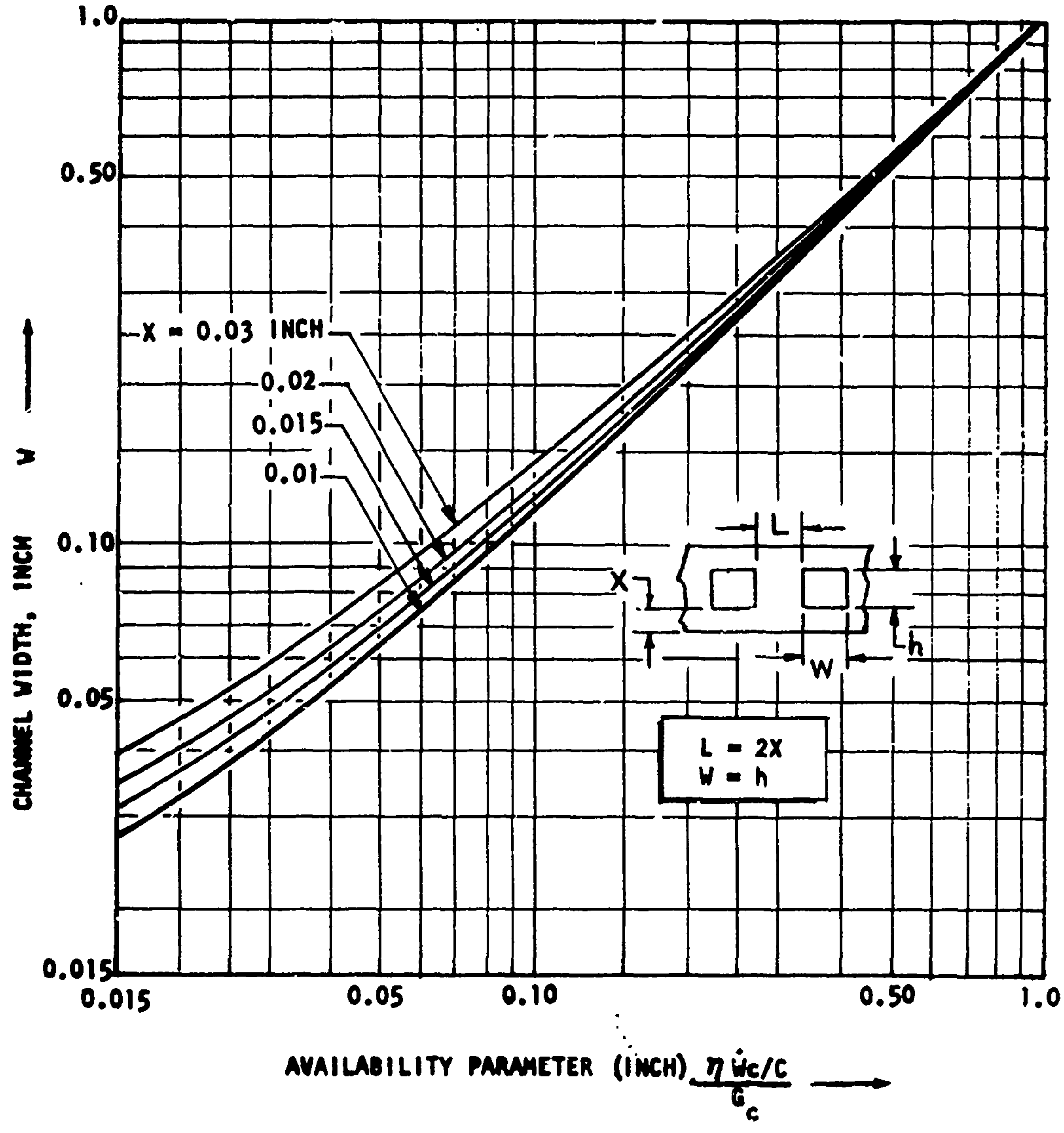

Figure 13 . Cooling Passage Width for Square Channels (U)

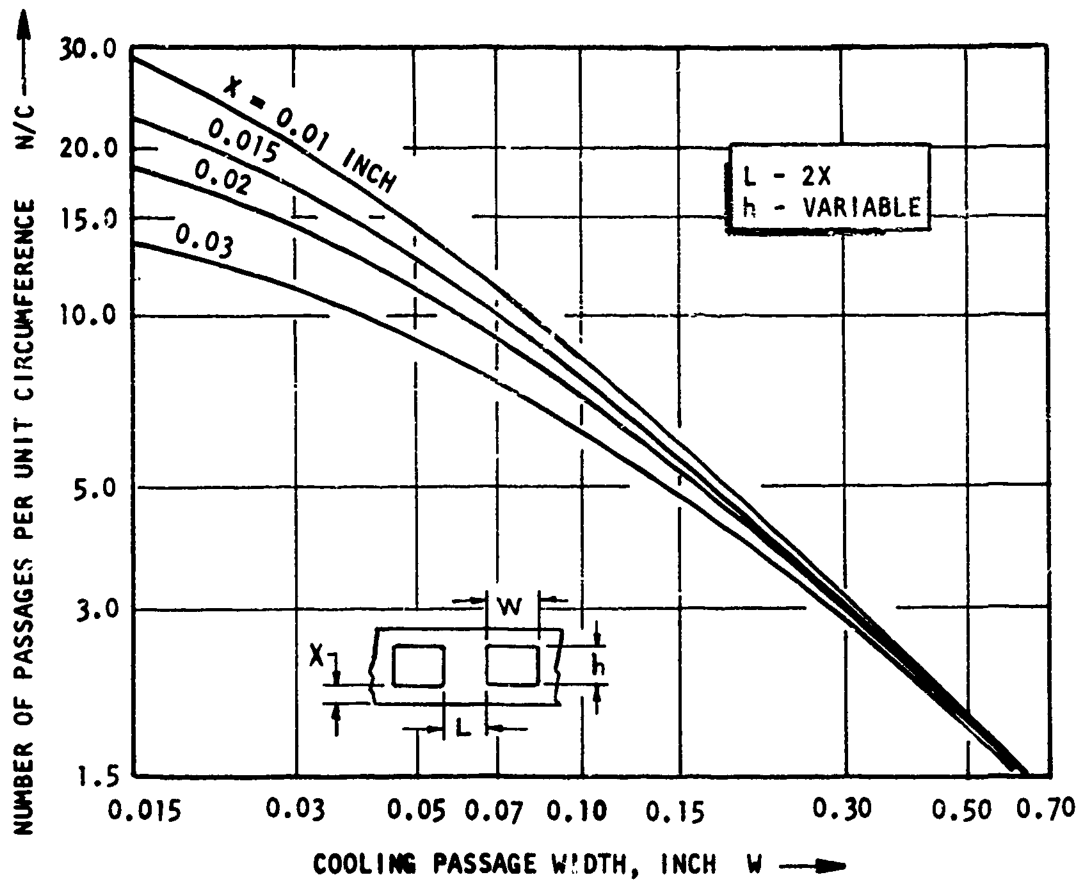

Figure 14. **Number of Cooling Passages as a Function of Channel Width for Typical Wall Thickness** (U)

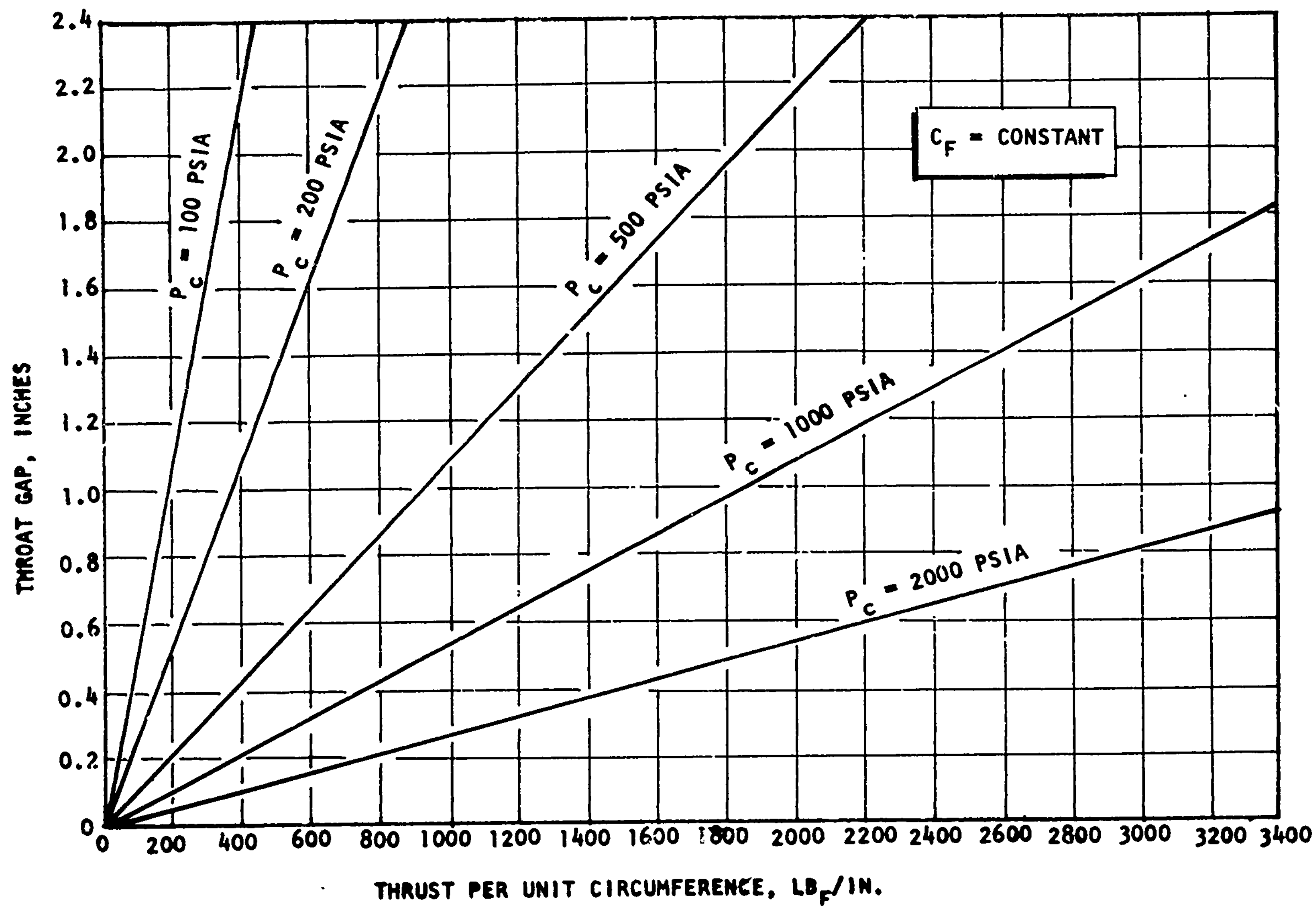

Figure 15. **Throat Gaps for Aerospike Configurations (U)**

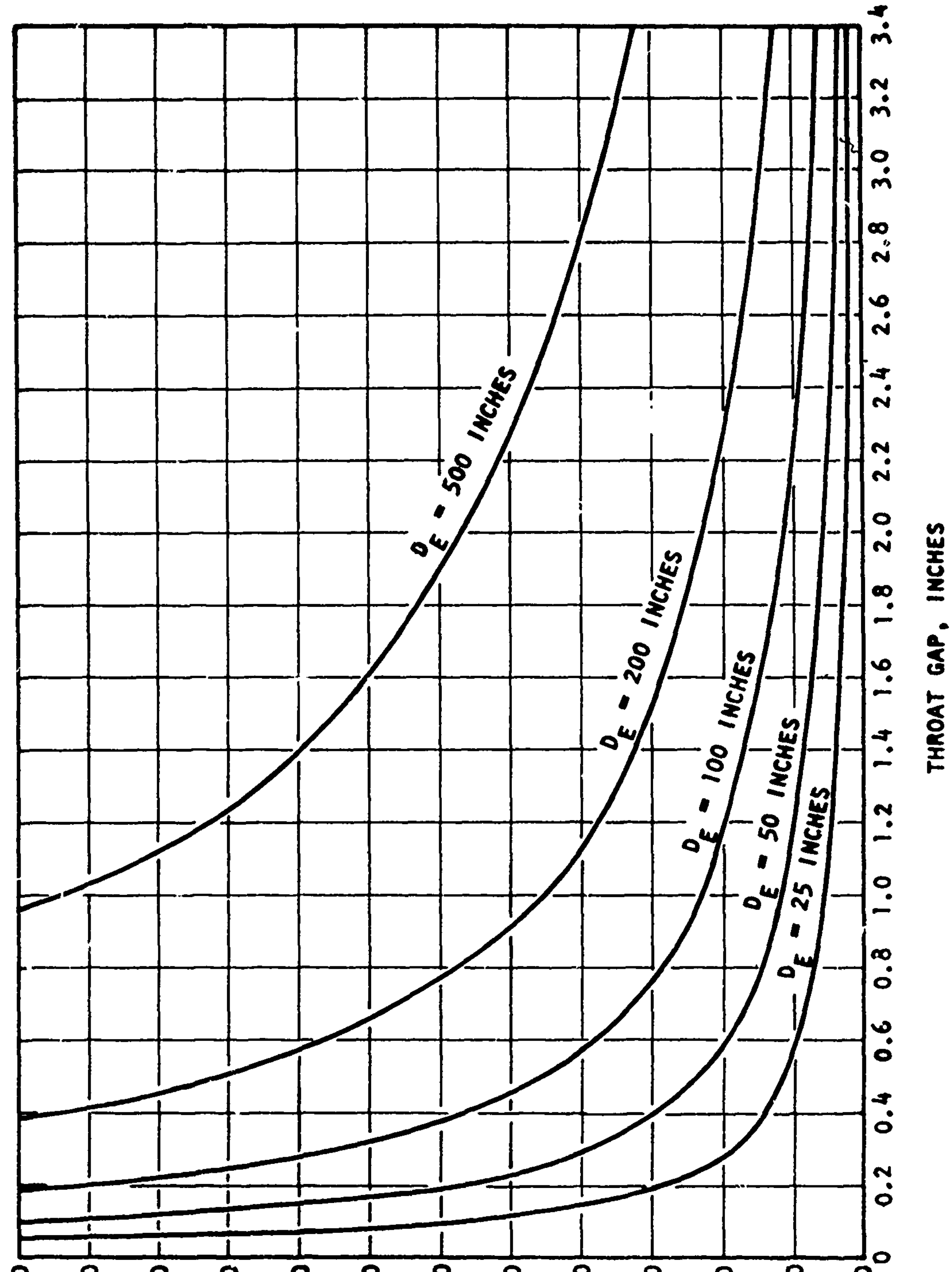

Figure 16 . Engine Area Ratios for Aerospike Configurations (U)

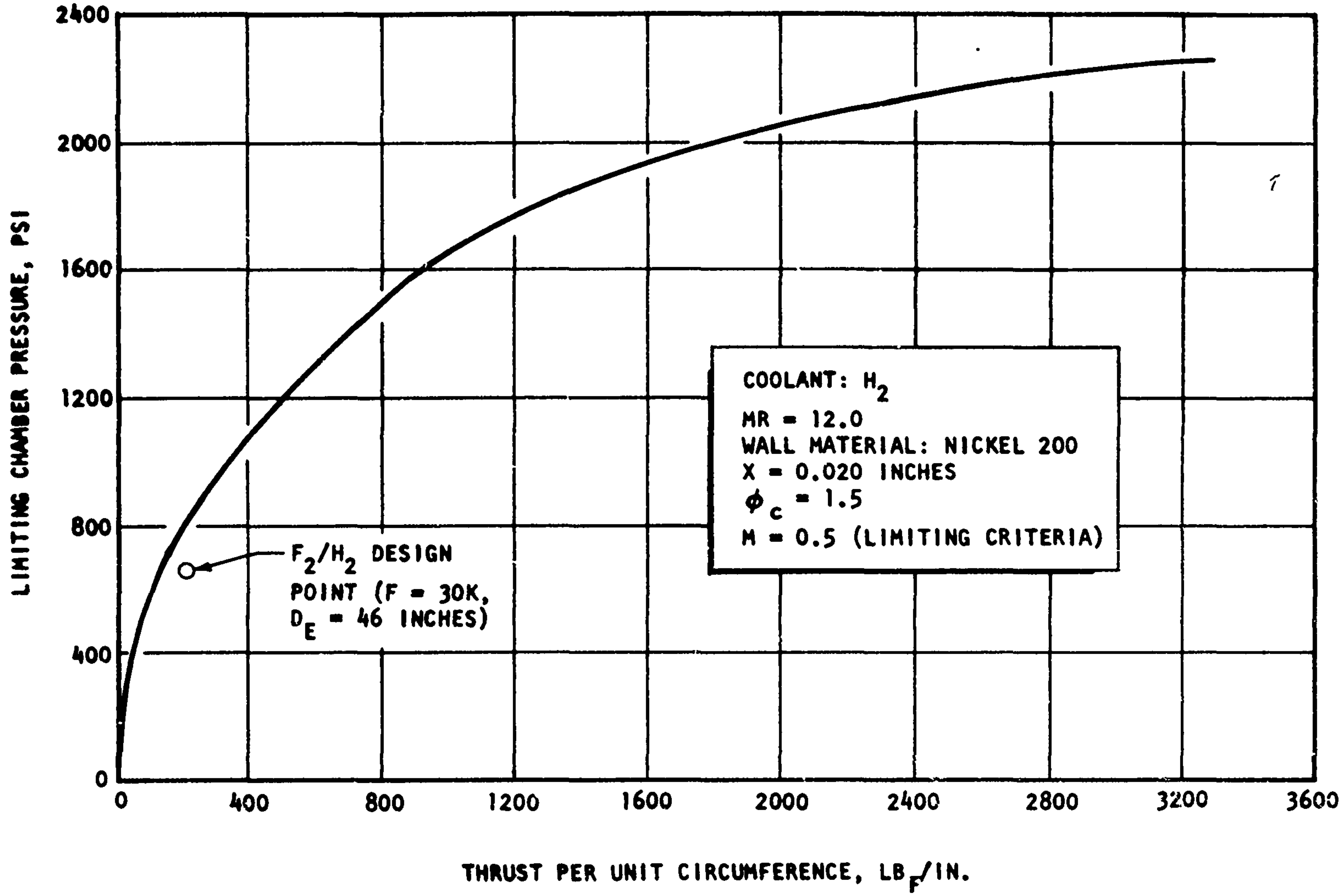

Figure 17. Chamber Pressure Limit for F_2/H_2 Aerospike Configurations (U)

The last pass represents the critical location because the required mass flux is a maximum and the allowable value is near a minimum, as shown previously.

(C) A typical design point was chosen at a relatively low thrust per inch value of 210 lbf/in., and 650 psia chamber pressure with the aid of Fig. 17. The thrust level was selected at 30K and the engine diameter was then fixed at 46 inches, as an example. Additionally, Nickel 200 was considered for the hot gas wall material at a maximum hot gas wall temperature of 1600 F (0.020 thick wall). Substitution of beryllium copper for the nickel would yield similar limits.

(U) Coolant pressure losses are plotted parametrically in Fig. 18 as a function of chamber pressure over a range of thrust per unit circumference. The cooling pressure losses shown are minimum values and are subject to several optimum design conditions. For example, the parametric study does not consider the additional coolant flowrate needed for baffles, which becomes significant at low thrust levels, as mentioned previously. Restrictions on channel depth variations imposed by fabrication limitations are not incorporated in the study, nor are the possible differences in cooling circuit channel geometry that may be dictated by specific system cooling requirements. Inclusion of these features would raise the coolant pressure drop above those predicted here, especially at the lower thrust levels, but it would unnecessarily complicate the parametric study.

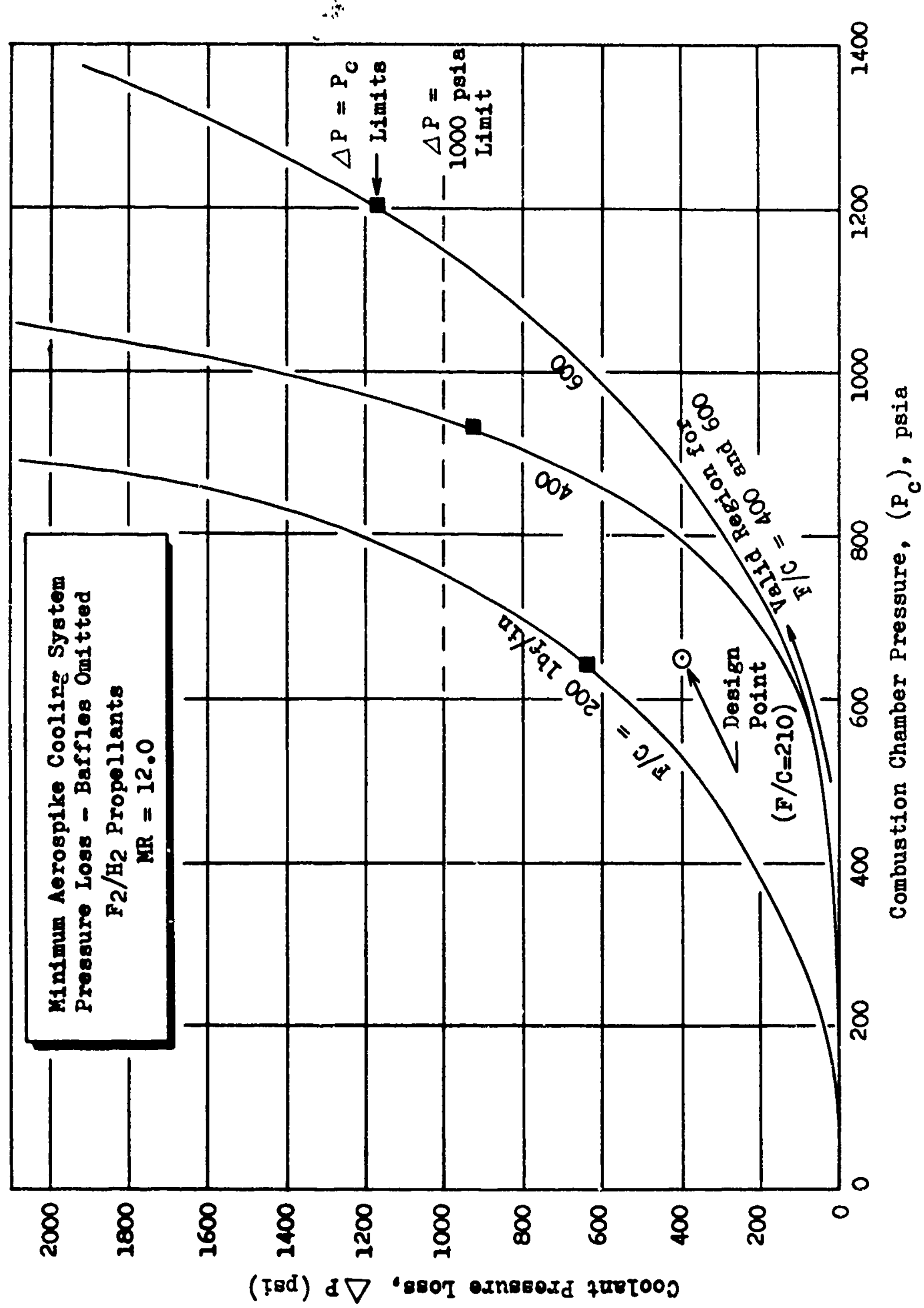

Fig. 18. Minimum Aerospike Cooling System Pressure Loss (U)

(C) It is apparent that the 30K design point is within the maximum pressure drop allotment of being equal to chamber pressure however, a substantial gain in chamber pressure cannot be achieved without substantial increases in pressure losses as shown in Fig. 18. Physically, the coolant is exceeding Mach 0.5 and approaching a choked condition at the throat as the chamber pressure and mass flux are raised. The inlet pressure must be increased to prevent choked flow.

(U) Lower thrust levels may be obtained with the use of several alternatives. Approaches that are evident are to reduce the engine diameter and chamber pressure. The other methods are a heat exchange in a double-layered panel between the F_2 and H_2, a refractory metal, and/or a thermal coating, which are discussed in detail in a later section. These methods help reduce the coolant bulk temperature at the throat location with additional benefits of a reduced heat flux in the cases of a refractory metal and a coating. Lower coolant bulk temperatures and heat fluxes at the throat location result in a lowering of the required hydrogen mass fluxes. It appears to be possible to achieve an aerospike design at the 10K-thrust level with some combination of the alternatives discussed. Increasing the thrust level to 100K or higher results in thermally conservative designs with F_2/H_2 propellants.

(U) N_2H_4 Regenerative Cooling. The parametric study of annular thrust chambers with CPF/N_2H_4 propellants assumed the use of the fuel as the coolant for the thrust chambers and nozzle section to the shroud termination plane. Below this plane the nozzle was considered to be oxidizer cooled.

(U) Hydrazine cooling provides characteristics that are quite different from H_2. The strongest influence of these characteristics on the design of thrust chambers is the limit of 300 to 350 F in coolant bulk temperature that must be placed on N_2H_4 because of its exothermic chemical instability. For this study a single-pass cooling circuit with the inner and outer body in series was selected to minimize the coolant bulk temperature at the throat of the last pass, and still maintain acceptable cooling passage sizes and simplify the physical design.

(U) Available coolant flowrate, and the fuel bulk temperature at the exit of the cooling system (injection temperature) is given in Fig. 19. This bulk temperature is the sum of shroud, combustion chamber, and nozzle coolant bulk temperature rises plus the inlet temperature. These limits indicate the allowable design limits in terms of thrust per unit circumference, and facilitates in the selection of a design point (F = 100K, P_c = 650 psia, D_e = 40 inches).

(U) The other parameter governing the selection of a design point is coolant pressure drop, which is a strong function of chamber pressure. The engine diameter and thrust level were fixed at 40 inches and 100K, respectively, and the coolant pressure loss was calculated for a wide variation in chamber pressure within the coolant bulk temperature limits. The resulting variation in pressure drop is plotted in Fig. 20, where a maximum chamber pressure is chosen for the design condition at 650 psia which was limited by coolant bulk temperature.

(U) Results showed that a thrust level of 100K is approaching the lower limit for the CPF/N_2H_4 Aerospike. Although thrust levels above 100K were not specified as an area to be studied, aerospike designs with CPF/N_2H_4 are particularly attractive at high thrust levels. The beneficial effect of increasing thrust may be observed in the preceding parametric curves.

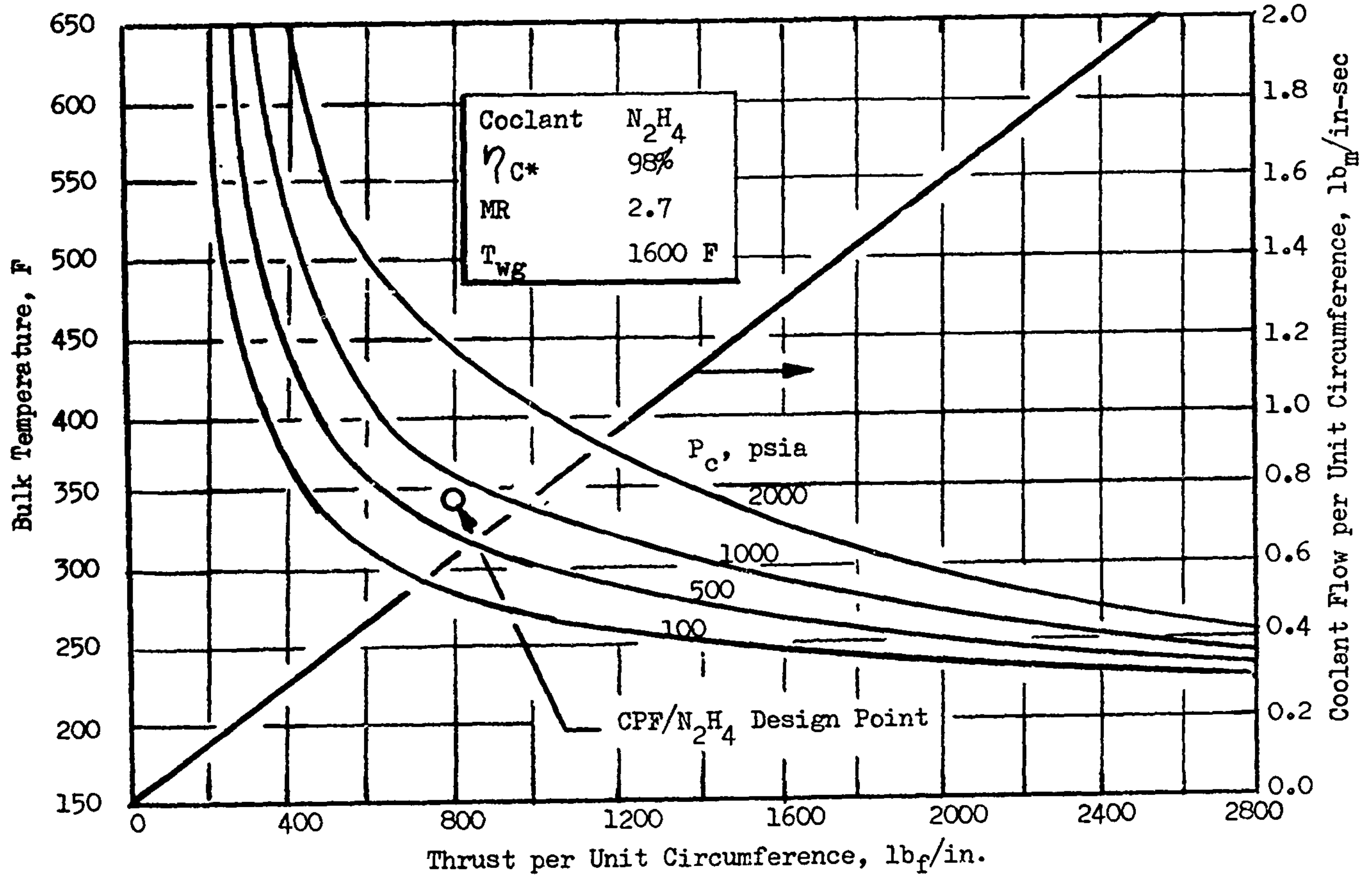

Fig. 19. Available Coolant Flowrate and Outlet Bulk Temperature for CPF/N_2H_4 Aerospike Configurations (U)

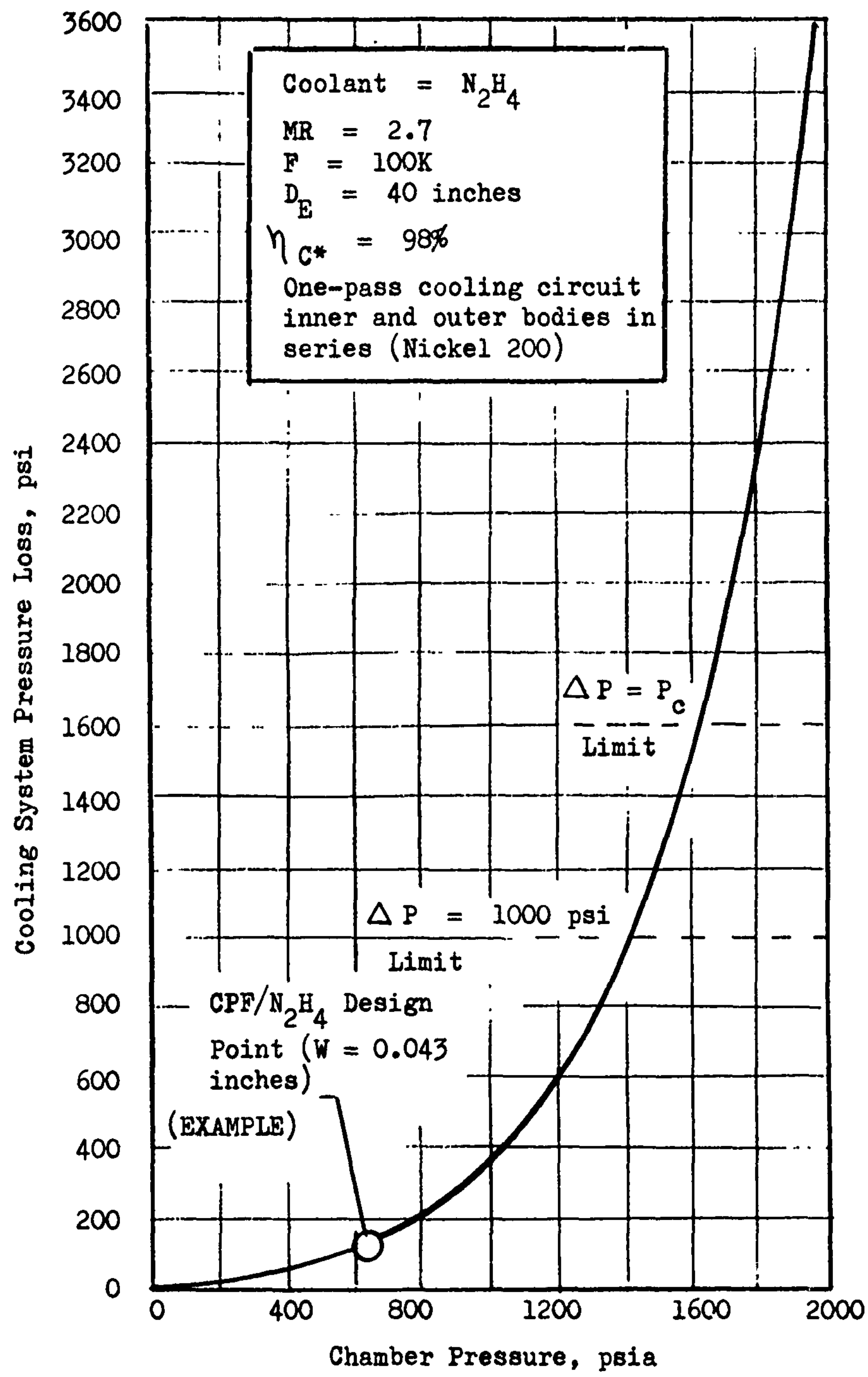

Figure 20. Coolant Pressure Loss for CPF/N_2H_4 Aerospike Design (U)

(U) <u>Oxidizer Heat Exchange Panels</u>. Non-tubular construction provides a convenient technique for using both propellants as coolants. The fuel is the primary coolant with the oxidizer employed in a heat exchange technique through the use of multiple layer of coolant passages (Fig. 21).

(U) Provision of a gaseous oxidizer for injection will allow for a reduction in combustion chamber volume because of a lack of a length requirement for propellant vaporization (assuming the oxidizer vaporization rate limits the combustion process, as is the usual case in a hydrogen-cooled system).

(U) The reduction of adjacent structure temperature in applications where fuel temperatures are high due to a high integrated heat input or high mixture ratio will result in decreased structure thermal stress and possibly reduced backup structure weight. With the heat exchange from the fuel coolant to the oxidizer, a reduced fuel temperature is accomplished at no additional pressure loss to the main fuel coolant. In the case with compressible hydrogen fuel as a regenerative coolant, a reduced coolant temperature will result in a substantially lower pressure drop and an increased margin for gas-side wall temperature. Extension of regenerative cooling limits in thrust chamber configurations where fuel temperature is relatively high can be obtained as a result of the added heat sink capacity provided by the oxidizer.

(U) Heat exchange to the oxidizer section is limited by the thermal resistance for three respective controlling influences: (1) Fuel side convection resistance, (2) Wall conduction thermal resistance and (3) Oxidizer side convection resistance.

(U) A heat flux balance from the heated fuel (T_f) temperature to the colder oxidizer temperature (T_o) may be expressed at any point along the passage length as

$$q/A_s = \frac{T_f - T_o}{\frac{1}{h_f} + \frac{x}{K_W} + \frac{1}{h_o}}$$

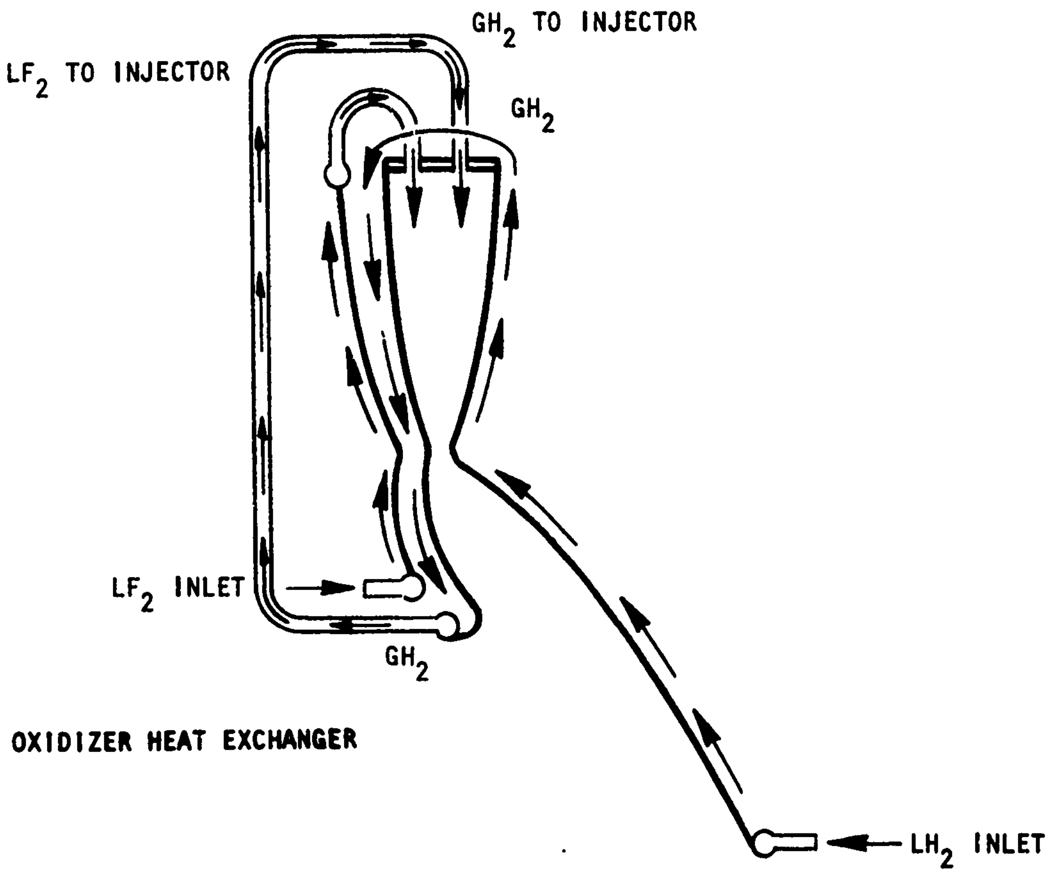

(B) OXIDIZER HEAT EXCHANGER

Figure 21. Flow Schematic for Oxidizer Heat Exchange Concept. (U)

with an effective conductance h' expressed as

$$h' = \frac{1}{\frac{1}{h_f} + \frac{x}{K_W} + \frac{1}{h_o}}$$

(U) Consideration of a controlling conductance on the oxidizer side results in the relationship

$$\frac{h'}{h_o} = \frac{1}{\frac{h_o}{h_f} + \frac{h_o x}{K_w} + 1} = \frac{1}{\frac{h_o}{h_f} + N_{Bi_o} + 1}$$

(U) Variations of fuel film coefficient and improved wall conduction will result in a reduced thermal resistance. Design configurations analyzed for backup panels with cryogenic oxidizers result typically in

$$\frac{h_o}{h_f} \cong 0.4$$

$$N_{Bi_o} \cong 0.3$$

(U) As a result, the effective overall heat transfer coefficient enthalpy absorbed by the relationship

$$\frac{\dot{W}_o \quad H_o}{A_s} = \frac{h_o \, (T_f - T_o)}{\frac{h_o}{h_f} + N_{Bi_c} + 1}$$

(U) Relating the oxidizer Stanton number to the flow mass velocity,

$$h_o = G_o C_{p_o} N_{ST_o} = \frac{\dot{w}_o}{A_o} C_{p_o} N_{ST_o}$$

(U) The solution of the above relationships yields the surface area to flow cross-sectional area in terms of the enthalpy ratio:

$$\frac{A_s}{A_c} = \frac{\frac{h_o}{h_f} + N_{Bi_o} + 1}{N_{ST_o}} \left[\frac{\Delta H_o}{H_f - H_o}\right]$$

(C) For nickel coolant passages with moderately low oxidizer transfer heat fluxes ($Q/A \sim 5.0$ Btu/in.^{2}-sec) the finned surfaces can be assumed to enhance the effective surface area for conduction. For the limiting case with high conduction $A_s/A_c = (4 \ \ell/d)$, a simplified expression for the controlling passage length to diameter becomes

$$\ell/d = \frac{\frac{h_o}{h_f} + N_{Bi_o} + 1}{f \, N_{ST_o}} \left[\frac{\Delta H_o}{H_f - H_o}\right]$$

(C) The passage length to diameter requirement is related to the enthalpy increase required by the oxidizer and the enthalpy difference between the high and low temperature fuel and oxidizer conditions respectively. Heat exchange backup panel ℓ/d values are shown in Fig. 22 for the F_2/H_2 design range. Coolant passage ℓ/d to achieve complete vaporization of the F_2 are shown to be in the range of 60 to 80. Verification of this criteria was accomplished during experimental oxygen and fluorine cooling study.

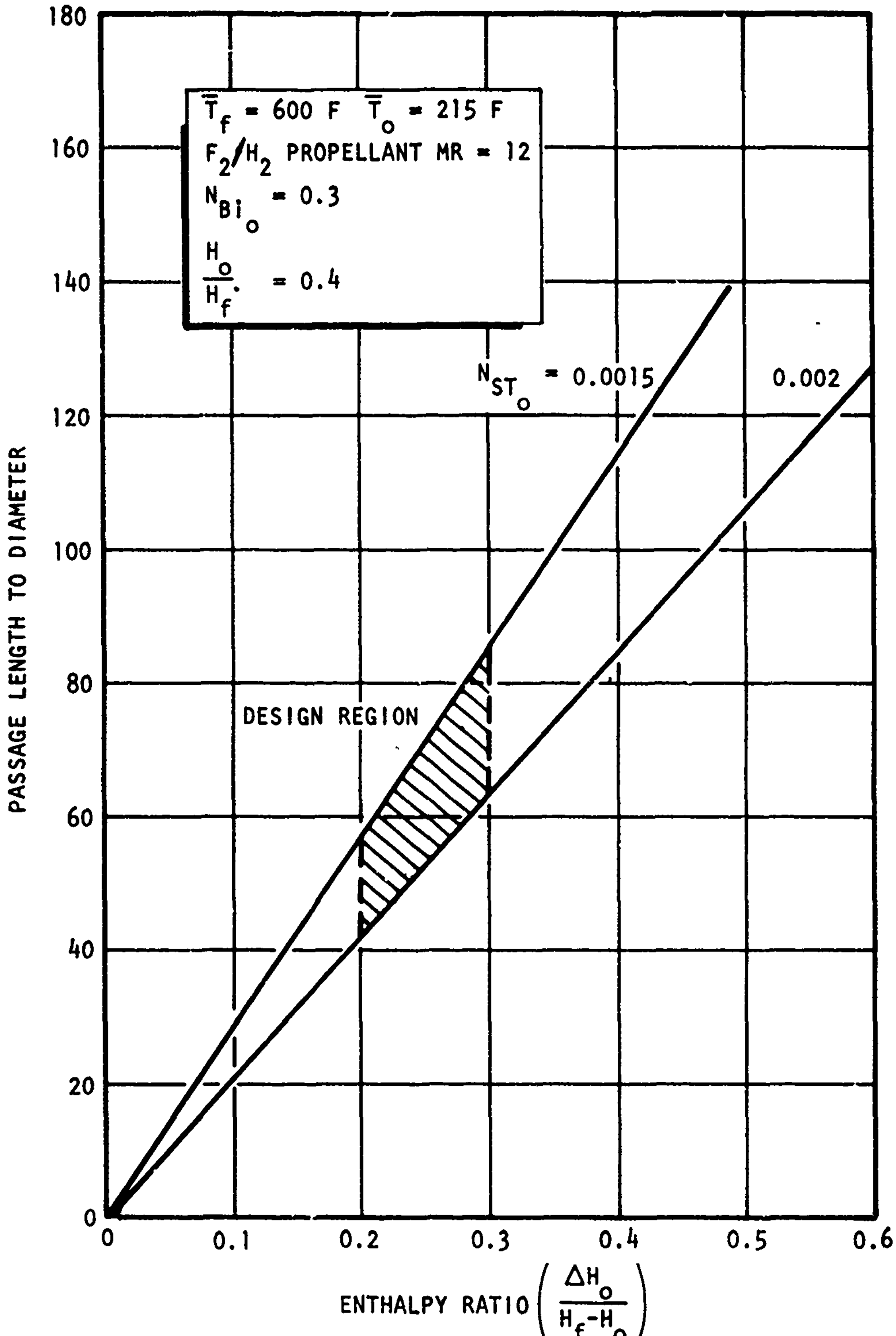

Figure 22. Backup Panel Cooling Channel ℓ/d vs Enthalpy Ratio (U)

(U) Selected combustion zone fluorine-cooled heat exchange panel materials for both annular and bell chambers include nickel, copper (alloys), and aluminum because of the relatively high heat transfer rates, low temperature differences involved, and ease of manufacture.

(C) To illustrate the potential advantage of the multiple panel heat exchange concept the following example was evaluated:

Engine Configuration	Aerospike
Propellants	F_2/H_2
Mixture Ratio	12:1
Thrust Level, pounds	30,000
Chamber Pressure, psia	650
Engine Diameter (throat centerline, inches)	45.7
Area Ratio	60:1

(C) The heat exchange panel concept was compared to a tube wall design at the above operating conditions. It was determined that the heat exchange panel concept utilizing the oxidizer to reduce the heat load on the fuel benefits the original design in three ways (although not all benefits are necessarily achieved simultaneously): (1) Reduce fuel coolant pressure drop, (2) Increase allowable chamber pressure, and (3) Fuel cooling circuit simplification.

(C) Substituting the double panel concept directly for the tube wall design (i.e., same fuel cooling circuit) reduced the required fuel coolant manifold inlet pressure approximately 15 percent. If the fuel inlet pressure were maintained at the current value, the chamber pressure could be increased to about 850 psia resulting in a substantial increase in performance.

(C) The double-panel allows greater flexibility in selecting the cooling circuit since the total heat load to the hydrogen is reduced. In the tube design it is necessary to cool the nozzle portion of the chamber last to minimize the hydrogen temperature in the throat region. This requires numerous fuel lines to and from the nozzle with resulting fuel pressure losses and increased weight. The double-panel approach would allow simplification of the fuel circuit in that the nozzle does not have to be cooled last. One attractive fuel cooling circuit configuration (Fig. 21) would be to introduce the fuel into the coolant circuit at the nozzle exit plane, single uppass cool the nozzle and inner body and then double pass the outer body, ending up at the injector inlet manifold. An oxidizer heat exchange panel would be incorporated on the outer body. This would eliminate many of the fuel lines now required in the tube wall design. A fuel pressure drop savings of 150-200 psi would also be realized.

dimensional thermal analyses of the critical regions of the various designs were performed to assure that wall temperatures were not excessive. A typical isotherm plot is shown in Fig. 23 for the cooling circuit discussed previously. This plot represents conditions at the throat of the last pass in the outer body. The peak temperature of the beryllium copper fuel channels is 1194 F. The use of nickel for the oxidizer panel results in back wall temperatures less than 200 F.

(U) Coating Material Thermal Resistance. The coating resistance effects accomplished by the elevation of the coating surface temperature toward the adiabatic wall temperature value have been analyzed. Figure 24 illustrates typical selected Al_2O_3 and ZrO_2 coating temperature drop values vs wall thickness. Composite gradated mixtures of Inconel or tungsten with zirconia are shown to improve the thermal conduction of

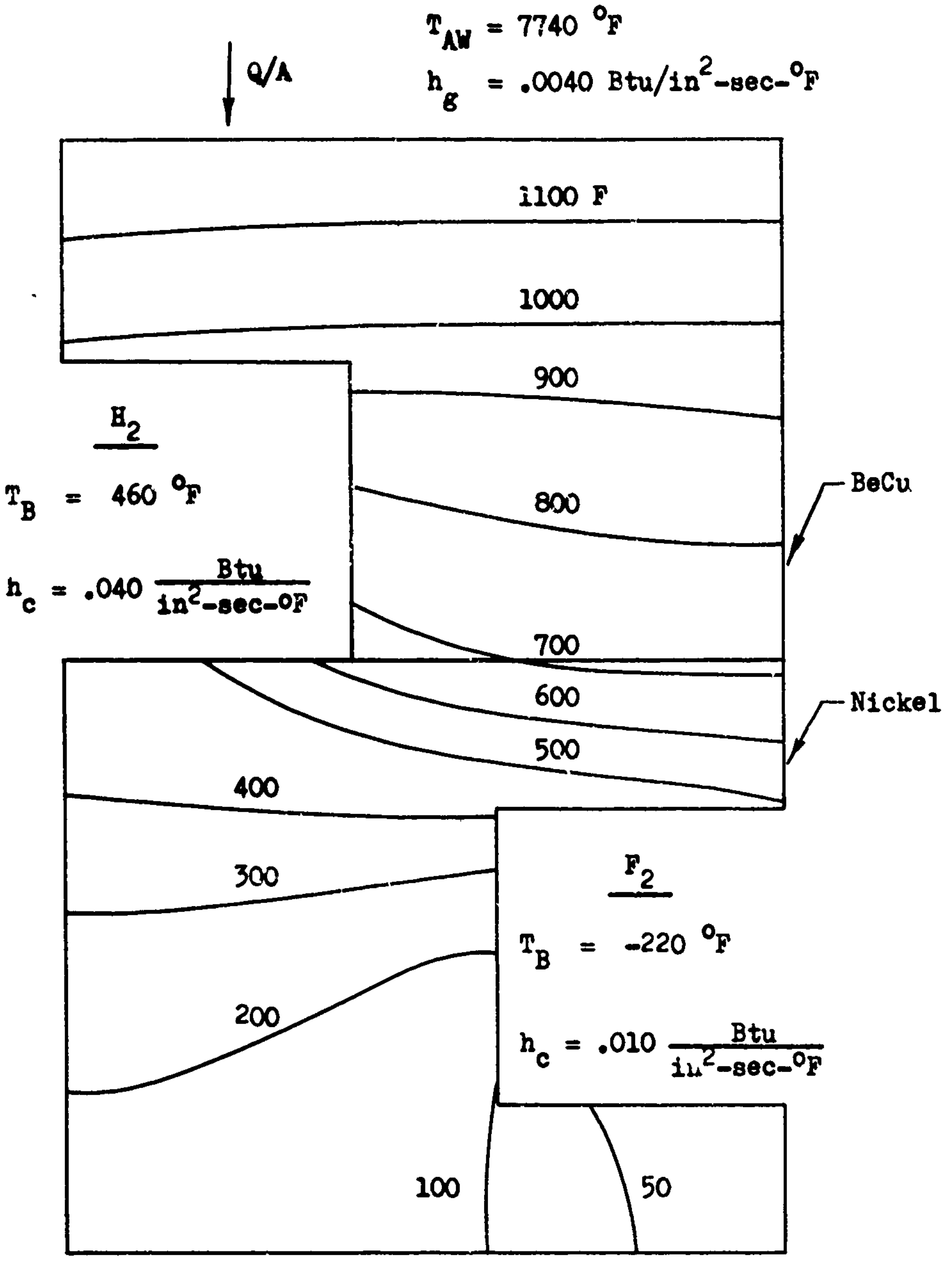

Fig. 23. Typical Isotherm Profiles in a F_2/H_2 Double Panel Cooling Design (U)

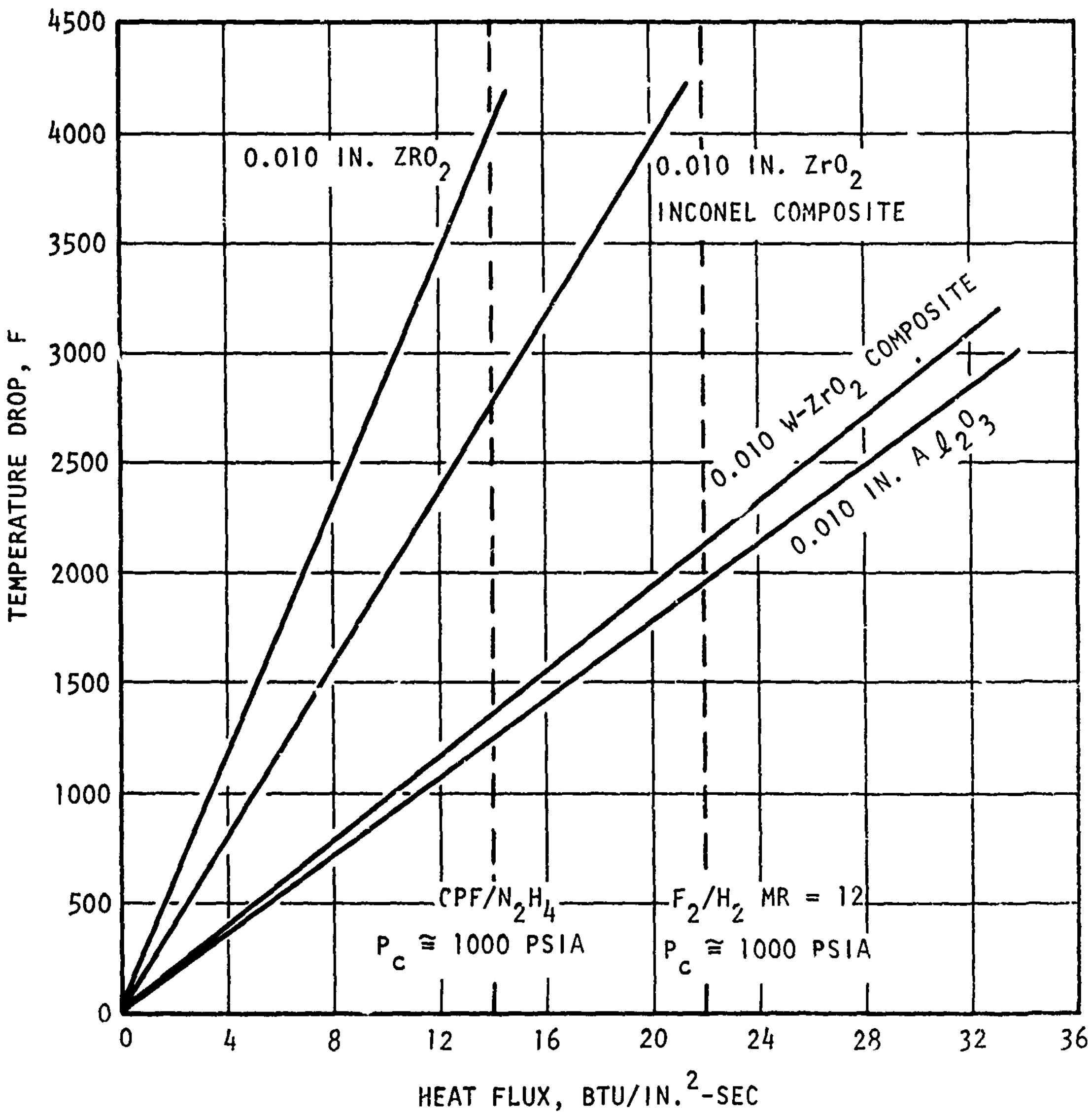

Figure 24. Coating Temperature Drop vs Heat Flux (U)

the coating layer so that a greater coating thickness is required for reduction to a given heat flux level. Composite coating thickness requirements at the throat for a 1000 psia chamber pressure level are shown to range from 0.010 to 0.015 inch dependent upon the acceptable wall temperature. Proportional reductions in the combustion zone and nozzle are accomplished with a coating thickness directly proportional to the area ratio. Acceptance of thermal coating benefits for reductions in high heat flux region wall temperatures appear beneficial to life and thermal fatigue capability. Designs, however, should allow for local spalling of the coating material without failure of the coolant passage.

Parametric Stress Analysis

(U) As a part of the Phase I - Task 1 Parametric Design and Limits Study, a parametric stress analysis was completed to establish the structural limits and requirements of coolant channels and external structure. A detailed description of the analytical technique was given in Ref. 1.

(U) Hot Gas Wall Analysis. The parametric pressure strength analysis of the hot gas wall included rectangular and U-shaped coolant channel geometries (Fig. 25).

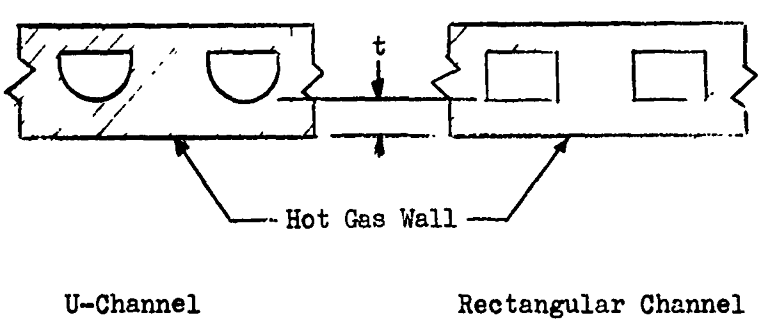

Figure 25. Coolant Channel Geometries (U)

(U) For each, the proportions of the hot wall can be described in terms of the channel width to wall thickness (a/t) ratio, and the pressure strength of the hot wall is ideally the same for any combination of a/t ratio and material strength. It then follows that the pressure capabilities of these two geometries may be parametrically presented for any given material in terms of the a/t ratio and material temperature conditions. Thus, the results of the analysis were plotted as the maximum wall pressure differential which may be safely sustained, versus the wall a/t ratio, for selected wall temperature conditions as established by the heat transfer study.

(U) Pressure Strength Analytical Philosophy and Safety Factor. The prediction of the maximum safe operating pressure for a channel wall resolves into an analysis of the limit bending or limit shear strength of the wall, and applying a suitable design safety factor to determine the maximum safe operating pressure. The theory of limit design was used to determine the limit bending strength. This is different from the elastic theory ordinarily used in structural analysis, in that limit design theory presupposes ductile or semi-ductile stress distribution. In it, the emphasis is shifted from permissible stresses to permissible deformations. Larger safety factors than those applied to elastic strength predictions are therefore desirable.

(U) In this study, a design safety factor of two was used for all cases. This factor was applied to the wall pressure differential. A pressure of over twice that indicated in the figures will thus bring the hot wall to a condition of gross distortion, with the wall permanently deformed. The cooling characteristics of the wall could be affected by such deformation, resulting in higher wall temperatures. A progressive failure mechanism could thus be initiated leading to the eventual rupture of the wall.

(U) Mechanical Restraint and Bending Strength. The analysis of the limit bending strength of the channel wall is complicated by thermo-plastic strains which act in combination with the bending strains. These thermo-plastic strains are normally compressive, and are the result of restraint against thermal expansion of the heated wall. They cause no reduction in the limit bending strength of the wall. It is possible, however, to design a thrust chamber with a high degree of elastic deflection in the hoop direction, and thus greatly reduce the mechanical restraint. The pressure strength of such a partially restrained wall is considerably reduced, because of tensile loads which develop in the heated wall in combination with the bending stresses.

(U) As a practical matter, most thrust chamber designs have sufficient mechanical restraint to justify the use of the limit bending strength analytical model. This study was therefore based on the assumption of a biaxially restrained hot wall for all cases.

(U) Parametric Analysis. The parametric structural limits, curves of the rectangular and U-channels, are shown in Figs. 26, 27, and 28 for a number of candidate materials.

(U) Coolant Channel Closeout and Backup Structure Analysis. Coolant Channel Closeout thicknesses for bell and annular chambers plus jacket hoop reinforcement thicknesses of the combustor sections of bell chambers were also analyzed for several typical cases: (1) Electroformed nickel and sintered nickel closeout and backup structure, (2) Inconel 718 closeout and backup structure, (3) Inconel 718 backup structure, and (4) Cast Aluminum (Tens-50) backup structure.

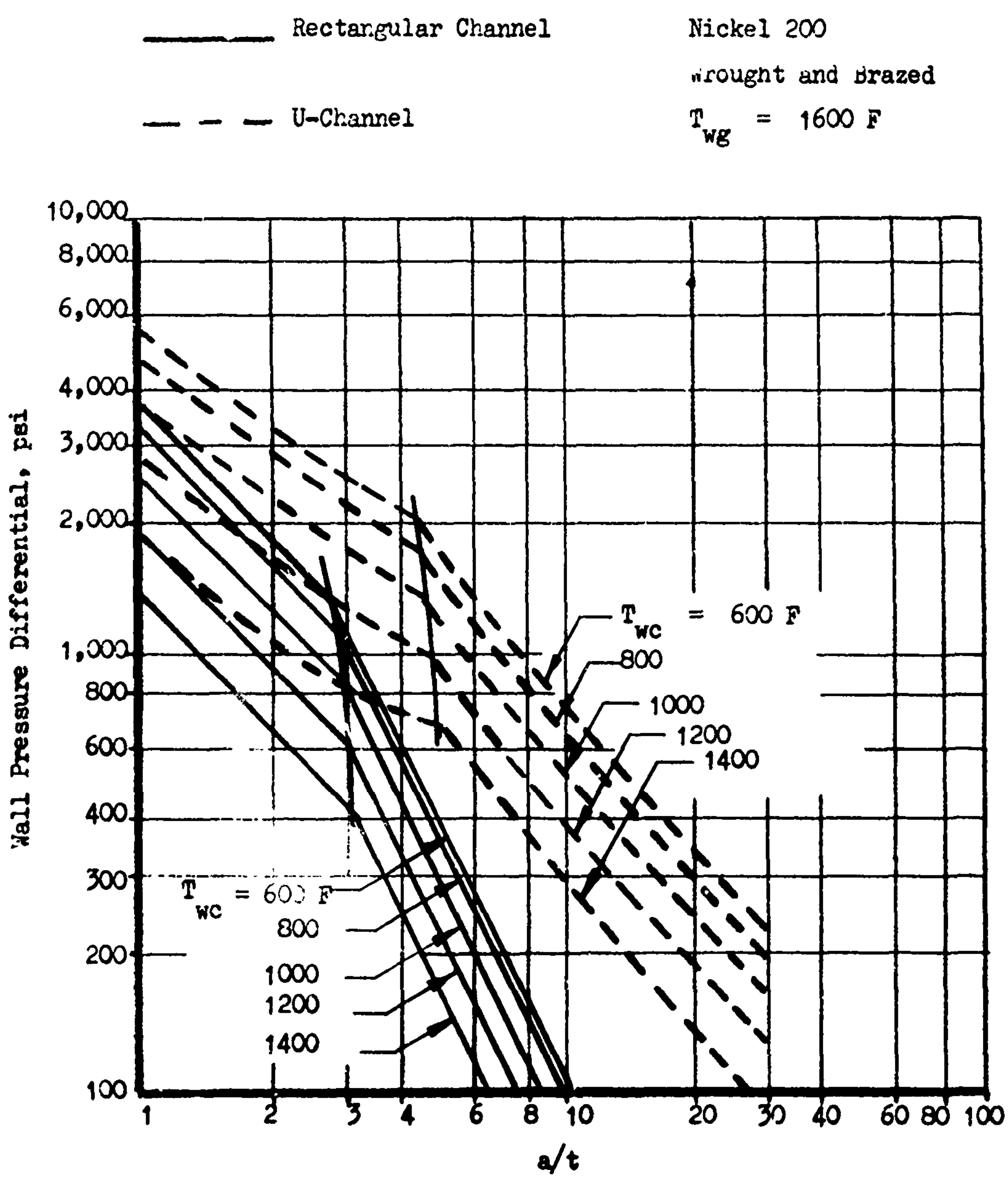

Figure 26. Structural Limits for Nickel 200 Channel Walls (U)

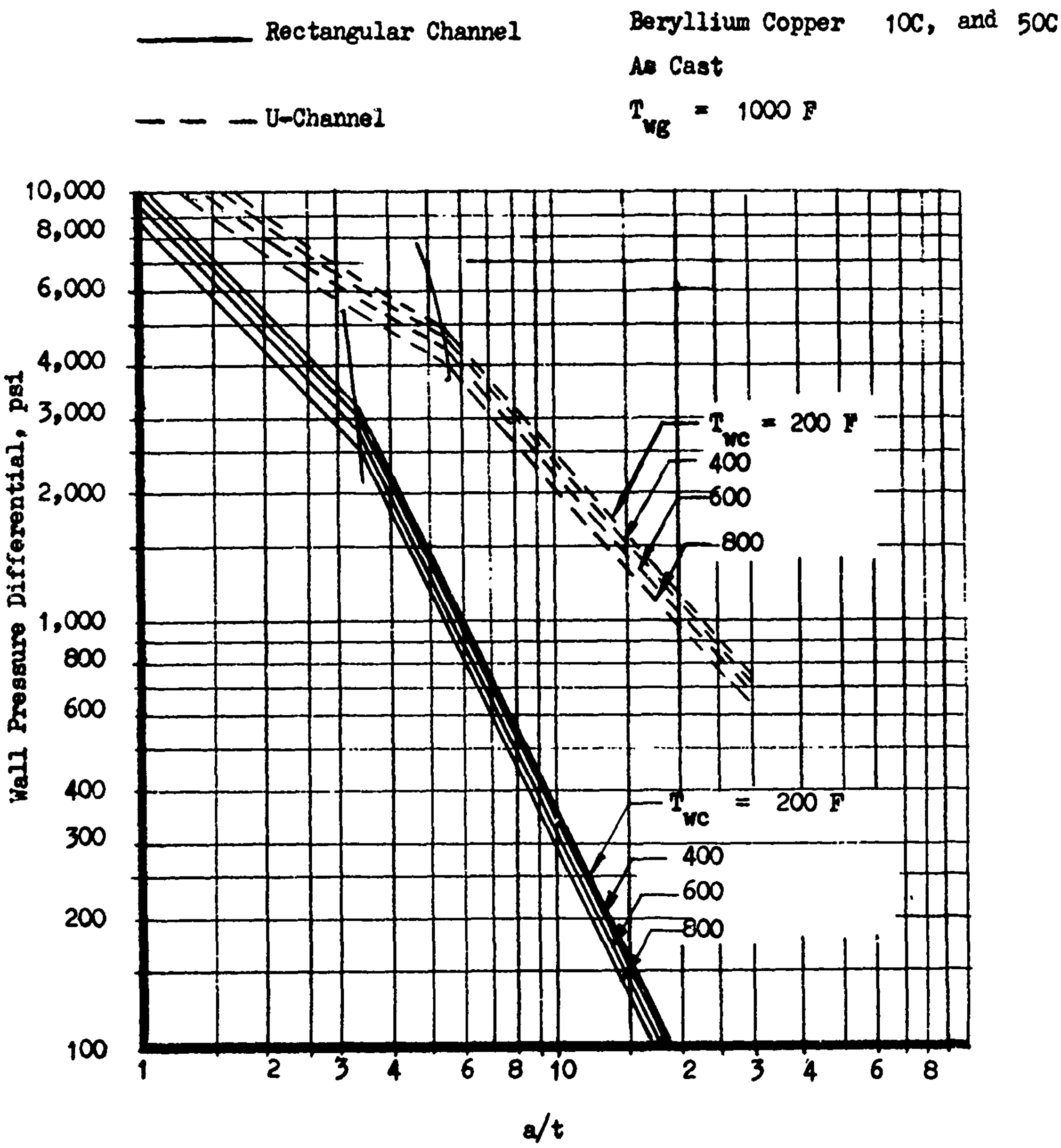

Figure 27. Structural Limits for Beryllium Copper 10C, and 50C Channel Walls (U)

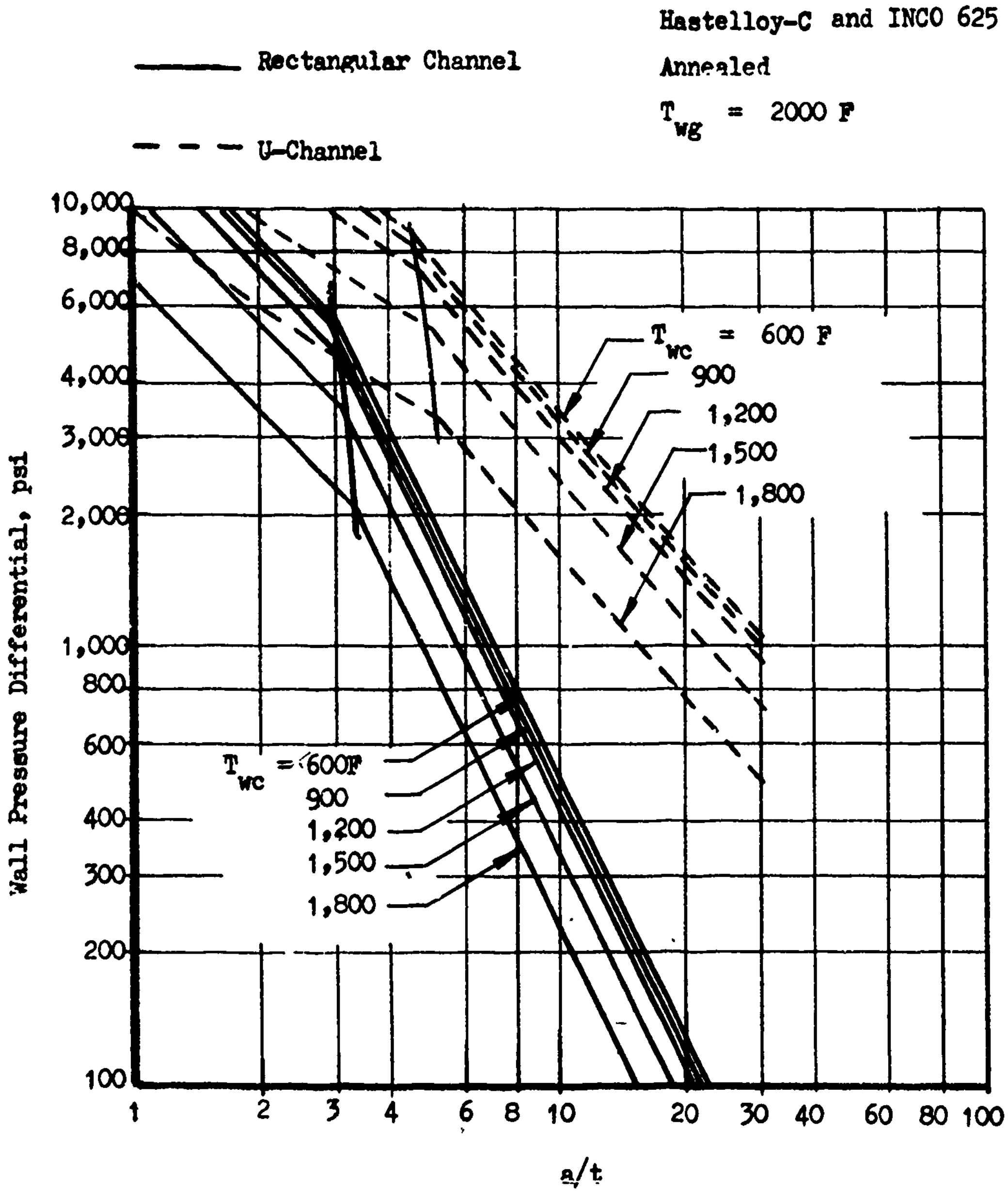

Figure 28. Structural Limits for Hastelloy-C and Inco 625 (U)

(U) The results are shown in Fig. 29. In those cases that considered electroformed nickel as a closeout only, the thickness of the electroformed nickel layer was sized to resist a room temperature proof pressure test (120 percent of nominal channel operating pressure) prior to addition of the backup structure. Additionally, a minimum thickness of 0.020 inches was established for this closeout.

(U) The coolant channel closeout and backup structure thicknesses were assumed to be the same for cast beryllium copper, sintered nickel and electroformed nickel hot gas walls and coolant channel lands since the yield strengths are essentially the same.

TASK II - MATERIALS STUDY

(U) The objective of Task II was to obtain material physical, mechanical and compatibility data and to assess the state of the art of the candidate fabrication techniques to be considered in the Task III study.

(U) Data for this study was obtained from a literature survey and numerous industrial surveys. Contributors include: Battelle Memorial Institute of Columbus, Ohio (through subcontract effort on this program); Camin Laboratories of Brooklyn, New York (through a 5-year exclusive licensing agreement that Rocketdyne has with Camin); from the Los Angeles, Columbus and El Toro divisions of North American Rockwell Corporation and numerous specialty vendors with extensive experience using such fabrication techniques as forging, casting, spinning, chem milling and explosive bonding.

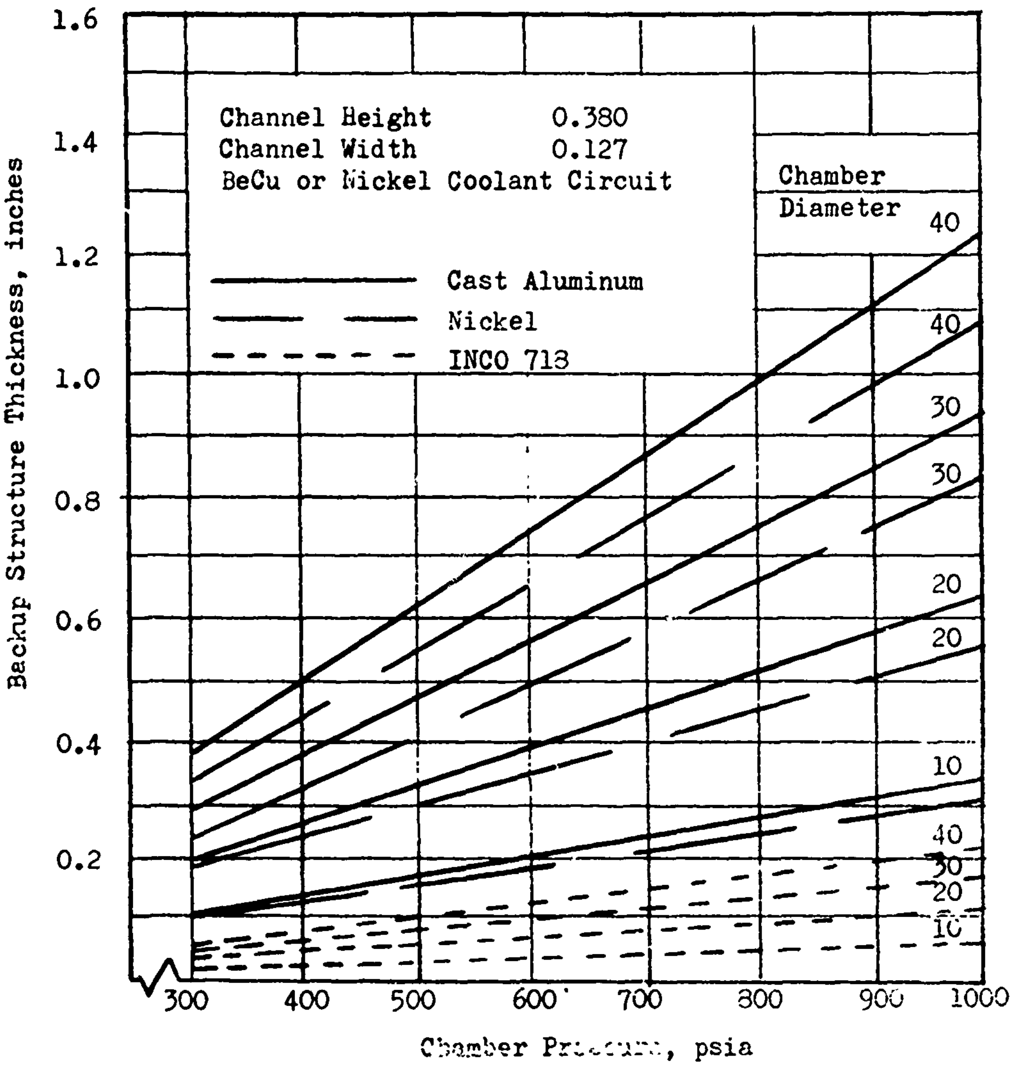

Figure 29. Minimum Thickness Requirements of Cast Aluminum, Inconel 718 and Nickel (Electroformed or Sintered) Backup Structure for Bell Chambers (U)

Selected Materials

(U) As a result of concurrent studies performed under Tasks I and III in Phase I, the number of materials of interest, for both coolant circuit use and for backup structure use were narrowed to a selected few. The selected materials are listed below.

Coolant Circuit.

(U) Nickel: wrought, electroformed, and sintered (powder metal)
Beryllium Copper: wrought and cast
Hastelloy C alloy
Inco 625 alloy
Unalloyed tungsten

Structure.

(U) Inconel 718 alloy
Cast aluminum (Tens-50)

(U) Yield strength data for these materials are shown in Fig. 30.

Material Compatibility

(U) A review was made of the compatibility of the candidate materials with H_2, F_2, CPF and N_2H_4 + 10% EDA and the combustion products of the propellant combinations H_2/F_2 and CPF/N_2H_4 + 10% EDA. The results of the review and information survey is reflected in Table I for the previously selected materials plus others of possible use. In several cases the material has not been physically evaluated with the specific propellant

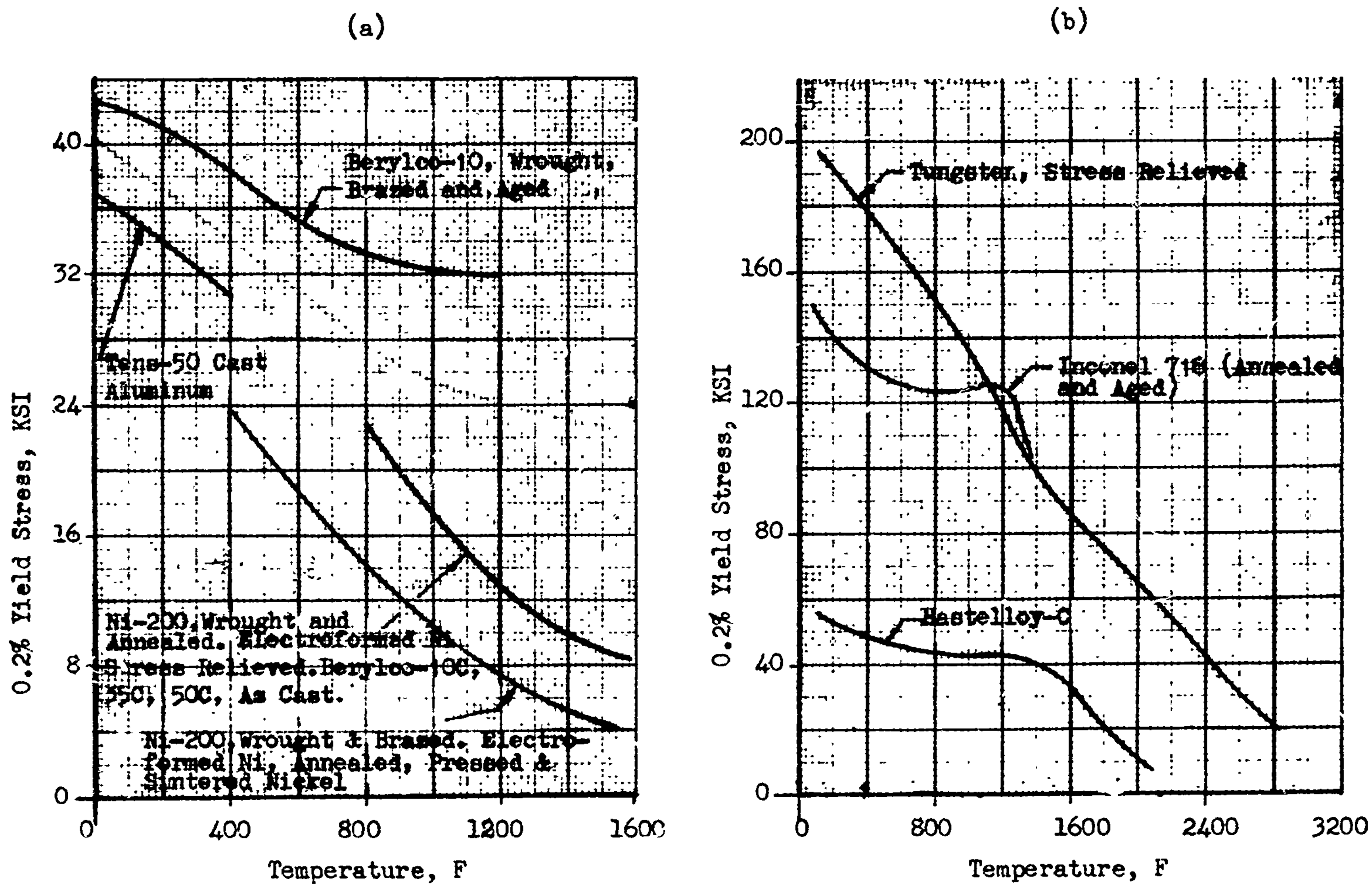

Figure 30. Material Yield Strength at Elevated Temperatures (U)

TABLE I

SUMMARY OF COMPATIBLE CANDIDATE COOLANT CIRCUIT MATERIALS (U)

Environment / Material	Nickel 200 & Electroformed Nickel	BeCu-10, -10C and -50C	Hastelloy-X & C INCO 625	Tungsten	W-Zr_2O_3 Gradated Coating	Inconel Zr_2O_3 Coating
H_2	S	S	S	S	NA	NA
F_2	S	TBD	S	TBD	NA	NA
H_2/F_2 Combustion Products	S	S	S	S	S	S
N_2H_4 + 10% EDA	(S)	U	(S)	S	NA	NA
CPF	S	S	S	TBD	NA	NA
CPF/N_2H_4 Combustion Products	S	S	S	(S)	(S)	(S)

CODE:

S - This rating implies that the material (1) has a low rate of corrosion, (2) does not react with the environment rapidly, and (3) does not act as a catalyst toward the environment, within the projected life and operating conditions of the chamber system. It does not imply, however, that the material is completely unaffected and resistant to change in the environment or that some protection may not be required.

U - This rating implies that the literature has indicated a serious problem in one of the aspects discussed above and that the material should not be considered for use.

TBD - Available data is inconclusive and compatibility must be explored should the materials be employed in any advanced fabrication concept.

NA - Not applicable.

( ) - Predicted from the reaction with similar materials.

or in the products of combustion and the compatibility had to be predicted on the basis of free energy relationships and/or the reaction of similar materials in the same or similar environments.

Fabrication Methods

(U) Basic fabrication methods which were reviewed in the construction of non-tubular, regeneratively cooled thrust chambers included the following:

Electroforming	Forging
Spinning	Machining
Explosive forming	Hot Isostatic pressing*
Casting	Powder Metallurgy

(U) In addition, the following joining processes were investigated:

Electroforming	Solid state diffusion bonding:
Welding	Creep deformation bonding
Brazing	Gas pressure bonding*
Liquid interface diffusion bonding	Thermovac bonding*
Hot isostatic pressing*	Explosive bonding*

(U) A brief description of each fabrication method as related to this program is presented in the following paragraphs. A detailed discussion of each method was presented in Ref. 1.

* Inputs from Battelle Memorial Institute

(U) Electroforming. A process of controlled electrolytic deposition of metal on a mandrel or other materials; differing from plating in the thickness of deposit usually obtained. Either nickel or copper can be deposited on numerous substrates.

(U) Spinning. A process for fabricating a surface of revolution wherein material is physically formed over a mandrel by applying roller pressure to a spinning metal blank; applicable to most metals.

(U) Explosive Forming. Forming method accomplished by a pressure shock wave generated in a hydraulic medium by an explosive charge; applicable to most metals.

(U) Casting. A method of generally obtaining a complex shape by pouring molten metal in or around a mold — subsequently freezing — then removing the mold. Of the candidate materials under consideration, it is currently limited to beryllium copper and aluminum.

(U) Forging. A form method where metal is physically formed over a die from a solid blank by high energy mechanical means (e.g. press and drop hammer); applicable to most metals.

(U) Machining. A process used to obtain a final shape by physically removing material by tool cutting (milling, lathe turning, etc.), spark discharge removal (electrical discharge machining - EDM), electrolytic removal (electrochemical machining - ECM), and chemical removal (chem milling).

(U) Hot Isostatic Pressing. A method by which a metal powder is simultaneously pressed and sintered in a high pressure autoclave employing an inert gas at elevated temperature. A thin metal container is used to support the powder around a mandrel and transmit the pressure forces. The elevated temperature is attained from a resistance heater located within the autoclave. High temperature, hard tooling is required during the hot pressing cycle. This tooling is subsequently leached out. Applicable to axisymmetric and flat hardware.

(U) Powder Metallurgy. A fabrication method similar to hot isostatic pressing except that pressing and sintering are not accomplished simultaneously. Initial pressing is accomplished at room temperature with the powder supported around the mandrel by a polyethylene container which also transmits the pressure forces to achieve a self supporting free standing part. The part is then sintered at elevated temperature but as a free standing part. No pressure is applied during sintering, precluding the need for internal hard tooling. Coolant passage tooling is fabricated from low melting temperature material. Applicable to axisymmetric and flat hardware.

(U) Welding. A method of joining similar materials by controlled application of temperature and/or pressure to the joining interface either with or without the use of an intermediate filler material to obtain fusion of the joint.

(U) Brazing. Similar to welding except accomplished usually at lower temperatures and a relatively nonfusible filler material is always used.

(U) Liquid Interface Diffusion Bonding. Essentially a brazing process employing moderate pressures and plating on the mating surfaces rather than filler material to attain higher metallurgical bond strengths at the joining interface; applicable to flat or contoured hardware.

(U) Solid State Diffusion Bonding. A general terminology defining the process of joining similar materials by the application of pressure and temperature, the magnitudes of which are a function of the particular materials involved.

(U) Creep Deformation Bonding. A diffusion bonding method distinguished by the use of mechanical pressure applied by hard tooling platens. No tooling is required in the coolant passages. Requires accurate fitup between the platens and the part to assure good bond joints. Most applicable to flat or large radius of curvature parts.

(U) Gas Pressure Bonding. A diffusion bonding method accomplished in an autoclave at high pressure and elevated temperature. Hard tooling is required in the coolant passages to restrict deformation. After bonding the tooling must be leached out. Applicable to flat or contoured parts.

(U) Thermovac Bonding. Similar to gas pressure bonding except that a lower pressure is employed negating the use of hard tooling to maintain the required geometry. Requires more accurate fitup than gas pressure bonding but has a potentially lower cost. Applicable to flat or contoured parts.

(U) Explosive Bonding. Similar to gas pressure bonding except that bonding force is applied by the detonation and subsequent shock wave of an explosive. Requires hard tooling in the coolant passages that is subsequently leached out. Most applicable to flat or large radius of curvature part.

TASK III - FABRICATION STUDY

(U) The objective of the Task III Fabrication Study was to evaluate and rank advanced fabrication concepts that would be lower in cost and/or have performance advantages and extended range of application over conventional tubular wall thrust chambers.

Design Concepts

(U) In order to complete the ranking of fabrication concepts, it was necessary to select design concepts that were representative of the design cases considered in Task I and allowed for exploration of the regenerative cooling limits established by the parametric heat transfer study. Briefly, the results of the heat transfer study showed:

1. H_2 and N_2H_4 were better coolants than F_2 and CPF respectively.
2. H_2 cooled chambers have an almost unlimited range of application with conventional (nickel and/or beryllium copper) materials.
3. N_2H_4 cooled bell chambers have a good range of application with conventional (nickel) materials.
4. Low to moderate thrust N_2H_4 cooled bell chambers, that throttle 10:1 have an extended range of application if a hot wall ($\sim$2000F) is used rather than a more conventional (1600F) wall temperature.

5. Refractories operating at a hot gas wall temperature of 2800F extend the regenerative cooling limits of N_2H_4 cooled chambers. However, due to exothermic decomposing tendencies of N_2H_4, the coolant side wall temperature cannot exceed $\sim$ 600F, resulting in an exceptionally thick wall if the maximum benefits (2800F wall) are to be realized with the refractory.

6. Decomposed N_2H_4 is a good coolant; however, due to the decomposition temperature of the coolant ($\sim$1400F), a refractory chamber is required.

7. The use of multiple layers of coolant passages considerably extends the limits of regeneratively cooled chambers that operate on F_2/H_2 propellants. Hydrogen is used as the primary coolant and fluorine is used as the backup coolant to remove heat from the hydrogen. The CPF/N_2H_4 propellant combination does not experience the same benefits since there is a relatively small difference in the bulk temperatures of the two propellants.

(U) Using these results and the material compatibility data of Task II, the six design concepts, listed in Table II were selected for consideration in the ranking of fabrication concepts.

(U) In all cases the chambers were considered to terminate at a low area ratio, at which point a nozzle is attached and continues to higher area ratios. Fabrication methods considered for the chamber are also applicable to the fabrication of regeneratively cooled nozzles.

Fabrication Methods Ranking

(U) The various methods of fabricating thrust chambers which were considered in the Task III study were presented previously in Task II.

TABLE II

SELECTED DESIGN CON

NO.	T/C	PROPELLANT	COOLANT	COOLANT CIRCUIT MATERIA
1	BELL	F_2/H_2	H_2	BERYLLIUM COPPER
2	BELL	F_2/H_2 OR CPF/N_2H_4	H_2 OR N_2H_4	NICKEL
3	BELL	CPF/N_2H_4	N_2H_4 (DECOMPOSED)	REFRACTORY
4	BELL	CPF/N_2H_4	N_2H_4	NICKEL WITH "HOT
5	A/S	F_2/H_2 OR CPF/N_2H_4	H_2 OR N_2H_4	NICKEL
6	A/S	F_2/H_2	H_2 + F_2 HEAT EXCH.	BERYLLIUM COPPER AND/OR NICKEL

TABLE II

CTED DESIGN CONCEPTS (U)

COOLANT CIRCUIT MATERIAL	COMMENTS
ERYLLIUM COPPER	• Parametric heat transfer and stress studies show beryllium-copper bell thrust chambers to have wide range of application. •• Good range of P_c and throttling. • Refractory materials are not needed with H_2 coolant.
ICKEL	• Parametric study showed nickel to have a good range of application with both H_2 and N_2H_4 coolant. •• N_2H_4 considered over wide range of both throttling and nonthrottling chambers. •• H_2 considered over complete range for both throttling and nonthrottling chambers.
EFRACTORY	• Heat transfer studies showed that decomposed N_2H_4 ($\sim 1400^{\circ}F$ coolant temperature) requires refractory materials ($\sim 2800^{\circ}F$ wall temperature) for coolant circuit.
ICKEL WITH "HOT WALL"	• "Hot Wall" needed for N_2H_4 cooled nonthrottling bell chambers below a thrust level of 10K lbs. and for high thrust levels $\sim$30K lbs. when throttled 10 : 1.
ICKEL	• Parametric study showed nickel to have a good range of application with both H_2 and N_2H_4 coolant.
ERYLLIUM COPPER AND/OR NICKEL	• Beryllium copper and nickel have good range of application. • Beryllium copper has lower system pressure drop (ΔP) than nickel at the same operating point. • Beryllium copper design can facilitate greater manufacturing tolerances than nickel from a heat transfer standpoint. • Heat exchange concept very attractive for systems payoffs. •• At a given P_c, heat exchange offers higher I_s and/or reduced ΔP and gas-gas propellant injection.

(U) The Development Risk ranking of the candidate combinations of the previously listed fabrication methods was accomplished using the criteria and weighted ranking factors presented in Table III .

(U) Ranking of the various fabrication methods with respect to the construction of regeneratively cooled thrust chambers is presented in Table IV through VII, which considered individually the fabrication of; coolant circuits, backup structures and hot-gas wall liners for both bell and annular thrust chamber configurations. A numerical range of 1 through 10 was selected to rank the fabrication methods; the better the fabrication method, the higher the number.

(U) The ranking numbers which appear in the fabrication methods ranking charts (Tables IV through VII) depict the relative rank of each fabrication method to the other methods listed in terms of that ranking parameter heading. The numbers also include the relative importance of the weighting factor for that ranking parameter.

(U) For both the bell and annular coolant circuit ranking charts (Tables IV and V), the candidate methods under each heading (inner or hot gas wall, coolant passages, and closure) defines the fabrication methods which may be applied to a specific portion of the total coolant circuit assembly. The arrangement, in sequence, from left to right depicts a logical approach to the coolant circuit construction steps, but does not necessarily preclude the reverse arrangement of the headings; the closure portion of the coolant circuit may be constructed first and the inner wall constructed last, depending upon the convenience of producing a specific item of hardware.

TABLE III

FABRICATION METHODS RANKING CRITERIA (U)

RANKING CRITERIA	DEFINITION
Structural Integrity	Confidence that the chamber fabricated by the subject fabrication method and process will reliably and repeatably withstand the stresses imposed during fabrication, inspection and testing.
Sealing	Confidence that the chamber fabricated by the subject fabrication method and process will not leak coolant into the chamber or overboard (i.e., permeability, cracks, porosity).
Plugging	Confidence that the chamber fabricated by the subject fabrication method or process will have no plugged or restricted coolant passag (i.e., braze plugging, crushing, incomplete removal of tooling from passages, etc.).
Fabrication Turn-Around-Time	Flow time required to fabricate new tooling after a design change i released to the shop (coolant circuit and/or combustor change).
Fabrication Time	The shop flow time required to fabricate a chamber using the specif fabrication method and process
In-Process Inspection	The degree to which the fabrication method and process lends themse to inspection at various stages of fabrication prior to and after completion.
Tolerance Sensitivity	The ability to achieve close and repeatable tolerances as fabricate

CRITERIA (U)

	WEIGHTED FACTORS	REASONS
ct fabrication hstand the testing.	1.5	Fabrication method/process must have inherent structural integrity to be applied to T/C construction.
ct fabrication hamber or over-	1.0	A small amount of leakage does not preclude the use of the method/process within the limits of performance and reliability.
ct fabrication d coolant passages of tooling from	1.5	Irrespective of the low cost or fabrication time of fabrication method, if coolant slots are plugged or severely restricted, the application is severely compromised.
design change is tor change).	1.0	Important only to the degree it affects cost and delivery schedule. Most important during R&D or technology programs
sing the specified	1.0	Important only to the degree it affects cost and delivery schedule. May influence amount of facility expansion required.
es lends themselves to and after	1.3	Important that method/process lends itself to inspection during fabrication such that inferior component can be rejected prior to spending a great deal of time and money on it.
es as fabricated.	1.0	Tolerance variation is important only within the bounds of its effect on wall temperature (reduced life) and system ΔP.

TABLE IV

FABRICATION METHODS RANKING CHART (U)

ANNULAR CHAMBER COOLANT CIRCUIT

FABRICATION METHOD: HOT GAS WALL	PASSAGES	CLOSURE	NO.	MATERIALS & PROCESS DEVELOPMENT FACTORS: STRUCTURAL INTEGRITY 1.5	SEALING 1.0	PLUGGING 1.5	TURN AROUND TIME: REVISE CONTOUR 1.0	REVISE PASSAGE 1.0	FAB. TIME 1.0
ELECTROFORM (ELF)	ELECTROFORM	ELECTROFORM	1	15	10	15	7	8	4
		BRAZE	2	12	8	9	6	8	7
		* DIFFUSION BOND 1	3	10	8	15	5	8	6
		DIFFUSION BOND 2	4	13	8	15	6	8	6
		DIFFUSION BOND 3	5	13	8	14	6	5	5
		DIFFUSION BOND 4	6	13	8	14	6	5	5
		WELD	7	9	9	11	7	7	7
	MACHINE	ELECTROFORM	8	15	10	15	7	8	3
		BRAZE	9	12	8	9	6	8	3
		* DIFFUSION BOND 1	10	10	8	15	5	8	4
		DIFFUSION BOND 2	11	13	8	15	6	8	4
		DIFFUSION BOND 3	12	13	8	14	6	5	3
		DIFFUSION BOND 4	13	13	8	14	6	5	3
		WELD	14	9	9	11	7	7	5
			15						
MACHINE	MACHINE	ELECTROFORM	16	15	10	15	8	8	7
		BRAZE	17	12	8	9	7	8	7
		* DIFFUSION BOND 1	18	10	8	15	6	8	6
		DIFFUSION BOND 2	19	13	8	15	7	8	6
		DIFFUSION BOND 3	20	13	8	14	7	5	5
		DIFFUSION BOND 4	21	13	8	14	7	5	5
		WELD	22	9	9	11	8	7	7
	ELECTROFORM	ELECTROFORM	23	15	10	15	8	8	6
FORGE	ELECTROFORM	ELECTROFORM	24	15	10	15	6	8	6
	MACHINE	ELECTROFORM	25	15	10	15	6	8	5
		BRAZE	26	12	5	9	5	8	7
		* DIFFUSION BOND 1	27	10	8	15	4	8	6
		DIFFUSION BOND 2	28	13	8	15	5	8	6
		DIFFUSION BOND 3	29	13	8	13	5	5	5
		DIFFUSION BOND 4	30	13	8	13	5	5	5
		WELD	31	9	9	10	6	7	7
MECHANICALLY FORM	MECHANICALLY FORM	ELECTROFORM	32	15	10	15	5	6	6
		BRAZE	33	12	8	9	4	6	9
		* DIFFUSION BOND 1	34	10	8	15	3	6	7
		DIFFUSION BOND 2	35	13	8	15	4	6	7
		DIFFUSION BOND 3	36	13	8	13	4	4	6
		DIFFUSION BOND 4	37	13	8	13	4	4	6
		WELD	38	9	9	11	5	5	9
	MACHINE	ELECTROFORM	39	15	10	15	6	8	5
		BRAZE	40	12	8	9	5	8	7
		* DIFFUSION BOND 1	41	10	8	16	4	8	6
		DIFFUSION BOND 2	42	13	8	15	5	8	6
		DIFFUSION BOND 3	43	13	8	14	5	5	5
		DIFFUSION BOND 4	44	13	8	14	5	5	5
		WELD	45	9	9	11	6	7	7
	ELECTROFORM	ELECTROFORM	46	15	10	15	6	8	6
CAST	CAST	ELECTROFORM	47	12	8	15	4	3	8
		BRAZE	48	9	5	9	3	3	9
		* DIFFUSION BOND 1	49	7	6	15	2	3	8
		DIFFUSION BOND 2	50	9	6	15	3	3	9
		DIFFUSION BOND 3	51	9	6	14	3	1	4
		DIFFUSION BOND 4	52	9	6	14	3	1	4
		WELD	53	6	7	10	4	2	10
		CAST	54	10	7	14	2	2	10
	MACHINE	ELECTROFORM	55	12	8	15	5	8	5
		BRAZE	56	9	5	9	4	8	7
		* DIFFUSION BOND 1	57	7	6	15	3	8	6
		DIFFUSION BOND 2	58	9	6	15	4	8	6
		DIFFUSION BOND 3	59	9	6	14	4	5	6
		DIFFUSION BOND 4	60	9	6	14	4	5	6
		WELD	61	6	4	11	5	7	7
	ELECTROFORM	ELECTROFORM	62	12	8	16	5	8	6
** HIP	** HIP	HIP	63	10	7	14	6	5	7
		BRAZE	64	9	5	9	5	7	8
		* DIFFUSION BOND 1	65	7	6	15	4	7	8
		DIFFUSION BOND 2	66	9	6	15	5	7	8
		DIFFUSION BOND 3	67	9	6	14	5	5	7
		DIFFUSION BOND 4	68	9	6	14	5	5	7
		WELD	69	6	4	11	6	6	8
	MACHINE	HIP	70	10	7	14	6	5	6
		ELECTROFORM	71	10	8	15	6	8	5
		BRAZE	72	9	5	9	5	8	8
		* DIFFUSION BOND 1	73	7	6	15	4	8	8
		DIFFUSION BOND 2	74	9	6	15	5	8	8
		DIFFUSION BOND 3	75	9	6	14	5	5	7
		DIFFUSION BOND 4	76	9	6	14	5	5	7
		WELD	77	6	4	11	6	7	8
	ELECTROFORM	ELECTROFORM	78	10	8	15	6	8	8

HART (U)

UIT

FACTORS		IN PROCESS INSPECTION	TOLERANCE SENSITIVITY	TOTALS
D TIME ISE PASSAGE 1.0	FAB. TIME 1.0	1.3	1.0	
8	4	8	10	77
8	7	9	8	67
8	6	8	6	66
8	6	8	7	78
5	5	8	8	67
5	5	8	8	67
7	7	10	7	67
8	3	8	10	76
8	5	9	8	65
8	4	8	6	64
8	4	8		69
5	3	8	8	65
5	3	8	8	65
7	5	10	7	68
8	7	9	10	80
8	7	10	8	69
8	6	9	6	69
8	6	9	7	74
5	5	9	8	69
5	5	9	8	69
7	7	13	7	70
8	6	9	10	81
8	6	9	9	78
8	5	9	9	77
8	7	10	7	63
8	6	9	5	68
8	6	9	6	71
5	5	9	7	66
5	5	9	7	66
7	7	13	6	68
6	6	9	7	73
6	9	10	6	64
6	7	9	4	63
6	7	9	8	68
4	6	9	6	64
4	6	9	6	62
5	9	13	5	65
8	5	8	8	76
8	7	10	6	65
8	6	9	4	65
8	6	9	5	70
5	5	9	7	66
5	5	9	7	66
7	7	13	6	67
8	6	9	8	77
3	8	9	7	66
3	9	10	5	55
3	8	9	4	55
3	9	9	5	59
1	4	9	6	53
1	4	9	6	53
2	10	13	5	55
2	10	9	5	59
8	5	9	7	69
8	7	10	6	58
8	6	9	5	60
8	6	9	6	63
5	6	8	7	59
5	6	8	7	59
7	7	13	6	58
8	6	9	7	70
5	7	8	6	63
7	8	10	5	59
7	8	9	3	60
7	8	9	4	63
5	7	8	6	60
5	7	8	6	60
6	8	12	6	57
5	8	8	6	62
8	8	9	7	65
8	8	10	6	60
8	8	9	4	62
8	8	9	5	65
5	7	8	6	60
5	7	8	6	60
7	8	12	5	68
8	8	9	7	63

* DIFFUSION BOND
1 - CREEP DEFORMATION
2 - THERMOVAC
3 - EXPLOSIVE
4 - GAS PRESSURE

** H.I.P.
HOT ISOSTATIC PRESSING

TABLE V

FABRICATION METHODS RANKING CH

BELL CHAMBER COOLANT CIR

FABRICATION METHOD: HOT GAS WALL	PASSAGES	CLOSURE		NO	MATERIALS & PROCESS DEVELOPMENT: STRUCTURAL INTEGRITY 1.5	SEALING 1.0	PLUGGING 1.5	TURN AROUND: REVISE CONTOUR 1.0	REVIS
ELECTROFORM (ELF)	ELECTROFORM	ELECTROFORM		1	15	10	15	6	
		BRAZE 1 & 2		2	12 2	2 6	5 6	6 4	8
		DIFFUSION * BOND	1	3	13	6	15	4	
			2	4	13	6	14	4	
			3	5	13	6	14	4	
		WELD		6	9	8	9	5	
	MACHINE	HIP		7	12	6	14	5	
		ELECTROFORM		8	15	10	15	6	
		BRAZE 1 & 2		9	12 12	2 6	5 6	5 4	8
		DIFFUSION * BOND	1	10	13	6	15	4	
			2	11	13	6	14	4	
			3	12	13	6	14	4	
		WELD		13	9	8	9	5	
POWDER METAL	POWDER METAL	POWDER METAL		14	8	7	15	4	
		BRAZE 1 & 2		15	7 7	2 5	5 6	4 3	6
		DIFFUSION * BOND	1	16	8	5	15	3	
			2	17	8	5	14	3	
			3	18	8	5	14	3	
		WELD		19	6	5	9	4	
	MACHINE	ELECTROFORM		20	10	7	15	3	
		POWDER METAL		21	8	6	15	5	
		BRAZE 1 & 2		22	7 7	2 5	5 6	5 4	8
		DIFFUSION * BOND	1	23	8	5	15	4	
			2	24	8	5	14	4	
			3	25	8	5	14	4	
		WELD		26	6	5	9	5	
	ELECTROFORM	ELECTROFORM		27	10	7	15	5	
HIP	** HIP	HIP		28	10	8	15	4	
		BRAZE 1 & 2		29	9 9	2 5	5 6	4 3	6
		DIFFUSION * BOND	1	30	10	6	15	3	
			2	31	10	6	14	3	
			3	32	10	6	14	3	
		WELD		33	6	6	9	4	
	MACHINE	ELECTROFORM		34	12	8	15	3	
		HIP		35	10	8	15	5	
		BRAZE 1 & 2		36	9 9	2 5	5 6	5 4	8
		DIFFUSION * BOND	1	37	10	6	15	4	
			2	38	10	6	14	4	
			3	39	10	6	14	4	
		WELD		40	6	6	9	5	
	ELECTROFORM	ELECTROFORM		41	12	8	15	5	
MACHINE (FROM BILLET)	MACHINE			42					
		HIP		43	10	6	14	6	
		ELECTROFORM		44	15	10	15	10	
		BRAZE 1 & 2		45	12 12	2 6	5 6	10 6	10
		DIFFUSION * BOND	1	46	13	6	15	7	
			2	47	13	6	14	6	
			3	48	13	6	14	6	
		WELD		49	9	8	9	7	
	ELECTROFORM	ELECTROFORM		50	15	10	15	10	
FORGE	ELECTROFORM	ELECTROFORM		51	15	10	15	5	
	MACHINE	HIP		52	10	7	14	5	
		ELECTROFORM		53	15	10	15	5	
		BRAZE 1 & 2		54	12 12	2 5	5 6	5 4	8
		DIFFUSION * BOND	1	55	13	7	15	4	
			2	56	13	7	14	4	
			3	57	13	7	14	4	
		WELD		58	9	8	9	5	
MECHANICALLY FORM (EXPLOSIVE SPINNING ETC)	MECHANICALLY FORM	HIP		59	10	7	14	6	
		ELECTROFORM		60	15	10	15	6	
		BRAZE 1 & 2		61	12 12	2 6	5 6	6 5	4
		DIFFUSION * BOND	1	62	13	7	15	5	
			2	63	13	7	14	5	
			3	64	13	7	14	5	
		WELD		65	9	8	9	5	
	MACHINE	HIP		66	10	7	14	6	
		ELECTROFORM		67	15	10	15	7	
		BRAZE 1 & 2		68	12 12	2 6	5 6	7 5	8
		DIFFUSION * BOND	1	69	13	7	15	5	[illegible]
			2	70	13	7	14	5	[illegible]
			3	71	13	7	14	5	[illegible]
		WELD		72	9	8	9	4	[illegible]
	ELECTROFORM	ELECTROFORM		73	15	10	15	7	[illegible]
CAST	CAST	HIP		74	11	6	14	2	
		ELECTROFORM		75	12	8	15	3	[illegible]
		BRAZE 1 & 2		76	9 9	2 5	5 6	3 2	3
		DIFFUSION * BOND	1	77	10	6	15	2	[illegible]
			2	78	10	6	14	2	
			3	79	10	6	14	2	
		WELD		80	6	7	9	3	[illegible]
CAST	ELECTROFORM	ELECTROFORM		81	12	8	15	3	[illegible]
	MACHINE	HIP		82	9	8	14	4	[illegible]
		ELECTROFORM		83	12	8	15	4	[illegible]
		BRAZE 1 & 2		84	9 9	2 6	5 6	4 3	8
		DIFFUSION * BOND	1	85	10	6	15	3	[illegible]
			2	86	10	6	14	3	[illegible]
			3	87	10	6	14	3	[illegible]
		WELD		88	6	7	9	4	[illegible]

RANKING CHART (U)

R COOLANT CIRCUIT

EVELOPMENT FACTORS				IN PROCESS INSPECTION	TOLERANCE SENSITIVITY	TOTAL
NG	TURN AROUND TIME		FAB TIME			
	REVISE CONTOUR 1.0	REVISE PASSAGE 1.0	1.0	1.3	1.0	
	6	8	6	8	10	78
6	6 4	8 8	7 7	9 9	6 6	55 58
	4	8	6	8	7	67
	4	6	2	8	8	69
	4	6	2	8	8	61
	5	7	8	10	7	63
	5	4	2	8	8	56
	6	8	5	8	10	77
6	5 4	8 8	6 6	9 9	6 6	54 57
	4	8	5	8	7	66
	4	4	2	8	6	59
	4	4	2	8	8	59
	5	5	7	10	7	59
	4	6	12	7	6	65
6	4 3	6 6	9 9	9 9	4 4	46 49
	3	6	8	8	5	58
	3	4	4	8	5	51
	3	4	4	8	5	51
	4	5	9	10	4	52
	3	8	5	8	7	63
	5	6	8	8	5	61
6	5 4	8 8	7 7	9 9	4 4	47 50
	4	8	6	8	5	59
	4	4	2	8	6	51
	4	4	2	8	6	49
	5	5	7	10	5	52
	5	8	6	8	7	66
	4	6	7	8	7	65
6	4 3	6 6	6 6	9 9	5 5	46 49
	3	6	5	8	5	58
	3	4	4	8	6	55
	3	4	4	8	6	55
	4	5	6	10	5	51
	3	8	6	9	8	69
	5	6	6	9	7	67
6	5 4	8 8	7 7	9 9	5 5	50 53
	4	8	5	9	5	63
	4	4	3	9	6	56
	4	4	3	9	6	56
	5	5	6	10	5	52
	5	8	6	9	8	71
	6	4	2	9	8	59
	10	10	7	9	10	86
6	10 6	10 8	6 6	10 8	6 6	61 60
	7	8	5	9	7	71
	6	4	2	9	8	62
	6	4	2	9	8	62
	7	5	7	13	7	65
	10	10	6	9	10	85
	5	8	6	9	9	77
	5	4	4	9	8	61
	5	8	6	9	9	77
6	5 4	8 8	7 7	10 10	6 6	55 58
	4	8	6	9	7	70
	4	4	3	9	8	62
	4	4	3	9	8	62
	5	8	7	13	7	63
	6	2	5	9	7	60
	6	4	8	9	8	75
6	6 5	4 4	8 8	10 10	5 5	52 56
	5	4	7	9	6	67
	5	2	4	9	7	61
	5	2	4	9	7	61
	5	3	8	13	6	61
	6	4	8	9	8	66
	7	4	4	8	9	73
6	7 5	8 8	7 7	10 10	6 6	57 60
	5	8	6	9	7	71
	5	4	3	9	8	63
	5	4	3	9	8	63
	6	8	7	13	7	64
	7	8	6	9	9	77
	2	1	10	8	6	59
	3	3	8	9	7	68
6	3 2	3 3	9 9	10 10	4 4	45 48
	2	3	8	9	5	59
	2	1	4	9	6	52
	2	1	4	9	6	52
	3	2	9	13	5	64
	3	8	7	9	8	70
	4	4	3	9	7	55
	4	8	6	9	8	70
6	4 3	8 8	7 7	10 10	5 5	50 53
	3	8	6	9	4	64
	3	4	3	9	7	66
	3	4	3	9	7	56
	4	4	8	13	6	67

* DIFFUSION BOND
1-THERMOVAC
2-EXPLOSIVE
3-GAS PRESSURE

** HIP-
HOT ISOSTATIC PRESSING

BRAZE:
1. WIRE WRAP
2. SPLIT SHELLS

TABLE VI

FABRICATION METHODS RANKING CHART-
LINERS AND BELL CHAMBER BACKUP STRUCTURE (U)

[BELL CHAMBER BACKUP STRUCTURE]

CONFIGURATION	FABRICATION METHOD	NO.	MATERIALS: STRUCTURAL INTEGRITY 1.5	PROCESS DEVELOPMENT: TURN AROUND TIME 1.0	PROCESS DEVELOPMENT: FAB TIME 1.0	IN PROCESS INSPECTION 1.5	TOLERANCE SENSITIVITY 1.0	TOTALS
INTEGRAL	ELECTROFORM	1	15	10	4	12	10	51
	POWDER METAL *HIP	2	9	7	7	10	7	39
		3	10	6	6	10	7	39
	CAST, INTEGRAL	4	12	5	10	10	8	44
WIRE	WIRE WRAP BRAZE	5	6	10	8	13	6	43
SPLIT SHELLS	THERMOVAC	6	13	7	7	8	7	42
	BRAZING	7	12	7	7	10	8	44
	GPB	8	13	6	6	8	7	40
	EXP	9	13	6	6	8	7	40
	EPOXY	10	7	8	8	10	6	40

[COMBUSTION CHAMBER LINER]
BELL

POWDER METAL *HIP	1	9	9	10	10	6	45
	2	10	6	8	10	6	41
MACHINE	3	13	4	4	10	10	44
PLASMA SPRAY	4	6	10	7	7	5	35
VAPOR DEPOSIT	5	3	10	7	7	5	32
MECHANICALLY FORM	6	12	8	8	10	8	47

[COMBUSTION CHAMBER LINER]
ANNULAR

POWDER METAL *HIP	1	9	7	10	10	6	43
	2	10	6	8	10	6	41
MACHINE	3	13	2	2	10	10	40
PLASMA SPRAY	4	6	10	6	7	5	34
VAPOR DEPOSIT	5	3	10	6	7	5	31
MECHANICALLY FORM	6	12	9	9	10	8	49

TABLE VII

FABRICATION METHODS RANKING CHART - ANNULAR CHAMBER BACKUP STRUCTURE (U)

WEB	RIBS (R)	(W) TO (R) JOINT	NO.	MATERIALS & PROCESS DEVELOPMENT: STRUCTURAL INTEGRITY 1.5	MATERIALS & PROCESS DEVELOPMENT: TURN AROUND TIME 1.0	MATERIALS & PROCESS DEVELOPMENT: FAB TIME 1.0	IN PROCESS INSPECTION 1.3	TOLERANCE SENSITIVITY 1.0	TOTALS
MACHINE	MACHINE	NONE	1	15	10	3	12	10	50
		CREEP DEFORM	2	10	7	4	8	7	36
		THERMOVAC	3	10	7	4	8	7	36
		GAS PRESSURE	4	10	6	2	8	8	34
		BRAZE	5	7	7	4	10	8	37
		WELD	6	9	8	5	13	6	41
			7						
	FORGE	CREEP DEFORM	8	10	6	4	8	6	34
		THERMOVAC	9	10	6	4	8	6	34
		GAS PRESSURE	10	10	5	2	8	7	32
		BRAZE	11	7	6	4	10	7	35
		WELD	12	9	7	5	13	5	39
	EXTRUDE	CREEP DEFORM	13	10	6	4	8	6	34
		THERMOVAC	14	10	6	4	8	6	34
		GAS PRESSURE	15	10	5	2	8	7	32
		BRAZE	16	7	6	4	10	7	35
		WELD	17	9	7	5	13	5	39
	CAST	CAST	18	7	3	7	9	4	31
		CREEP DEFORM	19	9	5	5	7	5	30
		THERMOVAC	20	9	5	5	7	5	30
		GAS PRESSURE	21	9	4	3	7	6	28
		BRAZE	22	6	5	5	9	6	31
		WELD	23	7	6	6	12	4	35
FORGE	MACHINE		24						
		CREEP DEFORM	25	10	6	5	8	6	35
		THERMOVAC	26	10	6	5	8	6	35
		GAS PRESSURE	27	10	5	3	8	7	33
		BRAZE	28	7	6	5	10	7	36
		WELD	29	9	7	6	13	5	40
	FORGE	NONE	30	15	4	10	12	6	47
		CREEP DEFORM	31	10	5	6	8	5	34
		THERMOVAC	32	10	5	6	8	5	34
		GAS PRESSURE	33	10	4	4	8	6	32
		BRAZE	34	7	5	6	10	6	35
		WELD	35	9	6	7	13	4	39
	EXTRUDE	CREEP DEFORM	36	10	5	6	8	5	34
		THERMOVAC	37	10	5	6	8	5	34
		GAS PRESSURE	38	10	4	4	8	6	32
		BRAZE	39	7	5	6	10	6	35
		WELD	40	9	6	7	13	4	39
	CAST	CAST	41	7	2	8	9	3	30
		CREEP DEFORM	42	9	4	6	7	4	29
		THERMOVAC	43	9	4	6	7	4	29
		GAS PRESSURE	44	9	3	4	7	5	28
		BRAZE	45	6	4	6	9	5	31
		WELD	46	7	8	7	12	3	34
CAST	MACHINE		47						
		CREEP DEFORM	48	9	5	6	7	6	32
		THERMOVAC	49	9	5	6	7	6	32
		GAS PRESSURE	50	9	4	4	7	7	31
		BRAZE	51	6	5	6	9	7	33
		WELD	52	7	6	7	12	3	37
	FORGE		53						
		CREEP DEFORM	54	9	4	7	7	5	31
		THERMOVAC	55	9	4	7	7	5	31
		GAS PRESSURE	56	9	3	5	7	6	29
		BRAZE	57	6	4	7	9	6	32
		WELD	58	7	5	8	12	4	36
	EXTRUDE	CREEP DEFORM	59	9	4	7	7	5	31
		THERMOVAC	60	9	4	7	7	5	31
		GAS PRESSURE	61	9	3	5	7	6	29
		BRAZE	62	6	4	7	9	6	32
		WELD	63	7	5	8	12	4	36
	CAST	CAST	64	12	1	10	8	3	34
		CREEP DEFORM	65	9	3	7	7	4	30
		THERMOVAC	66	9	3	7	7	4	30
		GAS PRESSURE	67	9	2	5	7	5	27
		BRAZE	68	6	3	7	9	5	29
		WELD	69	7	4	8	12	3	34

(U) The Annular Chamber Backup Structure chart, Table VII , indicates in sequence from left to right the logical approach to annular chamber backup structure construction (fabrication of baffles, fabrication of ribs, and joining the baffles to the ribs). A typical annular backup structure is shown in Fig. 31, in this case, for a segmented configuration.

Fabrication Concept Ranking

(U) By combining the results of the Task I Parametric Study and Task II Material Study with the selected design concepts and the highest ranked fabrication methods, and applying the guidelines discussed below, fifteen bell and thirteen annular thrust chamber fabrication concepts were derived for additional evaluation and ranking.

(U) The following ground rules and/or guidelines were established in the selection of these fabrication concepts.

1. Hot-gas wall liners were eliminated from further consideration since they are generally not needed to meet the regenerative cooling requirements of the selected design concepts.

2. Only integral bell backup structures were considered further for the bell fabrication concepts because integral structure reduces the complexity of the coolant circuit to structure joint, therefore, offering the most potential for low production costs.

3. Backup structure configurations for annular chambers are very dependent upon system operational requirements and field support philosophy, e.g., requirements may dictate designs varying

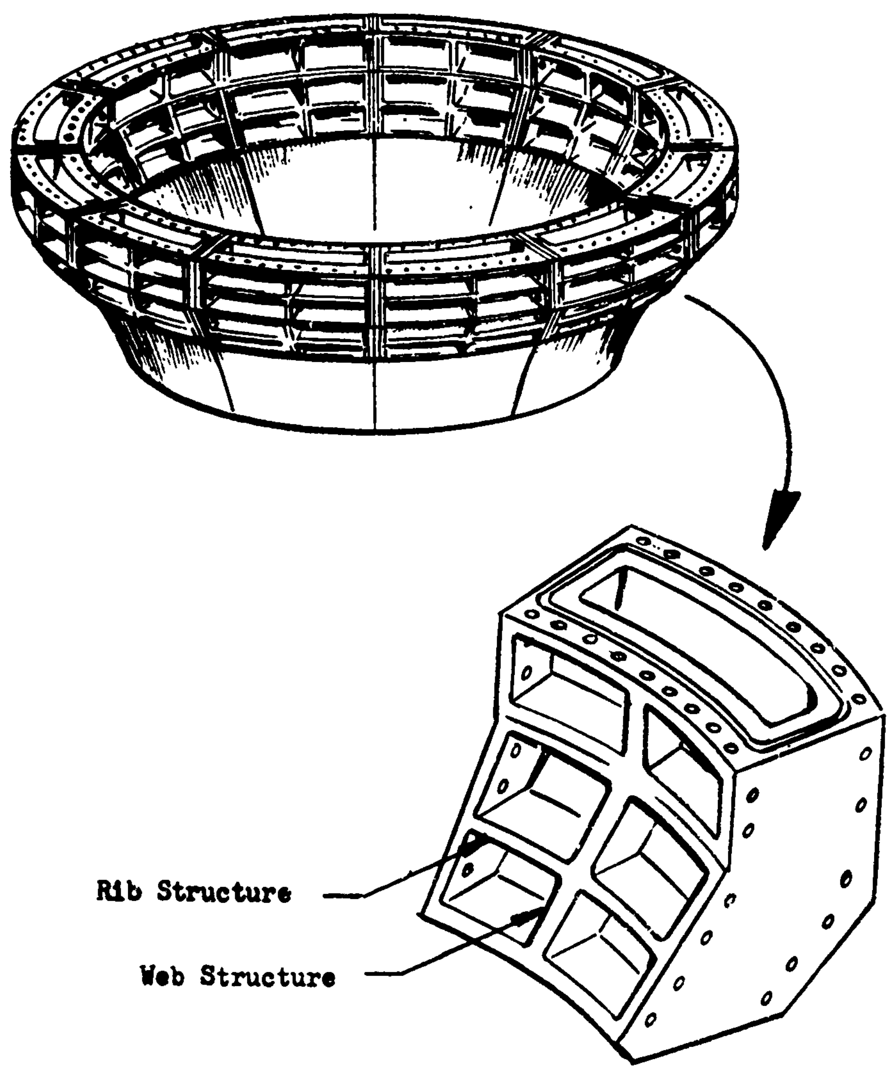

Figure 31. Typical Segmented Annular Chamber Structure. (U)

anywhere from complete unitized construction to field replaceable segments of many possible sizes and shapes. It was therefore determined prudent at this time, in light of Phase III program objectives and lack of definition of operational requirements, to restrict all further annular chamber fabrication concept evaluation efforts to the coolant assembly.

(U) All of the fabrication concepts selected were then evaluated and ranked in three key areas of consideration: "Development Risk", "Range of Application", and "Production Costs". A weighting factor was assigned to the ratings achieved in each of the areas (Table VIII) reflecting the relative importance associated with each aspect of consideration in selecting the final fabrication concepts. The fabrication concepts which were thus ranked using these factors are presented in Table IX .

(U) Development Risk. The ranking values defined within the Development Risk sections of Table IX are based upon adjusted values tabulated from the Fabrication Methods Ranking charts.

(U) Range of Application. The fabrication concepts Range of Application subtotals are obtained as the summation of the individual numerical values in each ranking parameter column combined with the weighting factor of 1.2 and reduced by the factor of 10 in order to again maintain the proper perspective with the other two ranking headings.

(U) Production Costs. The numerical ranking values appearing in the production cost section of Table IX reflect the estimated production cost of the fabrication concepts relative to one another based on the results of the production cost studies. (A detailed discussion of the production cost

TABLE VIII

WEIGHTED RANKING FACTORS - FABRICATION CONCEPTS

RANKING CRITERIA	DEFINITION
Development Risk	Ranking of the total risk involved in the development of a specific tion concept considering the aggregate fabrication methods developme (from respective charts) of the specific thrust chamber components: circuit, backup structure, and liner.
Range of Application	The ability of a specific fabrication concept to achieve the maximum limits of operation in terms of the following ranking parameters: 1. <u>Thrust Chamber Diameter</u>. The largest diameter is considere difficult to fabricate by all methods and therefore is rank highest. 2. <u>Passage Size</u>. The smaller, being the more difficult to achi ranked highest. 3. <u>Wall Thickness</u>. The thinnest, being the more difficult to ac ranked highest. 4. <u>Throttle Limit</u>. Throttling capability of concept within ran program applicability (10 : 1); the largest range ranking hi 5. <u>Thrust and P_c Limits</u>. Thrust/unit circumference (annular) o total thrust (bell) corresponding to the analytically predic limit of regenerative cooling; lowest value F/C ranking high 6. <u>Weight</u>. The lower weight concept ranked highest.
Production Cost	Average cost per chamber to produce the designated quantities (2, 20 of the selected fabrication concepts.

ATION CONCEPTS (U)

	WEIGHTING FACTOR	REASONS
of a specific fabrica- hods development risks r components: coolant	1.0	In this ranking chart, this factor has lowest value weighting factor. Because of fact that have already weighted this overall factor on previous fabrication method ranking charts.
ve the maximum desirable parameters: r is considered most refore is ranked fficult to achieve, difficult to achieve, cept within range of ange ranking highest. nce (annular) or lytically predicted P_c /C ranking highest. est.	1.2	Relative weighting factor required here since for a Technology Program the greatest knowledge is obtained when the results are applicable to a relatively broad range of applications.
ntities (2, 20 and 250)	1.5	Highly important in that if fabrication concept does not offer reduced fabrication cost comparable to other concepts, including tubular wall construction, its significance is lost.

TABLE IX

FABRICATION CONCEPTS RANKIN(

(BELL THRUST CHAMBE

DEVELOPMENT RISK													
FABRICATION CONCEPT NUMBER	COOLANT SYSTEM	COOLANT CIRCUIT MATERIAL	COOLANT CIRCUIT FABRICATION METHOD NUMBER	COOLANT CIRCUIT FABRICATION METHOD RANK	BACK UP STRUCTURE MATERIAL	BACK UP STRUCTURE FABRICATION METHOD NUMBER	BACK UP STRUCTURE FABRICATION METHOD RANK	LINER MATERIAL	LINER FABRICATION METHOD NUMBER	LINER FABRICATION METHOD RANK	SUB TOTAL	THRUST CHAMBER DIAMETER	WALL THICKNESS
1	F_2/H_2 OR CPF/N_2H_4	Ni	1	7.8	Ni	1	5.1	NA	—	—	6.5	10	10
2			14	6.1		2	3.9		—	—	5.0	6	7
3			14	6.1	AL	4	4.4	NA	—	—	5.3	5	7
4			67	7.3		4	4.4		—	—	5.9	5	8
5			67	7.3	Ni	1	5.1	NA			6.2	10	8
6	F_2/H_2	BERYLCO 10 & Ni	75	6.5	AL	4	4.4	NA	—	—	5.5	5	6
7			75	6.5	Ni	1		NA	—	—	6.3	5	6
8			67	7.3		1	5.1				6.2	10	8
9		BERYLCO 10	74	5.9	AL	4	4.4	NA	—	—	5.2	5	6
10													
11	CPF/N_2H_4 (HOT WALL)	HI TEMP ALLOY & Ni	67	7.3	Ni	1	5.1	NA	—	—	6.2	10	6
12			20	6.3		1	5.1		—	—	5.7	6	7
13			53	7.7		1	5.1		—	—	6.4	6	8
14			34	6.9		1	5.1		—	—	6.0	4	7
15			67	7.3	AL	4	4.4				5.9	5	8
16	DECOMPOSE CPF/N_2H_4	REFRACT	14	6.1	REFRACT	2	3.9	NA	—	—	5.0	6	7
17			69	7.1		6	4.2		—	—	5.7	8	6
18													

(ANNULAR THRUST CHAM

DEVELOPMENT RISK													
FABRICATION CONCEPT NUMBER	COOLANT SYSTEM	COOLANT CIRCUIT MATERIAL	COOLANT CIRCUIT FABRICATION METHOD NUMBER	COOLANT CIRCUIT FABRICATION METHOD RANK	BACK UP STRUCTURE (1) MATERIAL	BACK UP STRUCTURE (1) FABRICATION METHOD NUMBER	BACK UP STRUCTURE (1) FABRICATION METHOD RANK	LINER (1) MATERIAL	LINER (1) FABRICATION METHOD NUMBER	LINER (1) FABRICATION METHOD RANK	SUB TOTAL	THRUST (2) CHAMBER DIAMETER	WALL THICKNESS
1	F_2/H_2 DOUBLE PANEL	BERYLCO 10	19	7.4	CAST AL	—	—	NA	—	—	7.4	—	10
2			48	5.5		—	—		—	—	5.5	—	6
3			50	5.9		—	—		—	—	5.9	—	6
4						—	—		—	—		—	
5		BERYLCO 10 & Ni	16&1	8.0		—	—	NA	—	—	8.0	—	10
6			17	6.9		—	—		—	—	6.9	—	10
7			47&8	7.1		—	—		—	—	7.1	—	7
8		NI	16&1	8.0		—	—	NA	—	—	8.0	—	10
9			17	6.9		—	—		—	—	6.9	—	10
10						—	—		—	—		—	
11	F_2/H_2 OR CPF/N_2H_4 PANEL	Ni	16	8.2	INCO 718	—	—	NA	—	—	8.2	—	10
12			17	6.9		—	—		—	—	6.9	—	10
13			39	7.6		—	—		—	—	7.6	—	8
14		BERYLCO 10	50	5.9		—	—	NA	—	—	5.9	—	6
15			17	6.9		—	—		—	—	6.9	—	10
16						—	—		—	—		—	
17		BERYLCO 10 & Ni	47	6.6		—	—	NA	—	—	6.6	—	6
18						—	—		—	—		—	

(1) NOT CONSIDERED FOR PRODUCTION COSTS

(2) SEGMENTATION ALLOWS FOR WIDE RANGE OF THRUST CHAMBER DIAMETERS

IX

PTS RANKING (U)

UST CHAMBER)

RANGE OF APPLICATION						FABRICATION CONCEPT RANKING SUBTOTAL	PRODUCTION COST (1.5)			FABRICATION CONCEPT RANKING		
							PRODUCTION QUANTITIES			PRODUCTION QUANTITIES		
WALL THICKNESS	PASSAGE SIZE (IN x IN)	P_c LIMIT, THROTTLED	THRUST LIMIT	WEIGHT	SUB TOTAL (X1.2)		2	20	250	2	20	250
10	9	6	6	7	5.8	12	12	11	11	24	23	23
7	7	6	6	5	4.4	9	15	15	15	24	24	24
7	7	6	6	9	4.8	10	15	15	15	25	25	25
8	10	6	6	10	5.4	11	11	12	12	22	23	23
8	10	6	6	7	5.6	12	11	9	9	23	21	21
6	5	7	7	9	4.7	10	9	13	13	19	23	23
6	5	7	7	6	4.3	11	8	12	12	[illegible]	23	23
8	10	7	7	6	5.8	12	11	9	9	23	21	21
6	5	8	8	8	4.8	10	9	14	14	[illegible]	24	24
6	10	9	9	5	6.1	12	11	9	9	23	21	21
7	10	9	9	4	5.4	11	12	12	12	23	23	23
8	10	9	9	5	5.6	12	2	6	9	12	18	21
7	10	9	9	5	5.3	11	4	8	8	15	19	19
8	10	9	9	8	5.9	12	11	12	12	23	24	24
7	7	10	10	2	5.0	10	15	15	15	25	25	25
6	10	10	10	2	5.8	12	3	4	4	15	16	16

THRUST CHAMBER)

	RANGE OF APPLICATION						FABRICATION CONCEPT RANKING SUBTOTAL	PRODUCTION COST (1.5)			FABRICATION CONCEPT RANKING		
								PRODUCTION QUANTITIES			PRODUCTION QUANTITIES		
UST② BER TER	WALL THICKNESS	PASSAGE SIZE (IN x IN)	P_c LIMIT, THROTTLED	THRUST LIMIT	WEIGHT	SUB TOTAL (X1.2)		2	20	250	2	20	250
	10	10	10	10	4	5.3	13	9	5	5	22	18	18
	[illegible]	8	10	10	4	4.6	10	8	15	15	[illegible]	25	25
	6	8	10	10	4	4.6	11	8	14	14	19	25	25
	10	10	10	10	5	5.4	13	12	9	9	25	22	22
	10	10	10	10	5	5.4	12	9	6	6	21	18	18
	7	9	10	10	5	4.9	12	9	14	14	21	26	26
	10	10	8	8	6	5.0	13	12	8	8	25	21	21
	10	10	8	8	6	5.0	12	9	5	5	21	17	17
	10	10	5	5	10	4.8	13	15	11	11	23	[illegible]	24
	10	10	5	5	10	4.8	12	12	5	5	24	[illegible]	17
	8	10	5	5	10	4.6	12	13	11	11	25	[illegible]	23
	6	8	7	7	7	4.2	10	5	9	9	15	19	19
	10	10	7	7	7	4.9	12	12	6	6	24	18	18
	6	8	6	6	8	4.1	11	8	15	15	19	26	26

studies is presented in Appendix A). The higher the numerical rank the lower the relative cost. The numerical values include the 1.5 weighting factor previously discussed. The production cost studies were completed at a selected point design and then reviewed to determine what effect, if any, a change in physical size or operational parameters (P_c, F, ϵ) would have on the results.

(U) The total fabrication concept ranking for production quantities of 2, 20 and 250 units are presented in the last three columns of the Fabrication Concept ranking charts, the final rankings being the summation of the individual rankings from Development Risk, Range of Application, and Production Costs. Production Costs have the greatest influence on the final fabrication concept ranking because of the weighting factors considered and the averaging techniques used to obtain the Development Risk and Range of Application numerical rankings. The highest ranking fabrication concepts are listed in Table X.

TABLE X

HIGHEST RANKED FABRICATION CONCEPTS (U)

BELL CHAMBERS

Nickel Coolant Circuit (F_2/H_2 or CPF/N_2H_4)

- Powder Metal Nickel Chamber
- All Electroformed Nickel Chamber

Beryllium Copper Coolant Circuit (F_2/H_2)

- Cast (Open Face) With Electroformed Nickel Closeout

High Temperature Hot Gas Wall (CPF/N_2H_4)

- Spun Hastelloy or Inco 625 Liner with Machined Slots and Electroformed Nickel Closeout
- Powder Metal Refractory Liner with Machined Slots and Electroformed Nickel Closeout

Refractory Chamber (Decomposed N_2H_4 Coolant)

- Powder Metal

ANNULAR CHAMBERS

Nonsegmented Chambers

- Single Panel (Beryllium Copper and/or Nickel)
  - Cast Panel Segment (Open Faced) With Electroformed Nickel Closeout
  - Explosively Formed Nickel Shell (360°) Machined Slots and Electroformed Nickel Closeout
- Double Panel (Beryllium Copper and/or Nickel)
  - Cast H_2 Panel (Open Faced) Electroformed Nickel Closeout and F_2 Panel
  - Cast H_2 and F_2 Panels (Open Faced) Plus Nickel Closeout Sheet Brazed Together
  - Machined Beryllium Copper for H_2 Panel, Electroformed Nickel Closeout and F_2 Panel

Segmented Chambers

- Cast Beryllium Copper Segment (Open Faced) With Electroformed Nickel Closeout and F_2 Panel

Recommendation and Selection of Fabrication Concepts

(U) In an effort to establish the broadest fabrication technology base within the scope of the study, the remaining fabrication concepts were screened on the following basis.

(U) 1. Fabrication concepts which have been or are under evaluation in other programs were not considered as prime candidates for Phase II and III development (i.e., all electroformed bell chambers).

(U) 2. The fabrication concepts which assure the broadest possible range of application and advancement in fabrication technology without combining more than one major development area in any one concept are preferred.

(U) 3. Concepts predicated upon the use of a decomposed N_2H_4 coolant were eliminated from further consideration in the Phase III evaluation because of the test facility development required.

(U) Following this screening procedure, the six fabrication concepts outlined below were selected and reviewed with AFRPL program management.

Annular Chamber:

Cast Beryllium Copper segment with electroformed nickel close-out and double panel (oxidizer heat exchanger) on one side. (H_2 coolant)

A. Single coolant panel (annular fabrication concept No. 17, Table IX.

B. Double coolant panel (annular fabrication concept No. 7, Table IX.

Bell Chamber:

C. Powder metal nickel thrust chamber. H_2 coolant (Bell Fabrication Concept No. 2, Table IX)

D. Spun Hastelloy or Inco 625 liner with machined passages, electroformed nickel closeout and integrally cast aluminum structure. N_2H_4 coolant (Bell Fabrication Concept No. 15, Table IX)

E. Powder metal refractory (Tungsten wall with machined coolant slots and electroformed nickel closeout. N_2H_4 coolant (Bell Fabrication Concept No. 15, Table IX)

F. Cast beryllium copper with electroformed nickel closeout and integrally cast aluminum structure. H_2 coolant (Bell Fabrication Concept No. 6, Table IX)

(U) Each of these concepts along with the rationale for their selection is outlined in Table XI.

(U) The three fabrication concepts subsequently approved by AFRPL for experimental evaluation in Phases II and III are described below.

(U) Powder Metal Nickel Bell Thrust Chamber. The first concept selected for evaluation was a F_2/H_2 bell chamber fabricated by the power metal process. The chamber is pressed at room temperature and sintered (free standing) in a vacuum. This fabrication method has been used on other

TABLE X

EVALUATION OF RECOMMENDED FA

	Concept A & B	Concept C	Concept D
	Fabrication Concept No. 47 & 48 (Table IV) Cast Berylco Segment with electroformed nickel closeout and double panel (oxidizer heat exchanger) - (H_2 coolant).	Fabrication Concept No. 14 (Table V) Powder Metallurgy nickel bell chamber - (H_2 coolant).	Fabrication Concept No. 67 (Table V Spun Hastelloy body with machined c passages, electroformed nickel clos cast aluminum structure (N_2H_4 coola
DEVELOPMENT RISK	Ranks average in fabrication time due to electroforming. Development required to establish casting dimensional control capability and structural integrity. Double panel must be 100 percent leak proof between propellants. No coolant passage plugging problems since passage tooling is low melting temperature alloy. Ranks low in fabrication turnaround time due to long lead time required to fabricate pattern.	No plugging problems (ranks high in plugging column; Table V) since passage tooling is low melting temperature alloy. Ranks high in fabrication time (Table V)) Ranks average on structural integrity and sealing. Ranks low on turnaround time due to need to make new mandrels and cores. Ranks low on tolerance sensitivity due to unknowns in fabricating hardware using this fabrication concept.	Ranks quite high on structural inte plugging. The only tooling in the passages is low melting temperature Ranks good on sealing, tolerance se and inspection. Ranks low on turnaround time due to new spinning die and machining temp Requires development to establish c criteria for integrally cast alumin structure. Cast aluminum structure ranks quite all areas except turnaround time wh just average (due to need to build when change contour).
RANGE OF APPLICATION	Beryllium copper has good range of application as compared to nickel (higher conductivity and comparable strength result in lower coolant ΔP at same P_c, F, etc.) Coolant enhancement due to coolant passage roughness can be readily incorporated into pattern, thus extending regenerative cooling limit. Double panel (oxid. heat exchange) extends range of application by reducing fuel ΔP and T_B. Increases performance (I_s) by (1) reduced ΔP at same P_c and/or (2) increased P_c at same pump discharge pressure. Gas/gas injection extends throttling range, improves combustion stability and allows for reduced combustor cross section.	Fabrication technology generated here will establish base for extended range of application using other materials or material combinations. Coolant enhancement due to coolant passage roughness can be readily incorporated into cores, thus extending regenerative cooling limit. Nickel coolant circuit covers full range of H_2 regenerative cooling and major portion of range with N_2H_4 cooling (Fig. 6 and 8). Ranks average on geometrical range of application due to facility limits; however applicable to most chambers within scope of program.	Hastelloy hot gas wall (higher gas temperature and lower conductivity to nickel) extends limits of regen cooling with N_2H_4 (Fig. 9). Good range of application relative size and wall thickness since cool are machined. Cast aluminum structure offers lig approach to non-tubular thrust cha construction. Range of applicatio upon system (coolant bulk temperat Technology developed under this co applicable to other concepts (mach of spinnings; integrally cast alum structure).
PRODUCTION COSTS	Potentially lowest cost approach to fabricating segments of an annular chamber of any method explored in Phase I (Appendix A). Technology also applicable to cast panel of a nonsegmented annular chamber and also results in lowest cost for this design concept (Appendix A). Additional cost payoff, e.g., increased performance, reduced injector costs, etc., due to gas-gas injection Potential for even greater cost savings by casting with internally cored passages and elimination of need for electroforming.	Potentially lowest cost approach to fabricating bell thrust chambers of all methods explored in Phase I (Appendix A).	Integrally cast aluminum structure low cost approach to adding struct chambers (Appendix A). Electroforming lowest cost approac fabrication methods investigated i coolant passage closure to slotted body (Appendix A).

TABLE XI

ION OF RECOMMENDED FABRICATION CONCEPTS (U)

Concept D	Concept E	Concept F
abrication Concept No. 67 (Table V) pun Hastelloy body with machined coolant assages, electroformed nickel closeout and ast aluminum structure (N_2H_4 coolant)	Fabrication Concept No. 20 (Table V) Powder metal tungsten bell chamber with machined slots and electroformed nickel closeout (N_2H_4 coolant).	Fabrication Concept No. 75 (Table V) Cast Berylco bell chamber with electroformed nickel closeout and integrally cast aluminum structure (H_2 coolant).
anks quite high on structural integrity and lugging. The only tooling in the coolant assages is low melting temperature alloy. anks good on sealing, tolerance sensitivity nd inspection. anks low on turnaround time due to need for ew spinning die and machining templates. equires development to establish design riteria for integrally cast aluminum tructure. ast aluminum structure ranks quite high in ll areas except turnaround time where it is ust average (due to need to build new molds hen change contour).	Ranks quite high on plugging since the coolant passage tooling is low melting temperature alloy. Ranks good on sealing, tolerance sensitivity and inspection. Ranks low on turnaround time due to need for new mandrel and machining templates. Requires development to establish fabrication technology for P/M tungsten with machined slots and ELF closeout. Requires less development than internally cored design. Technology for this concept developed by Concept C.	Ranks average in fabrication time due to electroforming. Development required to establish casting dimensional control capability and structural integrity. No coolant passage plugging problems since passage tooling is low melting temperature alloy. Integrally cast aluminum structure technology developed on Concept D is applicable here. Ranks low on fabrication turnaround time due to long lead time on pattern fabrication. Casting technology developed on Concept A/B applicable here.
astelloy hot gas wall (higher gas side wall emperature and lower conductivity compared o nickel) extends limits of regenerative ooling with N_2H_4 (Fig. 9). ood range of application relative to passage ize and wall thickness since coolant passages re machined. ast aluminum structure offers light weight pproach to non-tubular thrust chamber onstruction. Range of application dependent pon system (coolant bulk temperature). echnology developed under this concept pplicable to other concepts (machining f spinnings; integrally cast aluminum tructure).	Electroformed nickel closeout lighter weight than pressed tungsten closeout Tungsten hot gas wall (2800 F) extends range of application of N_2H_4 cooled chambers (Fig. 9). Good range of application relative to passage size and wall thickness since coolant passages are machined. Tungsten wall quite thick and heavy to achieve goal of 2800 F hot gas wall (N_2H_4 coolant limits coolant side wall to $\sim$ 600 F).	Berylco has good range of application as compared to nickel (higher conductivity and comparable strength) (Results in lower ΔP for same P_c). Double panel development of concept A/B applicable here. Berylco can not be used with Amine coolants due to lack of compatibility.
Integrally cast aluminum structure extremely ow cost approach to adding structure to hambers (Appendix A). lectroforming lowest cost approach of all abrication methods investigated for adding oolant passage closure to slotted inner ody (Appendix A).	Low cost approach to fabricating "hot gas wall" concept. Electroforming lowest cost approach of all fabrication methods investigated for adding coolant passage closure to slotted inner body. Powder metallurgy extremely low cost approach to fabricating thick wall inner body.	Potential for extremely low production cost comparable to Concept C (Appendix A). Cast aluminum structure is lowest cost approach of all methods investigated for adding additional light weight structure to chamber (Appendix A). Electroforming lowest cost approach of all fabrication methods considered for adding coolant passage closeout to slotted chamber. Potential for even greater cost savings by casting with internally cored passages, thus eliminating need for electroforming.

components at Rocketdyne and is potentially the lowest cost fabrication technique for bell chambers of any investigated in Phase I. The process is amenable to fabricating the complete thrust chamber (coolant circuit, flanges and manifolds) as a unit. Also the technique can be used on any material or material combinations which are available as a powder.

(U) During Phases II and III only the coolant circuit and structural shell were fabricated by the powder metal process; machined flanges and manifolds were subsequently welded in place. The fabrication development effort completed here established the fabrication technology base required for later extension of the process to other materials and to fabricating the complete chamber as a unit.

(U) Spun Hastelloy or Inco 625 Liner with Machined Coolant Passages, Electroformed Nickel Closeout and Integrally Cast Aluminum Structure. The second concept selected for experimental evaluation was a CPF/N_2H_4 bell chamber which incorporated a spun INCO 625 or Hastelloy-C liner with machined passages, an electroformed nickel closure and an integrally cast aluminum shell around the chamber. Use of Inco 625 or Hastelloy-C as the hot gas wall material and operation at a gas side wall temperature of 2000 F, extends the range of application of N_2H_4 cooled chambers beyong the regenerative cooling limits of conventional nickel walled chambers that are limited to a hot gas wall temperature of 1600 F.

(U) Also, the integrally cast aluminum structure offers a low cost and lighter weight approach (as compared to all nickel or wire wrap and braze) to adding structure to chambers. The cast aluminum experience developed on this concept is applicable to the powder metal bell chamber or any other future concept where the system operating parameters

(coolant bulk temperature and back side wall temperature) do not preclude the use of aluminum as a structural member.

(U) Cast Beryllium Copper Segment with Electroformed Nickel Closeout and Oxidizer Backup Panel. The third concept selected for evaluation, was a segment of F_2/H_2 annular chamber which incorporated multiple layers of coolant passages on one side of the chamber to investigate an oxidizer heat exchange in this application. The selected fabrication approach was to cast the complete segment (contoured walls and supersonic baffles) open faced (hot gas .. and coolant passage lands) and then electroform the closure and oxidizer heat exchange panel. Casting of segments offers a potentially low cost approach to fabricating annular chambers. Also, the potential exists for reducing the fabrication costs even lower by internally coring of the coolant passages such that electroforming is no longer required to close out the fuel coolant passages.

(U) The oxidizer heat exchange technique offers significant system payoffs. The primary coolant (hydrogen) bulk temperature and pressure drop are reduced allowing for increased specific impulse (higher P_c and ϵ) with the same hydrogen pump discharge pressure or operation at the same chamber pressure and area ratio with reduced pump discharge pressure (this will also result in increased performance due to the reduced turbine power requirements).

(U) The gasification of the oxidizer (fluorine) results in gas-gas injection with a subsequent increase in performance and an extended throttling range since the injection ΔP reduces approximately linearly with P_c (with liquid injection the ΔP reduces as a square of the change in P_c, i.e., flowrate).

TEST HARDWARE DESCRIPTION

(U) After selection of the three fabrication concepts for experimental evaluation in Phases II and III, the physical size and operating parameters of the three were established. To provide meaningful fabrication and test data and yet to maintain a reasonably small size on the hardware, while remaining consistent with the sizes of hardware on other programs being developed for and by the AFRPL, the geometry shown in Figs. 32, 33 and 34 was selected. Operating parameters and basic design criteria are discussed in detail in the Phase III section.

(C) The bell chamber size is consistent with the secondary engine on contract F04611-67-C-0116 and with injectors being developed by the AFRPL. The annular chamber segment is a straight, three-inch long section of a nominal 30,000-pound thrust annular chamber under development by Rocketdyne for the AFRPL (F04611-67-C-0116). This segment duplicates the full scale hardware in all dimensions except arc length.

(U) LF_2/GH_2 propellants were to be used in all three concepts to provide the combustion environment with both bell thrust chamber concepts designed to use the same injector. The powder metal nickel bell chamber was to be cooled with GH_2 while the spun INCO 625 bell chamber was water cooled (simulating the amine fuels). The cast segment was to be GH_2 cooled in the primary circuit with LF_2 as the coolant in the heat exchange panel.

(U) Also, all hardware was to be designed with a bypass coolant circuit such that the operation of the injector was independent of the coolant; allowing independent variation of each as required during testing.

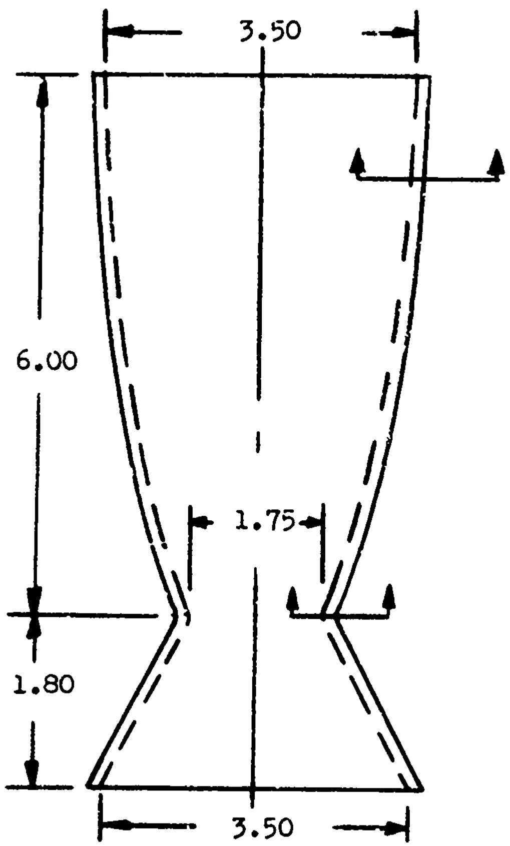

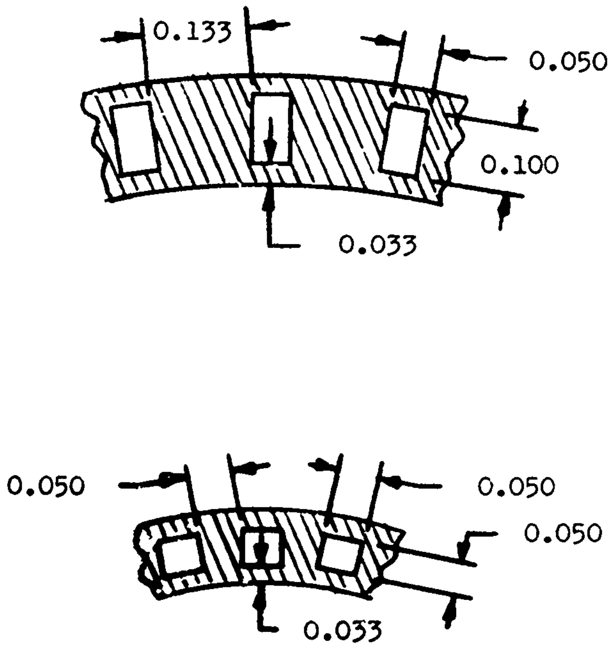

Thrust (to ϵ = 60) lbs	3300
Chamber Pressure, psia	750
Propellants	LF_2/GH_2
Coolant	GH_2
Mixture Ratio	12:1
Maximum Hot Gas Wall Temperature, F	1600

Figure 32. Design Criteria for Powder Metal Nickel Bell Chamber. (U)

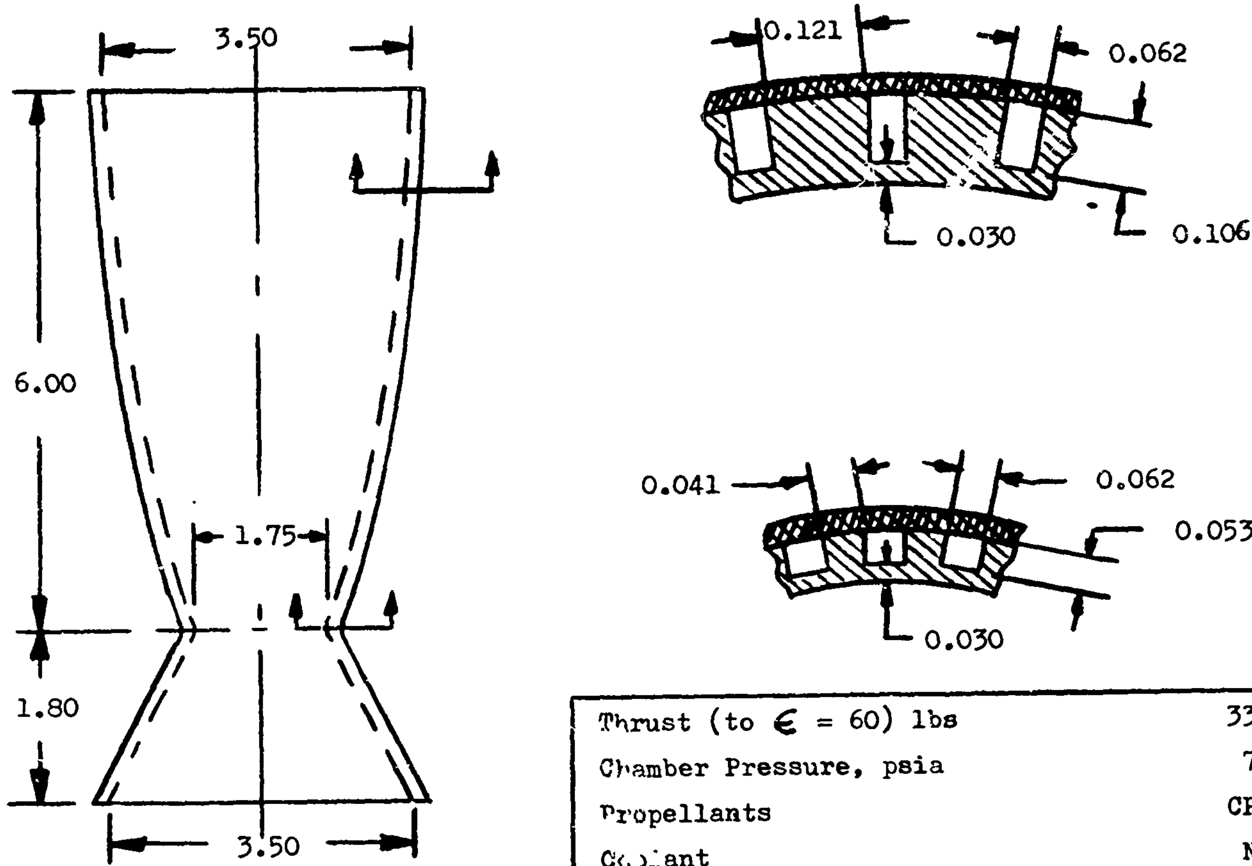

Thrust (to ϵ = 60) lbs	3300
Chamber Pressure, psia	750
Propellants	CPF/N_2H_4
Coolant	N_2H_4
Mixture Ratio	2.7
Maximum Hot Gas Wall Temperature, F	2000

Figure 33. Design Criteria for Spun Bell Chamber (U)

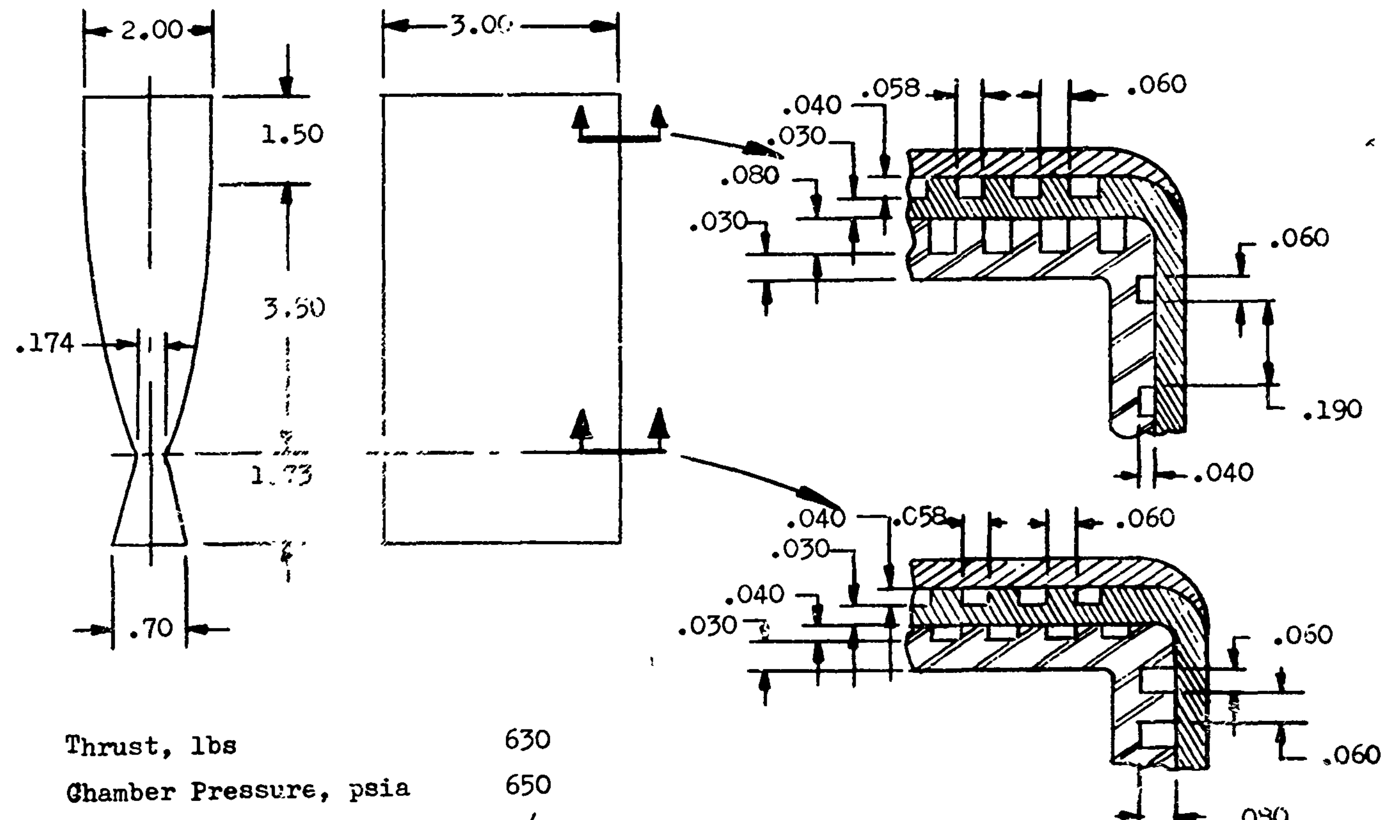

Thrust, lbs	630
Chamber Pressure, psia	650
Propellants	LF_2/GH_2
Coolant	GH_2 (Primary)
	LF_2 (Secondary)
Mixture Ratio	12:1

Figure 34. Design Criteria - Cast BeCu Segment. (U)

PHASE II FABRICATION PROCESS EVALUATION

(U) The objective of Phase II was to experimentally evaluate, in the laboratory, the selected fabrication concepts. This evaluation was to establish process parameters, structural and heat transfer limits (dimensional repeatability) through destructive testing and to establish nondestructive inspection techniques applicable to the Phase III hot firing hardware.

(U) To accomplish these objectives test panels, full-size sections and complete chambers and/or segments representing each of the three concepts were fabricated and laboratory tested.

CONCEPT NO. 1 - POWDER METAL NICKEL BELL CHAMBER

(U) The first bell chamber fabrication concept selected for experimental evaluation in Phase II utilized the powder metal fabrication technique for producing an internally cored (regeneratively cooled) thrust chamber using high purity nickel powder.

(U) Fabrication of internally cored hardware by Rocketdyne's powder metal process is a two step powder pressing operation in a hydroclave (room temperature pressing) followed by a sintering (high temperature) operation with all tooling removed and the part free standing in the furnace (no pressure applied). This fabrication sequence, which was shown schematically in Fig. 1, is discussed below.

(U) Initially, powder is packed and pressed around a hard steel mandrel which forms the internal diameter of the chamber. The outer surface of the as-pressed liner is then machined to the required hot gas wall thickness.

Soft tooling which forms the coolant passages is then stacked around the liner, additional powder is packed to form the lands and closure of the coolant circuit, and the entire unit pressed at a higher pressure. The as-pressed chamber is then machined on the outer surface, the hard mandrel removed, the coolant passage tooling flushed out with hot water and steam and the entire unit sintered as a free standing part in the furnace. Wrought nickel 200 flanges are then electron beam welded in place to complete the chamber.

(U) The operating parameters of the sintered nickel bell chamber, as well as a schematic representation of the chamber geometry as established by the preliminary heat transfer and structural analyses, is shown in Fig. 32.

(U) The detailed heat transfer and structural analyses of this concept performed using experimentally determined material properties are presented in the Phase III section.

Powder Blend Selection

(U) The nickel powder blend used here had been previously established on a company funded program. This blend is processed by blending and pressing into bars a mixture of 80 percent medium mesh (7-9 microns) powder with 20 percent fine mesh (2-3 microns) powder. These bars are then crushed, pulverized and screened to a 50-150 micron mesh and blended (in an 80-20 percent ratio) with additional fine powders to form the powder blend to be used in making the hardware.

(U) The resulting powder blend has very high purity, good compaction, ductility and flowing parameters (required for high fill densities), excellent sinterability, and good green strength allowing precision machining of as-pressed hardware to a very thin layer.

Fabrication Development

(U) Using this powder blend as a starting point, the Phase II fabrication development effort was initiated to evaluate pressing and sintering parameters to determine material physical properties, dimensional repeatability and structural integrity of sintered nickel hardware. Also, this development hardware was to be used to establish non-destructive inspection techniques for the Phase III hot firing hardware.

(U) Material Properties. Initially, a solid wall cylinder (Fig. 35) approximately 3-1/2 inches in diameter by 3 inches long was pressed at 50,000 psig, sintered at 2200 F for two hours, and sectioned for thermal conductivity and elevated temperature tensile testing.

(U) Thermal conductivity measurement of sintered nickel was determined by taking small (0.25 dia. by 0.060 to 0.125 long) bars from this cylinder, measuring thermal diffusivity on the apparatus shown in Fig. 36 and converting to thermal conductivity by means of the equation:

$$k = \alpha C_p \rho$$

where

k = thermal conductivity
α = thermal diffusivity
C_p = specific heat
ρ = density

Results are shown in Fig. 37 compared to experimentally determined wrought nickel 200 data and to National Bureau of Standards data for 99.94 percent pure nickel.

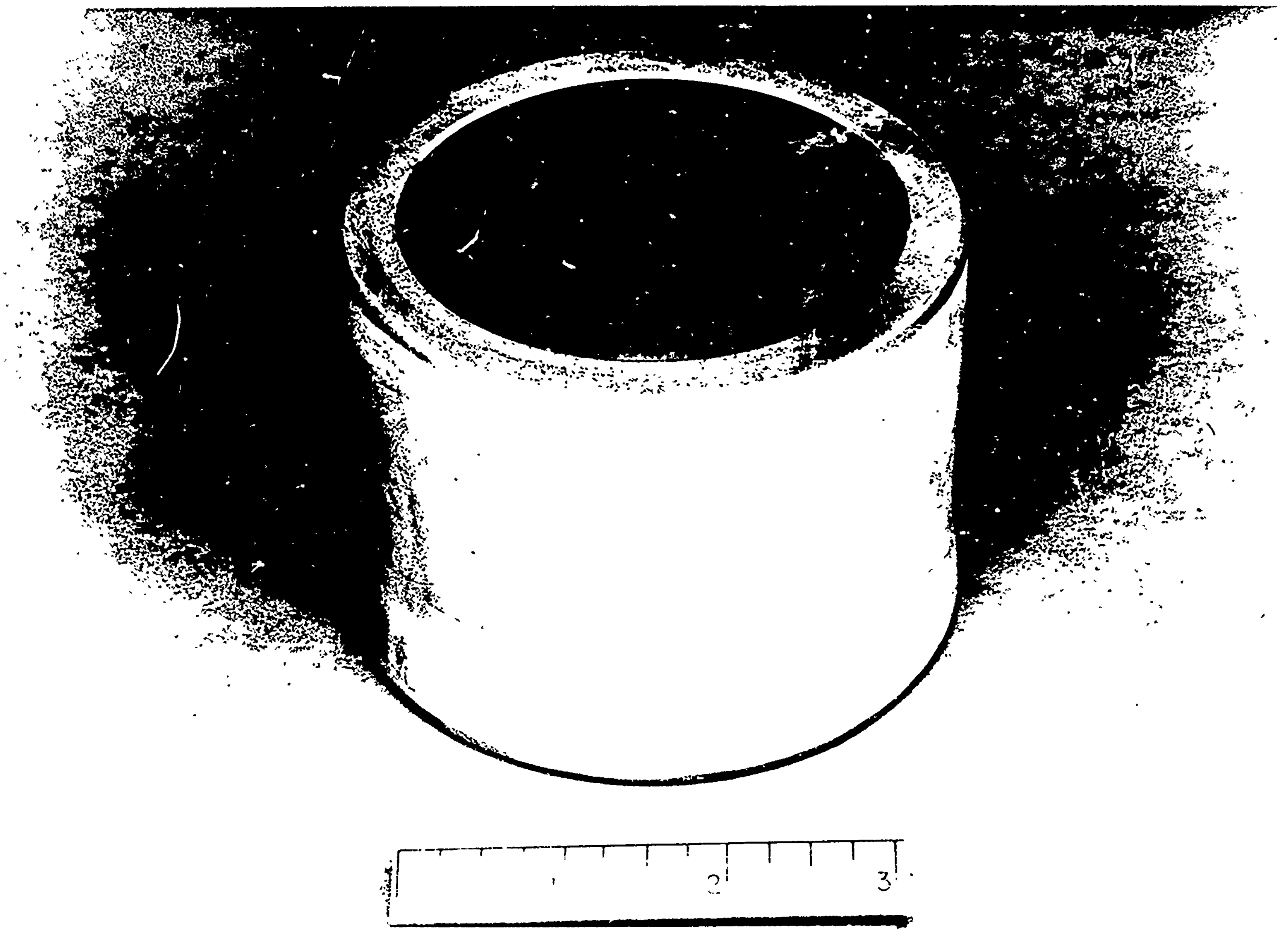

Fig. 35. Solid Wall Powder Metal Cylinder (U)

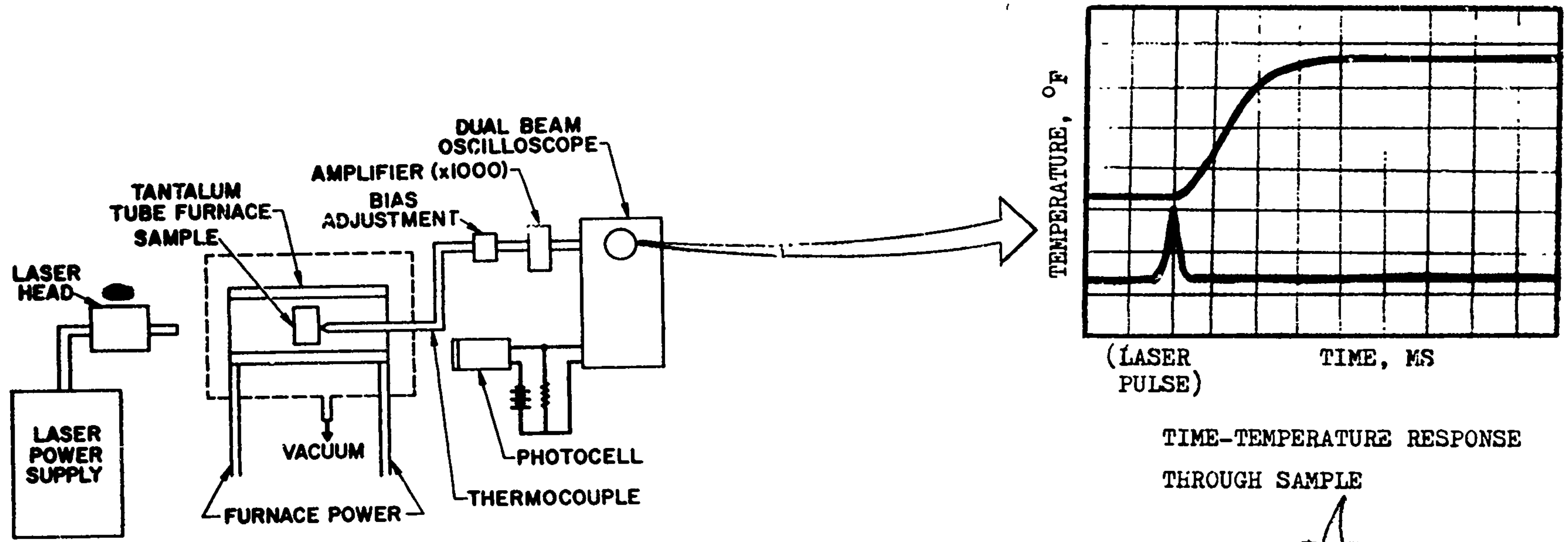

TIME-TEMPERATURE RESPONSE THROUGH SAMPLE

DETERMINATION OF THERMAL DIFFUSIVITY

CALCULATION OF THERMAL **CONDUCTIVITY** AS FUNCTION OF THERMAL DIFFUSIVITY, SPECIFIC HEAT, AND DENSITY

PROCEDURE:

-- MOUNT SAMPLE (1/4 DIA x .080 - .160 LENGTH)
-- HEAT FURNACE TO DESIRED TEMPERATURE
-- SINGLE LASER PULSE TO FRONT FACE OF SAMPLE

Figure 36. Elevated Temperature Thermal Conductivity Tests. (U)

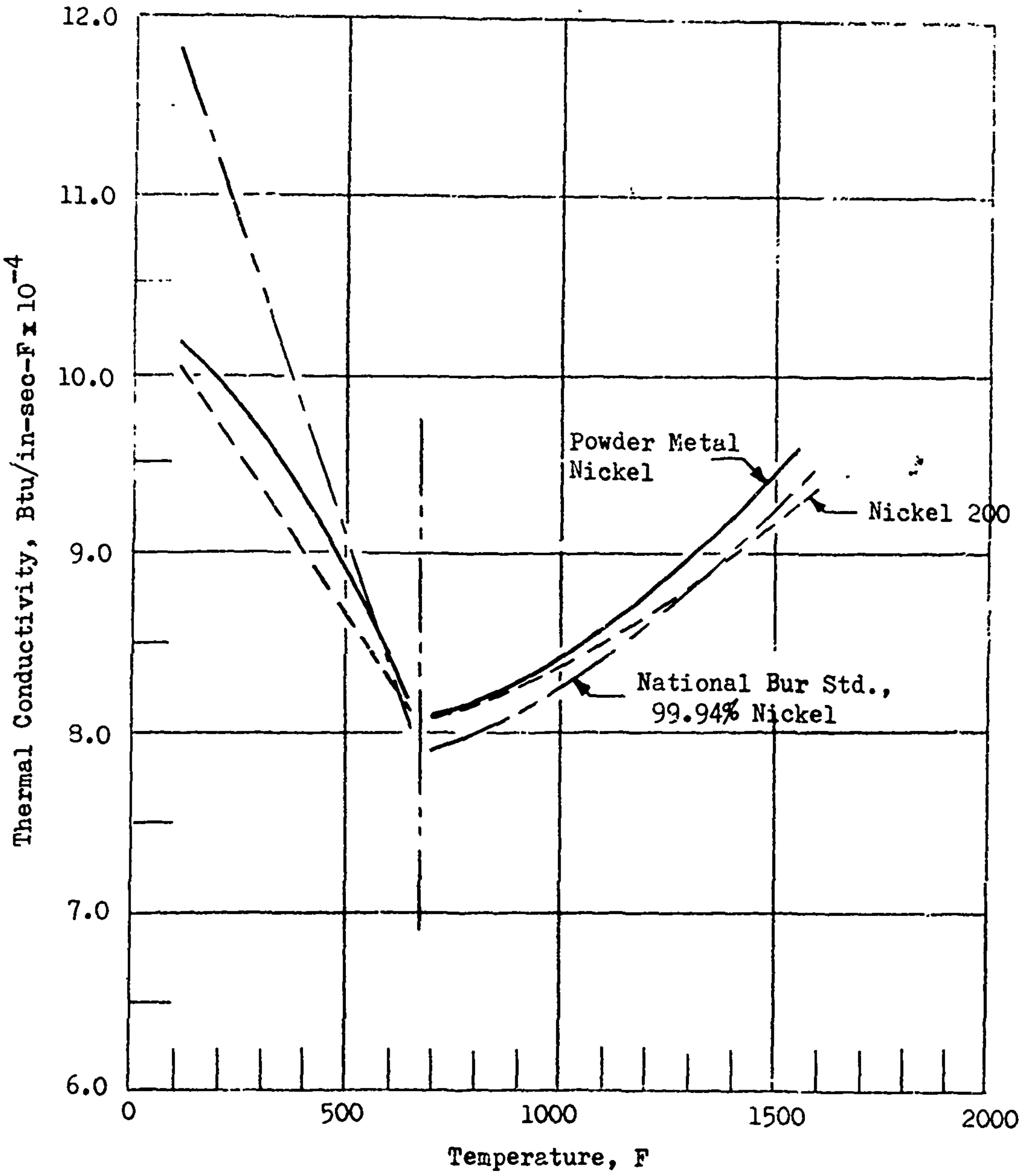

Figure 37. Thermal Conductivity of Pure Nickel. (U)

(U) Standard ASTM tensile bars were machined from the solid wall cylinder and tested at elevated temperature to determine physcial properties of sintered nickel. The tests, showed tensile properties to be quite similar to wrought, annealed nickel 200 (Fig. 38). Ductility of the sintered nickel was also good, ranging between 40 and 50 percent over the entire temperature range (Fig. 38).

(U) Coclant Passage Coring Study. The powder metal process utilizes soft tooling (cores) to form the coolant passages during the powder packing and room temperature pressing operation. This tooling is subsequently removed from the as-pressed hardware prior to sintering. Due to the nature of the powder metal hardware in the as-pressed condition (low strength and density) and in the interest of low cost and minimum fabrication time, it is desirable to use a low melting point, easily removable material to form these cores. This makes the Cerro-alloys prime candidates for this tooling due to the low melting temperatures and ease of workability. Typical alloys and their properties are listed in Table XII.

TABLE XII

TYPICAL CANDIDATE CERRO-ALLOYS (U)

Name	Bi	Pb	Sn	Cd	In	Others	Melting Range, F	Yield Temp, F
CERROLOW-105	42.91	21.70	7.97	5.09	18.33	4.00 HG	100-110	105
CERROLOW-136	49.00	18.00	12.00	--	21.00	--	136-136	136
CERROLOW-140	47.50	25.40	12.60	9.50	5.00	--	134-149	140
CERROBEND	50.00	26.70	13.30	10.00	--	--	158-158	158
CERROLOW-174	57.00	--	17.00	--	26.00	--	174-174	174
CERROMATRIX	48.00	28.50	14.50	--	--	9.00 SB	217-440	241
CERROTRU	58.00	--	42.00	--	--	--	281-281	281
CERROCAST	40.00	--	60.00	--	--	--	281-338	281

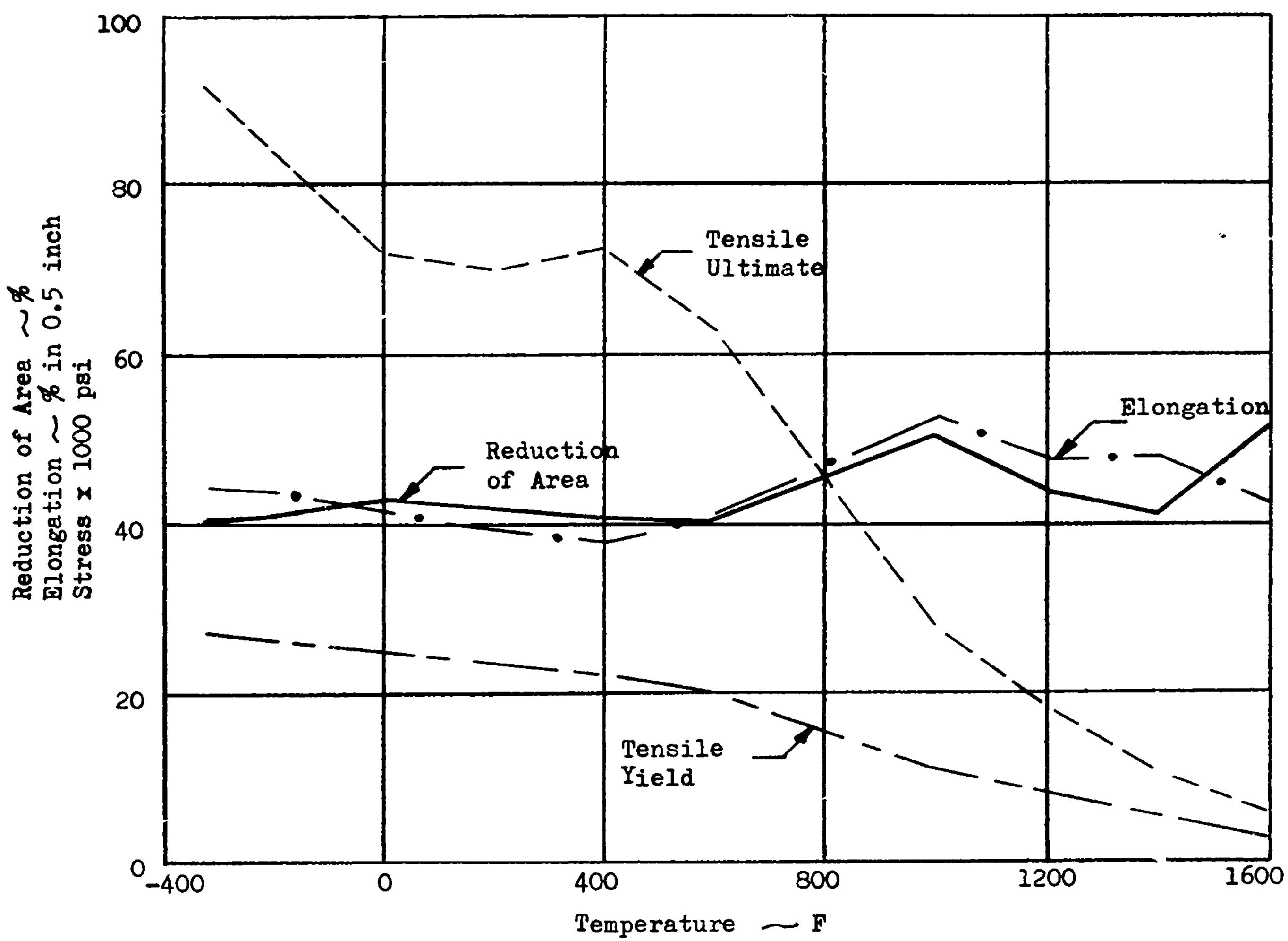

Figure 38. Short Time Tensile Properties of Powder Metal Nickel. (U)

(U) During the course of the company funded work on the powder metal process prior to this program, Cerrocast had been selected as the prime candidate to be used to form these cores. However, fabrication of the first internally cored cylinder using Cerrocast to form the coolant passages showed that all the Cerrocast was not removed from the passages prior to sintering, resulting in infiltration of the Cerrocast into the nickel during the sintering cycle with a subsequent embrittlement of the nickel. A study was then initiated to determine a more suitable coring material which could be completely removed from the coolant passages prior to sintering to eliminate this infiltration and embrittlement. Results showed that Cerrolow 136, which melts at 136 F, could be flushed with hot water and 100 percent removal obtained from the as-pressed hardware. Subsequently, a number of cylinders and chambers were fabricated verifying this removal technique for the Cerrolow 136.

(U) Structural Integrity and Dimensional Repeatability. The next step in the fabrication development study of the powder metal process consisted of fabricating, pressure testing and/or sectioning internally cored cylinders to evaluate dimensional results and structural integrity of sintered nickel hardware. The Cerrolow-136 cores deform considerably during pressing, thus the first internally cored cylinder fabricated using Cerrolow-136 cores (pressed at 50,000 psig and sintered at 2200 F for two hours) included a number of core configurations, (Fig. 39) to explore effects of core geometry, dimensional repeatability in the passages and verify core removal. Post-sintering sectioning of the cylinder showed that the Cerrolow-136 was successfully removed prior to sintering and that rectangular passages with small corner radii resulted in good dimensional repeatability.

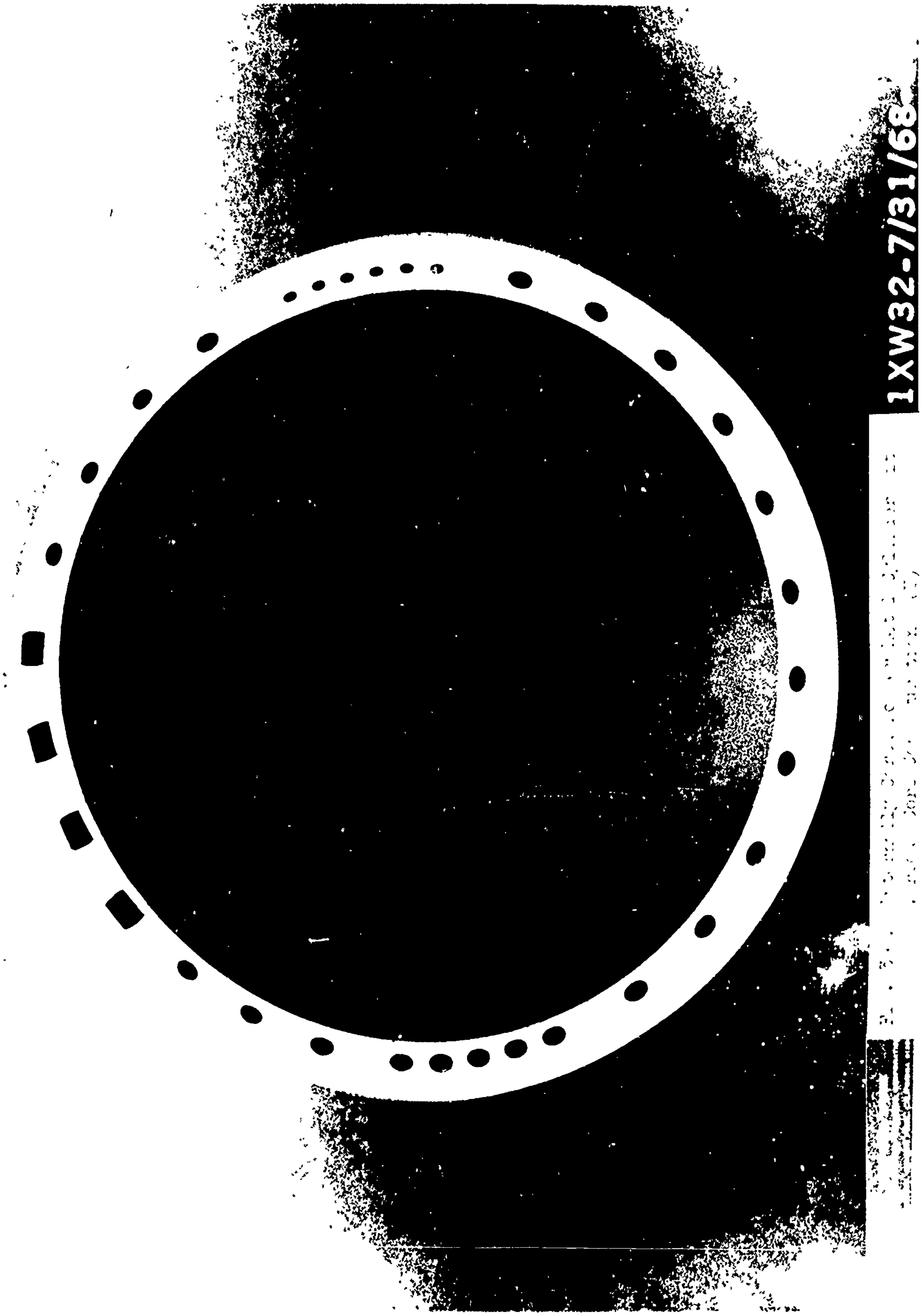
1XW32-7/31/68

(U) Data from this cylinder showed approximately 9 percent shrinkage for internally cored hardware. Also, an average Cerrolow-136 core deformation of 28 percent reduction in height and 7 percent increase in width was measured. These parameters were further verified by fabricating another internally cored cylinder and then used in the tooling design for the regeneratively cooled chambers (Fig. 40).

(U) After sintering, a wrought nickel flange was electron beam welded to a section of this sintered nickel cylinder to provide a pressurant supply manifold and to evaluate electron beam welding as a suitable technique for joining wrought nickel to sintered nickel. The manifold, weld joint and sintered nickel coolant passages were successfully pressure tested to 18,500 psig, demonstrating very good structural integrity.

(U) Subsequent sectioning and dimensional analysis of this cylinder showed good dimensional repeatability of the coolant passages and verified the shrinkage values which could be expected during sintering of internally cored hardware.

(U) This cylinder had been fabricated with an inner wall thickness and coolant passage spacing greater than that planned for the hot firing hardware. Consequently, another internally cored cylinder with a wall thickness and coolant passage cross section and spacing identical to the combustion zone dimensions of the full-size chamber was fabricated. This cylinder was pressure tested to 7500 psig, a value in excess of three times the design proof pressure requirement of the hot firing hardware. Dimensional results of this cylinder were quite good reflecting tolerances of $\pm$ 0.003 inches in passage and wall thickness dimensions.

Figure [illegible]. Internally Cored Powder Metal Cylinder with Various Sizes of Rectangular Cores. (U)

(U) Based on the experimental work on the internally cored cylinders, fabrication process parameters were established for the internally cored (regeneratively cooled) bell chambers. These parameters included a part shrinkage of 8.5 percent axially, 9.0 percent radially and 7 percent in wall thickness during sintering. Also post sintered densities ranged between 94.7 and 95.9 percent of theoretical. The pressing and sintering parameters were established as follows:

Press liner at 30,000 psig
Press complete chamber at 55,000 psig
Sinter at 2300 F for 2 hours

(U) Tooling Fabrication. The internal mandrel is a reusable item fabricated of tool steel and produces the chamber internal contour and surface finish. The mandrel is split in the throat plane for ease of removal after pressing and machining and prior to sintering.

(U) The Cerrolow cores which form the coolant passages are expendable items fabricated by casting into a split aluminum die. A number of completed cores are shown in Fig. 41. Numerous cores were fabricated using this die with satisfactory results, however for further improvement of core quality, it is recommended that on future programs steel dies be used to improve dimensional repeatability and tool life.

(U) Solid Wall Bell Chamber. Following completion of the internally cored cylinder effort, two full-size solid-wall bell chambers were fabricated to verify the pressing and sintering parameters and to proof the internal mandrel. These chambers were pressed at 55,000 psig, sintered at 2300 F for two hours and had average densities of approximately 96 percent of theoretical. During sintering of powder metal hardware, approximately 9 percent shrinkage occurs in the radial direction, resulting in

Fig. 41. Typical Cerrolox-1% Cores (U)

considerable movement of the hardware with respect to the base plate in the sintering furnace. Sintering of the first solid-wall bell chambers resulted in considerable distortion of the injector end of the chamber which was setting on the furnace base plate.

(U) This was attributed to the friction between the chamber and the furnace base plate, restricting movement of the chamber as it was shrinking. This was alleviated on the next solid wall chamber and all subsequent hardware by placing the as-pressed chamber on an as-pressed nickel plate which in turn rested on the furnace base plate. During sintering this nickel plate shrinks along with the chamber, minimizing the relative movement between the chamber and the plate. Results showed this approach to be highly satisfactory with no further out-of-roundness problems. This solid wall chamber is shown in Fig. 42.

(U) <u>Regeneratively Cooled Thrust Chambers</u>. Using the parameters established on the internally cored cylinders and the tooling proofed on the solid wall bell chambers, fabrication was initiated on the first of the internally cored bell chambers. First, the liner was pressed at 30,000 psig and machined to the prescribed thickness (Fig. 43). The Cerrolow cores were then positioned on the liner and the powder for the lands and outer shell packed in place. A typical liner, with cores in position along with the tooling used to locate and retain the cores is shown in Fig. 44. A partially packed chamber with the outer layer of powder packed over part of the combustion zone is shown in Fig. 45.

(U) The entire chamber, encapsulated in a PVC bag to retain the powder and to seal the powder from the pressurizing fluid (glycerin) in the press was then pressed at 55,000 psig. The as-pressed chamber is shown in Fig. 46. Subsequently, the outer surface of this chamber was machined, the tooling removed and the chamber sintered at 2300 F for 2 hours. Average density was 95.2 percent. The chamber, after sintering, is shown in Fig. 47.

Fig. 15. [illegible]

(This page is Unclassified)

CONFIDENTIAL

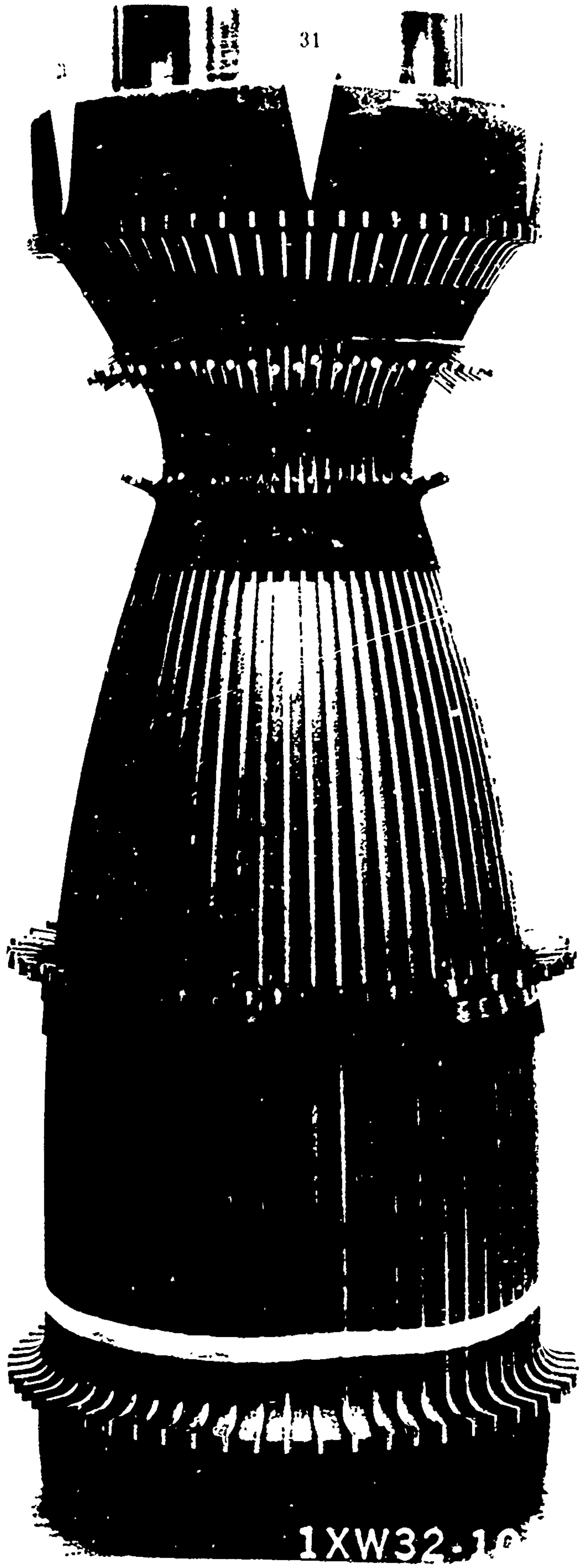

Fig. 44. [illegible]

CONFIDENTIAL

Fig. 45. [illegible] - powder [illegible] (U)

CONFIDENTIAL

Fig. 46. As-Pressed Powder Metal Nickel Bell Chamber Prior to Contour Machining. (U)

CONFIDENTIAL

CONFIDENTIAL

(U) Post-sintering inspection revealed what appeared to be a "contaminant" on the outer surface of the chamber (showing up as a shiny surface in Fig. 47). Chemical analysis showed this to be pure nickel, resulting from overheating and melting of localized areas of the chamber during the sintering cycle.

(U) This was attributed to the fact that the chamber is quite large in comparison to hardware normally sintered in the existing laboratory furnace and due to this large size receives an irregular heat input from the heating elements. This problem was corrected on subsequent chambers by placing the chamber inside a refractory shield such that heating is accomplished by reradiation from this shield resulting in a more uniform temperature gradient on the chamber and preventing temperature overshoot in localized areas. Additionally, the temperature was monitored on the shield and the inside diameter of the chamber to assure that the temperature did not exceed 2300 F at any time during the sintering cycle. This procedure was established and verified by exposing this regeneratively cooled chamber and the second solid wall chamber to simulated sintering cycles with adequate instrumentation on the chamber and the shield.

(U) Subsequently, this chamber was sectioned for dimensional analysis (Fig. 48). Results were quite encouraging, with wall thickness tolerances of $\pm$ 0.003 inches and coolant passage cross section dimensional tolerances of $\pm$ 0.003 in passage height and $\pm$ 0.002 in width. However, the hot gas wall thickness was below the design value. Detailed checkout of the machining templates and the tracer lathe used to turn the inner liner to the prescribed diameter showed this thinner wall to be a result of the machining, not the sintering, operation.

Fig. 43. [illegible] (U)

CONFIDENTIAL

(U) A longitudinal section of this chamber (Fig. 49) was pressure tested to determine structural integrity. Two adjacent passages in this section were proof pressure tested to 19,500 psig, at which time yielding of the hot gas wall could be seen. Pressure was then increased to 23,000 psig where leakage occurred between a pressurized and an unpressurized passage (a condition that would not occur in the hot firing hardware). Additionally, two passages located under a visual defect (apparent thin wall) in the nozzle section were pressure tested to 8000 psig, when a pin hole leak occurred in the defective area. These results were highly encouraging and verified the structural integrity of sintered nickel hardware in the configuration of interest for the hot firing hardware of Phase III.

(U) The post sintering inspection of this chamber revealed some indications of localized "blistering" of the hot gas wall coincident with the coolant passages. This was attributed to the thinner-than-design hot gas wall thickness, uneven deformation of the hot gas wall by the Cerrolow-136 cores during pressing, and/or excessive temperature during the sintering cycle.

(U) Consequently, it was decided to modify the fabrication procedure on the next chamber. To increase the density and strength of the as-pressed liner, thus increasing its resistance to deformation by the Cerrolow-136 cores during the second pressing, the pressing pressure of the liner was increased to 40,000 psig. Also, the Cerrolow-136 core casting technique was refined to produce smoother and more uniform cores.

(U) Using these parameters the liner for the next chamber was pressed and machined, the Cerrolow-136 cores stacked and the outer shell packed and pressed at 55,000 psig. After tooling removal, the chamber was sintered at 2300 F for 2 hours with the refractory shield placed around the

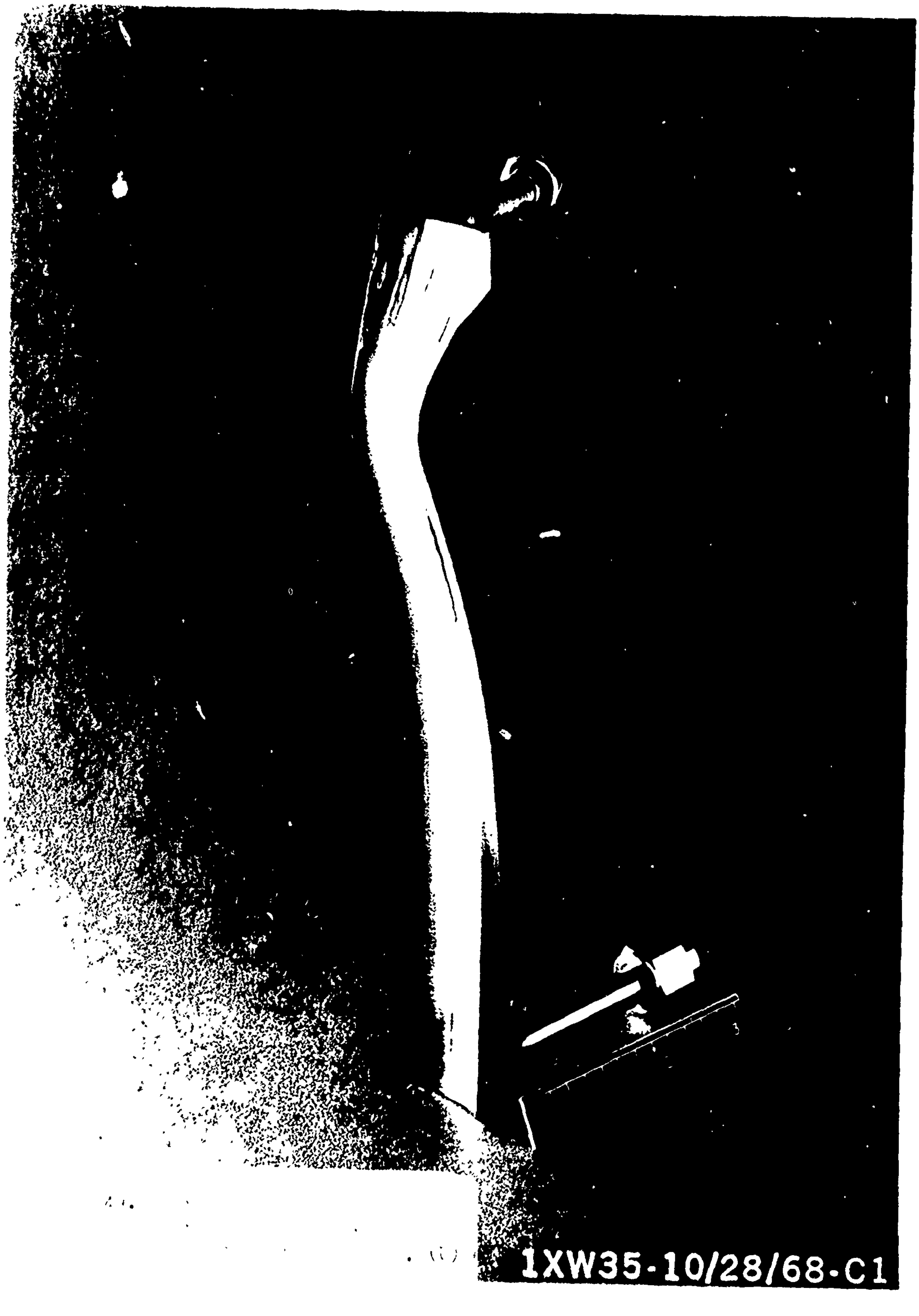
1XW35-10/28/68-C1

chamber in the furnace to more uniformly distribute the heat during the sintering cycle. Post sintering density of this chamber was 94.0 percent of theoretical, the lowest value measured to date.

(U) Post sintering evaluation of this chamber showed no evidence of blistering on the hot gas wall or overheating on the outer surface, indicating that modifications had worked as planned. Also, chamber interior dimensions were quite good.

(U) Wrought nickel 200 flanges were then electron beam welded to the sintered nickel chamber in preparation for pressure testing (Fig. 50).

(U) Pressure testing of the coolant passages revealed an inadequate bond between the first (liner) and second pressings (shell) as evidenced by the fact that separation occurred at pressures less than 850 psig. As discussed above, the liner had been pressed at 40,000 psig as compared to 30,000 psig on the first internally-cored chamber while the outer shell was pressed at 55,000 psig in both cases. Subsequent examination showed that with this lower pressure differential between the two layers, very little bonding takes place during the sintering cycle. The interior of the chamber was successfully proof pressure tested at 1400 psig to verify the structural integrity of the outer shell.

(U) Subsequently, this chamber was sectioned to determine dimensional repeatability. Results (Fig. 51) were excellent on both the hot gas wall and the passage cross section.

(U) In reviewing results on all powder metal nickel hardware fabricated and evaluated to this point, it was evident that good dimensional repeatability was achievable with reasonable care during liner machining, core stacking and powder packing. Also, to obtain good structural integrity

DESIGN

THROAT

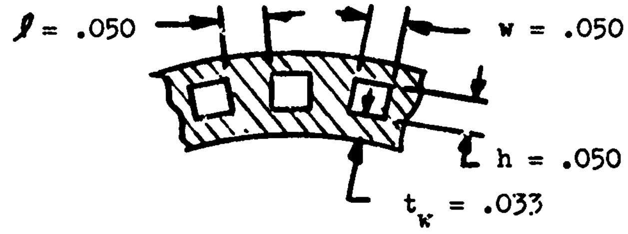

CHAMBER

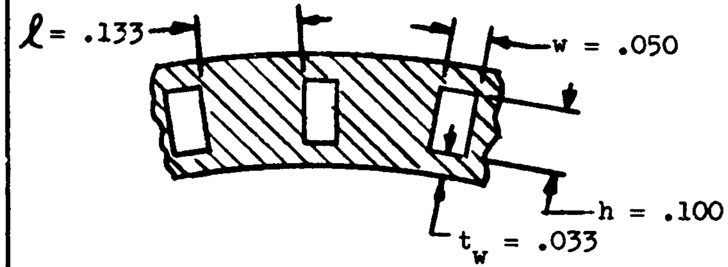

MEASURED

w	=	.052 - .055
h	=	.045 - .047
ℓ	=	.040 - .050
t_w	=	.036

w	=	.057 - .062
h	=	.076 - .078
ℓ	=	.130 - .151
t_w	=	.034

Figure 51. Dimensional Results of Internally Cored Powder Metal Bell Chamber. (U)

the liner should be pressed at 30,000 psig, the entire chamber pressed at 55,000 psig and sintering accomplished at 2300 F. Finally, the better quality cores and use of the refractory shield during sintering produced good quality chambers with no blistering on the hot gas surface.

(U) Using these parameters, the third internally-cored chamber was fabricated. Visual inspection of the green pressing after core removal and just prior to sintering revealed a small circumferential hair-line crack extending over two passages on the hot gas wall in the nozzle downstream of the throat. A small amount of copper-silver braze alloy was preplaced over the crack and successfully prevented propagation of the crack during sintering. This was the first occurrence of cracking of powder metal hardware fabricated on this program, and a review of the fabrication process uncovered no apparent causes for this crack. It was decided that this was a random failure with little likelihood of recurrence on subsequent hardware. After sintering, this crack was repaired by furnace brazing at 1950 F using a silver-palladium alloy. The average density of the chamber was approximately 95 percent of theoretical.

(U) The coolant passages were pressure tested to 1500 psig at which time a bulge approximately one-half inch in diameter occurred in the hot gas wall downstream of the throat. This bulge occurred in the same plane as the crack in the hot gas wall which had been sealed by brazing but removed about one inch circumferentially. (Subsequent sectioning and analysis of this bulge revealed contamination of the bond joint between the first-to-second layer of pressings by the braze alloy used to repair the crack in the liner; resulting in a reduced bond joint strength). The braze seal in the crack successfully withstood this pressure. This area of the coolant passages (from the throat plane to the exit) was then sealed off and the remainder of the chamber coolant circuit pressure tested to 5100 psig ($\sim$ 2.5 times the design proof pressure of 2120 psig

required for the hot firing hardware of Phase III). These tests demonstrated that the established parameters produced chambers wi .ı good structural integrity and lent confidence that a fabrication technology base had been established that would allow the fabrication of hot firing hardware for Phase III.

Non-Destructive Inspection Techniques

(U) During the course of the Phase II effort various non-destructive inspection techniques were found to be most appropriate in verifying the structural integrity and dimensional repeatability of sintered nickel hardware. These included; radiographics, density measurements, dimensional checks, hydrostatic proof pressure tests and water flow calibration of each passage.

(U) Successive dimensional checks of the internal mandrel, as-pressed liner, machined liner and outer layer and of the Cerrolow-136 cores were used to establish basic dimensional results. Also, X-ray of the as-pressed chamber just prior to sintering verified 100 percent core removal while X-ray of the sintered chamber verified no gross variations in coolant passage spacing. Average density measurements of the sintered chamber were compared to density values of destructively tested samples to verify attainment of satisfactory material properties. Finally, hydrostatic proof pressure tests of the coolant circuit and chamber interior, followed by water flow calibration of each coolant passage, were the final verification of the structural integrity and dimensional repeatability of the process.

Conclusions and Recommendations

(U) The Phase II fabrication development effort established a high confidence level that the powder metal process could be successfully used to produce hot-firing hardware for Phase III. This confidense level was attained by having successfully demonstrated and/or verified dimensional repeatability, structural integrity, and material properties for sintered nickel hardware. Recommended process parameters were (1) press first layer at 30,000 psig, (2) press second layer at 55,000 psig, and (3) sinter at 2300 F for 3 hours. Also, non-destructive inspection techniques to be used during the fabrication of the Phase III chamber included: progressive dimensional checks, average density measurement, X-ray to verify core removal and passage spacing, proof pressure tests and water flow calibration of the coolant passages.

CONCEPT NO. 2 - BELL CHAMBER WITH SPUN LINER, MACHINED PASSAGES AND ELECTROFORMED NICKEL CLOSURE

(U) The second bell chamber fabrication concept selected by the AFRPL for experimental evaluation in Phase II employed a spun and machined liner with an electroformed nickel closure. This fabrication sequence, illustrated in Fig. 2, is discussed below.

(U) Initially, a flat plate is spun into the chamber shape to form the liner. After annealing, the liner is machined on the I.D. and O.D. to the prescribed thickness. The coolant passages are machined into the outer surface of the spinning, and nickel is electroformed onto the outer surface to close off the coolant circuit and provide necessary structure to withstand chamber pressure loads. Subsequently, flanges and manifolds are electron beam welded in place.

(U) The chamber was designed to be regeneratively cooled with N_2H_4 (representing potential advanced regeneratively cooled engines). The operating parameters and physical size of the chamber are shown in Fig. 33. The detailed heat transfer and structural analyses of this chamber are presented in the section entitled Phase III Design and Performance Evaluation.

Fabrication Development

(U) The Phase II fabrication development associated with this concept is discussed in the following paragraphs.

(U) Spinning. Two materials (INCO 625 and Hastelloy C) were initially selected for evaluation as potential candidates for the hot gas wall.

(U) The design criteria of this concept (Fig. 33) reflected the need for a thick wall (0.136 inch), small diameter (1.75 to 3.50 inch inside diameter) liner. Three techniques were initially considered for spinning of the INCO 625 and/or Hastelloy C into the required chamber shape. These included:

1. Buying thick wall seamless tubing (3.50 diameter by 3/16 wall thickness) and form spinning into the chamber shape,
2. Rolling and butt welding plate stock into a cylinder and form spinning into the chamber shape, and
3. Form spinning a flat plate into the chamber shape.

(U) After considerable evaluation, including discussions with various tube suppliers and spinning vendors, the last approach (form spinning of a flat plate) was selected. This technique offers the most potential in that parent metal is used throughout, and it is amenable to any redesign such as a wall thickness or diameter change with a minimum affect on fabrication schedule during the development program.

(U) Use of thick wall seamless tubing which is subsequently spun into the chamber shape is a prime candidate when production quantities are being considered, however, extrusion die costs and delivery time prohibited the use of this technique on the current program.

(U) Rolling of plate stock into a cylindrical shape, butt welding the edges and subsequently spinning into shape was discarded due to the unknown ductility and porosity associated with the weld affected zone. Specifically, if the ductility in the weld zone was different than the remainder of the cylinder, this could affect spinning characteristics and possibly result in warping during post-spinning annealing and machining operations. Also, considering the potential use of bulk temperature limited amine-type fuel coolant for this concept, weld porosity or voids could cause stagnation points and/or contain contaminants resulting in instability or decomposition of the coolant.

(U) The spinning vendor, Tri-Metals, Inc., of Santa Fe Springs. California, successfully spun the INCO 625 and subsequently delivered acceptable spinnings to Rocketdyne (Fig. 52). Spinning of the INCO 625 from a flat plate into a converging-diverging shape required a number of intermediate steps in which the material was formed from a flat plate down through various breakdown dies into a cylinder and subsequently spun into the chamber shape (Fig. 53). Intermediate machining and torch annealing of the inner and outer surface was required to eliminate surface crazing and subsequent crack propagation in the next spinning operation (surface cracks were typically 0.005 of an inch deep). After spinning and inspection, the parts were furnace annealed and delivered to Rocketdyne.

(U) One spinning was sectioned for metallographic analysis and tensile bars extracted to determine what affect, if any, spinning had on the material. Results showed no adverse affect on the material with physical property data typically better than the minimum guaranteed properties of annealed INCO 625 plate stock.

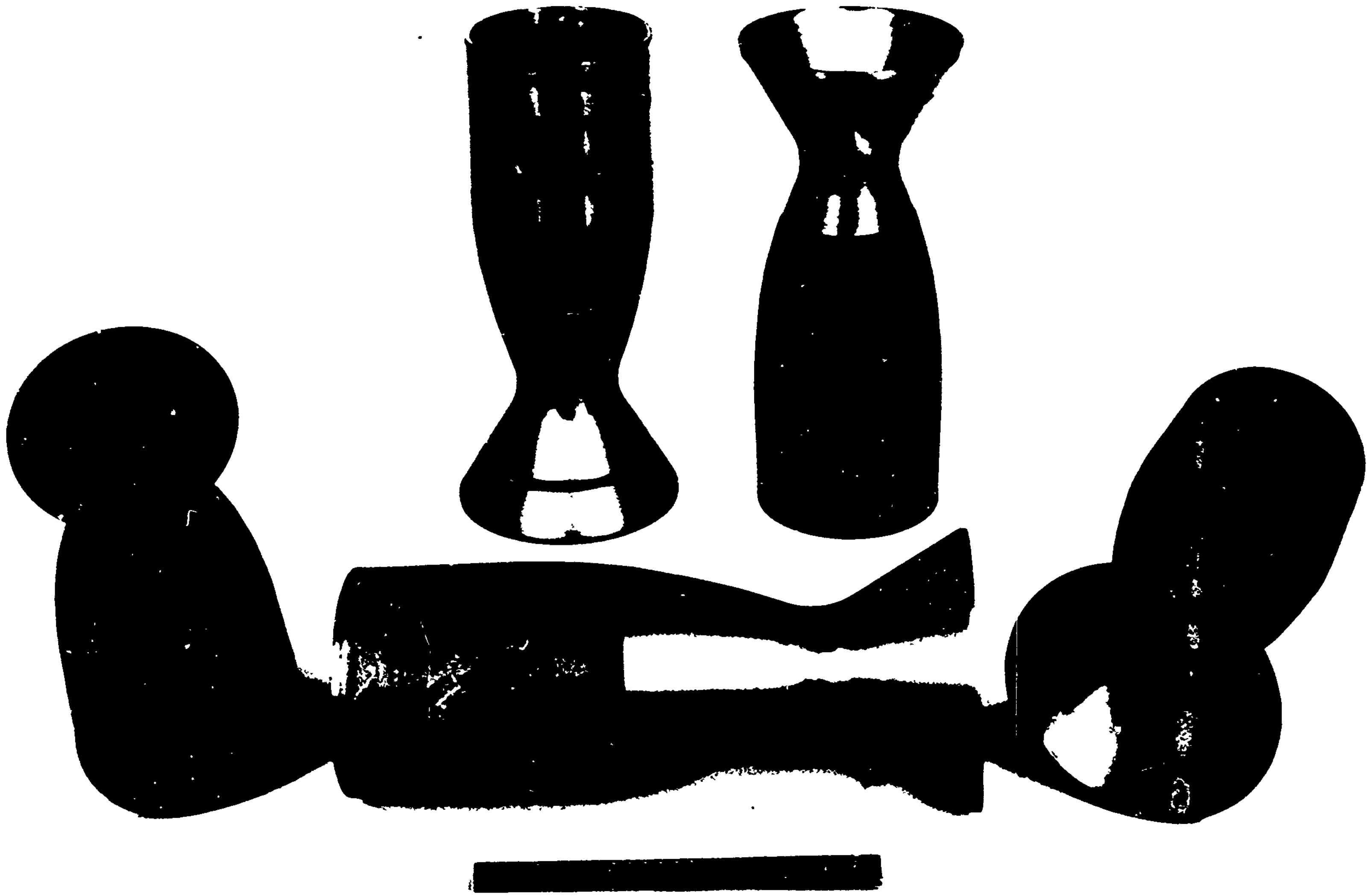

Fig. 52. INCO 6-5 Spinning As-Received

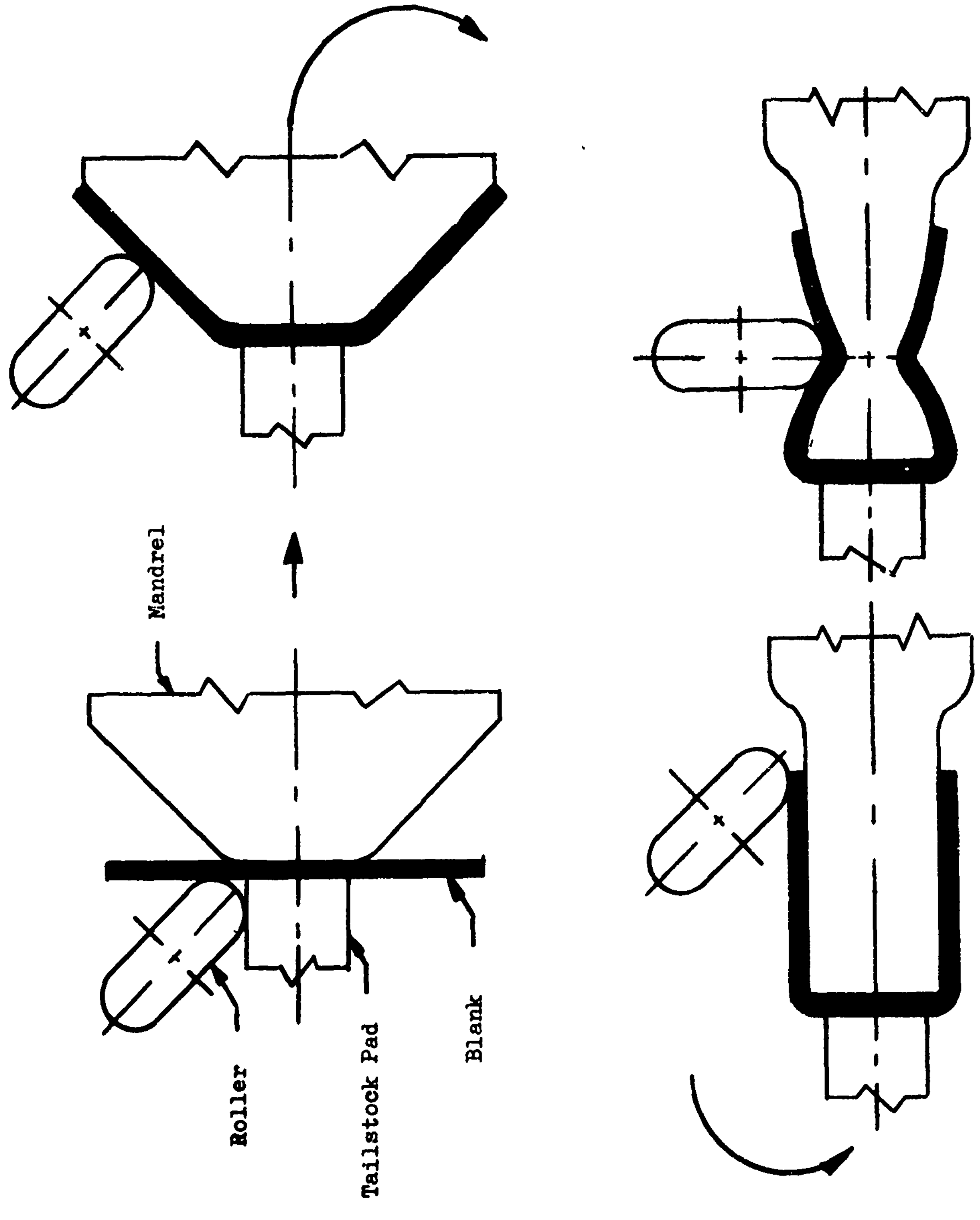

Figure 53. Fabrication Processes - Form Spinning.

(U) Tri-Metals also expended some effort trying to spin Hastelloy-C with unsatisfactory results. Material fracturing occurred during the intermediate spinning operations with the result that no chambers were successfully spun. Additional development effort is required before Hastelloy-C can be successfully spun to the chamber shape.

(U) Liner Machining. The next step in the fabrication process for this concept was machining of the liners (inner and outer surface and coolant passages). This operation is considered the most critical phase of the entire fabrication process in that it is the major factor affecting potential range of application (heat transfer limitations) and production costs.

(C) The heat transfer analysis of this concept had established a requirement for a hot gas wall thickness of 0.030 inch and sixty constant width (0.0625 inch) variable depth (0.053 to 0.106 inches) coolant passages.

(U) As a result of the Phase I cost studies, conventional machining was selected for cutting the constant width, variable depth coolant passages into the spun INCO 625 liners.

(U) Prior to machining the spinnings, slotting studies were conducted on flat panels. Results were: (1) saw cutters and key cutters produced a more satisfactory slot than end milling, and (2) depth of cut per pass is limited to approximately 0.050 inch, requiring multiple passes to cut each slot since maximum slot depth on the chambers exceeded 0.100 inch

(U) The first step in the machining of the spun liners was a tracer lathe operation to machine the internal contour of liners. Next an internal mandrel was centered in the liner to maintain concentricity of the part and all interstices between the mandrel and the liner filled with a rigid wax to support the liner during outer surface and passage machining. After surface machining on the

tracer lathe, the tooling was removed, the wall thickness measured, the tooling reinstalled and centered, and the coolant passages machined into the outer surface. Slotting was accomplished on a Hydrotel using a template offset from the inside diameter template by the thickness of the hot gas wall.

(U) The first spinning to be slotted was used to establish machining parameters (depth of cut, cutter feed and speed, and cutter life). Also, indexing characteristics of the Hydrotel were checked to establish tolerance variations that could be expected on subsequent chambers. This study established the following machining parameters:

1. Standard one-inch diameter -12 teeth key cutters which are ground and cyanided produce good slots and have exceptional life.
2. Three passes are required per slot.
3. Cutter speed should be 97 RPM (one-inch cutter) with a feed rate of 0.500 IPM in the nozzle and 1.500 IPM in throat and chamber.

(U) Using these parameters a representative grouping of eight passages were machined into this first spinning with good dimensional results. This slotted liner was then used to establish electroforming procedures. The configuration, all eight passages, was subsequently hydrostatically pressure tested successfully verifing the integrity of the electroformed nickel to INCO 625 bond. These results are discussed in detail in a ater section on electroforming.

(U) Next, fabrication was initiated on the Phase III prototype chamber. After inner and outer surface machining (Fig. 54), the 60 coolant passages were machined into the INCO 625 liner.

(U) The slotting procedure was as follows. Each slot was rough cut in a single pass approximately 0.050 deep. After cutting each slot, the part was rotated 6 degrees in the Hydrotel such that the cutting was progressive around the chamber. After the first revolution, a second pass ($\sim$.050 deep at either

Fig. 34. [illegible] Liner or [illegible]

end) was made through each slot to complete the rough cut. Again the chamber was rotated in 6 degree increments to progressively cut the slots. Upon completion of the second revolution, a third revolution was made to do the finish cut in each slot. The slotted chamber is shown in Fig. 55.

(U) Dimensional inspection of this chamber, (Fig. 56) showed good dimensional repeatability was obtained using this machining procedure. The hot gas wall thickness in the nozzle section was below the design value but presented no structural problem for hot firing hardware. Detailed checkout of the machine setup and the machining templates revealed this reduced dimension to be a result of misalignment of the template with respect to the part. Also, inspection of the chamber interior revealed some deformation of the hot gas wall in the nozzle section (Fig. 55). This was attributed to the fact that the rigid wax used to support the wall during machining did not completely fill in this region, leaving the liner unsupported. Consequently, the tool pressure yielded the wall during machining.

(U) This inspection showed the slotted INCO 625 liner capable in all respects of being used in the hot firing program of Phase III. However, the passage machining parameters were reviewed and recommendations which had been made to reduce machining time and/or further improve dimensional results were evaluated. This resulted in two major recommendations applicable to subsequent chambers. These were (1) completely machine each passage in one setup (eliminating the need for time consuming indexing to pick up a partially completed slot during successive slotting operations) and (2) use a more stable filler such as one of the Cerro alloys rather than the rigid wax that had been used inside the chamber to provide better liner support during the slotting operation.

(U) Using the previously established machining parameters and the refined procedures discussed above, another INCO 625 liner was slotted. On this chamber each slot was finished machined in three passes prior to rotating the chamber 6 degrees

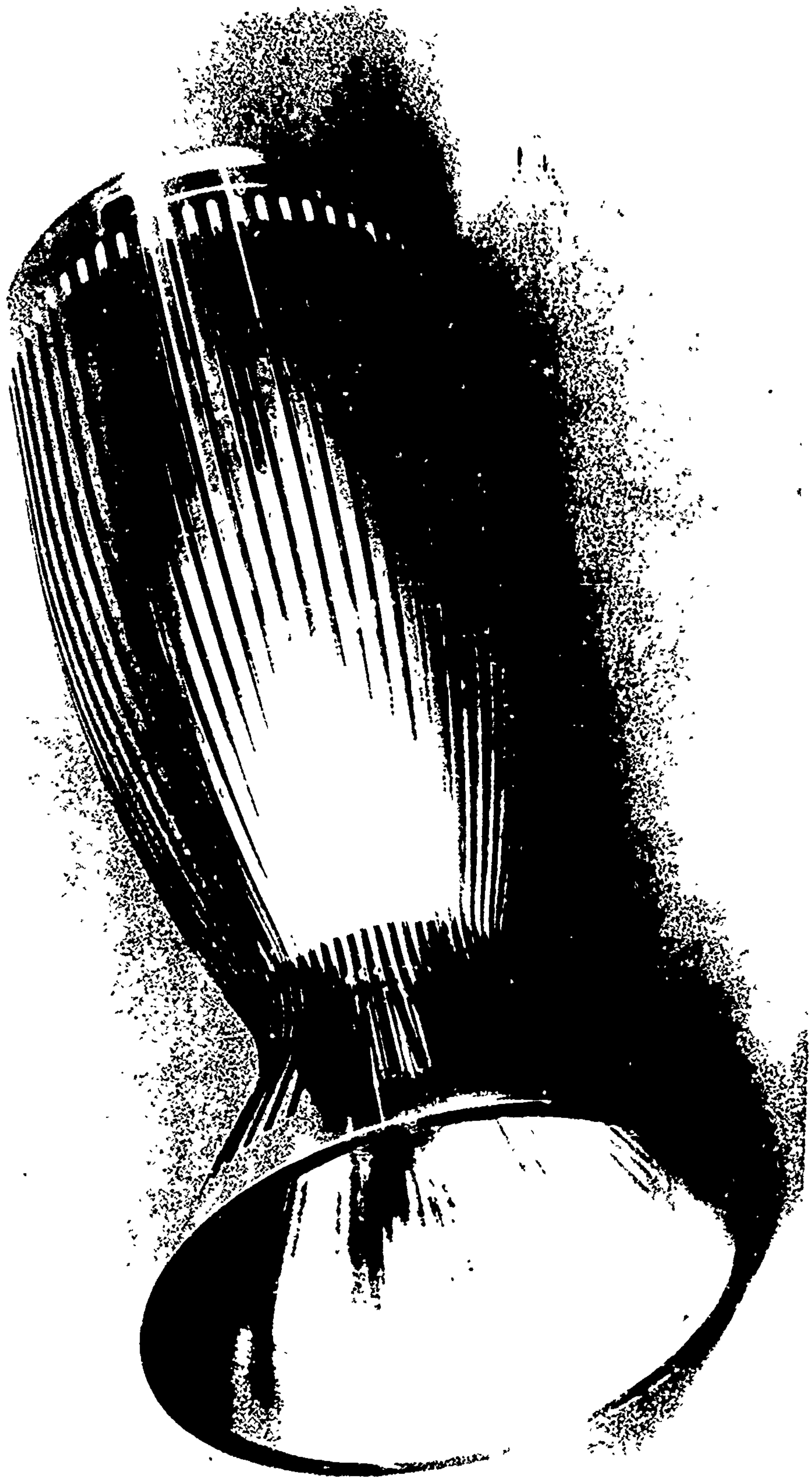

DESIGN

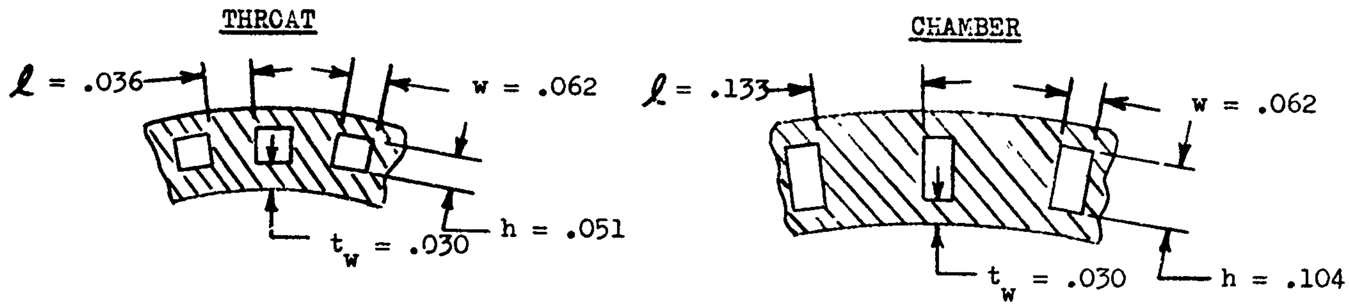

MEASURED

w	= 0.063 - 0.066		w	= 0.063 - 0.066	
h	= 0.047 - 0.053		h	= 0.104 - 0.111	
ℓ	= 0.035 - 0.040		ℓ	= 0.130 - 0.135	
t_w	= 0.030 - 0.036		t_w	= 0.030 - 0.032	

Figure 56. Dimensional Results of Machined Coolant Passages of Spun INCO 625 Bell Chamber. (U)

to cut the adjacent slot. Dimensional results on this chamber were good, however, there was some tolerance variation around the chamber, attributed to non-symmetrical movement of the chamber as one region of the chamber was slotted while another region was unslotted varying the degree of stiffness around the periphery of the part. To compensate for this on any future chamber, it is recommended that the slots be machined in 90 degree increments, i.e., finish machine a slot at 0 degrees, rotate 90 degrees and finish machine slot number two, rotate 90 degrees and finish machine slot number three, rotate 90 degrees and machine slot number four, then rotate 96 degrees for slot number five adjacent to the first slot. Repeat this procedure until all slots are machined into the liner. This procedure more uniformly removes the metal and minimizes distortion forces on the chamber.

(U) Results of this machining study in which two chambers were completely machined into the hot firing dimensions have shown that with conventional machines and machining techniques, tolerances in the range of ±0.003 are achievable in the critical region (throat) with overall tolerances of approximately ±0.005, which are acceptable for most applications. Further improvement of the dimensional repeatability is achievable by refinement in the indexing techniques and the machines used to cut the passages. It is anticipated that when required, tolerances of ±0.003 throughout the chamber could be maintained.

(U) Electroformed Nickel Closure. Initial studies to determine activation cycles and resultant adhesion of electroformed nickel onto nickel base alloys were performed using flat slotted panels of INCO 625 and Hastelloy-C. After depositing nickel to a thickness of 0.042 to 0.048, the panels were burst pressure tested and sectioned. Results (Table XIII) showed that in all cases the measured burst pressure exceeded the calculated burst pressure demonstrating the structural integrity of an electroformed nickel closure on a slotted INCO 625 or Hastelloy-C liner.

TABLE X[illegible]I

STRUCTURAL INTEGRITY VERIFICATION - SPUN LINER WITH ELECTROFORM NICKEL CLOSURE (U)

Item	Measured Pressure, psig	Calculated Pressure, psig	Results
Panel No. 1 (INCO 625)	23,000	14,600 (Burst)	Demonstrated good electroform nickel to liner bond
Panel No. 2 (INCO 625)	28,000	15,400 (Burst)	Demonstrated good electroform nickel to liner bond
Panel No. 3 (Hastelloy C)	17,500	16,200 (Burst)	Demonstrated good electroform nickel to liner bond
Panel No. 4 (Hastelloy C)	20,000	14,400 (Burst)	Demonstrated good electroform nickel to liner bond
Development Chamber (INCO 625)	14,800	2,120 (Proof)	Demonstrated structural integrity of fabrication process ~7 times required proof pressure of hot firing hardware

(U) Subsequently the first slotted INCO 625 liner was submitted to the electroforming laboratory for deposition of the nickel closure over the coolant passages. Initially, the coolant passages were filled with a rigid wax to the top of the lands and the surfaces sanded smooth. The wax surface was then silvered to make the surface electrically conductive and appropriate plexiglass shielding added to selectively control the rate of deposition during the plating cycle. The part was then processed through an anodic cleaning bath, flushed with distilled water, processed through a cathodic activation bath (which makes the surface active, assuring a structural bond between the base material and the electroformed nickel), flushed with distilled water and placed in the electroforming tank.

(U) In process inspection revealed the initial nickel deposition was of poor quality and the part was removed from the tank for analysis. Results revealed that (1) electrical conductivity of the silvered wax was extremely low (found to be caused by the initial anodic activation cycle and (2) the agitation technique (circular motion) was not preventing gas bubble buildup on the surface of the part. These were corrected by (1) modifying the activation cycle in that a nickel strike was added to the INCO 625 lands after filling the passages with the rigid wax but prior to silvering the wax surface (as a result, the part to be plated reacts like a nickel part and the activation cycle developed and proven for electroforming nickel onto nickel was used), and (2) by going to a push-pull agitation cycle (where the part is automatically moved back and forth in the electroforming tank) sufficient shearing action was achieved between the part and the fluid in the electroforming tank to scrub off any gas bubbles that collected on the surface. Also, the part was manually rotated at periodic intervals to provide uniform conditions around the periphery of the chamber. After the electroformed nickel layer was deposited, the part was removed from the tank, the shielding removed, and the wax melted out of the passages.

(U) A test panel taken from the first slotted INCO 625 liner (Fig. 57), dimensionally representative of the Phase III hardware, was successfully pressure tested to 14,800 psig (at which time the welded-on manifold ruptured), demonstrating the structural integrity of the electroformed nickel to INCO 625 bond in the configuration of interest for the Phase III hot firing hardware (Table XIII).

(U) Flange Welding Study. A flange welding study was conducted to (1) determine the E.B. (electron beam) welding parameters and (2) to isolate any problem that might be associated with E.B. welding nickel 200 flanges to an electroformed nickel chamber. The weld sample configuration duplicated the weld joint, and simulated the part-E.B. gun clearance problems which would be encountered on the chamber. The weld joint was made with a 0.002 to 0.006 inch interference (shrink) fit between the flange I.D. and cylinder O.D. and subsequently pressure tested to 18,000 psig without joint failure to verify the welding parameters for the full size chamber.

(U) Cast in Place Aluminum Study. As discussed in Phase I, the use of cast-in-place aluminum shells around the periphery of a bell thrust chamber provides a low cost, lightweight approach to incorporating structure to withstand the pressure stresses in the chamber.

(U) In specific applications, to incorporate this technique for adding additional structure to the chamber requires the development of a mechanical or eutectic bond between the aluminum and electroformed nickel. This bond must be of sufficient strength to withstand the separating loads experienced during the start and shutdown transient. Additionally, the electroformed nickel must be of sufficient thickness to prevent degradation of the nickel to INCO 625 bond due to dissolving the nickel by the aluminum.

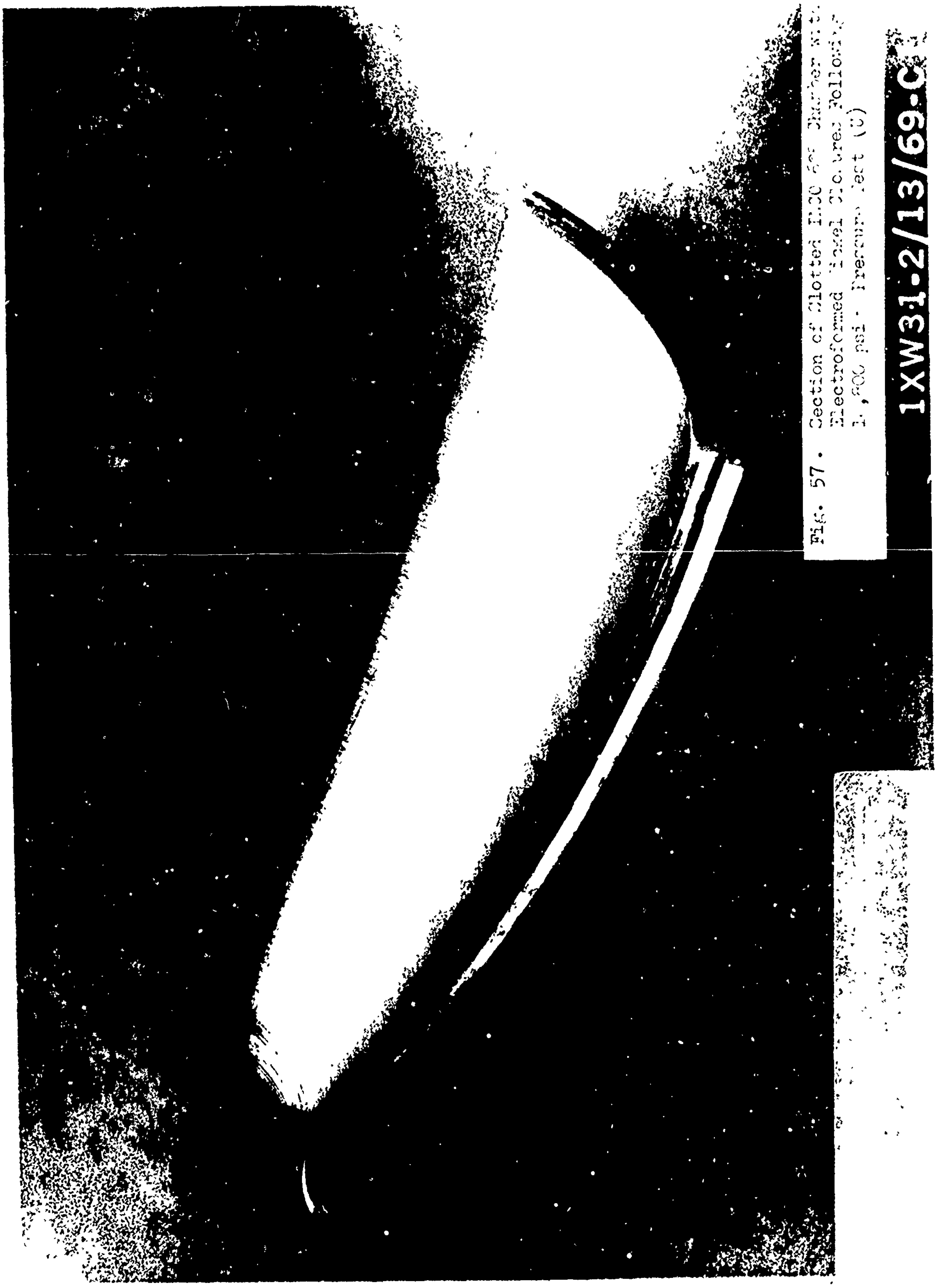

Fig. 57. Section of Slotted I.30 for Chamber With Electroformed Nickel Closures Following 1,800 psi Pressure Test (U)

(U) To evaluate the eutectic bond and minimum nickel thickness requirements stainless steel spools were machined and slotted, various thickness of nickel electroformed onto these spools and the specimens proof pressure tested to verify electroformed nickel to stainless steel bond. Subsequently, Tens-50 aluminum was cast around the spools and each unit pressure tested to 20,000 to 40,000 psig with no structural failures or leaks, demonstrating that there was no degradation of the nickel to stainless steel bond (Fig. 58). Subsequent sectioning of these parts revealed a complete lack of bond between the nickel and aluminum. Further experimentation on this concept including the use of various platings such as gold and tin on the electroformed nickel surface did not promote a reaction with the cast aluminum, however, on none of the samples was the nickel to stainless steel bond degraded by the casting of aluminum around the specimen.

(U) These results have demonstrated that this fabrication technique is a feasible approach for adding additional structure around a chamber. For those applications which require a structural bond between the nickel and aluminum further development is required to establish the necessary parameters (plating, melting and pouring temperature, chamber pre-heat temperature, cool down cycle, etc.) for successfully achieving this bond. Further, through proper design, mechanical means can be incorporated into the chamber to achieve the nickel to aluminum bond when required.

(U) In light of the potential advantages of reduced fabrication cost and lighter weight, that could be realized in incorporating this fabrication technique on flight type chambers, it is recommended that additional effort be undertaken to define bond requirements, establish the necessary process parameters to achieve this bond, and to demonstrace feasibility.

SLOTTED 321 CRES SPOOL

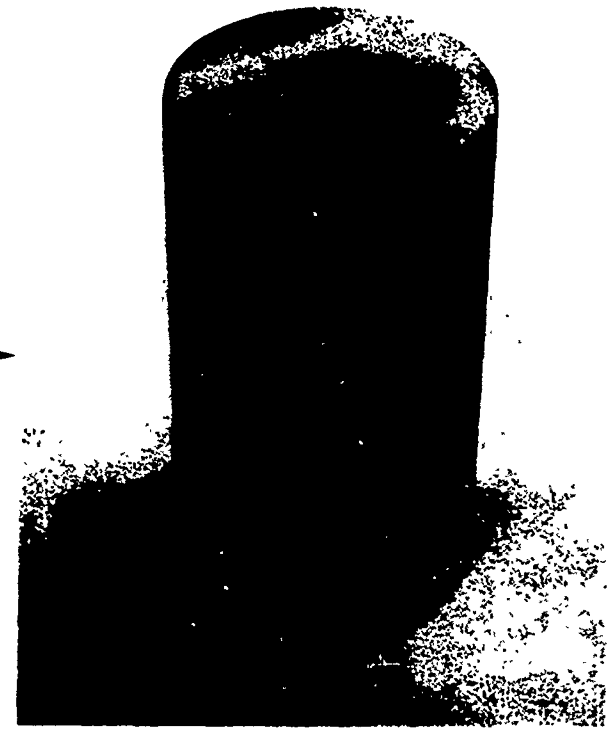

ELECTROFORMED NICKEL
(PROOF PRESSURE = 2600 PSIG)

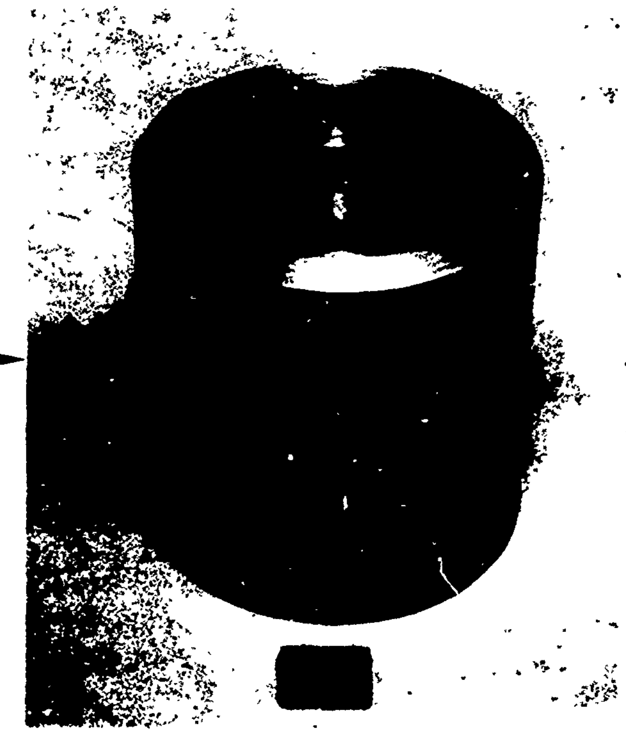

CAST ALUMINUM

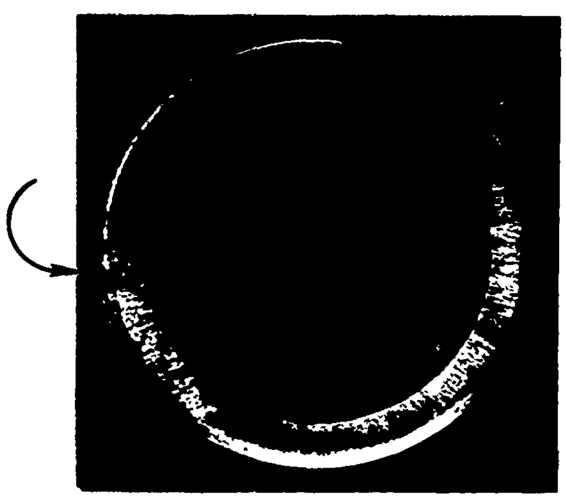

SECTIONED SAMPLE (AFTER PRESSURE TEST)

PRESSURE TEST -
PASSAGES PRESURIZED FROM 20,000 PSIG TO 40,000 PSIG WITH NO STRUCTURAL FAILURES OR LEAKAGE

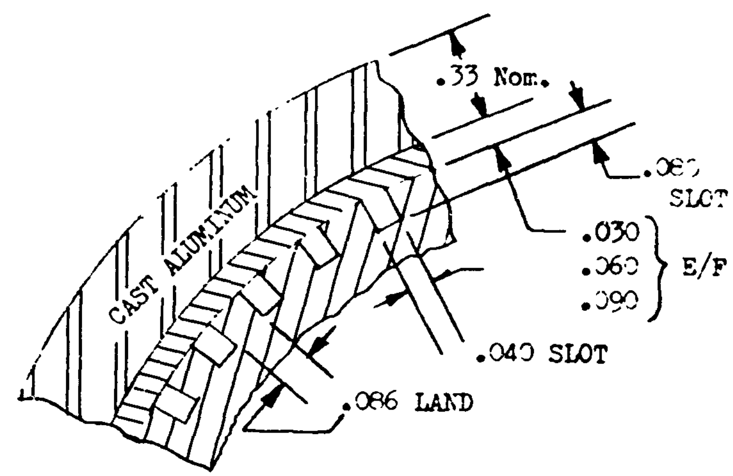

Fig. 58. Process Flow - Cast-in-Place Aluminum Body ( )

Non-Destructive Inspection Techniques

(U) During the course of the Phase II fabrication development, several destructive and non-destructive inspection techniques were used to verify the quality and structural integrity of this fabrication concept. These included, ultrasonic testing, dye penetrant inspection, radiographics, successive dimensional inspection, hydrostatic proof pressure testing and water flow of each coolant passage individually.

(U) Results showed that both ultrasonic testing and dye penetrant inspection were suitable techniques for verifying there were no internal or surface defects in the spun liners; however, these tests had to be conducted on the spun liners after inner and outer surface machining. The results of the radiographic evaluation of the quality of the spun liners were inconclusive, showing no correlation between apparent defects on the film and the known condition of the test samples.

(U) Progressive dimensional inspection of the liner after each machining operation and after electroforming was found to be the best check on repeatability of the machining and electroforming process.

(U) Hydrostatic proof pressure test of the coolant circuit and of the chamber interior, verified structural integrity of the electroformed nickel, of the spun INCO 625 liner and of the nickel to INCO 625 bond joint. Individual water flow of each passage verified that there were no coolant passage restrictions following removal of the wax used during the electroforming cycle.

Conclusions and Recommendations

(U) Results of the Phase II fabrication development studies have shown spinning of hot gas wall liners, followed by machining (surfaces and coolant passages), and electroforming of a nickel closure to be a feasible and economically practical fabrication technique for regeneratively cooled thrust chambers.

(U) Spinning feasibility was demonstrated with the INCO 625 liners spun on this program. The vendor responsible for this effort has expressed confidence and/or demonstrated capability in spinning other candidate materials such as Nickel 200, Inconel 605, Haynes-25, T.D. Nickel, Tantalum, Tungsten and Molybdenum. However, it has also been concluded that spinning of Hastelloy-C, although it should be entirely practical, requires further development.

(U) Machining of the spun liners produced adequate dimensional repeatability using conventional equipment and practices. Factors to be considered in assuring reproducibility at the lowest possible cost are (1) more positive locating techniques for positioning the machining template with respect to the liner and (2) better quality control of the standard off-the-shelf cutters to minimize tolerance and hardness (cutter life) range. Both of these factors influence quality and production rate (cost) of the finished part.

(U) Electroforming onto the slotted liners to close off the coolant circuit and provide the necessary structure to withstand the chamber pressure stresses has been demonstrated to be reproducible with good structural integrity.

(U) The feasibility of using cast-in-place aluminum structural shells around the chamber was successfully demonstrated. Aluminum was cast around slotted stainless steel spools which had electroformed nickel closures without a degradation of the nickel to stainless steel bond. However, in those applications which require a bond between the nickel and the aluminum, further development of the fabrication technique is required to establish the necessary procedures to achieving this bond. Also, more detailed analysis is required to establish bond requirements. Due to the potentially lighter weight system that would result with larger chambers, it is recommended that further development of this fabrication concept be undertaken.

(U) Based on these results, the Phase III effort was initiated on this concept using machined INCO 625 liners from the Phase II effort.

CONCEPT NO. 3 - CAST COPPER ALLOY SEGMENT WITH ELECTROFORMED NICKEL CLOSURE AND OXIDIZER HEAT EXCHANGE PANEL

(U) The third fabrication concept selected for experimental evaluation in Phases II and III incorporated the use of a precision investment cast segment, followed by successive layers of electroformed nickel to form the coolant circuit closures and manifolds.

(U) An added feature incorporated on this concept was an investigation of the fabrication feasibility and system advantages to be gained through the use of multiple layers of coolant passages. Fuel is used as the

primary coolant with oxidizer as a secondary coolant in the heat exchange panel. In this manner heat exchange occurs between the two propellants, lowering the bulk temperature (and pressure drop) of the primary coolant, while gasifying the secondary coolant, thus extending the range of application (regenerative cooling and/or throttling).

(C) The segment geometry selected for use on this fabrication concept was shown in Fig. 34, along with nominal operating parameters. The combustion zone geometry represents a straight full-size cross section of an annular chamber under development at Rocketdyne for the AFRPL on another program (F04611-67-C-0116).

(U) The fabrication sequence, shown previously in Fig. 3 , is as follows. The annular chamber segment (hot gas wall and lands of the coolant passages) is investment cast and an electroformed nickel closure added to close off the fuel coolant circuit. Coolant passages for the oxidizer heat exchange coolant panel are machined into the electroformed nickel closure on one contoured wall. A second layer of electroformed nickel is added to the segment to close off the oxidizer coolant circuit and to provide sufficient buildup for the coolant manifolds. After manifold machining, a third electroformed nickel layer is added to close off the manifolds. Subsequent final machining and welding and the addition of workhorse bolt-on structure completes the assembly.

(U) The fabrication development tasks undertaken to evaluate this concept and to establish non-destructuve inspection techniques applicable to the hot firing hardware of Phase III are discussed in the following paragraphs.

Fabrication Development

(U) Casting of Beryllium Copper Alloys. This fabrication concept was selected based on the Phase I fabrication ranking studies and some supplemental exploratory work underway on a company funded program. Initially, a survey of the casting industry and of candidate materials data was conducted to determine the most applicable material or materials for application in regeneratively cooled thrust chambers. Results showed the beryllium copper alloys to be most appropriate of the readily available, off-the-shelf castable materials. The properties of these materials are listed in Table XIV below.

TABLE XIV

CANDIDATE CASTABLE BERYLLIUM COPPER ALLOYS (U)

MATERIAL	SOLIDIFICATION RANGE, F	TENSILE PROPERTIES @ 800 F,ksi	DUCTILITY @ 800 F percent	THERMAL CONDUCTIVITY (percent of OFHC)
BeCu-20C	1575-1800	52 UTS 30 YS	1 E.L. 4 R.A.	28
BeCu-10C	1885-1995	42 UTS 17 YS	20 E.L. 22 R.A.	40
BeCu-50C	1855-1955	38 UTS 16 YS	20 E.L. 22 R.A.	40

(U) The 20C alloy is a readily castable alloy used extensively in structural applications; however, it has limited applicability in regeneratively cooled thrust chambers due to its low thermal conductivity and ductility. The 10C and 50C materials have satisfactory casting parameters but due

(U) to their lower strength are not as extensively used in the casting industry. However, their thermal conductivity and ductility properties make them attractive for use in regeneratively cooled thrust chambers. The literature data and discussions with representatives of various foundries and beryllium copper suppliers showed no strong technical preference for either 10C or 50C. Therefore, it was decided to concentrate the casting effort on the 10C material, because of its slightly better tensile properties and solidification range, with the 50C material to be used as an interchangeable alternate.

(U) The investment casting process makes possible the casting of a wide range of shapes and contours in moderate sized parts and offers low-cost solutions to close tolerance parts, with intricate contours and good surface finishes. Usually as-cast surfaces (requiring only sandblasting to remove superficial scale) can be used as final finishes. The investment casting process is as follows:

(U) Initially a very accurate aluminum pattern, the reverse image of the finished part, (Fig. 59) is machined. A special low thermal expansion wax is then injected into the pattern to form an expendable wax core identical in configuration to the final cast part (Fig. 60A). Next, wax risers and gates are attached to this wax core as required (Fig. 60B).

(U) The wax core is then dipped in a slurry composed of silica flour, water, and a bonding agent and dusted with fine-grain silica sand to form the initial layer of the investment shell. After drying, additional layers of investment are added and dried, giving the shell sufficient strength to retain the molten material during pouring. The wax core is then melted out, leaving a cavity the mirror image of the finished casting in the ceramic shell (Fig. 60C).

CONFIDENTIAL

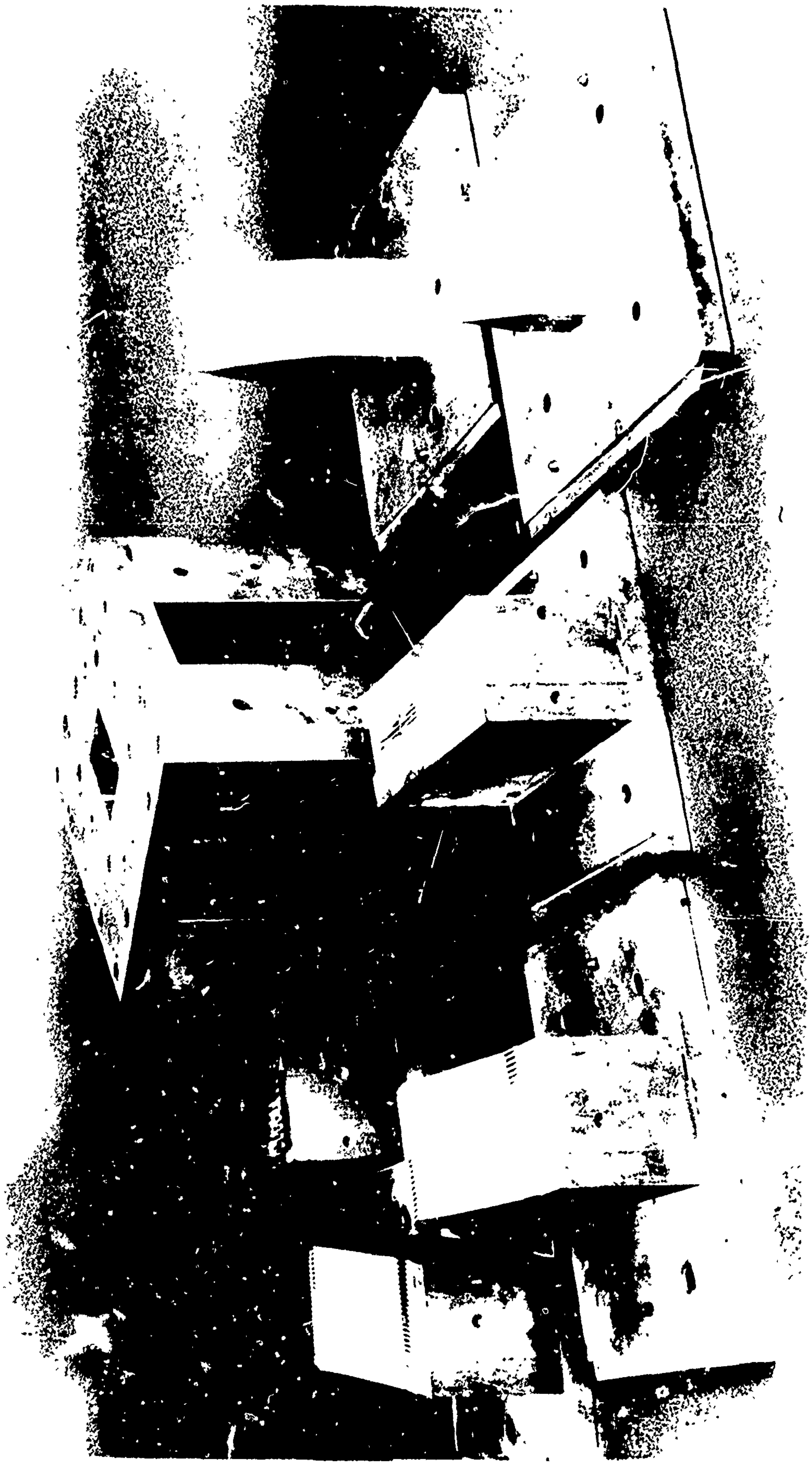

CONFIDENTIAL

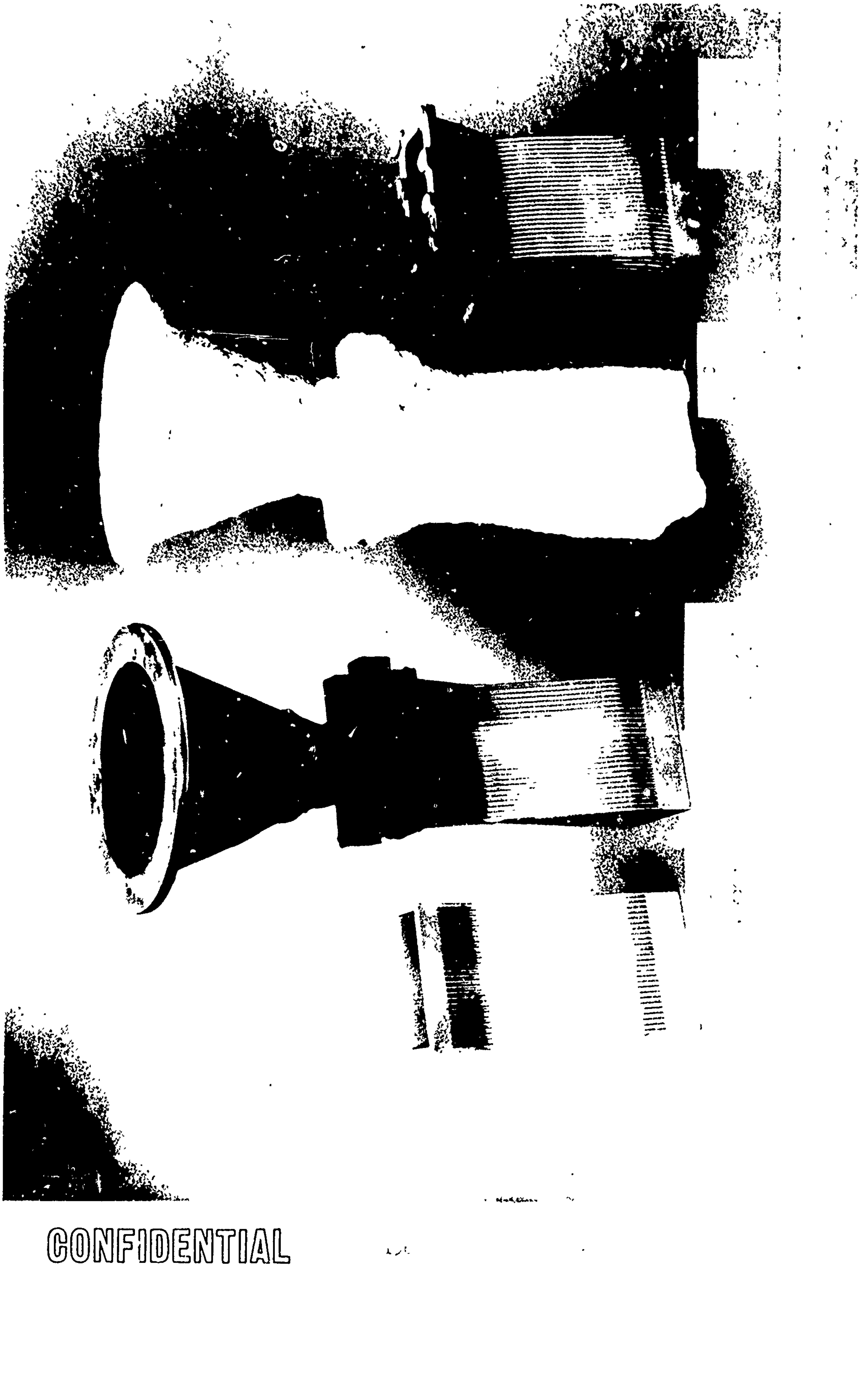

(U) Prior to pouring, the ceramic shell is heated to (1) cure the ceramic shell, (2) minimize the temperature gradient between the shell and the molten metal and (3) promote complete filling of the shell with the molten material prior to solidification. After solidification, the ceramic shell is removed by vibration and sandblasting with a very fine material, gates and risers are cu off and any minor surface protrusions removed by grinding (Fig. 60D).

(U) In reviewing the casting parameters and state-of-the-art on investment casting of the beryllium copper 10C and 50C, the foundry and Rocketdyne Materials and Processes personnel established minimum dimensional requirements which they felt should be maintained to assure maximum confidence in obtaining good quality castings at reasonable cost. These were a minimum hot gas wall thickness of 0.060 and minimum passage and land widths of 0.060 and 0.058, respectively. These dimensions along with the internal dimensions presented in Fig. 34 resulted in the segment liner design shown in Fig. 61.

(U) Based on the foundry experience with beryllium copper alloys, the initial castings were poured in air, had the injector end up and were top gated (Fig. 62). Inspection showed excellent dimensional repeatability (Table XV) but the presence of oxide inclusions and shrinkage in the casting hot gas wall.

(U) The oxides were attributed to the condition of the virgin ingots and to the ingot melting and pouring in an open air atmosphere. The ingots, as received from the supplier, had inclusions and large oxide entrapments plainly visible. The casting foundry had only limited success in cleaning these ingots by remelting in air and scraping the top of the molten metal. Subsequently, vacuum melting of the ingots was used and eliminated

CORE COORDINATES

STATION	COORDINATE X	TOL	COORDINATE Y	TOL
1	3.400		.957	
2	3.200		.894	
3	3.000		.851	
4	2.800		.808	
5	2.600		.764	
6	2.400	±.010	.720	±.005
7	2.200		.674	
8	2.000		.626	
9	1.800		.576	
10	1.600		.528	
11	1.400		.477	
12	1.200		.424	
13	1.000		.366	
14	.800		.308	
15	.600		.231	
16	.400		.151	
17	.300		.109	
18	.200	±.005	.080	±.002
19	.100		.063	
20	.000		.057	
21	-.100		.063	
22	-.200		.080	
23	-.300		.106	
24	-.500		.160	
25	-.700		.215	
26	-.900		.267	
27	-1.100	±.010	.321	±.005
28	-1.250		.361	
29	-1.732		.492	

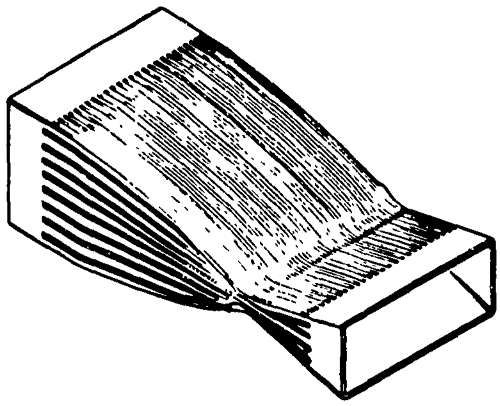

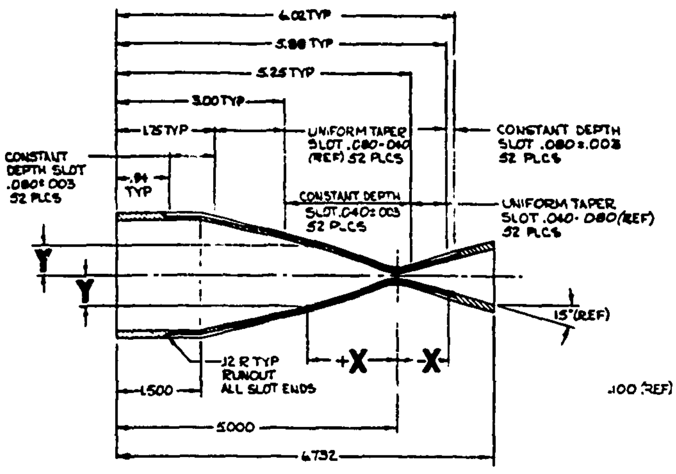

SECTION A-A

CONTOUR FACE

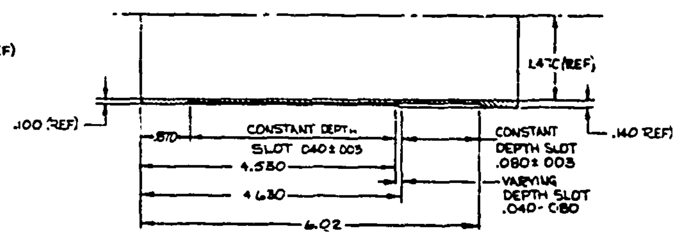

SECTION B-B

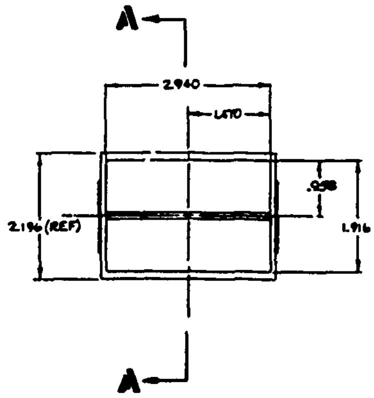

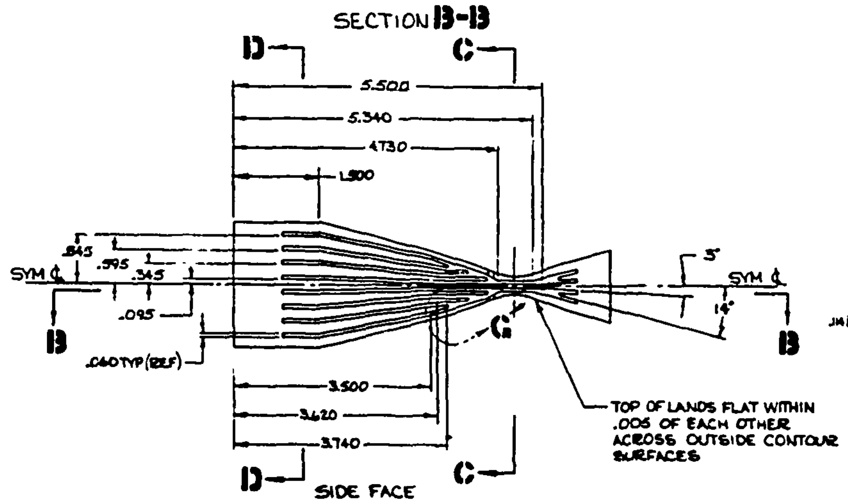

SIDE FACE

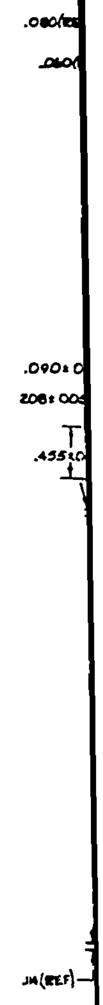

1

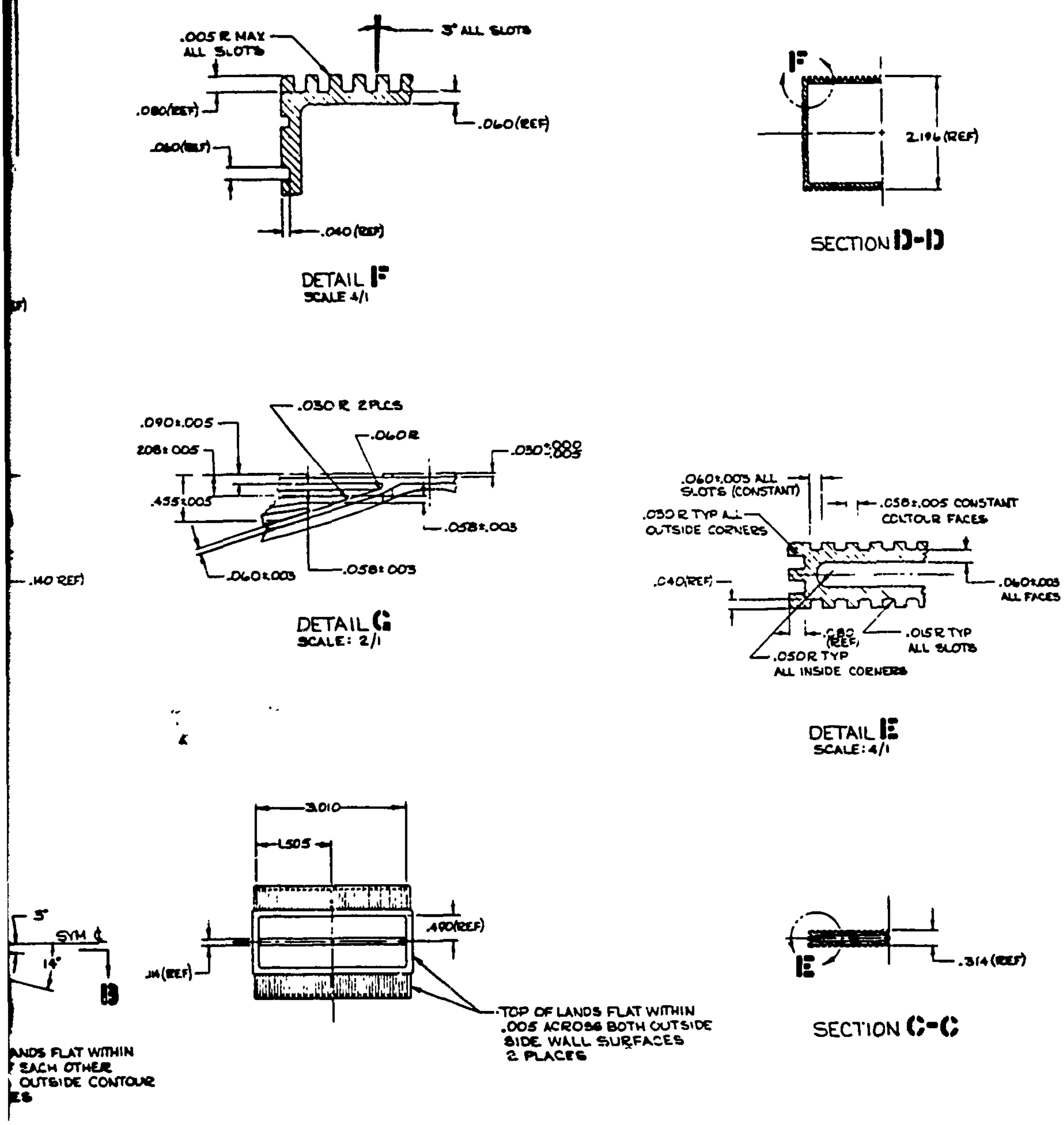

Figure 61. Design Layout of Cast Segment Liner. (U)

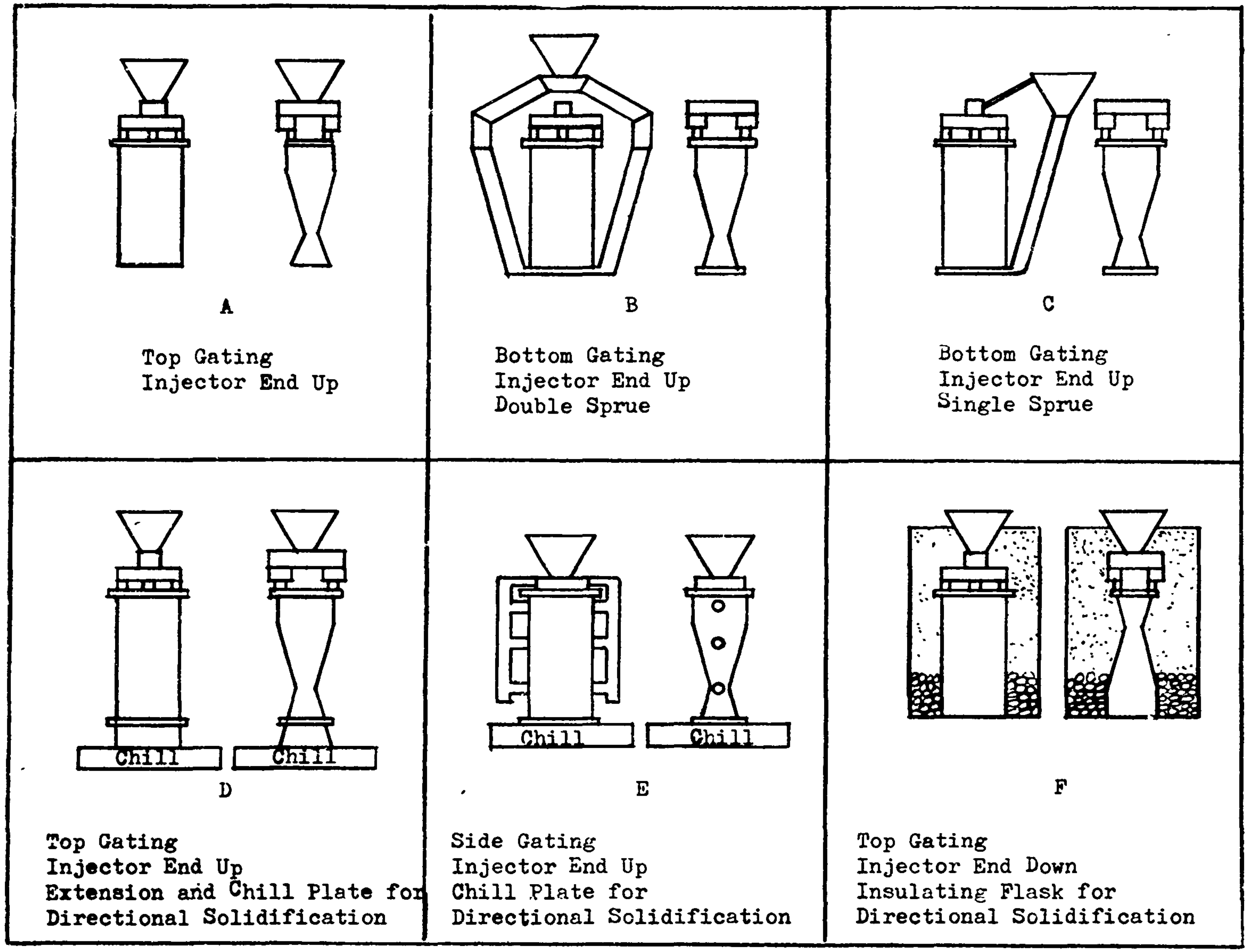

Figure. 62. Typical Gating Arrangements for Investment Cast BeCu Development Effort. (U)

TABLE XV

TYPICAL DIMENSIONAL RESULTS -

AS-CAST THROAT PLANE OF BeCu SEGMENTS (U)

DESIGN (THROAT PLANE)

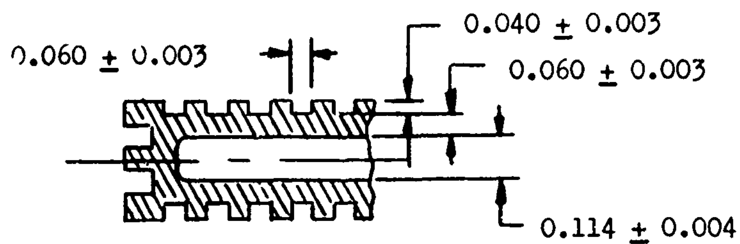

MEASURED

CASTING NO.	THROAT GAP in.	PASSAGE DEPTH in.	PASSAGE WIDTH in.	HOT GAS WALL THICKNESS in.
1	.116 (Ends) .132 (Center)	0.035 to 0.039	0.055 to 0.059	0.058 to 0.062
2	.115 (Ends) .125 (Center)	0.035 to 0.040	0.054 to 0.060	0.058 to 0.063
3	.114 (Ends) .126 (Center)	0.035 to 0.040	0.055 to 0.060	0.058 to 0.061
4	.116 (Ends) .122 (Center)	0.035 to 0.039	0.056 to 0.061	0.056 to 0.061
5	.118 (Ends) .128 (Center)	0.036 to 0.040	0.055 to 0.062	0.057 to 0.061

the problem of impurities in the ingots. However, as the ingot for each casting was melted prior to pouring and during the pouring itself some oxides were formed. Generally these could be floated out of, or minimized in, the cast segment by proper use of gates and risers.

(U) Shrinkage, or more accurately microshrinkage, (caused by a decrease in metal volume due to solidification) occurred because localized areas of the casting remained molten after surrounding areas had solidifed. This type of shrinkage occurs between individual dendrites and indicates the lack of directional solidification.

(U) Two conditions must be met in order to avoid microshrinkage; first, there must be a reservoir of liquid metal which will remain liquid until after the casting itself has solidified. This reservoir is usually provided in the form of a heavy section of metal placed at a carefully chosen point on the casting and is called a riser. The second condition is that there must be an open pathway for this reservoir of liquid metal to flow to the point in the casting that requires feed metal; that is, there must be directional solidification of the molten cast material toward the riser.

(U) As a result of the initial casting pours, it was considered necessary to explore various casting parameters in an attempt to eliminate this microshrinkage problem. Variables that were considered included; ceramic shell and metal pouring temperatures, various gating and riser arrangements, orientation during the pour (injector end up or down) and directional solidification. Typical examples were illustrated in Fig. 62. The ceramic shell temperature was varied between 1400 F and 1800 F. In general, higher shell temperatures produced better quality castings with less shrinkage and non-fills (metal solidified before mold was filled). Metal pouring temperatures were varied between 1950 F and 2200 F. Results

showed that maintaining the pouring temperature between 2100 and 2150 F provided better castings with less shrinkage and non-fills than did temperatures under 2000 F. Good directional solidification was achieved when the gate or gate-riser combination extended completely around the casting. This type of riser in conjunction with the pour cup kept the top of the poured casting hot enough to aid directional chilling.

(U) Also evaluated were various directional solidification techniques including; surrounding the shell with a mullite insulator or a graphite heat conductor, and copper chill plates positioned beneath the shell to promote progressive chilling from bottom to top. On some of the castings which used a chill plate, extensions were added to the casting to enhance filling and solidification.

(U) One other casting parameter evaluated on a limited basis was melting and pouring the casting in a vacuum. However, the foundry facility limitations precluded the use of chill plates in the vacuum chamber.

(U) A typical grouping of cast segments poured under these varying conditions is shown in Fig. 63 and a summation of results is presented in Table XVI. Generally, air pours combined with directional solidification gave good quality castings with no microshrinkage but, in some cases, the presence of oxides near the upper end of the cast segment. Conversely, the vacuum castings without directional solidification produced good quality castings with no oxides but the reoccurrence of microshrinkage in specific cases.

(U) It was concluded from this effort that to repeatably obtain hot firable castings required vacuum casting combined with directional solidification. However, a sufficient number of hot-firable castings to satisfy the Phase II and Phase III requirements had been obtained in this investigation and no further experimental effort was undertaken on this program.

CONFIDENTIAL

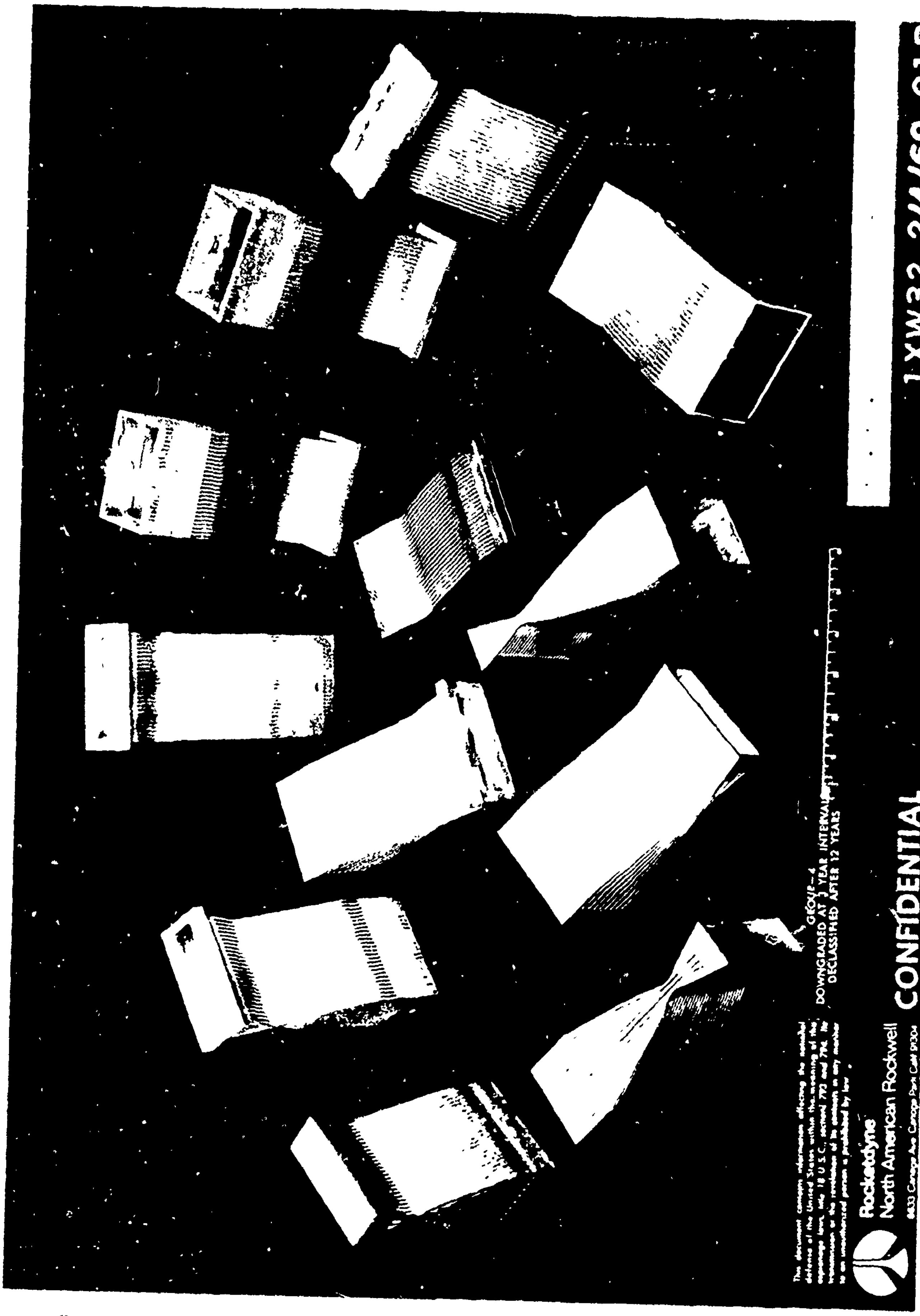

CONFIDENTIAL

TABLE XVI

TYPICAL RESULTS OF SEGMENT CASTING DEVELOPMENT PROGRAM

MATERIAL	SHELL TEMP F	MELT TEMP F	ENVIRON-MENT	CHILL PLATE	INJECTOR END	GATING ARRANGE-MENT	REMARKS AND CONCLUSIONS
BeCu-10C	1800	2125	Air	No	Up	Top	Initial attempt to cast BeCu-10C segments. Good dimensional results, however, castings had microshrinkage and oxides.
						Bottom	Good quality casting - acceptable for hot firing.
							Repeat of above. Casting had shrinkage and oxides. Show, parameters are marginal for repeatability.
				Yes		Side	Good quality part with no shrinkage or oxides. Acceptable for hot firing; side gates difficult to machine off.
				No			Repeat of above except no chill plate used. No shrinkage but some oxides. Again showed need for vacuum casting.
	1400	2100	Vac			Top	Initial attempt to cast in vacuum. Results promising. No oxides but some shrinkage. Indicated need for directional solidification.
BeCu-50C	1800	2100	Air	Yes	Down	Bottom	First attempt with alternate material. Good quality; no shrinkage or oxides.
BeCu-50C	1450	2100	Vac		Up	Bottom	Good quality casting acceptable for hot firing. Shell had been preplaced in container and surrounded with mullite in an attempt to aid directional solidification.

(U) Concurrently, a broader scope company funded program which was underway to explore alternate copper alloys and other configurations had initiated an effort to explore vacuum casting with directional solidification. Appropriate modifications were made to the vacuum chamber to allow for chill plates and for continuous recording of various temperatures associated with the casting.

(U) Initial effort considered the experimental verification of the directional solidification technique. Ceramic shells were instrumented with thermocouples, and mounted in a two-piece flask. Insulation was added around the flask, and after pre-heating to a prescribed temperature, the shell/flask assembly was placed on a chill block in the vacuum chamber and the castings poured. Continuous monitoring of the shell temperatures established basic requirements of shell temperature, pouring time and chilling time to produce good quality castings. This arrangement is illustrated in Fig. 64 and typical temperature traces are shown in Fig. 65. Subsequently, a number of excellent quality copper alloy castings were poured using these parameters and demonstrated that the vacuum casting technique combined with directional solidification repeatably produced top quality castings. Further, this company funded effort successfully produced castings with thinner hot gas walls and smaller cross section passages, thus extending the range of application of this fabrication concept.

(U) Material Properties. As a part of the evaluation of beryllium copper investment castings for use as thrust chamber hot gas wall liners, elevated temperature material properties were obtained for both BeCu-10C and -50C.

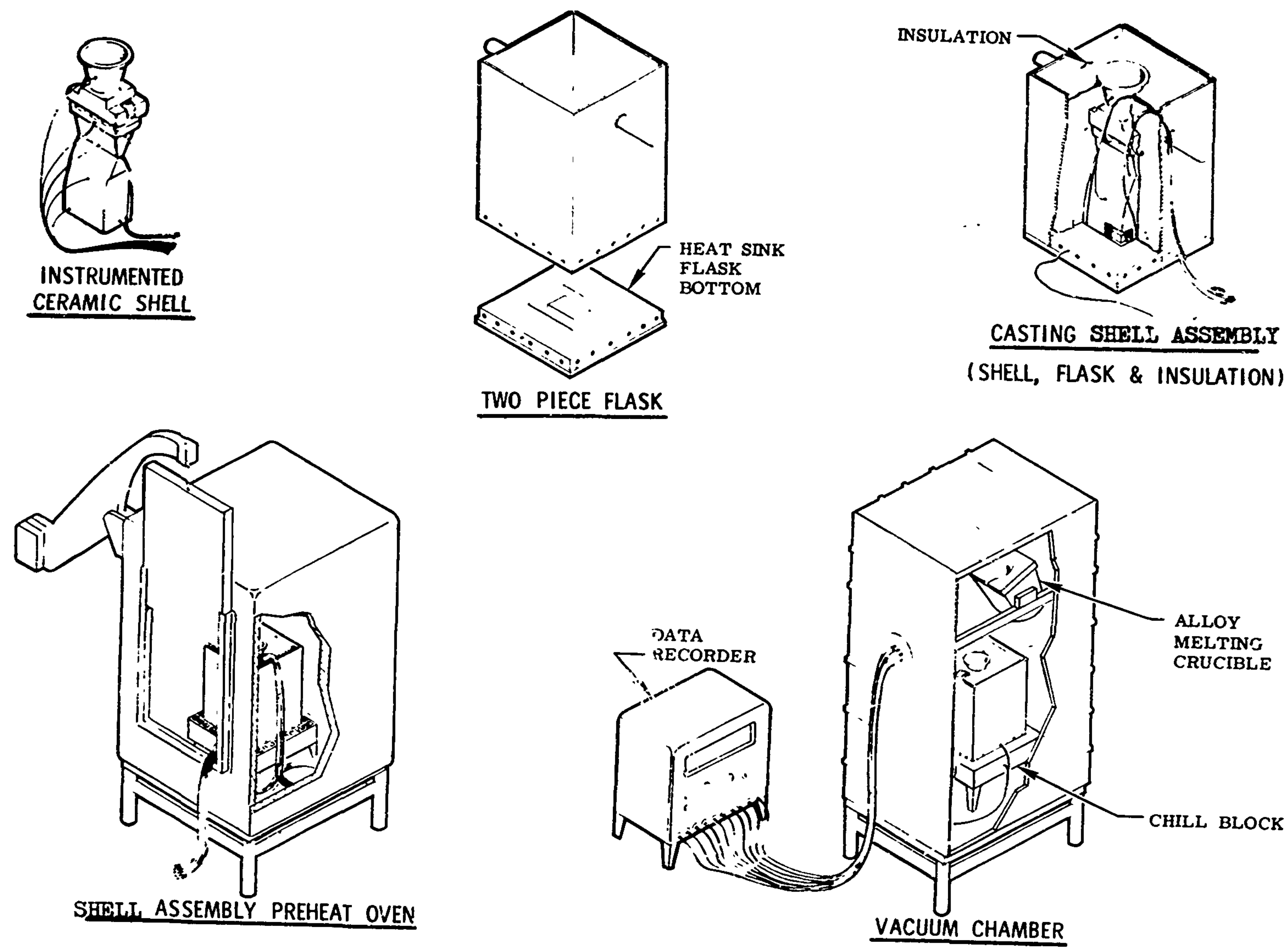

Figure 64. Test Procedure for Establishing Vacuum Investment Casting Parameters. (U)

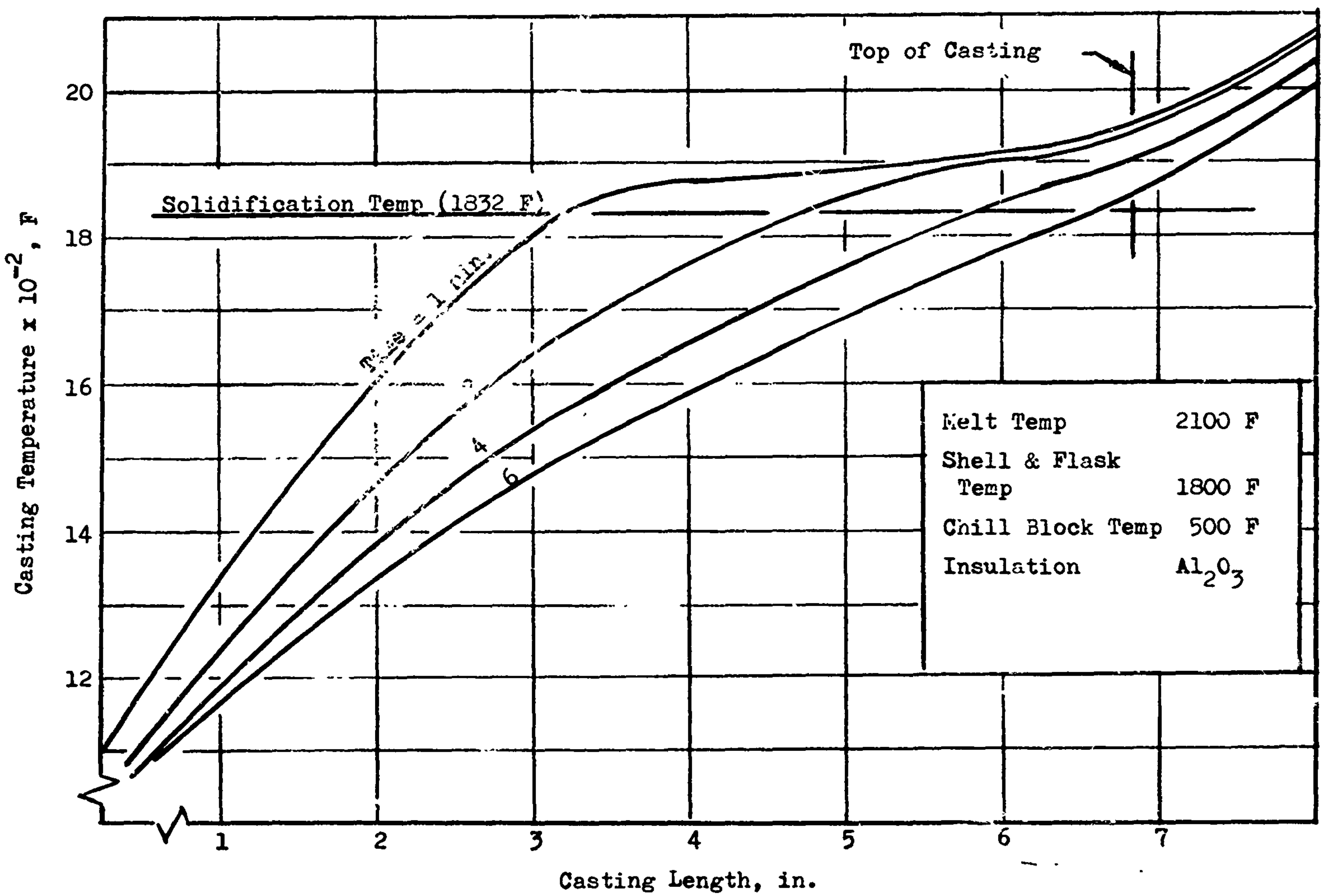

Figure 65. Typical Temperature Distribution for Vacuum Casting. (U)

(U) Tensile Properties. Standard ASTM tensile bars were cast and tested to determine elevated temperature tensile properties of as-cast and overaged specimens. The overaged specimens had been heat treated (1350 F for one and one half hours) to increase ductility and thermal conductivity. A detailed discussion of the overaging studies is presented in Appendix B along with as-cast tensile properties. Overaged tensile properties are presented in Figs. 66 and 67. The data presented in these figures show a low point in ductility at approximately 900 F with increasing value above this temperature and moderate tensile properties to temperatures as high as 1350 F, indicate maximum service temperature of cast beryllium copper segments is greater than the originally established 1000 F. In fact, operation at 1200 F or even higher should be acceptable in most applications, depending on specific system requirements.

(U) Thermal Conductivity. Thermal conductivity measurements (Fig. 68) were also completed on the 10C and 50C materials following the procedures previously described in the section on the Powder Metal Bell Chamber.

(U) Electroformed Nickel Closure on Cast Segments. Upon receipt of investment cast segments from the foundry, effort was initiated to evaluate the structural integrity of the electroformed nickel to cast beryllium copper bond. A layer of electroformed nickel was deposited on one of the Phase II fabrication development segments to close off the coolant circuit. Coolant transfer manifolds were then machined into this electroformed nickel closure. A second electroforming layer was added to closeout the manifolds and the coolant transfer tubes welded in place to complete the assembly; Figs. 69 and 70. The coolant circuit was hydrostatically pressure tested to levels as high as 10,500 psig; demonstrating the structural integrity of the electroformed nickel to beryllium copper bond, the electroformed nickel to electroformed nickel bond and the weld joint between the electroformed nickel and coolant supply tubes (Table XVII).

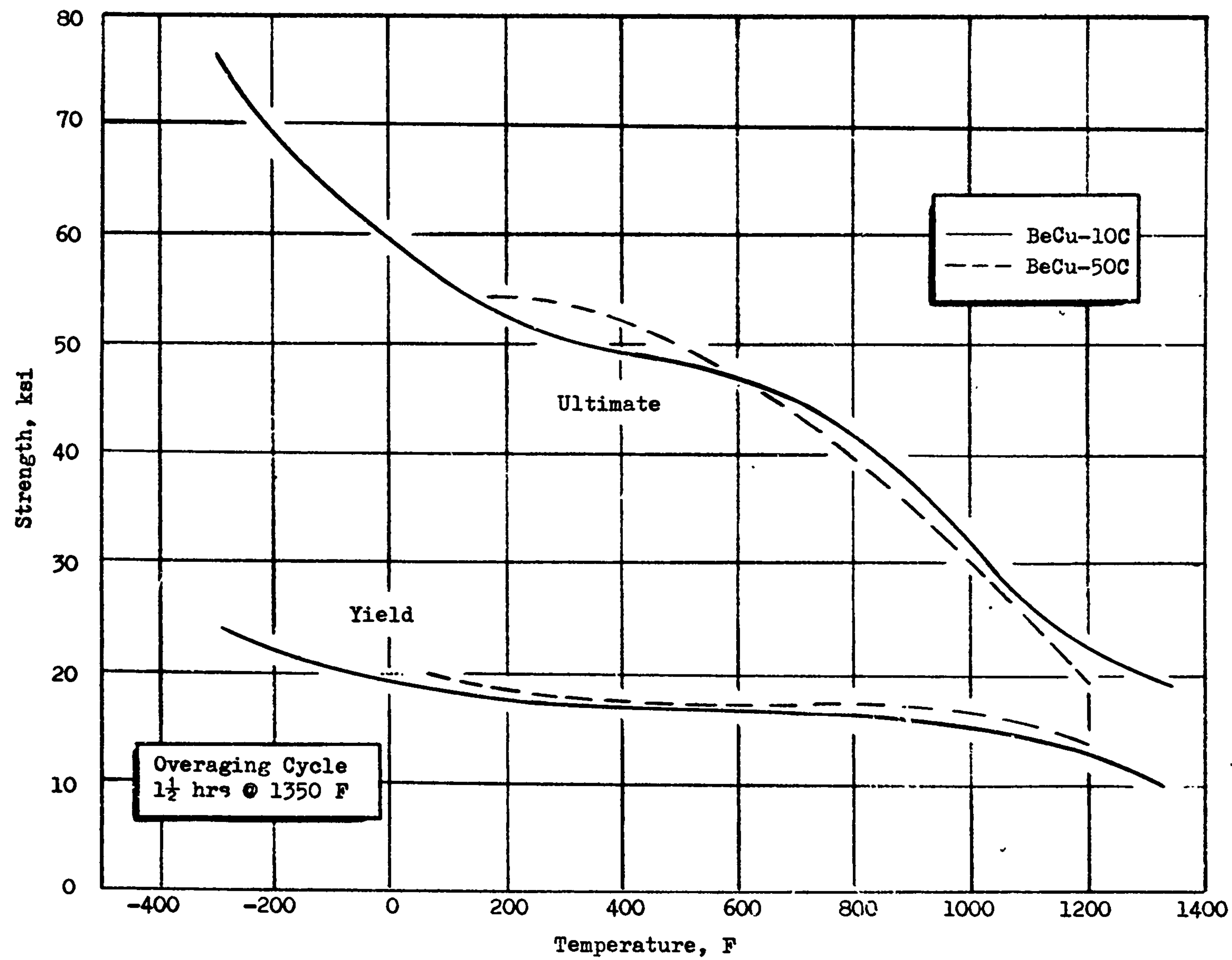

Figure 66. Material Properties of Overaged Beryllium Copper Castings. (U)

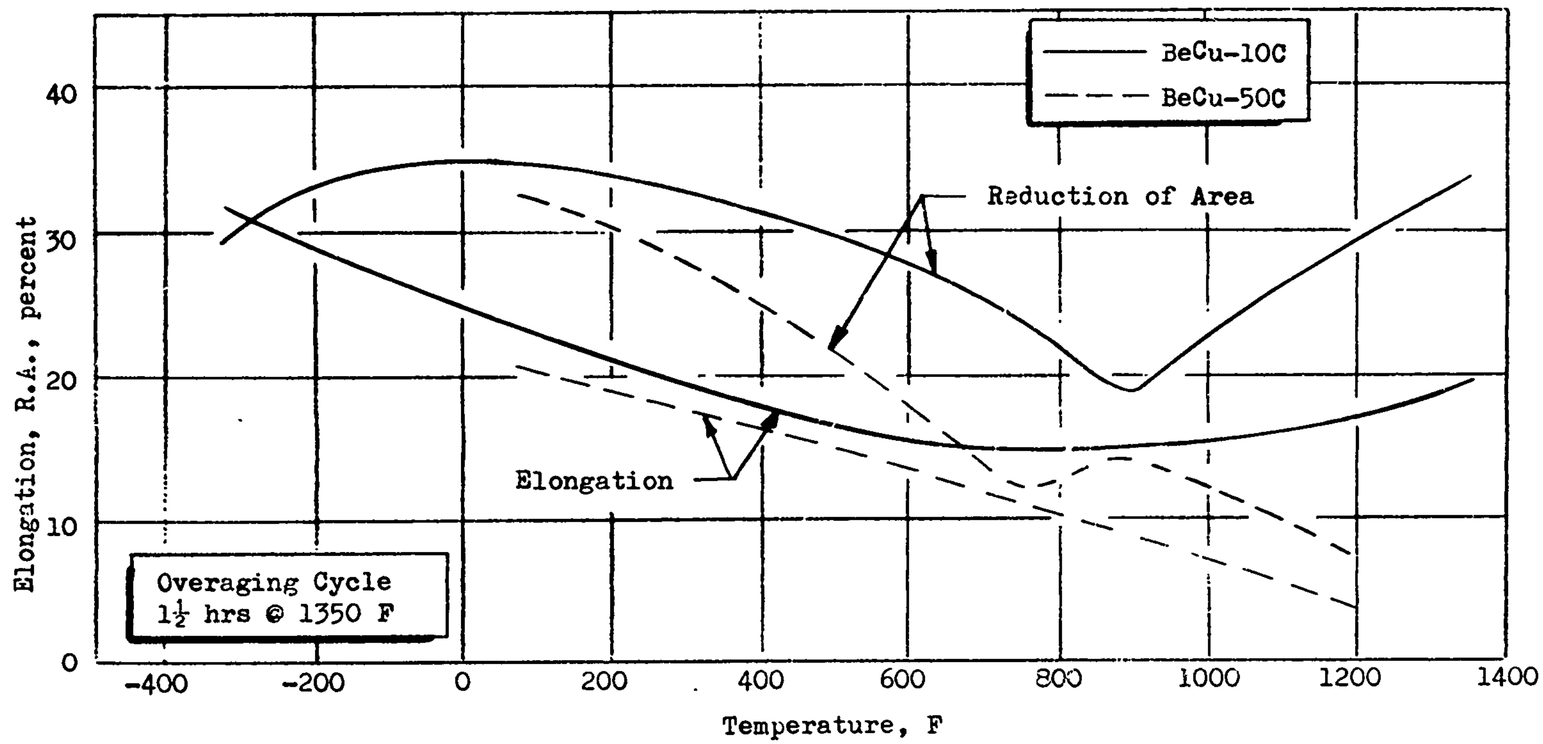

Figure 67. Material Properties of Overaged Beryllium Copper Castings. (U)

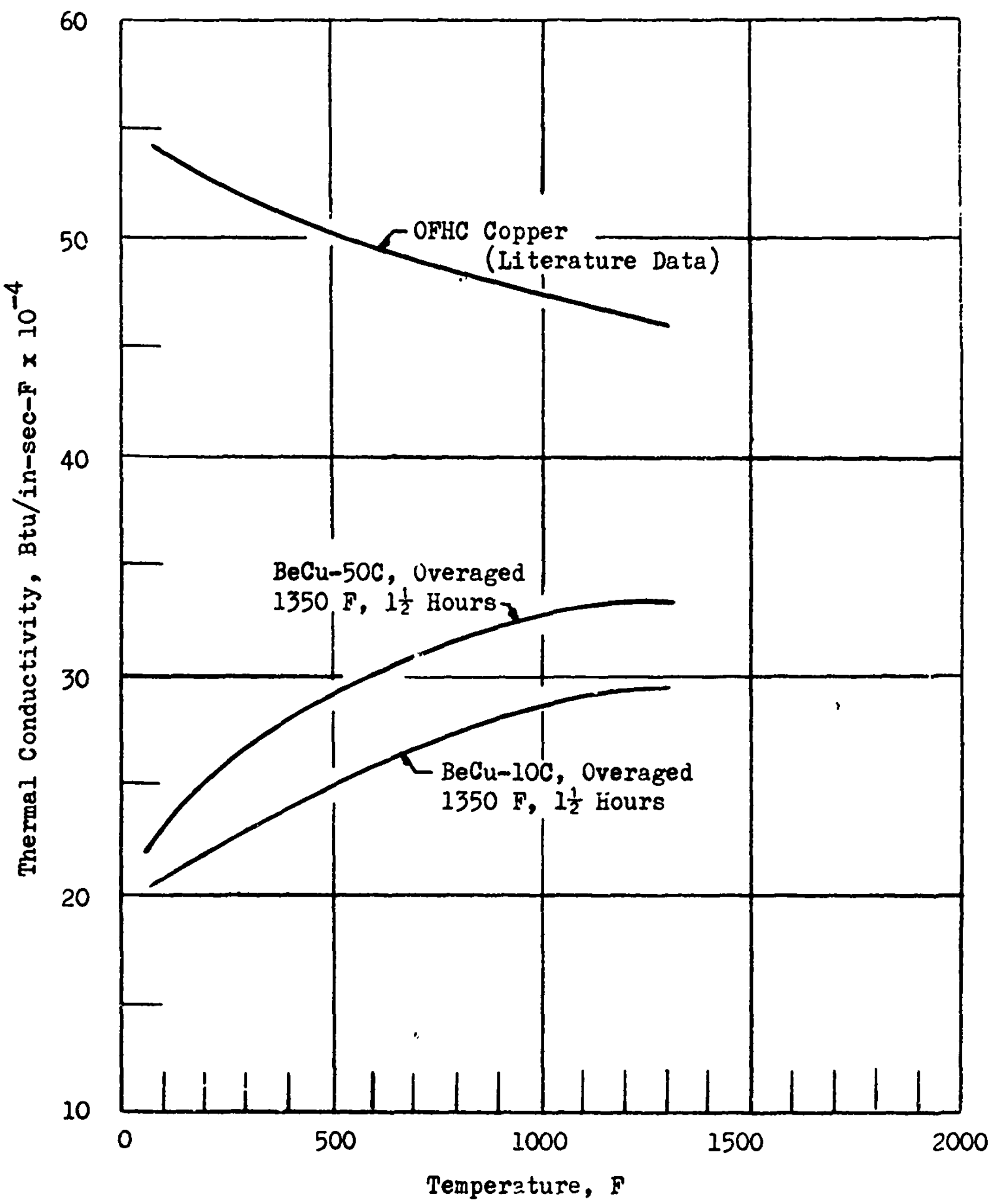

Figure 68. Thermal Conductivity of Overaged Beryllium Copper Castings. (U)

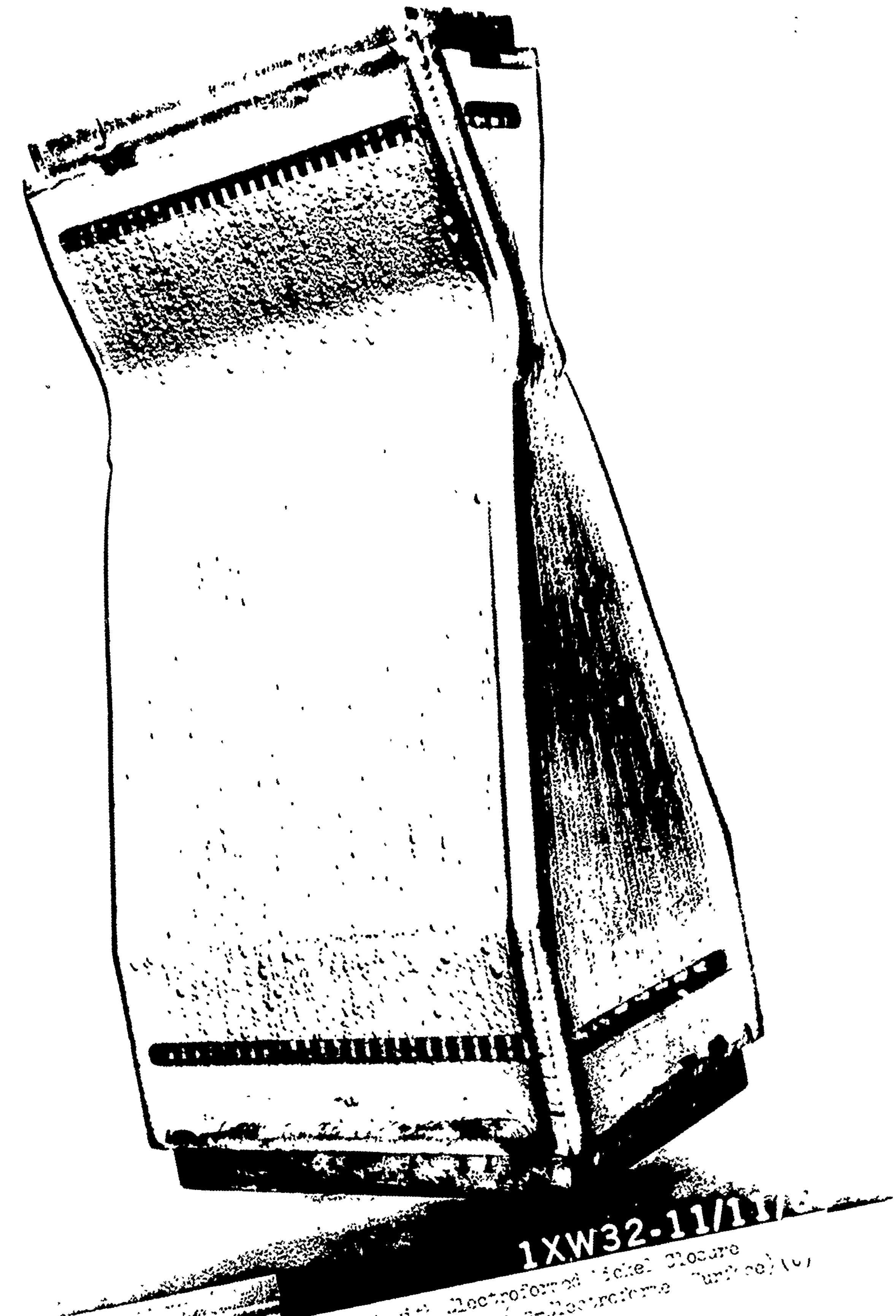

Fig. 69. Cast Segment with Electroformed Nickel Closure and Machined Manifolds (As-Electroformed Surface) (U)

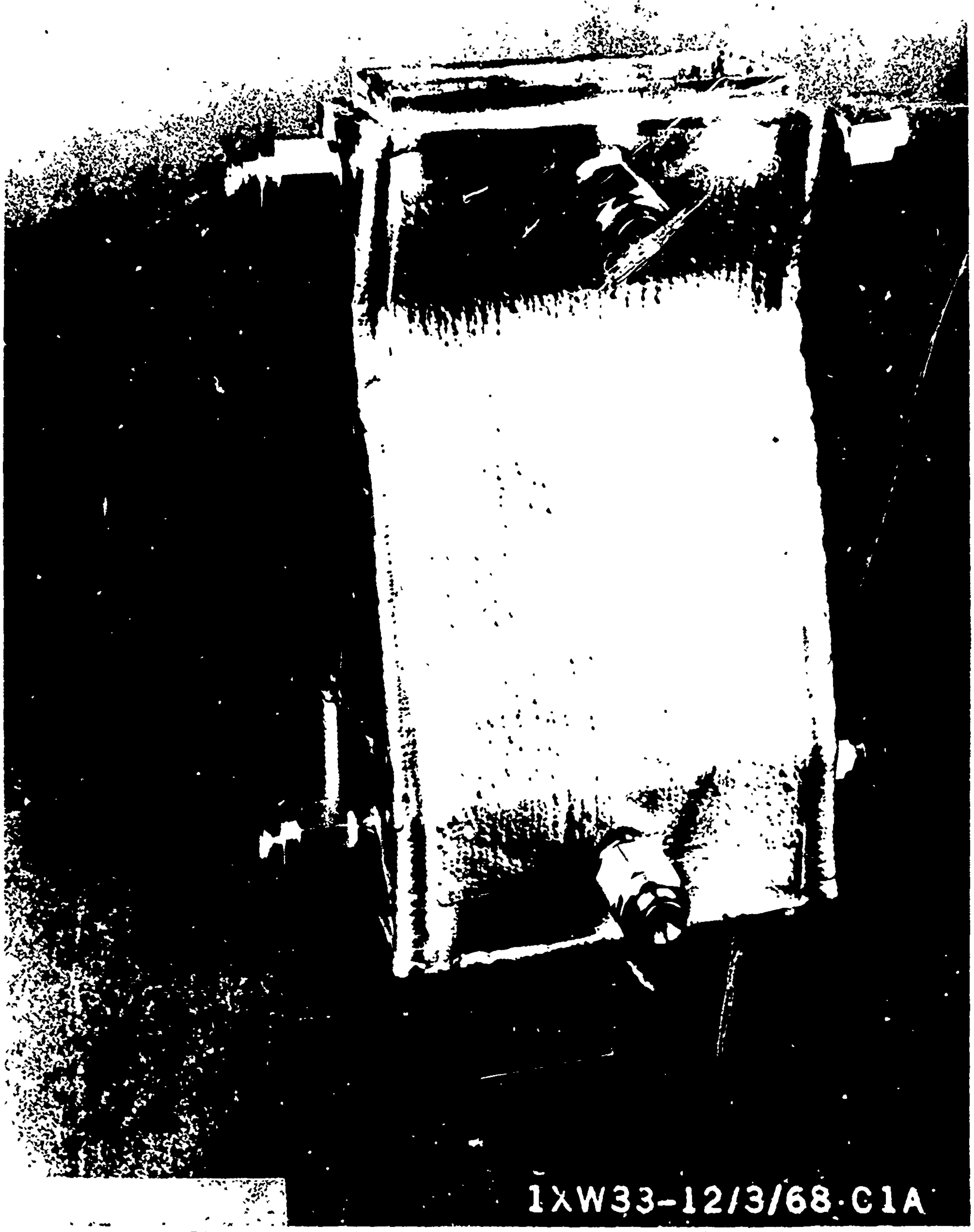

Fig. 70. Development Segment with Ni-Electroformed Surface and Welded on Pressurant Tubes (U)

TABLE XVII

STRUCTURAL INTEGRITY VERIFICATION -
CAST BeCu SEGMENT/ELF NICKEL CHAMBER (U)

ITEM	LOCATION	PRESSURE TEST psig	CONCLUSIONS
Fabrication Development Segment	Contoured Walls	10,500 Burst 2700 Proof	Demonstrated structural integrity
	Side Plates	10,500 Burst 2700 Proof	↓

(U) As discussed in more detail in a later section, this segment was then used to establish parameters for machining the coolant passages of the heat exchange panel into the electroformed nickel.

(U) Each electroformed cycle performed on the segment was done in a similar fashion. All coolant passages and manifolds, into which no electroformed nickel was desired were filled with wax. All surfaces were sanded smooth and all wax surfaces burnished with silver powder. This makes all surfaces conductive; assuring a proper bond and uniform deposition of the nickel onto the surface to be covered. The part was then shielded (Fig. 71) to control rate of buildup in various areas, cleaned in an anodic bath, activated in a cathodic bath, and placed in the electroforming tank.

(U) <u>Chemical Milling</u>. As discussed previously, the castings were poured with a hot gas wall thickness of 0.060. However, the heat transfer analysis of the cast beryllium copper segment in the test environment planned for Phase III showed that a hot gas wall thickness of 0.030 was required to maintain the hot gas wall temperature to the design value of 1000 F at 650 psia chamber pressure. Consequently, investigation was initiated into

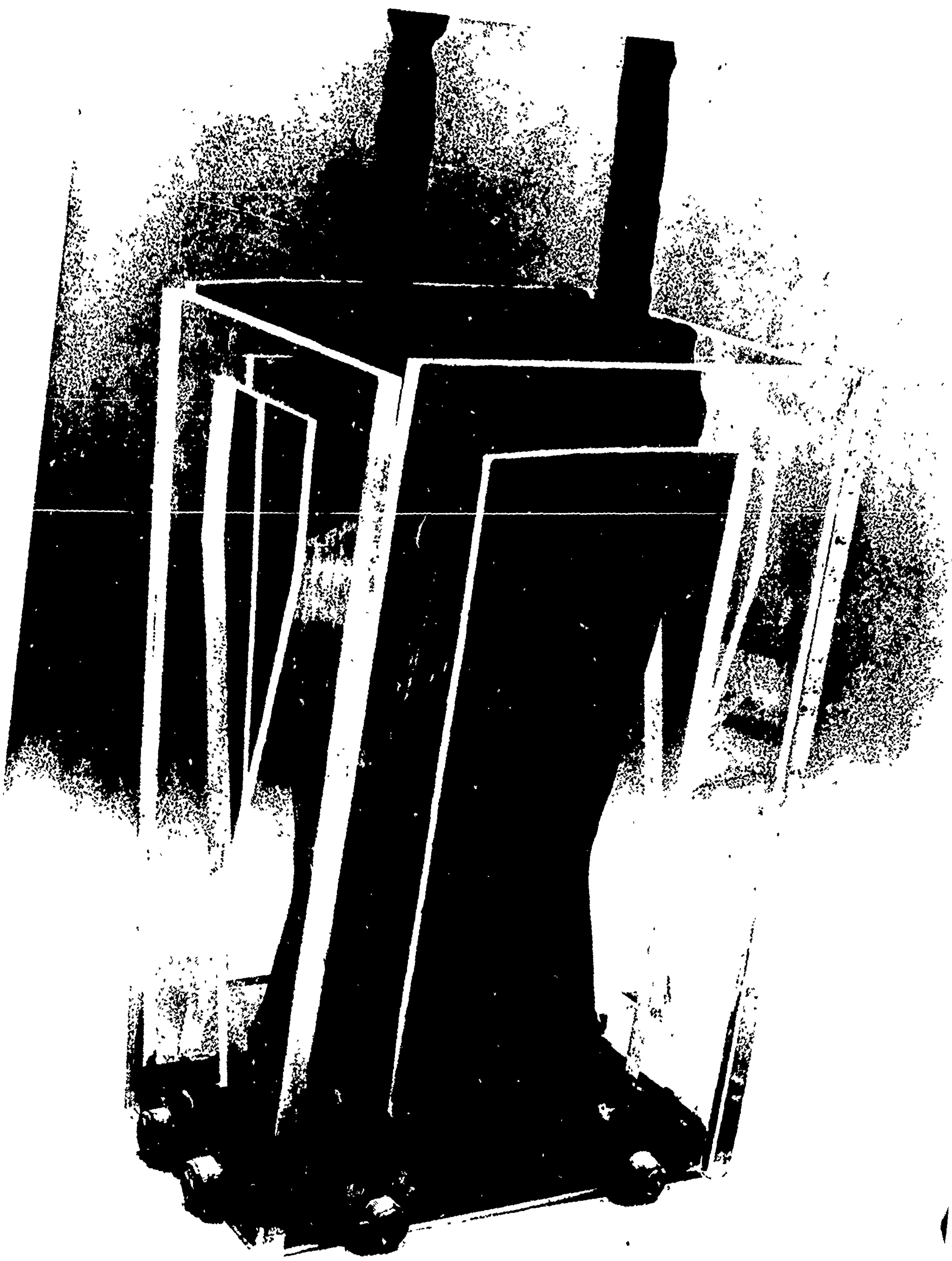

Fig. 71. Cast [illegible]Cu Segment Ready for Electroforming (U)

the feasibility of chemical milling the as-cast 0.060 inch thick hot gas wall of the cast segments to the design value of 0.030 inches with good dimensional repeatability and surface finish.

(U) The initial samples submitted for chemical milling showed good overall dimensional repeatability, however, there were some surface irregularities, due to the oxides and shrinkage fissures in the castings (which were rejects from the casting development program). It was concluded from these samples that chemical milling was feasible with good quality castings. This was later demonstrated in the company funded program where the hot gas walls of good quality copper alloy castings were chemical milled to a thickness of 0.030 $\pm$ 0.003.

(U) In consideration of the fact that the primary goal of the Phase III hot firing program was to demonstrate the integrity of the fabrication process in the thermal environment at a wall temperature of 1000 F and in view of the material properties which showed that the cast beryllium copper segments should be capable of operation at even higher gas side wall temperatures, it was decided to delete the chemical milling requirement and test the segments with the as-cast wall thickness of 0.060. Also, it should be noted that other techniques such as conventional, electrochemical and electro-deposition machining are applicable candidates for reducing the hot gas wall thickness below the as-cast dimensions if required. Further, the successes on the casting program lent confidence that castings with thinner walls can be repeatably cast, eliminating any need for further reduction in the hot gas wall thickness.

(U) <u>Heat Exchange Panel Machining</u>. Following the proof pressure test discussed previously, the Phase II fabrication development segment was used to establish heat exchange coolant circuit machining parameters and

segment tooling requirements. Single and multiple cuts per pass were completed with various cutter feeds and speeds using one and one half inch diameter jeweler saw cutters. Results showed that cutting three passages at a time with three saws on a single arbor and making cuts of .010 inch deep per pass produced good dimensional results (tolerances were typically ± 0.003 inch for passage width and depth).

Non-Destructive Inspection Techniques

(U) Non-destructive inspection techniques verified for use in inspecting the Phase III hot firing hardware included dimensional, radiographic and dye-penetrant inspection as well as hydrostatic proof pressure tests and gaseous helium leak checks.

(U) Dye-penetrant inspection was used to locate any surface defects and to verify that there were no fissures or micro-shrinkage cracks through the as-cast wall.

(U) Radiographic inspection was used to locate any internal defects in the as-cast wall. Various exposures were used to verify that the casting was free of defects in the thick as well as the thin sections (located in a land region between passages or over a passage). Radiographics were also used to establish the location of the heat exchange coolant passages in relation to the primary (fuel) coolant passages.

(U) Progressive dimensional checks using special fixtures were completed to verify wall thickness (hot gas wall and wall between coolants) as well as passage cross section and spacing dimensions.

(U) Structural integrity of the cast segment, the electroformed nickel and the electroformed nickel to cast segment bond joint was verified by proof pressure testing. Also, high pressure ($\sim$ 1500 psig) gaseous helium leak checks were used to verify there was no porosity in the as-cast wall, the electroformed nickel layer between the primary and heat exchange coolants or in the electroformed nickel closure itself.

(U) The fabrication sequence employed on this concept used successive layers of electroformed nickel to close off the coolant passages and manifolds. Verification of complete removal of the wax used to fill the passages and manifold cavities during the electroforming cycle was accomplished by infrared analysis of solvent flushed through the coolant circuit.

Conclusions and Recommendations

(U) The Phase II fabrication development studies demonstrated the capability and low-cost feasibility of this fabrication concept (investment cast hot gas wall liners followed by electroforming to closeout the coolant circuit) for production quantities of regeneratively cooled thrust chambers. Comments on each process involved in this fabrication concept are presented in the following paragraphs.

(U) Investment Casting. The feasibility of investment casting copper alloy segments for subsequent use as hot gas wall liners in regeneratively cooled thrust chambers was demonstrated on this program for two candidate beryllium copper alloys, BeCu-10C and -50C. Subsequently, a company funded program has demonstrated the feasibility of casting alternate copper alloys.

(U) For maximum quality and repeatability in the process, the castings should be poured in a vacuum and should incorporate directional solidification. It is recommended that additional investigation of the investment cast process be undertaken to further refine the casting parameters and that additional materials be explored. This would establish a family of materials from which to select for any specific application. Also, investigation is needed to determine casting limits in reduced hot gas wall thickness, various passage cross section dimensions and application to larger size and alternate shapes such as curved segments and/or bell chambers. Additional effort is required to more firmly establish operating temperature limits based on structural and thermal fatigue (cyclic life) characteristics.

(U) To further reduce the production cost of this fabrication technique, evaluation should be undertaken to explore the feasibility of integrally casting the coolant passages, thus eliminating the need for subsequent electroforming.

(U) <u>Chemical Milling</u>. Adequate investigation was completed on the company funded program to establish confidence that chemical milling can be effectively employed to reduce the hot gas wall thickness below the as-cast thickness if required.

(U) <u>Electroforming</u>. Electroforming nickel onto the beryllium copper and onto itself has been demonstrated to be a good technique for closing out the coolant passages and the manifolds, resulting in excellent structural integrity. However, further work is warranted to optimize shielding techniques and electroforming parameters to minimize production cost and time.

(U) <u>Heat Exchange Panel Machining</u>. Conventional machining techniques are acceptable for use in slotting the electroformed nickel layer to provide the coolant passages for the heat exchange panel.

PHASE III - DESIGN AND PERFORMANCE EVALUATION

(U) In Phase III thrust chambers and/or segments representing each of the three selected fabrication concepts were fabricated and hot fire tested to demonstrate the structural integrity and thermal performance of the three concepts when subjected to the combustion environment.

(U) As discussed previously, LF_2/GH_2 propellants were used in all three concepts to provide the combustion environment with both bell thrust chamber concepts designed to use the same injector. The powder metal nickel bell chamber was cooled with GH_2 while the spun INCO 625 bell chamber used water coolant (simulating the bulk temperature limited amine fuels). The cast segment used GH_2 as the primary coolant with LN_2 and subsequently LF_2 as the coolant in the heat exchange panel.

TEST HARDWARE DESCRIPTION

(U) Hardware requirements for the Phase III hot firing effort included chambers and/or segments of each fabrication concept, injectors, and solid wall chambers and segments for injector checkout.

Powder Metal Nickel Bell Chamber

(C) The application selected for experimental evaluation of the powder metal nickel bell chamber fabrication concept was a gaseous hydrogen cooled bell chamber identical in operating parameters to one being developed under AFRPL Contract F04611-67-C-0116. Design parameters are listed in Table XVIII.

TABLE XVIII

DESIGN PARAMETERS FOR PHASE III HARDWARE (U)

	POWDER METAL BELL	SPUN BELL	CAST SEGMENT
Thrust, pounds	3300 (to ϵ = 60)	3300 (to ϵ = 60)	630
Chamber Pressure, psia	750	750	650
Propellants	F_2/H_2	CPF/N_2H_4 (simulated with F_2/H_2)	F_2/H_2
Coolant	H_2	N_2H_4 (simulated with water)	H_2 (F_2 in heat exchange panel)
Hot Gas Wall Temp, F	1600	2000	1000
Area Ratio	4	4	4
Contraction Ratio	4	4	12
Combustion Zone Length, (Injector Face to Throat Centerline) in.	6	6	3.5

(U) The resulting heat transfer analysis, presented in more detail in a later section, established a requirement for sixty constant width variable depth coolant passages with a hot gas wall thickness of 0.032 inches. The design layout of the chamber is shown in Fig. 72.

(U) The Phase III chamber was fabricated using the process parameters developed in Phase II. The liner for the hot gas wall was pressed at 30,000 psig and machined to the prescribed thickness. Following core stacking (Fig. 73) and powder packing, the entire unit was pressed at 55,000 psig. After outer surface machining, the cores were flushed out with hot water and ultrasonics with core removal verified by X-ray. The chamber was then sintered at 2300 F for 3 hours.

(U) Post sintering inspection showed the chamber to be of excellent quality, free of surface imperfections and blistering. The average density of the chamber was 96.3 percent of theoretical and the shrinkage during sintering averaged 8.7 percent axially and 8.0 percent radially. The chamber is shown after sintering in Fig. 74.

(U) Subsequent X-ray of the chamber showed no gross variations in coolant passage spacing. A nickel 200 flange was then electron beam welded to the exit end of the chamber, the coolant circuit hydrostatically proof pressure tested to 1500 psig and each passage flow calibrated. Results showed that, with a back pressure of 50 psig, the passage to passage flowrate with water was within 8 percent of the average value; reflecting very good dimensional repeatability in the coolant passages. The forward flange was then welded in place and a final proof pressure test of the coolant circuit (1500 psig) and chamber interior (1000 psig) completed. The chamber is shown in Fig. 75.

CONFIDENTIAL

SECTION B - B

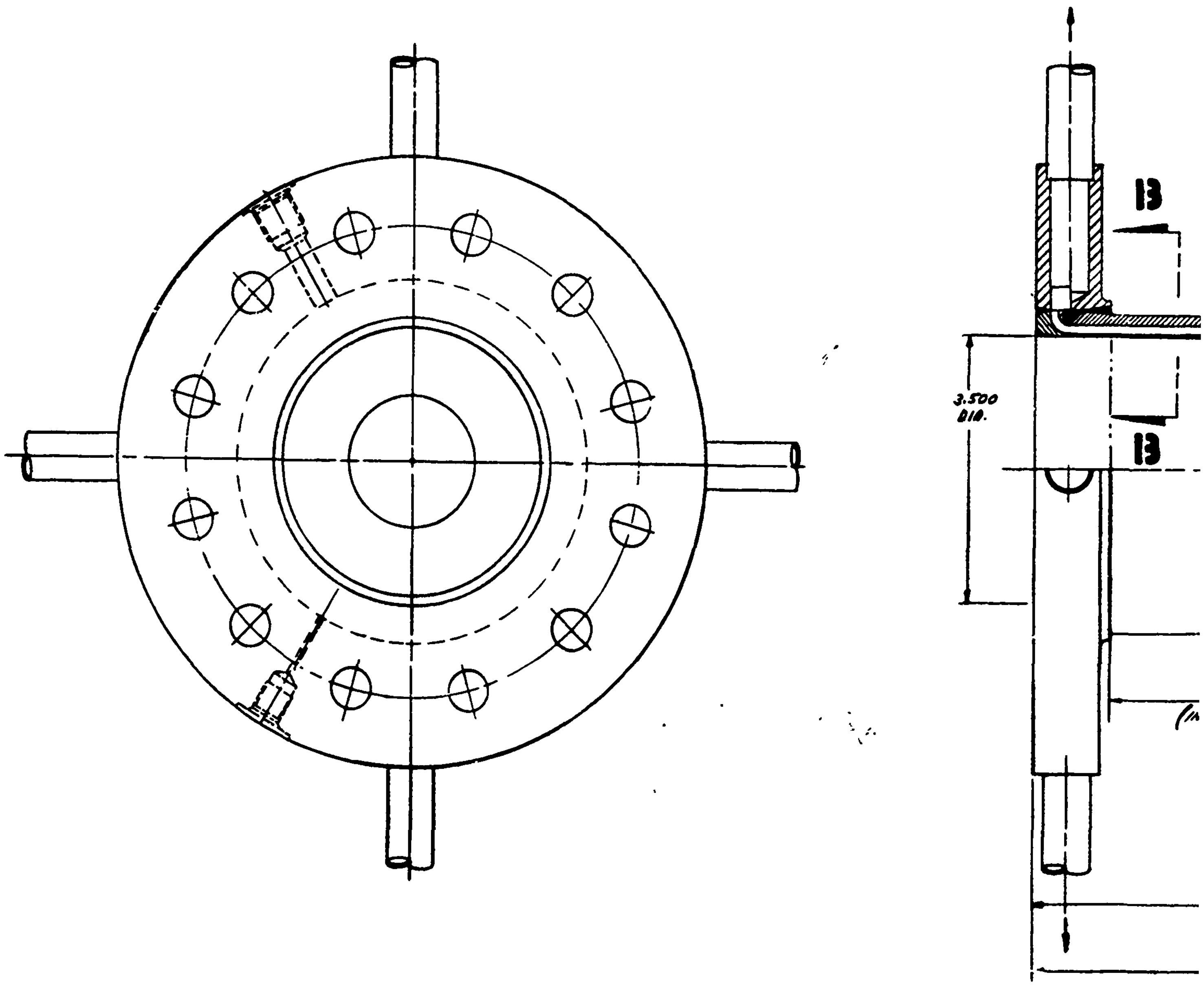

AL

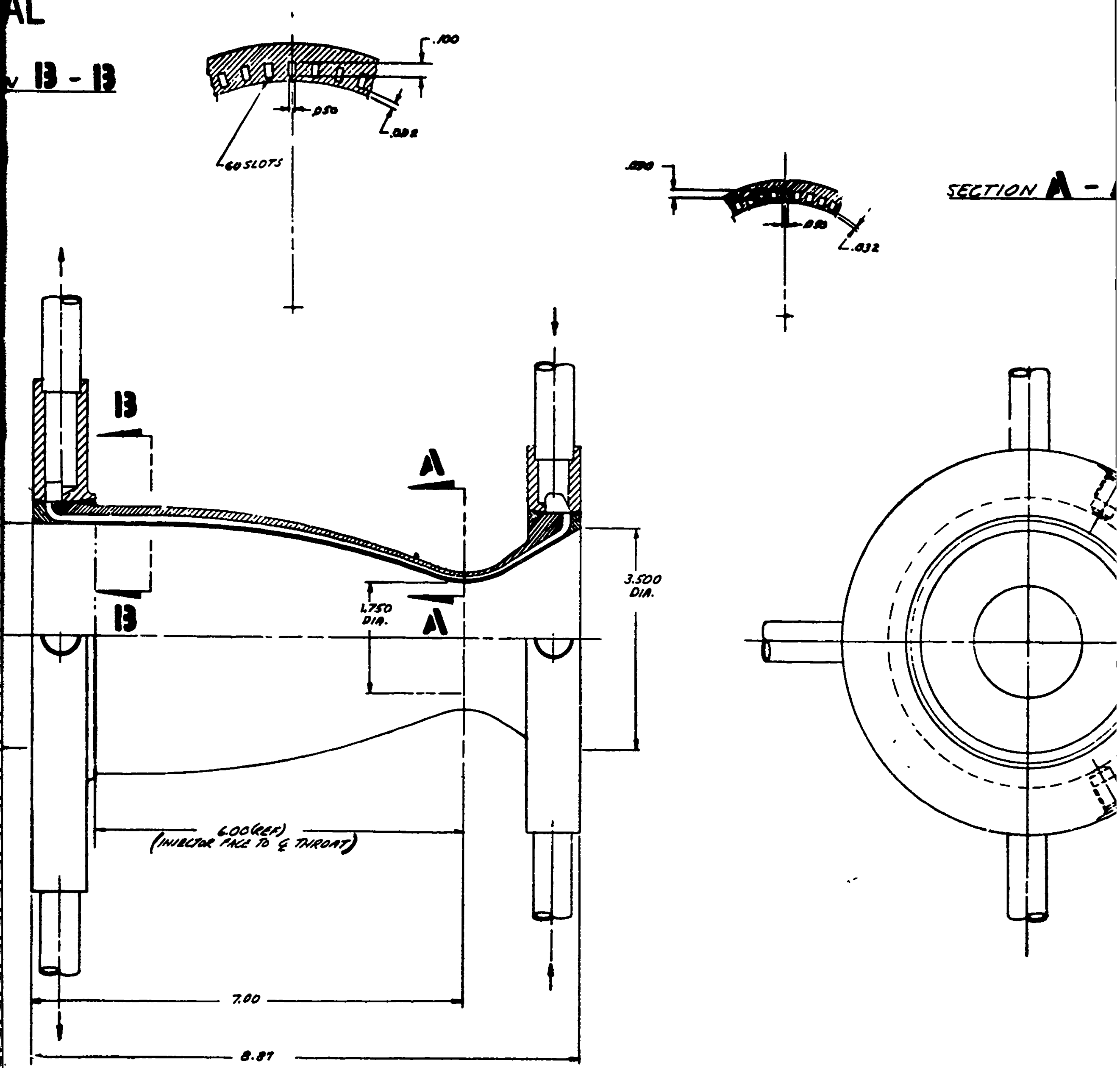

B - B
.100
.050
60 SLOTS
SECTION A -
.032
B
B
A
A
1.750 DIA.
3.500 DIA.
6.00(REF) (INJECTOR FACE TO ℄ THROAT)
7.00
8.87

Figure 72.

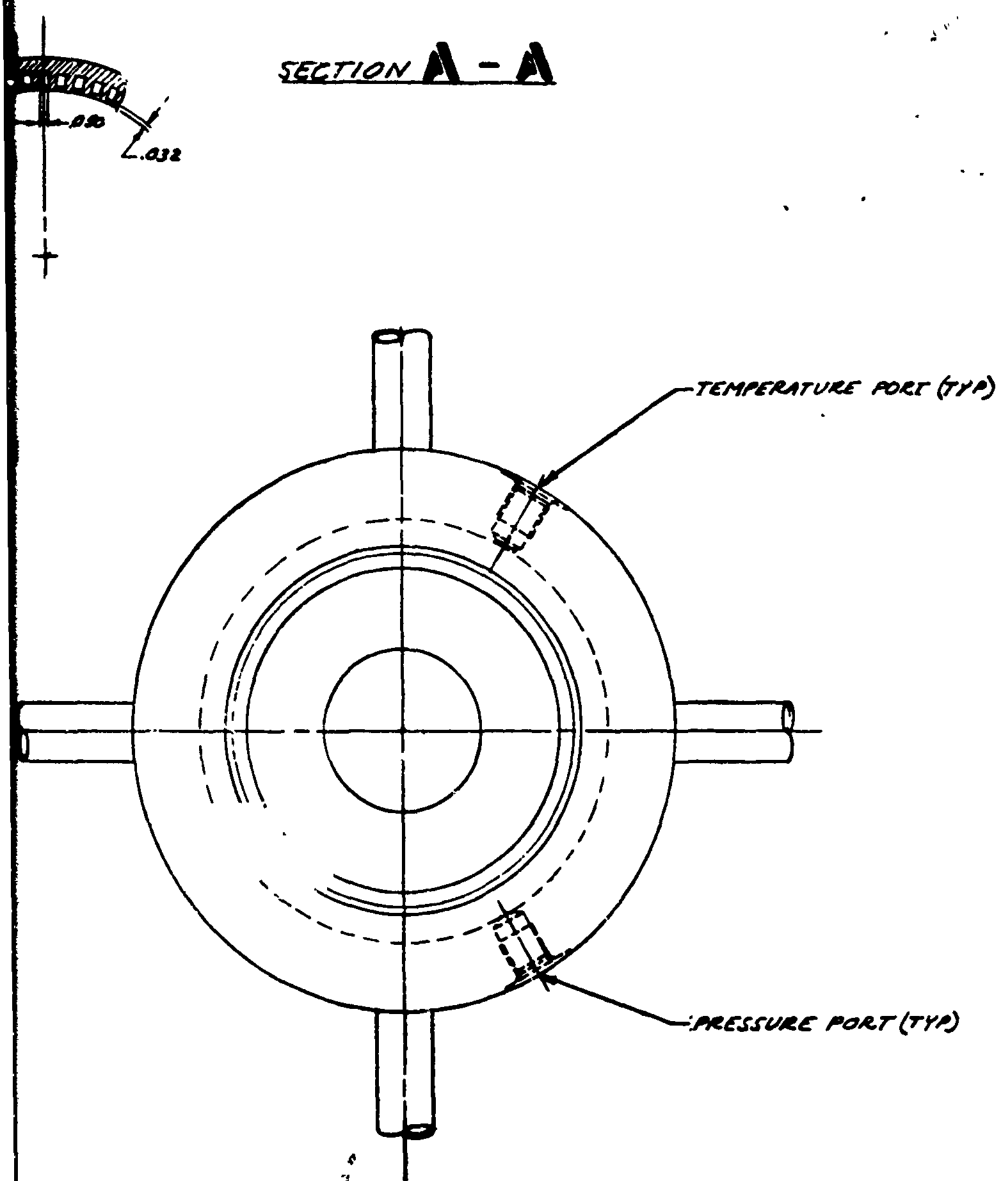

Figure 72. Design Layout of Powder
Metal Nickel Bell Chamber. (U)

NFIDENTIAL

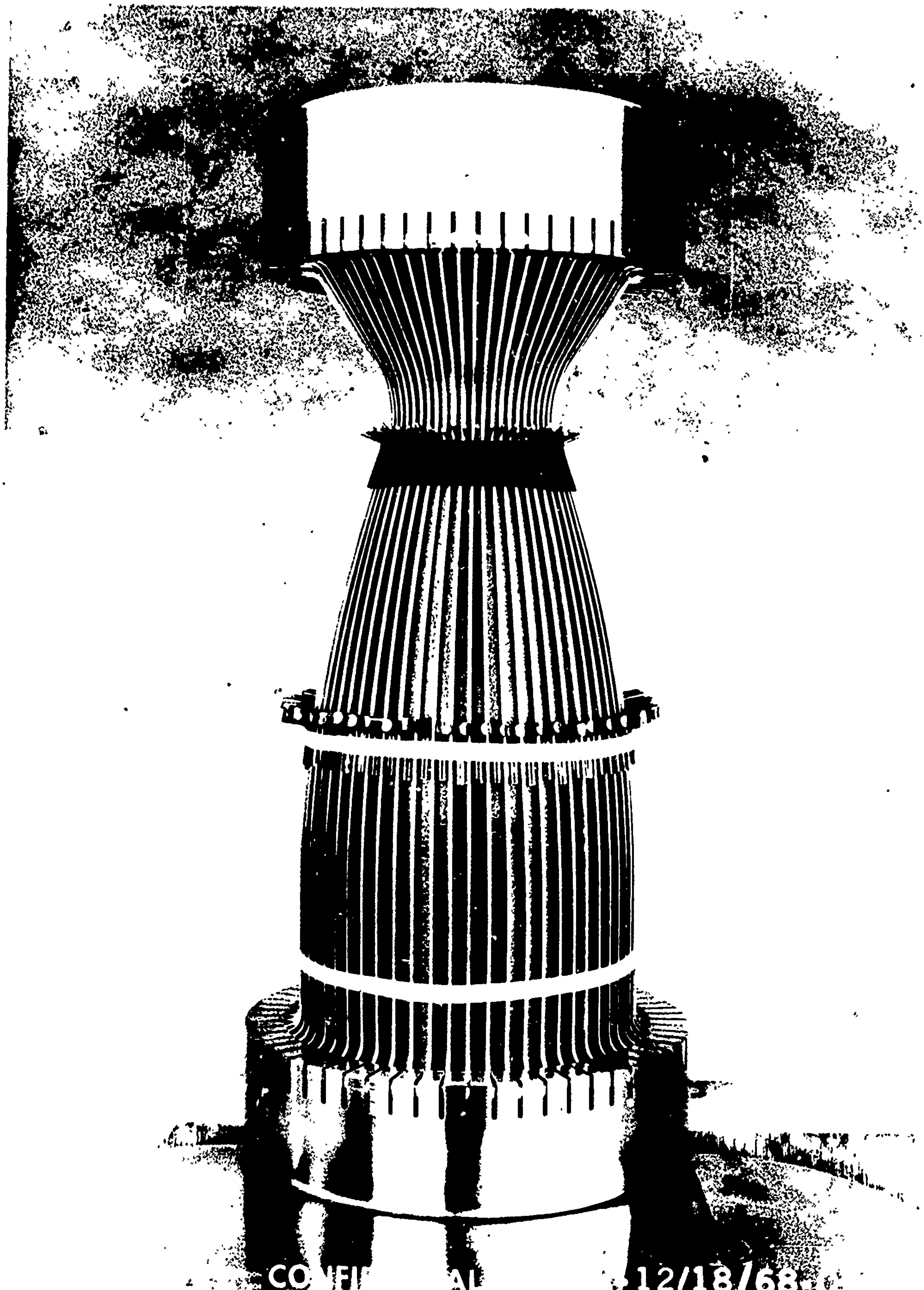

Fig. 73. Pressed and Machined Powder Metal Liner with Cerrolow Cores Stacked in Place Preparatory to Packing Powder for the Outer Shell (U)

CONFIDENTIAL

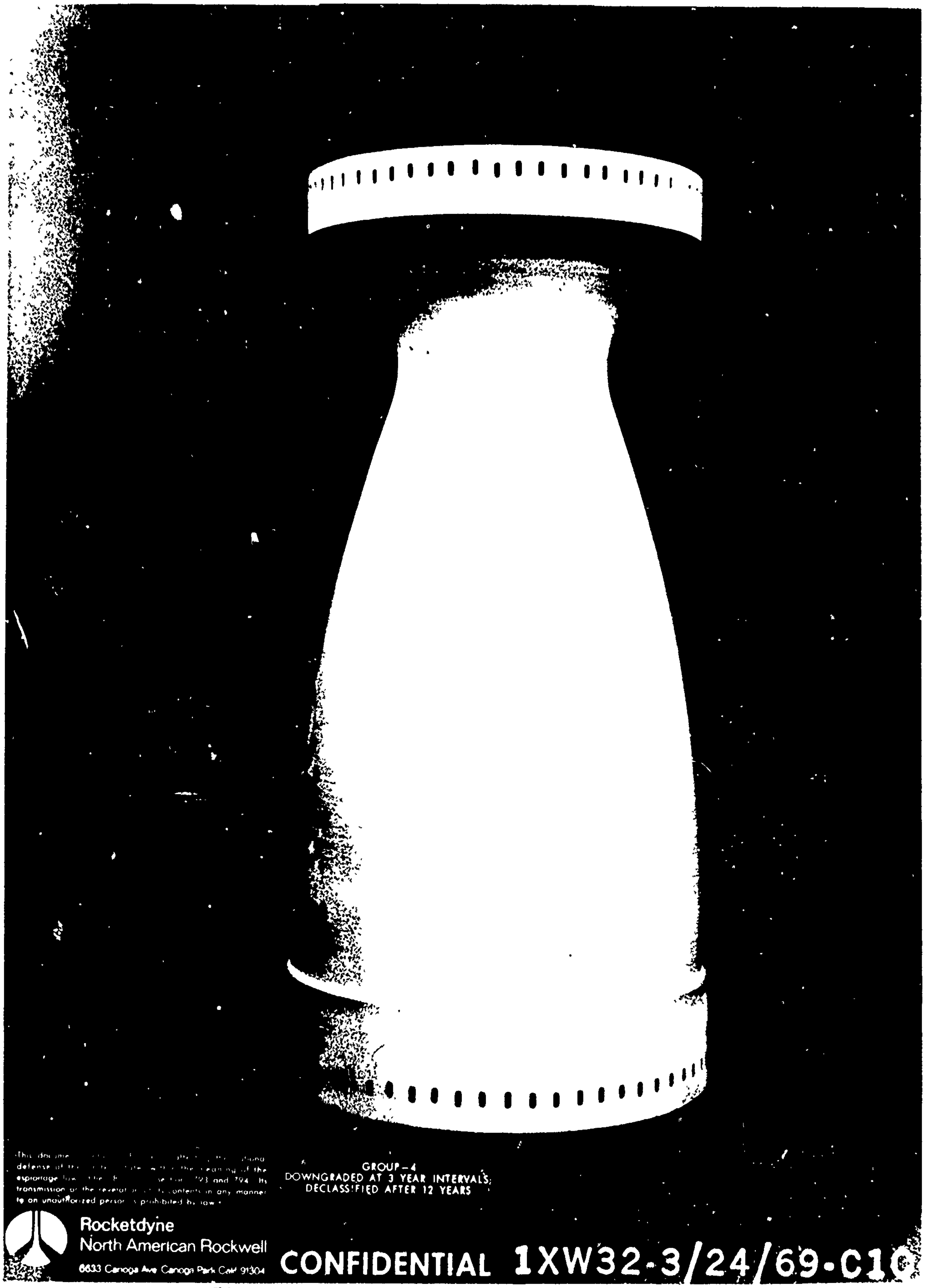

Fig. 74. Post Sintering View of Phase III Hot-Firing Powder Metal Bell Chamber (U)

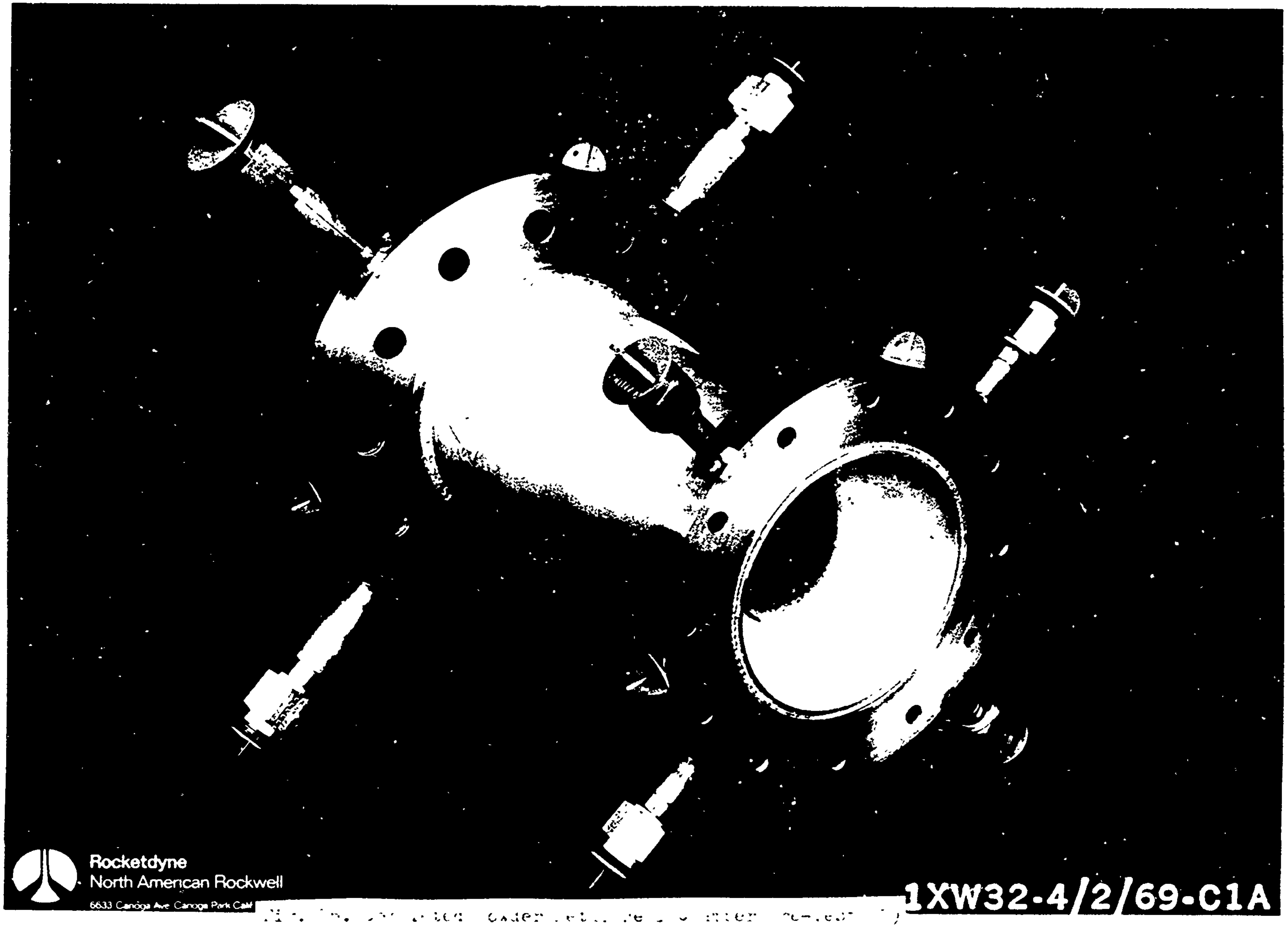
Rocketdyne
North American Rockwell
6633 Canoga Ave Canoga Park Calif
1XW32-4/2/69-C1A

Spun INCO 625 Liner with Machined Passages and Electroformed Nickel Closure

(U) The spun INCO 625 bell chamber fabrication concept was selected as an attractive low cost technique for extending the limits of regenerative cooling of CPF/Amine chambers cooled with the bulk temperature limited Amine-type fuels. Water was used as the coolant and the F_2/H_2 injector used with the powder metal nickel bell chamber provided the combustion environment. The higher heat fluxes experienced with F_2/H_2 propellants as compared with CPF/Amine propellants necessitated the operation of the injector at a lower chamber pressure to simulate the CPF/N_2H_4 design value of 750 psia chamber pressure (Fig. 4). Design parameters are shown in Table XVIII.

(U) The heat transfer analysis had established a requirement for sixty constand width, variable depth coolant passages and a hot gas wall thickness of 0.030 inches. The chamber design layout is shown in Fig. 76.

(U) The Phase III hot firing chamber was fabricated using one of the slotted INCO 625 liners from Phase II (shown previously in Fig. 55). After electroforming the nickel closure (Fig. 77) and machining (Fig. 78), the aft nickel 200 flange was electron beam welded in place and the coolant circuit hydrostatically proof pressure tested to 2200 psig. Subsequently, the forward nickel 200 flange was welded in place and a final hydrostatic proof pressure test completed on the coolant circuit (2200 psig) and chamber interior (1000 psig). The chamber is shown in Fig. 79.

(U) Non-destructive inspection techniques used to verify chamber quality included (1) dye penetrant check of the spun liner to assure integrity, (2) dimensional check of the machined liner and electroformed nickel shell and (3) hydrostatic proof pressure tests to assure structural integrity.

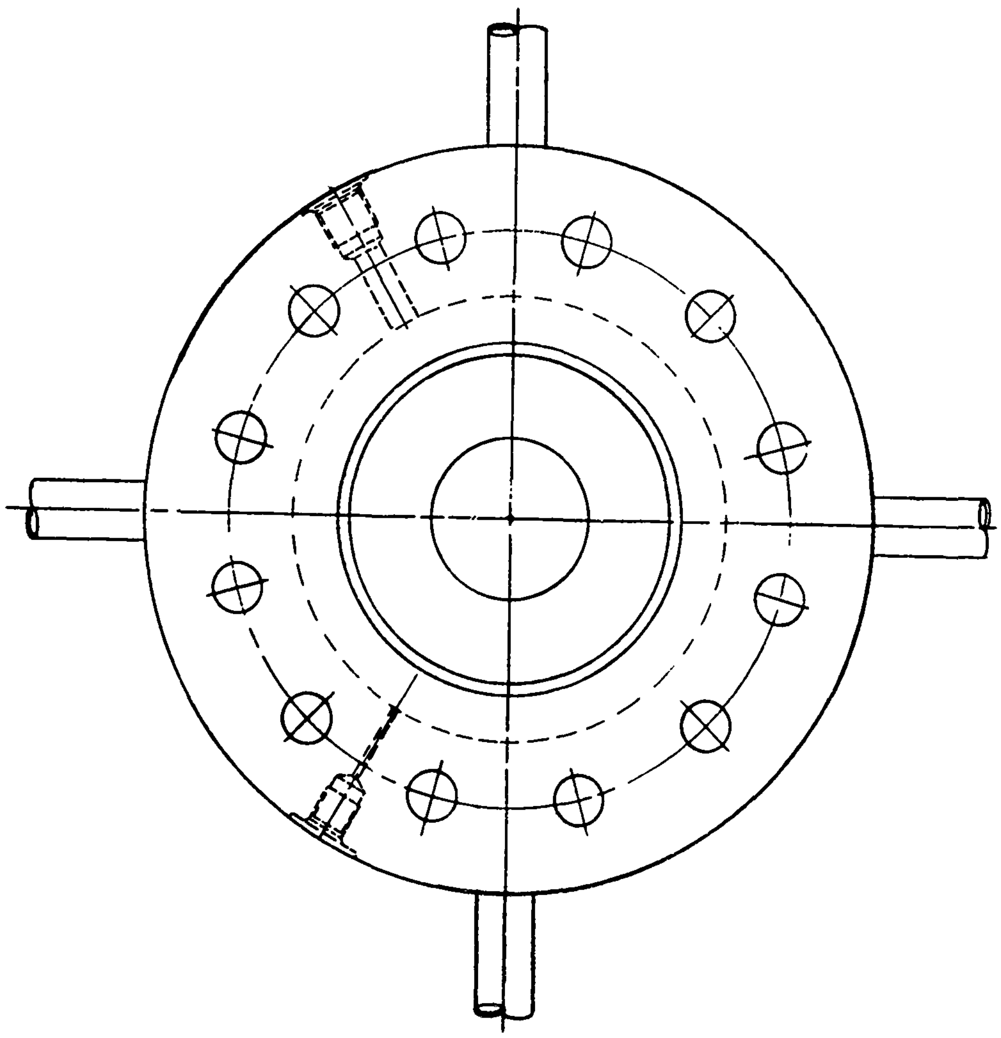

SECTI

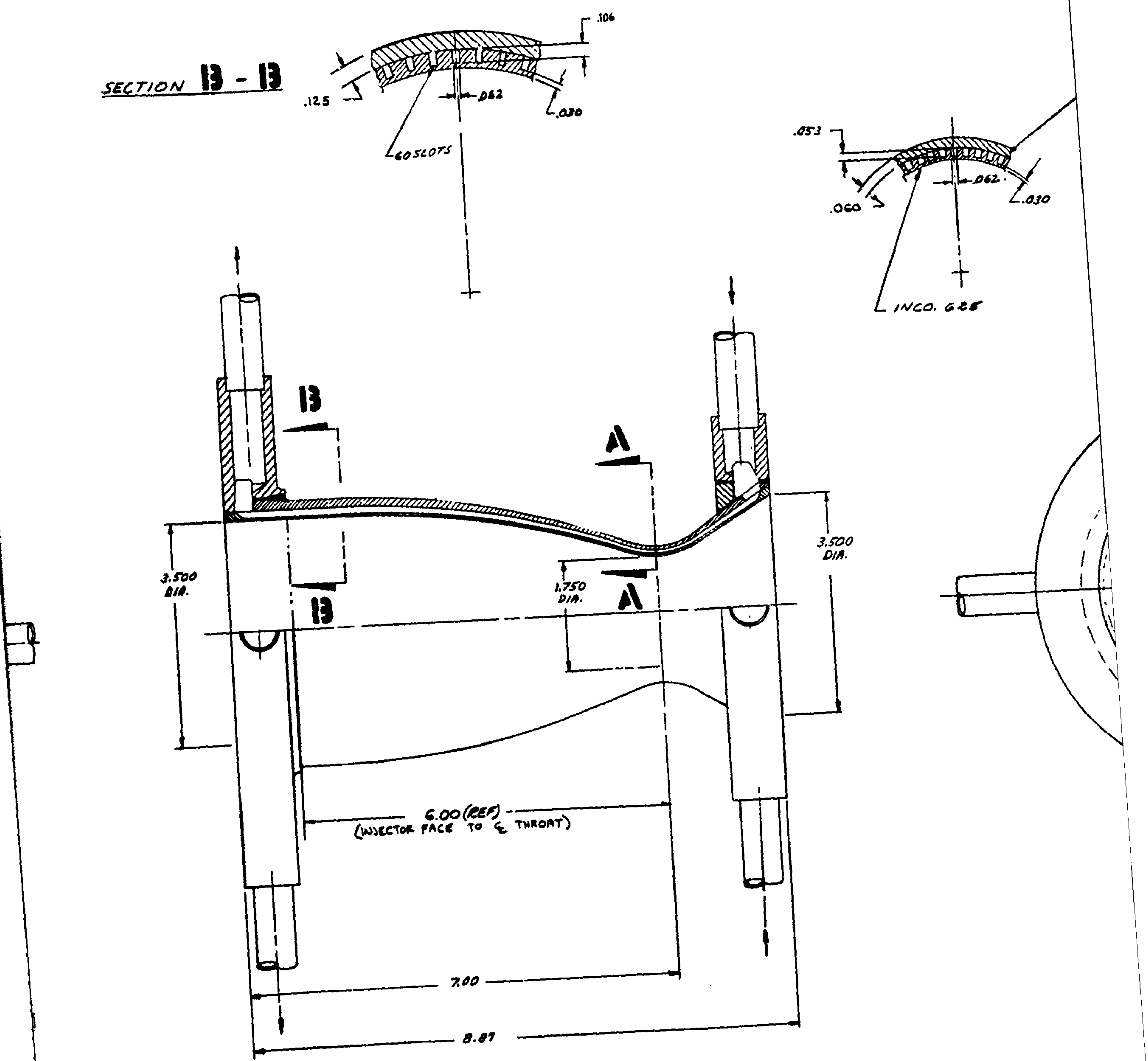
SECTION B - B
.106
.125
.062
.030
60 SLOTS
.053
.060
.062
.030
INCO. 625
B
B
A
A
3.500 DIA.
3.500 DIA.
1.750 DIA.
6.00 (REF)
(INJECTOR FACE TO ℄ THROAT)
7.00
8.87

Fig

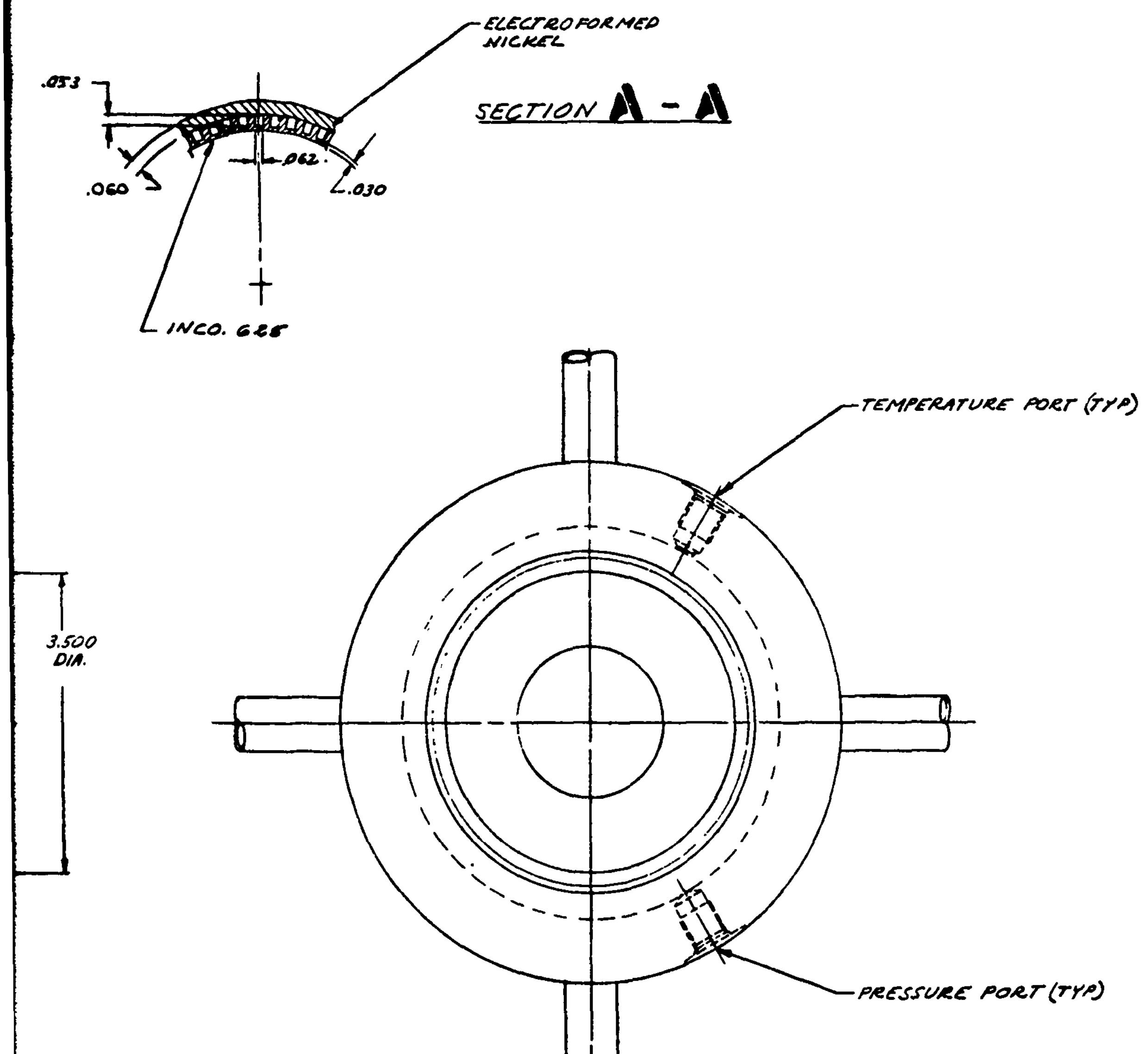

Figure 76. Design Layout of Spun INCO 625 Bell Chamber with ELF Nickel Closure. (U)

CONFIDENTIAL

CONFIDENTIAL

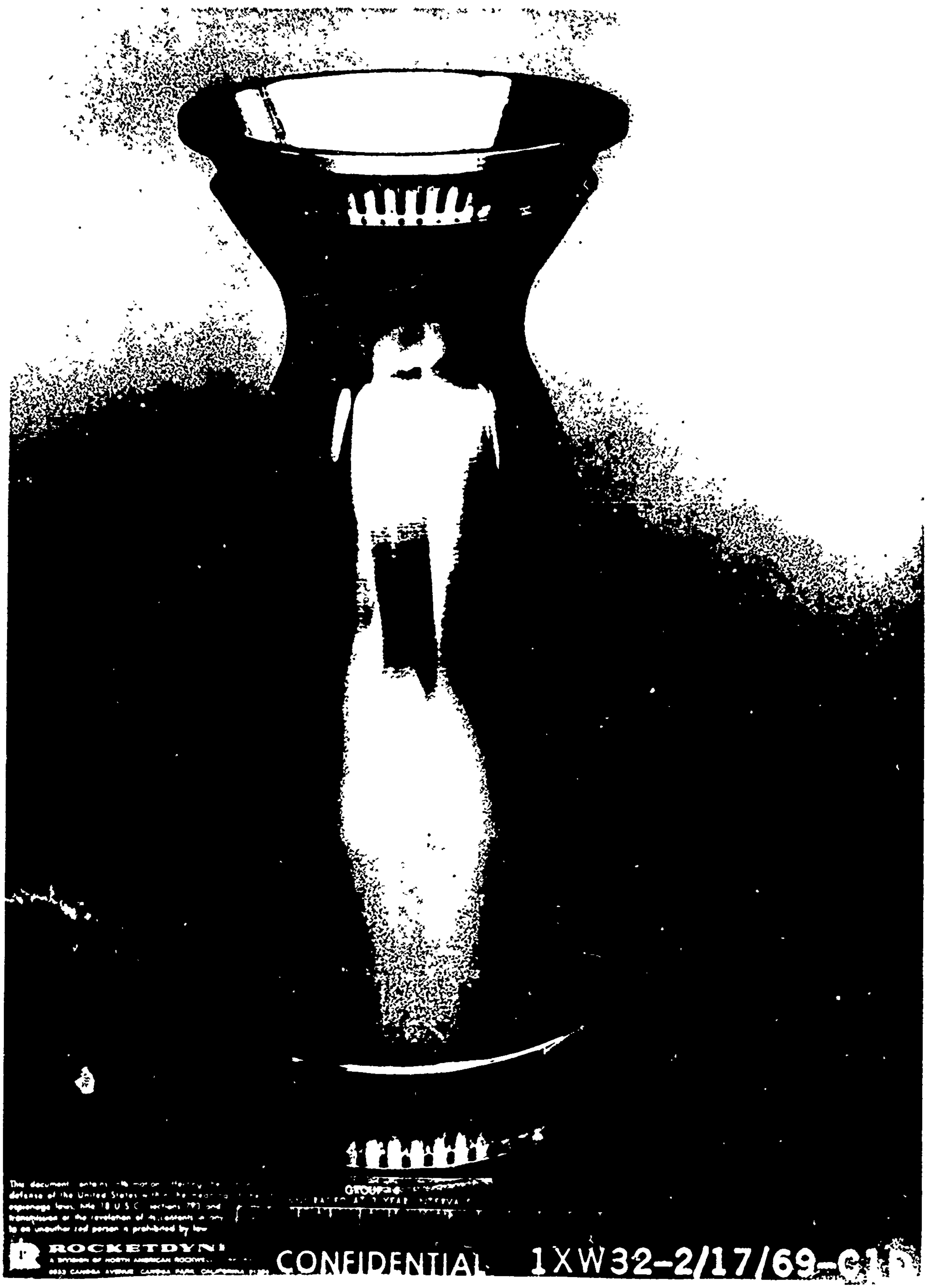

Fig. 78. Slotted INCO 625 Liner with Electroformed Nickel Closure - After Manifold and Surface Machining (U)

CONFIDENTIAL

[illegible] (U)

(This page is unclassified)

CONFIDENTIAL

Cast Segment with Electroformed Nickel Closure and Machined Heat Exchange Panel

(U) This concept was selected as an attractive fabrication technique for producing low cost segments of an annular chamber, or complete bell chambers. The heat exchange panel incorporated on one contoured wall of the segment offers significant system advantages as discussed previously.

(C) The application selected for demonstrating this fabrication concept was a full-size cross section of an annular chamber under development at Rocketdyne for the AFRPL (F04611-67-C-0116). The design parameters for this segment are listed in Table XVIII.

(U) The dimensional requirements for the cast segment liner were established based on the minimum dimensions the foundry and Rocketdyne Materials and Processes personnel felt could be confidently cast. The resulting design details of the segment liner were shown previously in Fig. 61. The electroformed nickel thickness requirements and the heat exchange panel dimensions were then established by the heat transfer and structural analyses. The segment assembly is shown in Figs. 80 and 81.

(U) The cast segment liner (Fig. 82) used for the Phase III hot firing segment was one of the BeCu-10C segments cast during the Phase II development effort. Initially, an electroformed nickel layer was added to this segment to close off the fuel coolant passages in the casting. Manifolds were then machined into the nickel on either end of the segment, and passages for the heat exchange panel machined on one contoured wall (Figs. 83 and 84).

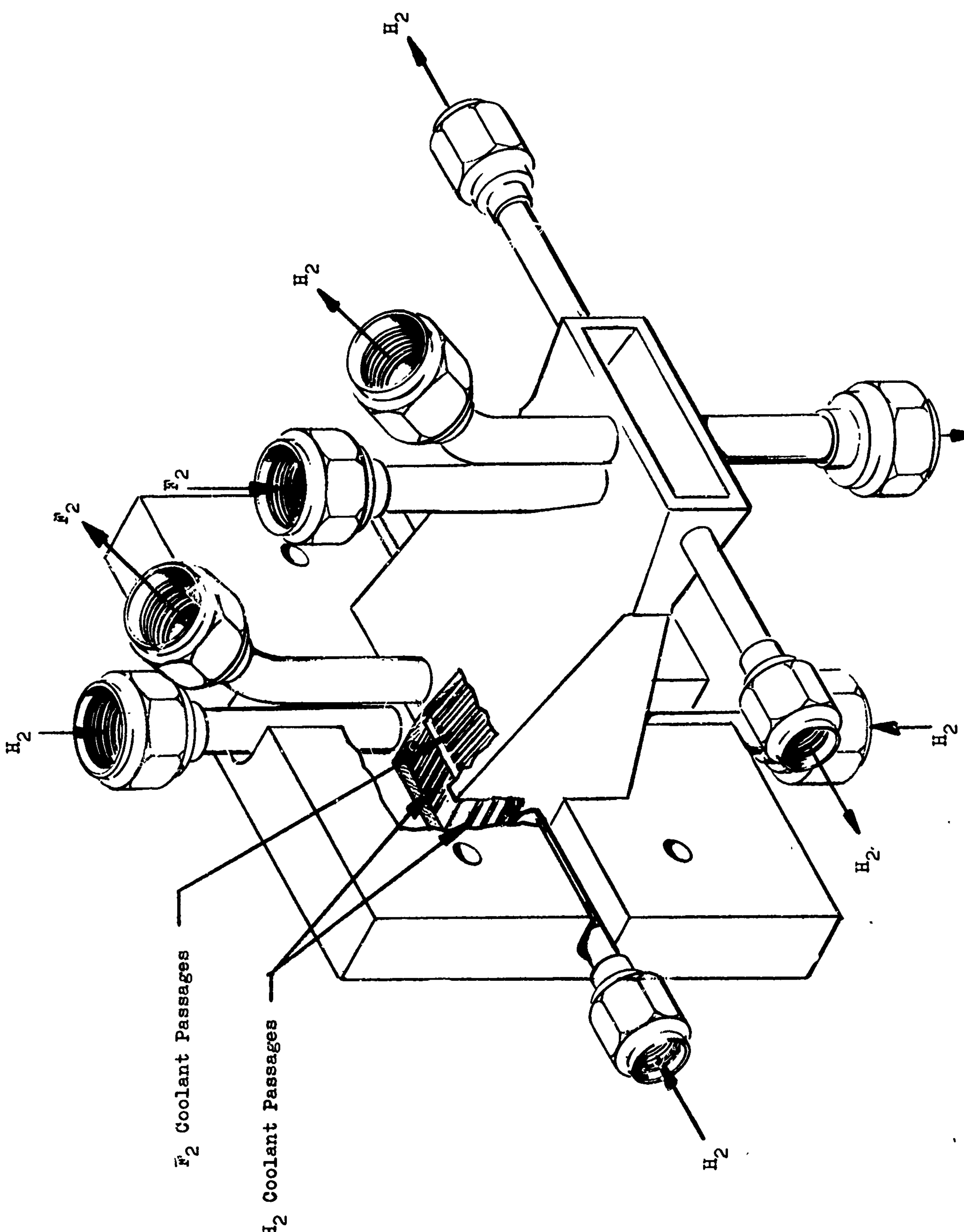

Figure 80 . Isometric of Cast Segment With Electroformed Nickel Closure and Heat Exchange Panel (Structure Removed for Clarity). (U)

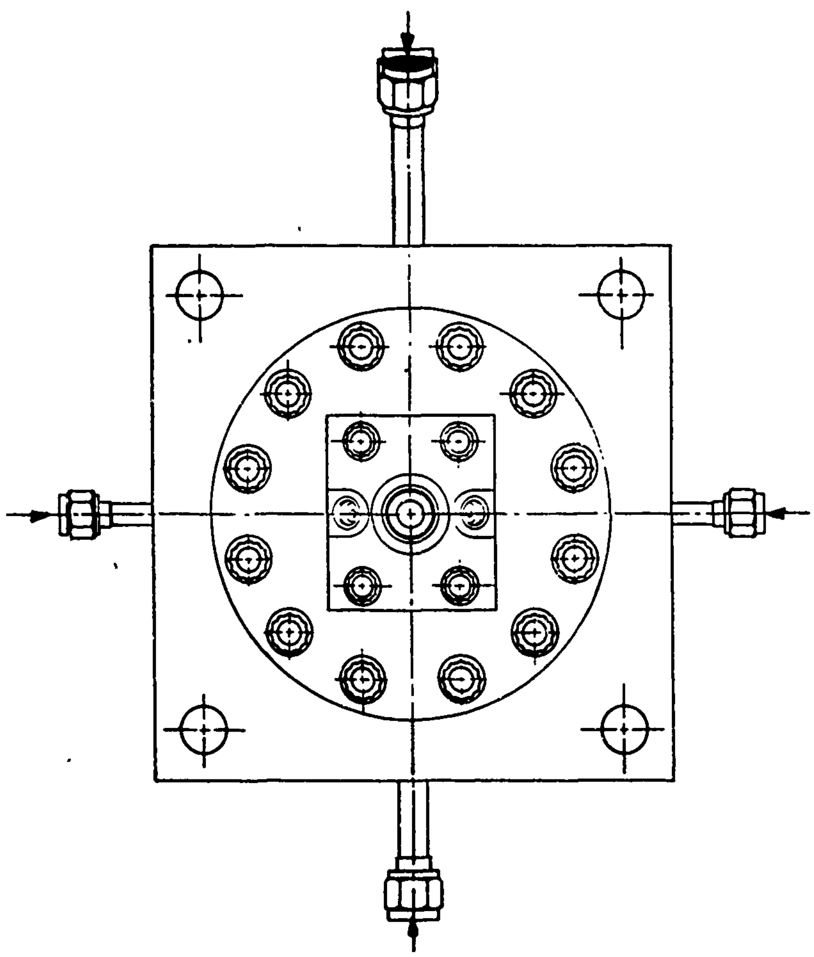

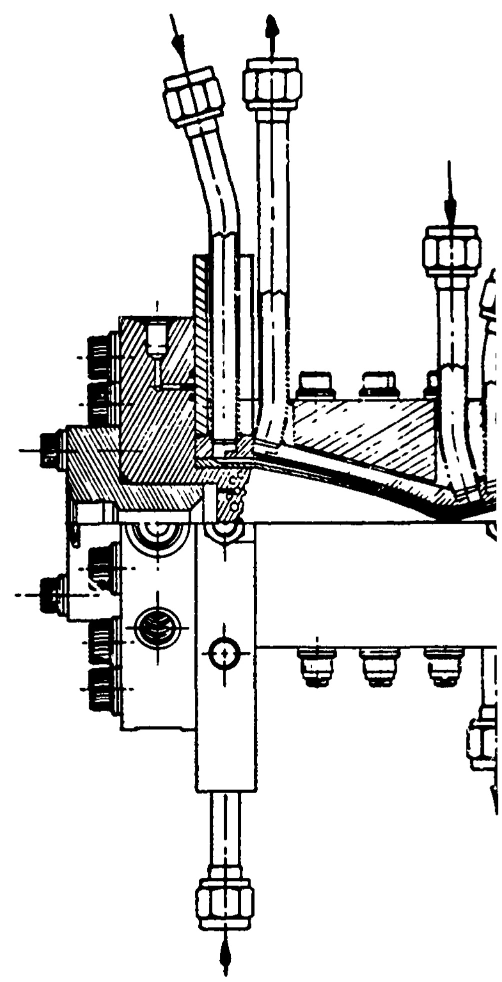

CONFIDENTIAL

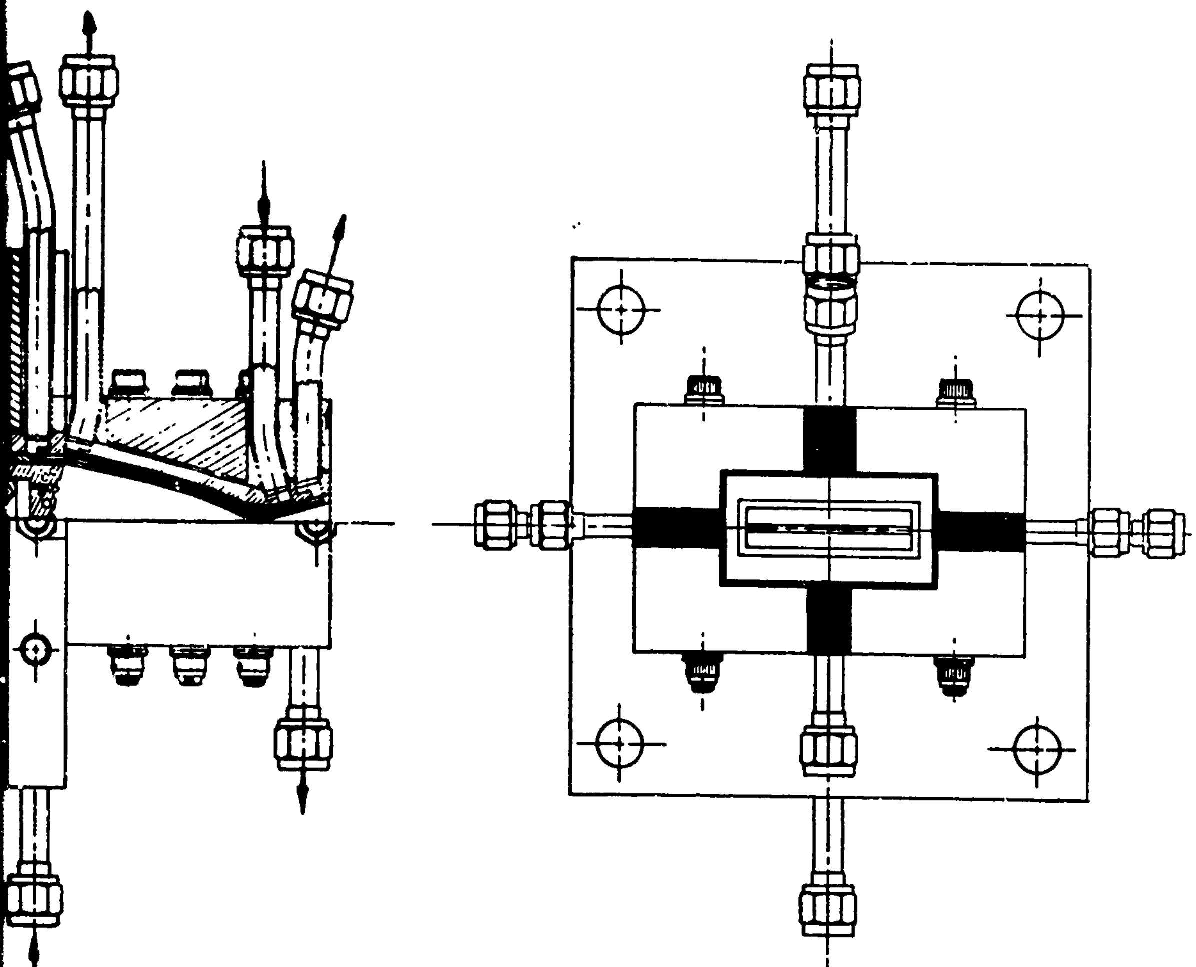

Figure 81. Cast BeCu Segment Assembly. (U)

CONFIDENTIAL

CONFIDENTIAL

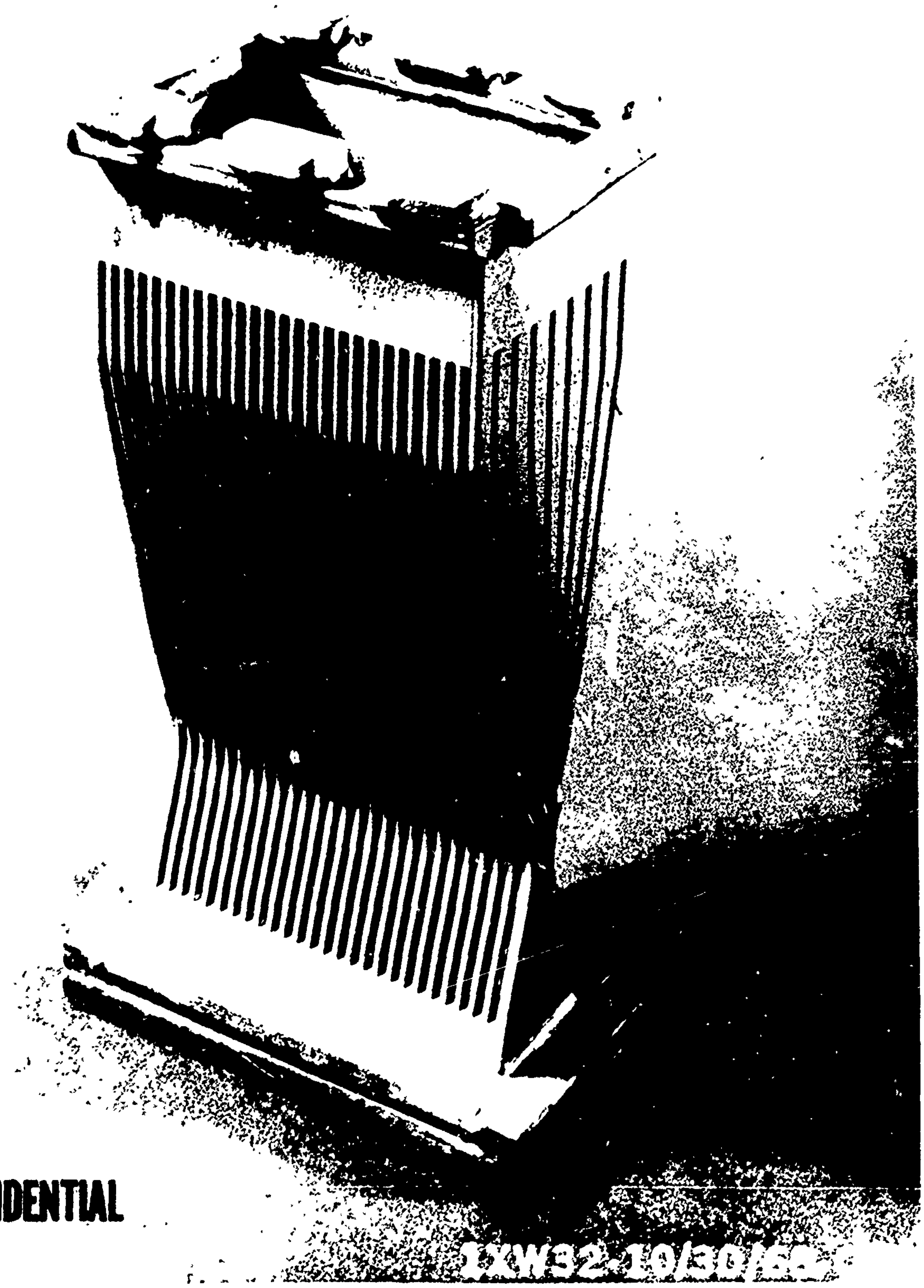

CONFIDENTIAL

CONFIDENTIAL

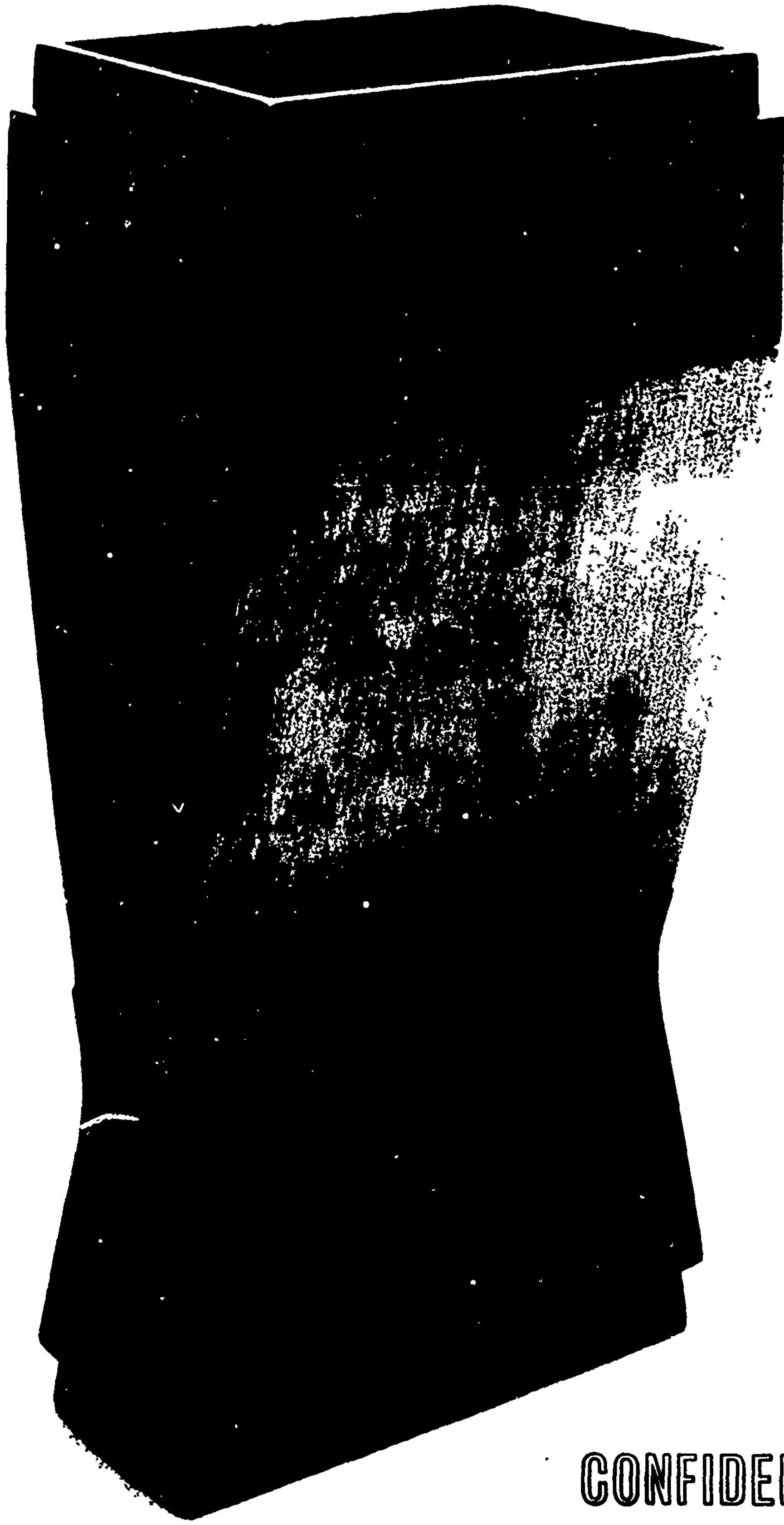

CONFIDENTIAL

Fig. 83. Cast BeCu Segment Just Prior to Machining Passages for Heat Exchange Panel (U)

CONFIDENTIAL

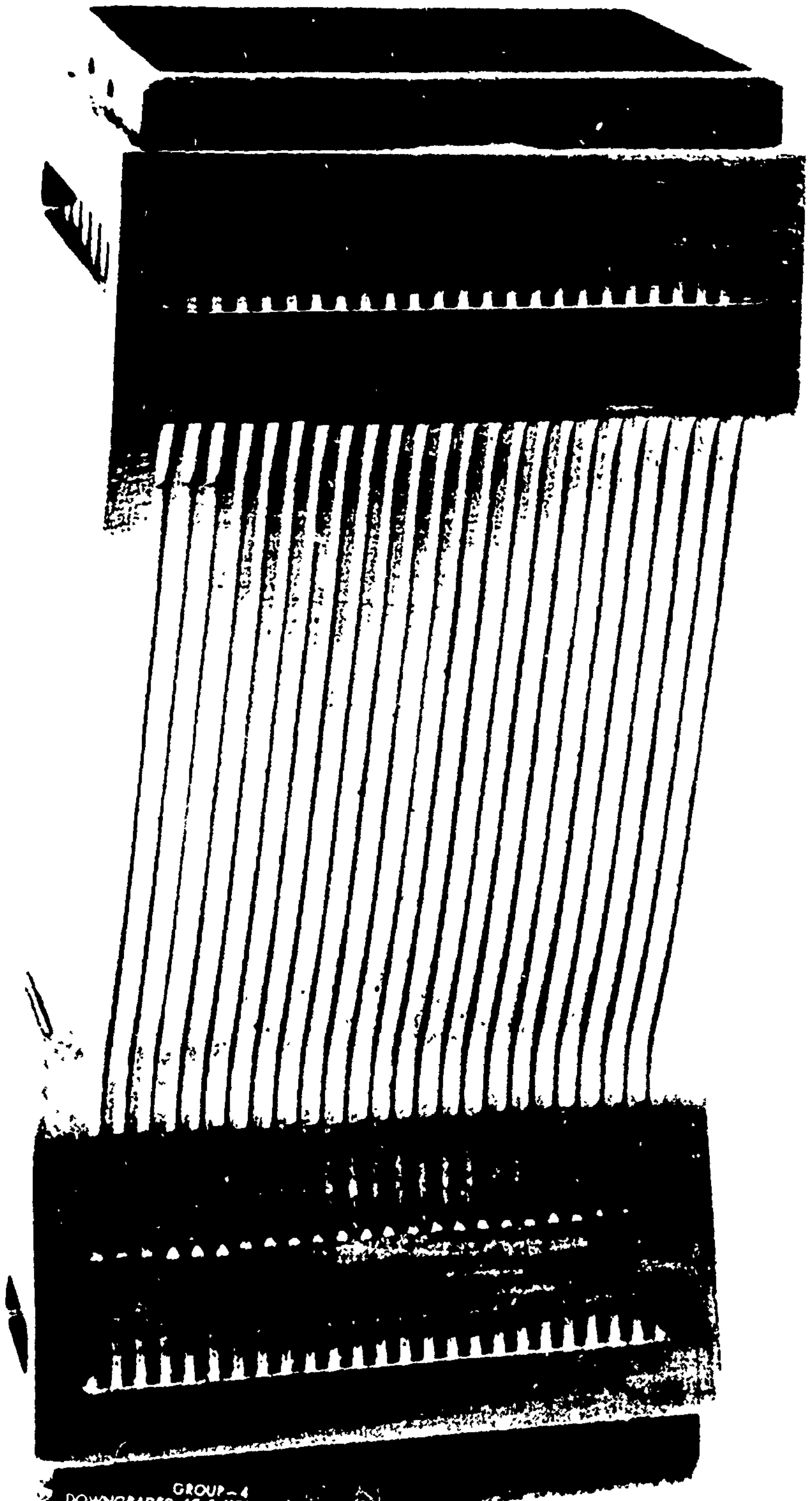

GROUP-4
DOWNGRADED AT 3 YEAR [illegible]
DECLASSIFIED [illegible]

Fi . 34. [illegible] (U)

(U) At this time the primary coolant circuit was hydrostatically proof pressure tested and helium leak checked verifying the integrity of the cast segment hot gas wall, the electroformed nickel layer and the nickel to beryllium copper bond.

(U) A second layer of electroformed nickel was added to closeout the passages in the heat exchange panel and to increase the depth of the manifolds to the design value. The manifolds were then machined, a clean up surface cut taken to smooth out the electroformed surface (Fig. 85), and the third (and last) electroforming cycle added to closeout the coolant manifolds. Subsequently, the part was machined as required, the coolant transfer tubes welded in place and the final assembly completed (Fig. 86 and 87).

(U) Non-destructive inspection techniques used to verify dimensional acceptability and structural integrity of the segment included; (1) dye penetrant and radiographic inspection of the cast liner, (2) successive dimensional checks to establish coolant passage and wall thickness values of the cast liner and the electroformed nickel, (3) successive hydrostatic proof pressure tests to 2700 psig and gaseous helium leak checks to 1500 psig to assure segment integrity (structurally and no interpropellant leaks), and (4) water flow calibration of each coolant circuit.

<u>Segment Injector</u>

(C) The design philosophy of the liquid fluorine-gaseous hydrogen injector to be used with the cast segment thrust chambers was based upon Rocketdyne experience with this propellant combination during the Advanced LF_2/LH_2 Propulsion System Concept Program, contract AF04(611)-10745, and related

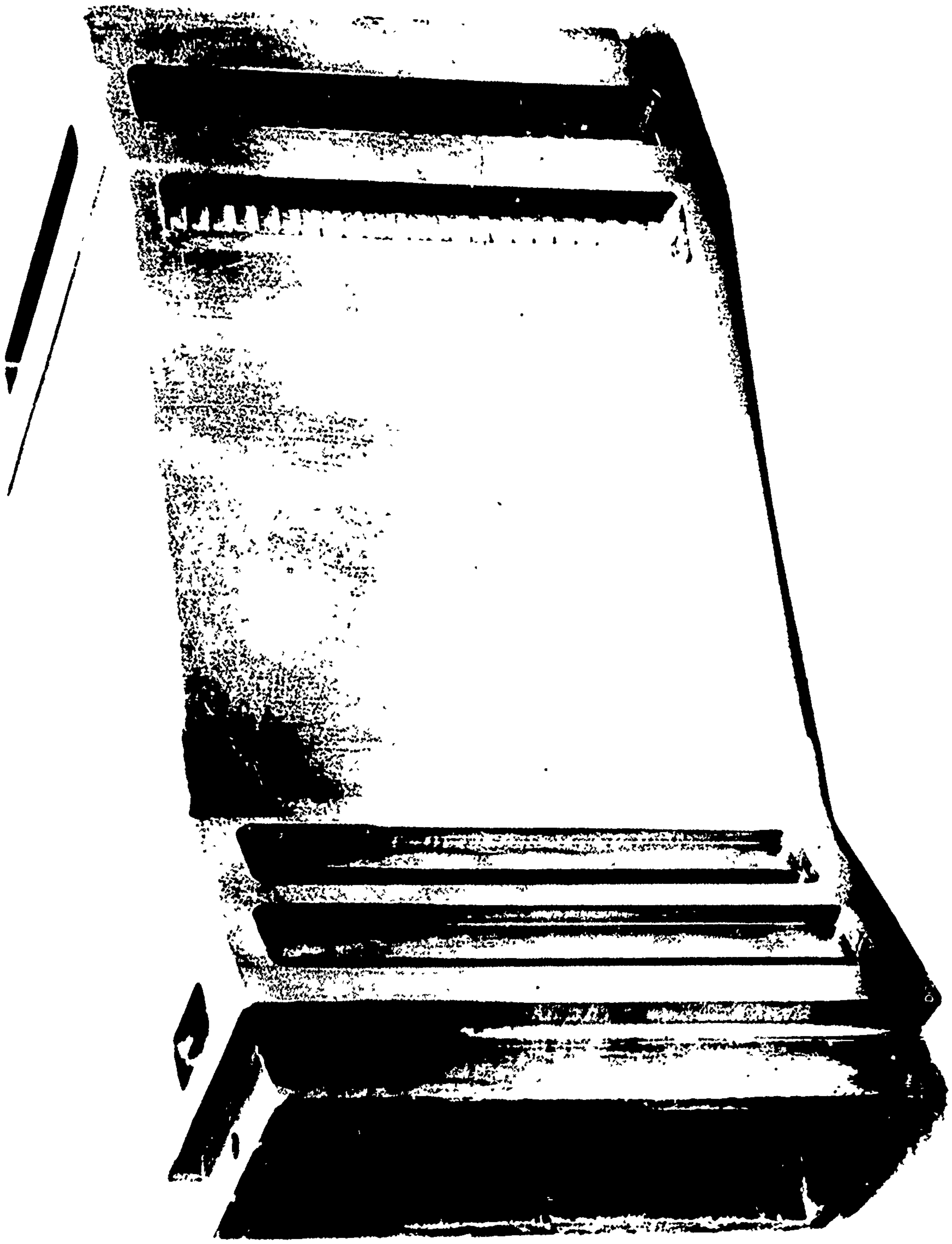

Fig. 85. Cast Mesh Segment Just Prior to Third Electroforming Cycle (U)

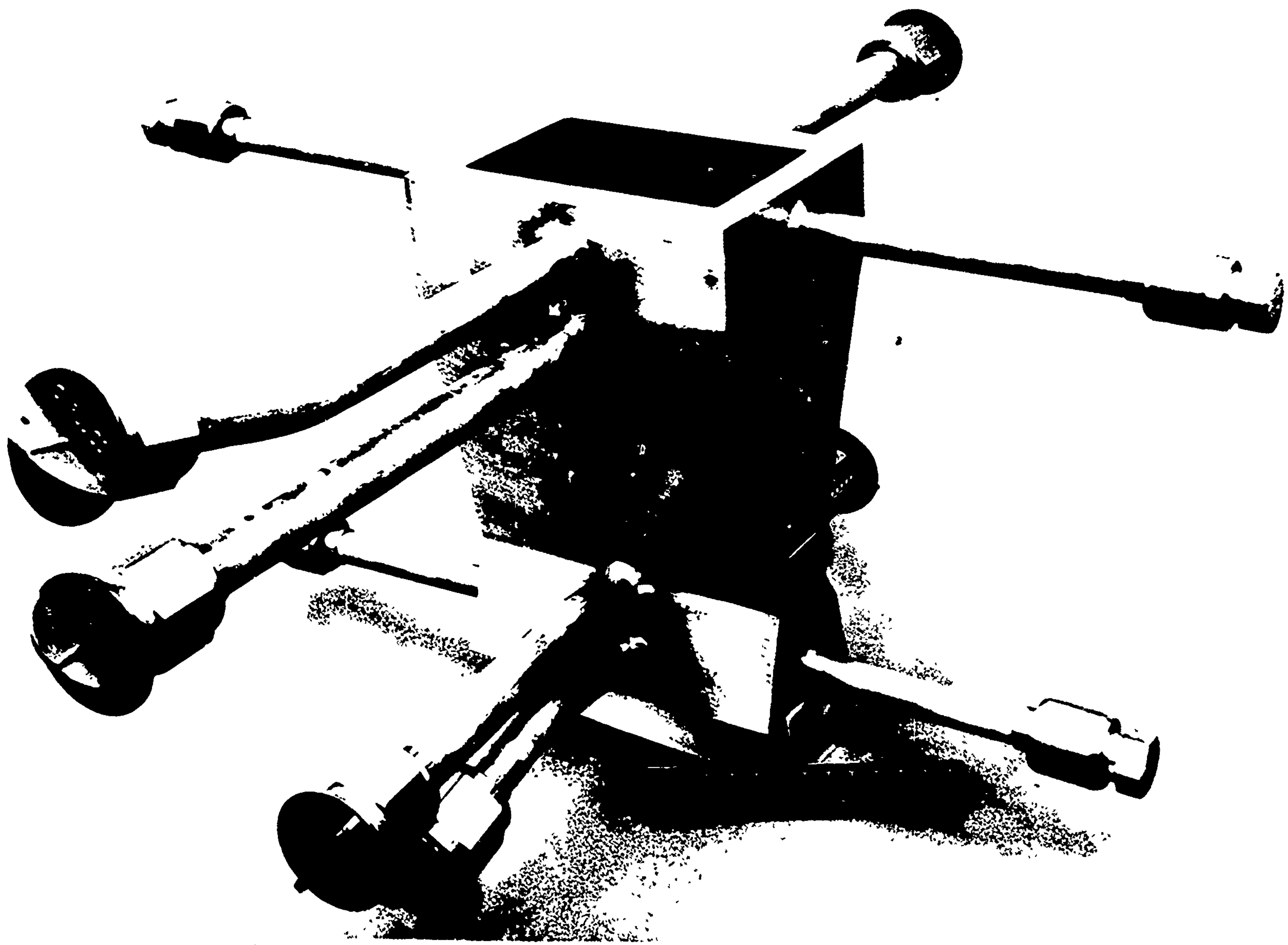

company funded studies. Basic requirements were a minimum C* efficiency of 92 percent and a throttling range of 2.5:1 using liquid fluorine-gaseous hydrogen propellants at a nominal mixture ratio of 12:1.

(C) The resulting design was a canted fan injector consisting of a 14-element, 3-row pattern, with the outer rows canted inward 12-degrees to match the chamber wall inclination, Table XIX and Fig. 88. In this pattern, two pairs of LF_2 orifices form fans on either side of a row of three GH_2 showerhead orifices. These fans intersect in a sheet directly downstream of the GH_2 orifices.

(U) The injector body was OFHC copper with an all parent metal face. The completed injector is shown in Fig. 89.

Bell Injector

(C) The design philosophy of the triplet/doublet injector used with the bell thrust chambers was based upon a study of Rocketdyne experience with this propellant combination, a requirement for a minimum of 92 percent C* efficiency over a 5:1 throttling range. Propellants were liquid fluorine-gaseous hydrogen (ambient) at a nominal mixture ratio of 12:1.

(U) The design consisted of an inner core triplet pattern (fuel showerhead-oxidizer doublets) with 30 elements staggered within six parallel rows to produce uniform distribution with ease of manifolding. The outer zone consisted of 20 unlike doublet orifice elements, designed to reduce chamber wall heat flux, Table XX and Fig. 90. The injector body was OFHC copper with an all parent metal face. The completed injector is shown in Fig. 91.

TABLE XIX

SEGMENT INJECTOR DESIGN CRITERIA (U)

Chamber Pressure, psia	300 to 750
Mixture Ratio (Nominal	12:1
Propellants	LF_2/GH_2 (ambient)
Combustion Efficiency (minimum), percent	92
Injector Delta-P (minimum), percent	0.1 P_c

	LF_2	GH_2
Number of Orifices	56	42
Orifice Diameters, inches	0.018	0.0225, 0.018
Doublet Impingement Angle, degrees	55	NA
Fan Impingement Angle, degrees	65	NA
Fan Impingement Distance, inches	.190	.190
Orifice L/D	5.5-6.9	5.0-6.2
Free Stream L/D	3.9	8.4-10.5

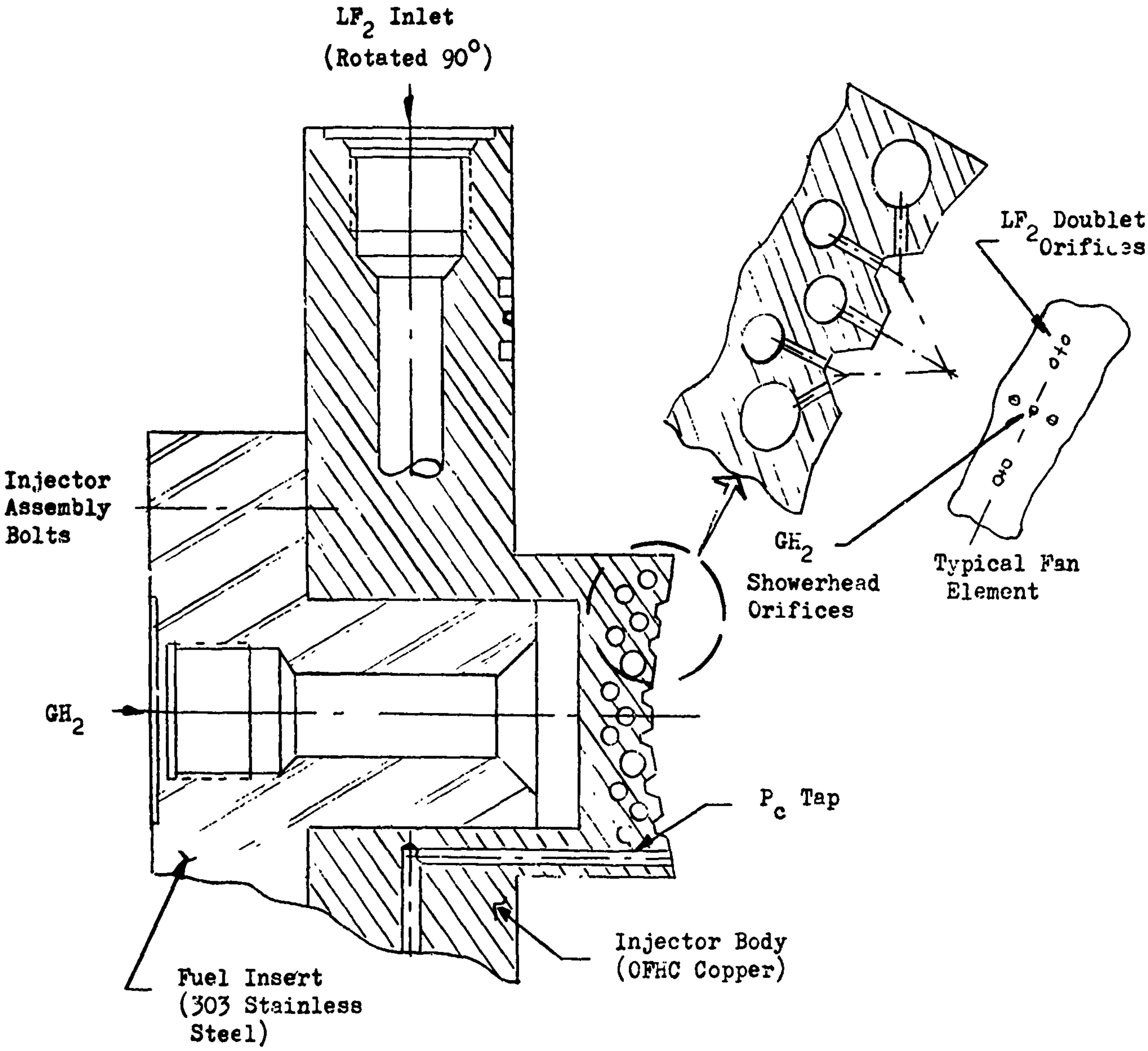

Figure 88. Canted Fan Injector Assembly, Showing Typical Orifice Feed Arrangements. (U)

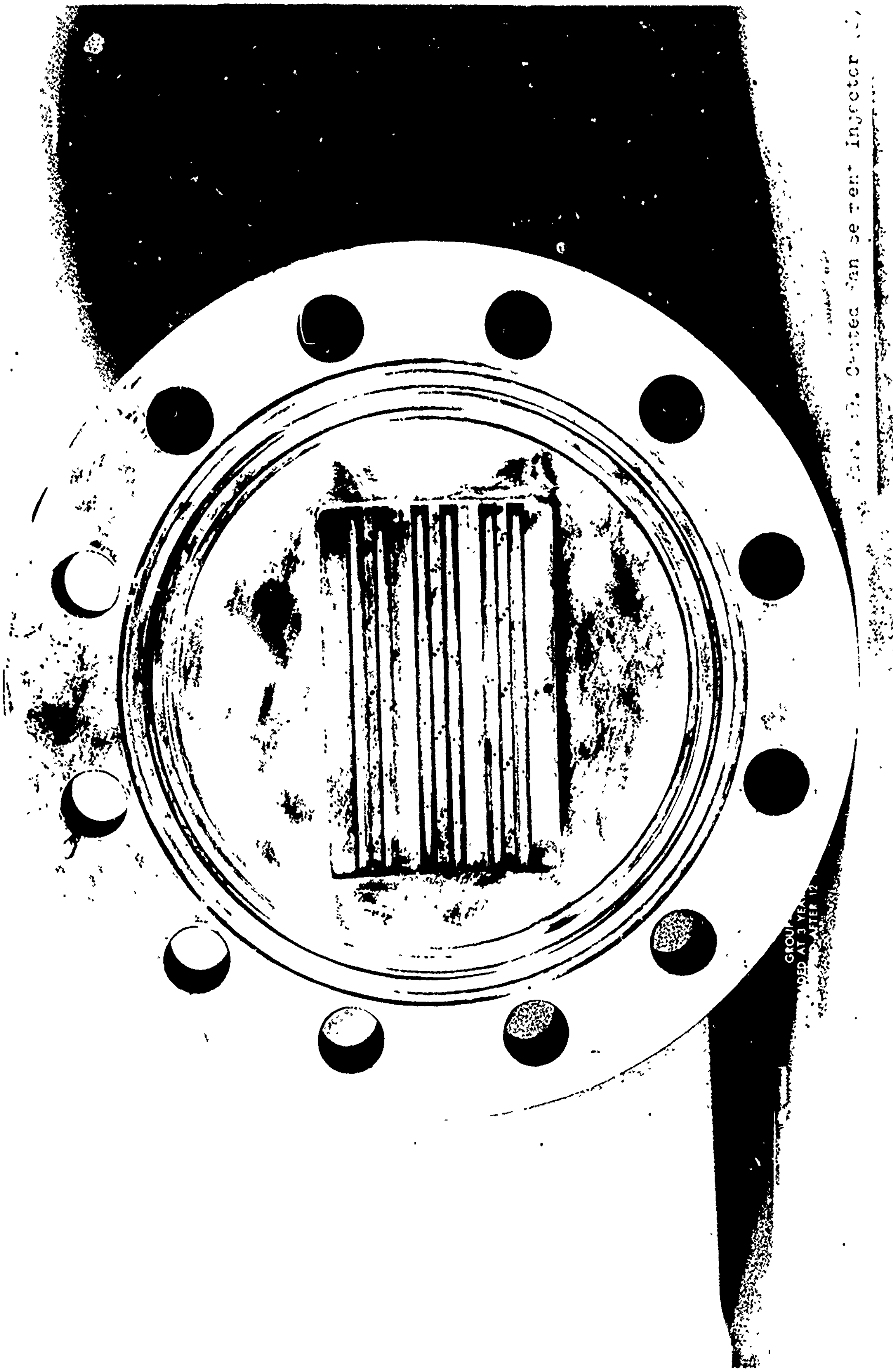

Fig. [illegible]. Coated Fan Segment Injector

CONFIDENTIAL

TABLE XX

BELL INJECTOR DESIGN CRITERIA (U)

Chamber Pressure, psia	200 to 1000
Mixture Ratio (Nominal)	12:1
Propellants	LF_2/GH_2 (ambient)
Combustion Efficiency (minimum), percent	92
Injector Delta P (minimum), percent	0.2 P_c

	LF_2		GH_2	
	Triplet	Doublet	Triplet	Doublet
Number of Orifices	60	20	30	20
Orifice Diameter, inches	0.031	0.031	0.055	0.055
Impingement Angle, degrees	45	12	—	—
Impingement Height, inches	0.25	0.30	0.25	0.30
Orifice L/D	7	7	20	20
Free Stream L/D	9	10	4	4

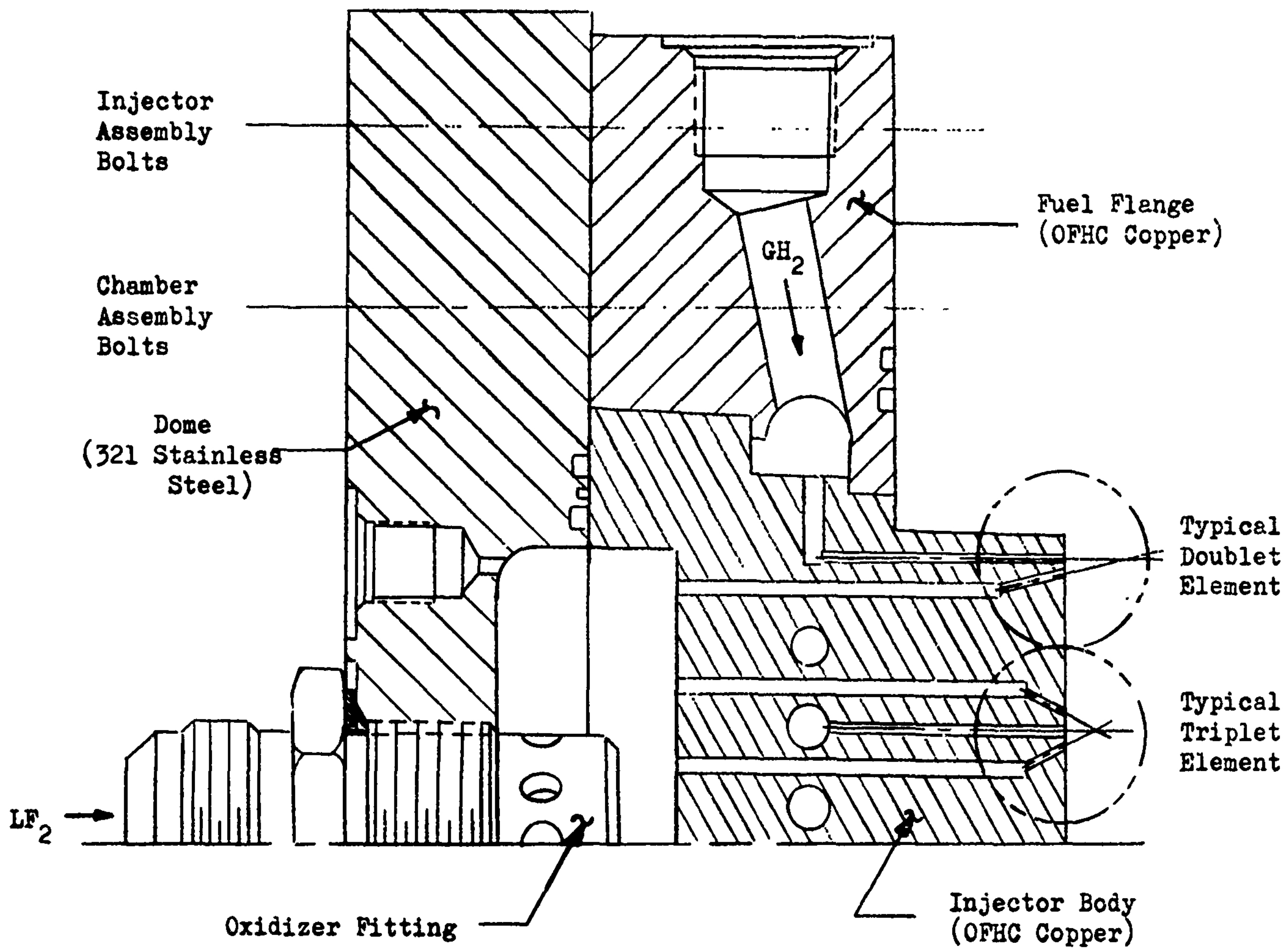

Figure 90. Triplet/Doublet Injector-Dome Assembly, Showing Typical Orifice Feed Arrangements. (U)

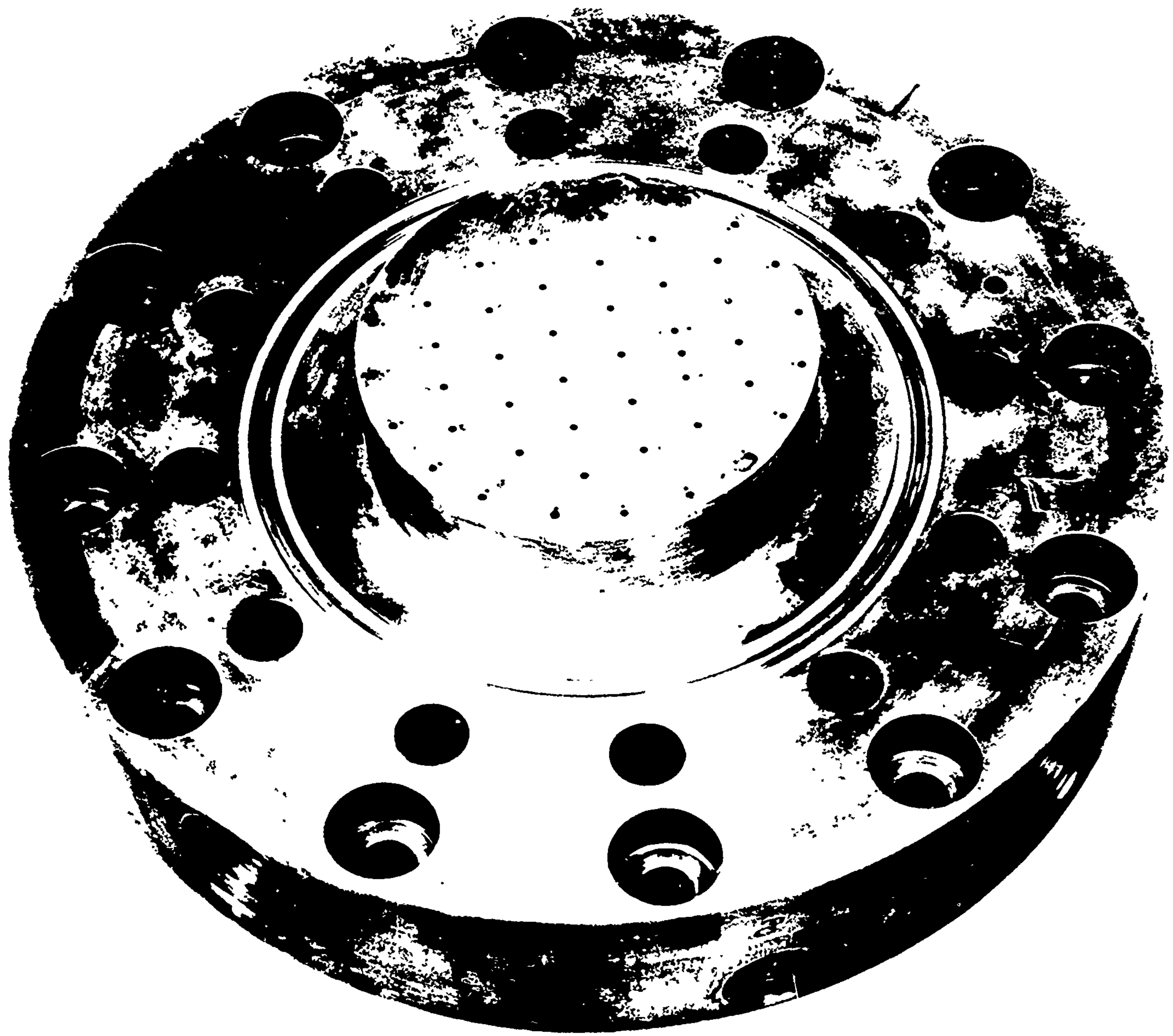

Fig. 91. Triplet/Doublet Injector (b)

Solid Wall Bell Chamber

(U) Short duration bell injector checkout tests were completed in a solid wall heat sink copper chamber which had the same internal dimensions as the regeneratively cooled bell chambers (Fig. 92A).

Solid Wall Segment

(U) The segment injector was checked out in an existing water cooled calorimeter segment available from another program (Fig. 92B).

TEST FACILITIES AND PROCEDURES

Test Facility

(U) The experimental firings were conducted on Roger Test Stand in the Propulsion Research Area, Santa Susana Field Laboratory. Liquid fluorine was obtained by condensation of GF_2 (supplied from manifolded high pressure cylinders) in a liquid nitrogen heat exchanger and was stored in a prechilled, 15-gallon, LN_2-jacketed run tank. The condensation and transfer procedures were carried out routinely and without difficulty. Following completion of a set of firings, remaining LF_2 in the tank was allowed to gasify back into the supply bottles by dumping the LN_2 in the cooling jackets and replacing it first with flowing GN_2, then with water.

(U) The fluorine flow system was chilled with jacketed LN_2 from the condenser to the injector inlet. In addition, use of a three-way main oxidizer valve permitted prerun chilldown of the manifold and injector

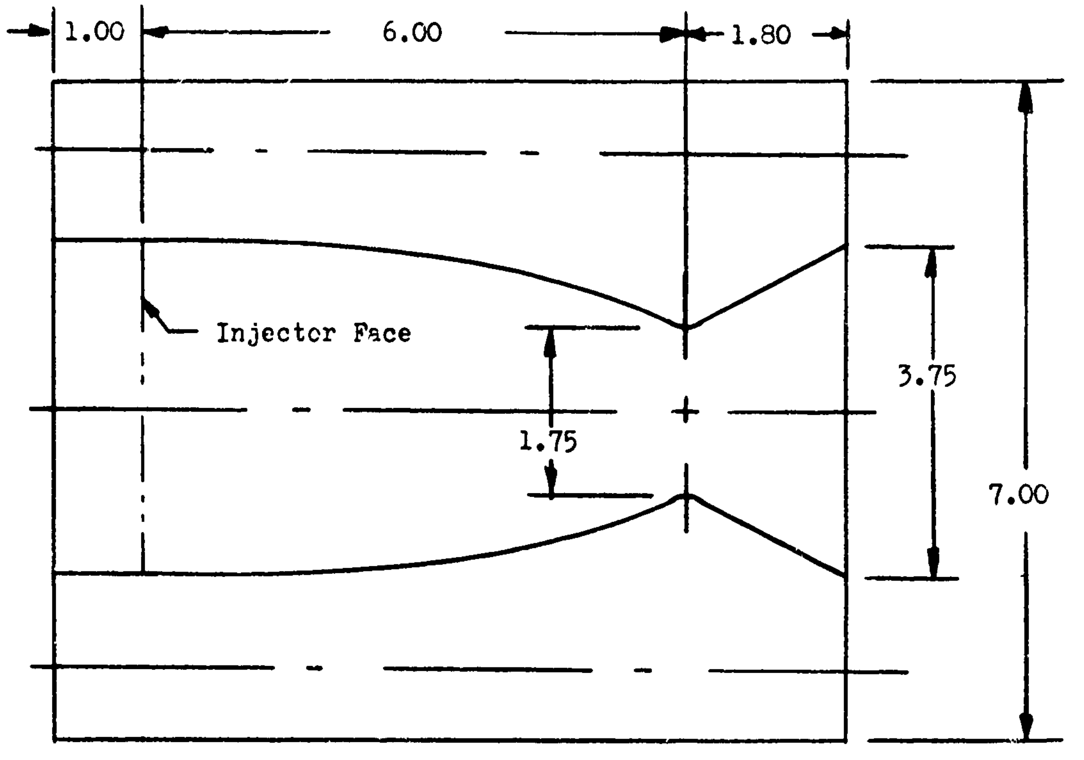

A. Solid Wall Copper Bell Chamber

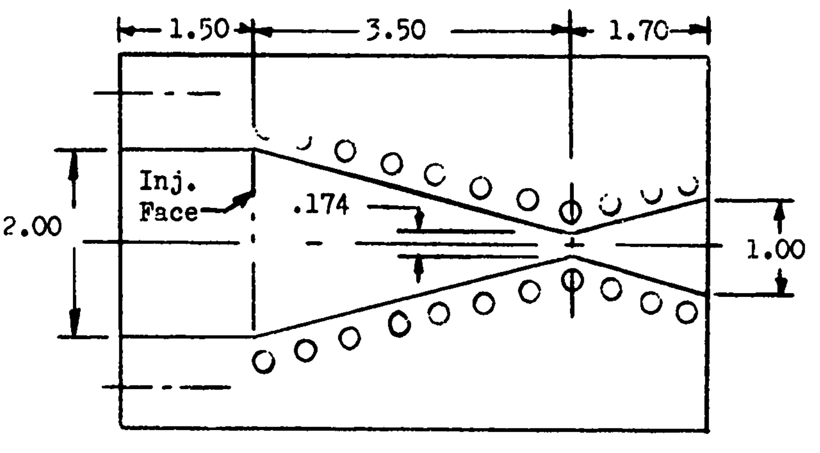

B. Water Cooled Copper Calorimeter Segment

Figure 92. Injector Checkout Chambers. (U)

by an LN_2 bleed directly through the injector and thrust chamber, thus preventing fluorine flashing in the initial portion of the firing and minimizing flow transients. Filtered helium was used for fluorine tank pressurization.

(U) Gaseous hydrogen was supplied from the area tank farm through a suitable pressure regulating system. Gaseous nitrogen purges were used on both oxidizer and fuel sides.

Instrumentation

(U) A schematic diagram indicating instrumentation locations are shown in Figs. 93 and 94 for the bell and annular chamber testing. The particular transducers used for the various types of measurements are described below.

(U) Pressure. All pressures were measured with bonded strain gage transducers. Chamber pressure was measured through the injector face with a close-coupled transducer.

(U) Hydrogen Flowrate. Gaseous hydrogen flowrates were measured by orifices machined to ASME standards and installed in flange-tap orifice-metering lines. The flowrates were obtained by using measured differential pressure across the orifice in conjunction with the density obtained from pressure and temperature measurements immediately upstream of the orifice. Standard ASME flow coefficients and expansion factors dependent upon

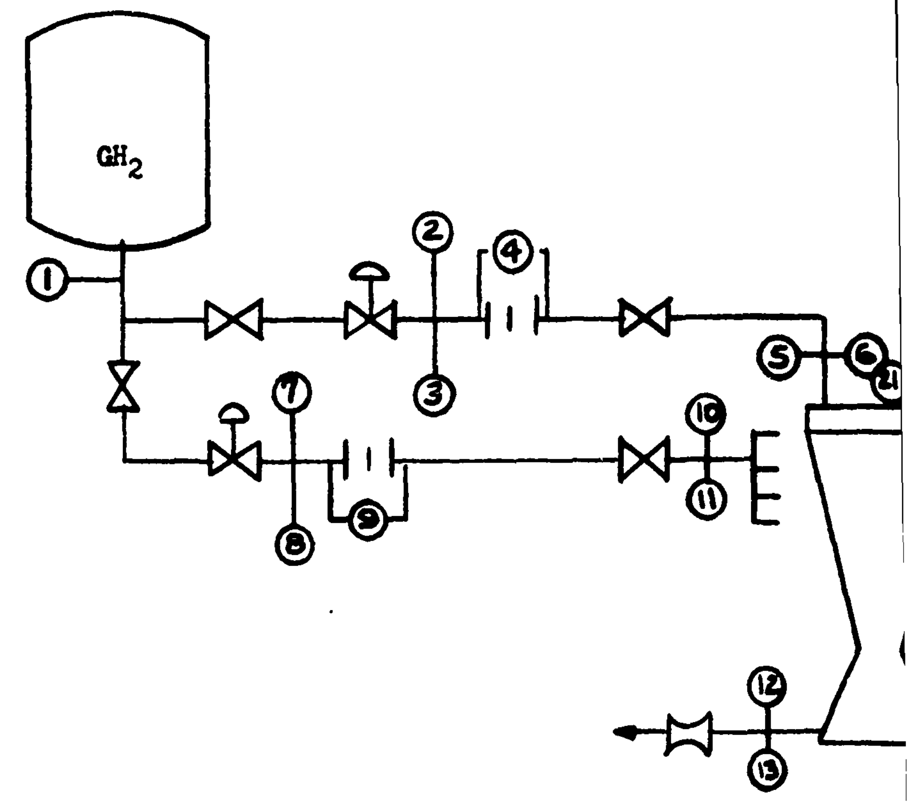

(TYPICAL 4 PLACES)

INSTRUMENTATION

1. HYDROGEN SUPPLY PRESSURE
2. GH_2 ORIFICE UPSTREAM PRESSURE
3. GH_2 ORIFICE UPSTREAM TEMPERATURE
4. GH_2 ORIFICE DELTA PRESSURE
5. GH_2 INJECTION PRESSURE
6. GH_2 INJECTION TEMPERATURE
7. GH_2 COOLANT ORIFICE UPSTREAM PRESSURE
8. GH_2 COOLANT ORIFICE UPSTREAM TEMPERATURE
9. GH_2 COOLANT ORIFICE DELTA-PRESSURE
10. GH_2 COOLANT PANEL INLET PRESSURE
11. GH_2 COOLANT PANEL INLET TEMPERATURE
12. GH_2 COOLANT PANEL VENTURI PRESSURE (4)
13. GH_2 COOLA
14. CHAMBER P
15. FLUORINE
16. FLUORINE
17. FLUORINE
18. FLUORINE
19. VENTURI IN
20. VENTURI IN
21. LF_2 INJECT
22. LF_2 INJECT
23. FLUORINE C
24. FLUORINE C

FIGURE 93 . SCHEMATIC FLOW CIRC
LOCATION OF INSTRUM

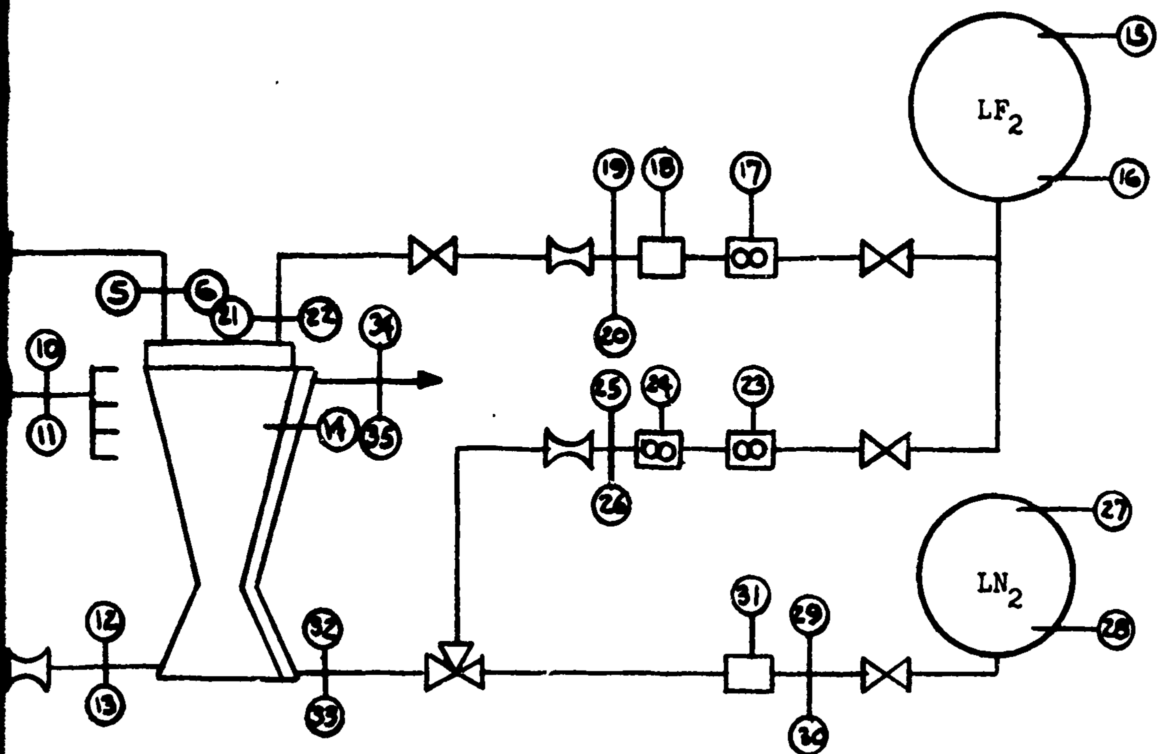

CAL 4 PLACES)

13. GH_2 COOLANT PANEL OUTLET TEMPERATURE (4)
14. CHAMBER PRESSURE
15. FLUORINE TANK PRESSURE
16. FLUORINE TANK TEMPERATURE
17. FLUORINE FLOWRATE
18. FLUORINE FLOWRATE
19. VENTURI INLET PRESSURE
20. VENTURI INLET TEMPERATURE
21. LF_2 INJECTION PRESSURE
22. LF_2 INJECTION TEMPERATURE
23. FLUORINE COOLANT FLOWRATE
24. FLUORINE COOLANT FLOWRATE
25. COOLANT VENTURI INLET PRESSURE
26. COOLANT VENTURI INLET TEMPERATURE
27. LN_2 TANK PRESSURE
28. LN_2 TANK TEMPERATURE
29. LN_2 COOLANT LINE PRESSURE
30. LN_2 COOLANT LINE TEMPERATURE
31. LN_2 COOLANT FLOWRATE
32. OXIDIZER COOLANT INLET PRESSURE
33. OXIDIZER COOLANT INLET TEMPERATURE
34. OXIDIZER COOLANT OUTLET PRESSURE
35. OXIDIZER COOLANT OUTLET TEMPERATURE

EMATIC FLOW CIRCUIT OF SEGMENT TEST SYSTEM SHOWING TYPES AND
CATION OF INSTRUMENTATION TRANSDUCERS. (U)

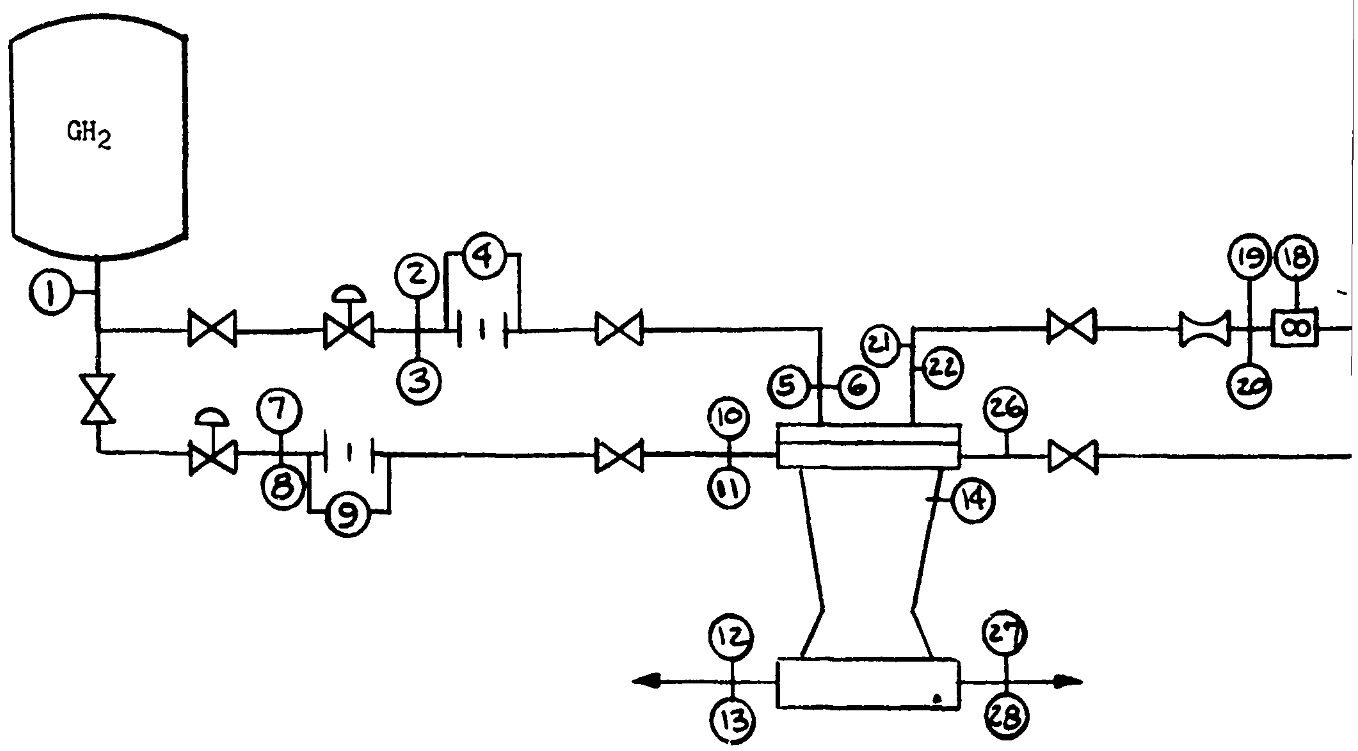

INSTRUMENTATION

1. HYDROGEN SUPPLY PRESSURE
2. GH_2 ORIFICE UPSTREAM PRESSURE
3. GH_2 ORIFICE UPSTREAM TEMPERATURE
4. GH_2 ORIFICE DELTA-PRESSURE
5. GH_2 INJECTION PRESSURE
6. GH_2 INJECTION TEMPERATURE
7. GH_2 COOLANT ORIFICE UPSTREAM PRESSURE
8. GH_2 COOLANT ORIFICE UPSTREAM TEMPERATURE
9. GH_2 COOLANT ORIFICE DELTA-PRESSURE
10. GH_2 COOLANT JACKET INLET PRESSURE
11. GH_2 COOLANT JACKET INLET TEMPERATURE
12. GH_2 COOLANT JACKET OUTLET PRESSURE
13. GH_2 COOLANT JACKET OUTLET TEMPERATURE
14. CHAMBER PRESSURE
15. FLUORINE
16. FLUORINE
17. FLUORINE
18. FLUORINE
19. VENTURI
20. VENTURI
21. LF_2 INJE
22. LF_2 INJE
23. WATER TA
24. WATER LI
25. WATER FL
26. WATER JA
27. WATER JA
28. WATER JA

FIGURE 94. SCHEMATIC FLOW CIRCUIT OF BELL CHAMBER TEST SYSTEM SHOWING TYPES AND LOCATION OF INSTRUMENTATION TRANSDUCERS. (U)

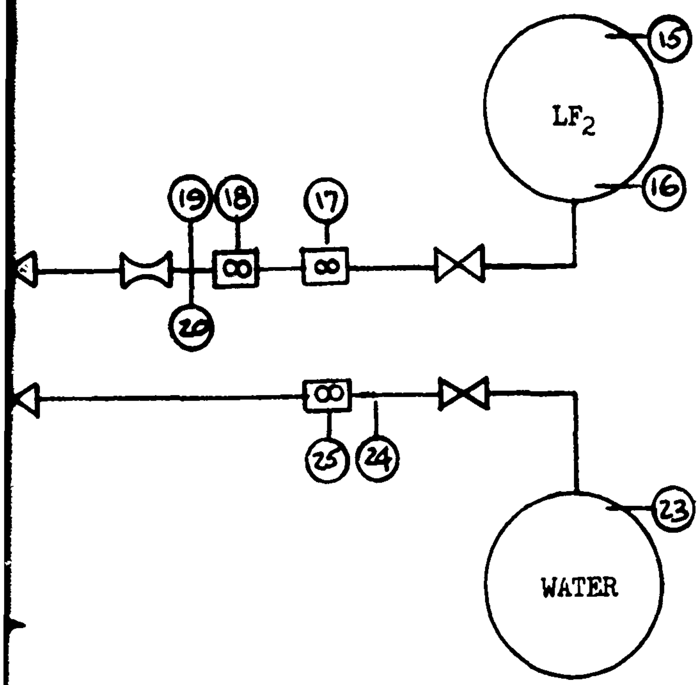

15. FLUORINE TANK PRESSURE
16. FLUORINE TANK TEMPERATURE
17. FLUORINE FLOWRATE
18. FLUORINE FLOWRATE
19. VENTURI INLET PRESSURE
20. VENTURI INLET TEMPERATURE
21. LF_2 INJECTION PRESSURE
22. LF_2 INJECTION TEMPERATURE
23. WATER TANK PRESSURE
24. WATER LINE TEMPERATURE
25. WATER FLOWRATE
26. WATER JACKET INLET PRESSURE
27. WATER JACKET OUTLET PRESSURE
28. WATER JACKET OUTLET TEMPERATURE

IOWING TYPES AND

specific diameter ratios (ρ), Reynolds Number (R_D) and pressure ratio ($\frac{\Delta P}{P_o}$) were used to define the flowrate equations. These orifices were calibrated against sonic venturies to assure accuracy of flowrate measurement.

(U) Fluorine Flowrate. Two turbine flowmeters in series were used to measure volumetric fluorine flowrates. In addition, a sonic venturi meter, with an adjustable area* was installed downstream of the flowmeters. The venturi meter functioned both as a redundant flow metering device and as a flow regulator. The density of fluorine was obtained from pressure and temperature measurements immediately u ..ream of the venturi.

(U) Hydrogen Temperature. Hydrogen temperatures upstream of the orifices were measured with iron-constantan thermocouples. Because temperatures were ambient and flowrate is a function of the square root of absolute temperature, the degree of accuracy of these measurements were satisfactory.

(U) Fluorine Temperature. Reliable measurement of fluorine mass flowrate requires accurate determination of liquid density. Density of liquid fluorine is a moderately sensitive function of temperature. Hence, it was important to make accurate measurements of fluorine as close to the flow metering devices as practical. This was done by use of a shielded platinum resistance bulb (Rosemount Model 176) immersed in the liquid stream, downstream of the second flowmeter and upstream of the venturi. This sensor is very sensitive to temperature changes in the cryogenic region and is the preferred method of measurement.

---

* Fox Valve Development Co., Inc., 2 Great Meadowlane, Hanover, New Jersey.

(U) <u>Data Recording</u>. All pressure, temperature, and flow measurements were recorded on tape during each firing by means of a Beckman Model 210 Data Acquisition and Recording System. This system acquires analog data from the transducers, which it converts to digital form in binary-coded decimal format. The latter are recorded on tapes which are then used for computer processing.

(U) The Beckman Data Acquisition Unit sequentially samples the input channels at a rate of 5625 samples per second. Programmed computer output consists of tables of time vs parameter values at approximately 10-millisecond minimum intervals during the firing, together with calibration factors, prerun and postrun zero readings, and related data. The same computed results are machine plotted and displayed as CRT outputs on appropriately scaled and labeled grids for sample determination of gradients, establishment of steady state, etc.

(U) Primary data recording for these firings was on the Beckman 210 system. In addition, the following auxiliary recording systems were employed:

1. An 8-channel Brush Mark 200 recorder was used in conjunction with the Beckman unit primarily to establish time intervals for computer data reduction and, for "Quick-look" information on the most important parameters. This is a direct-inking system, with display on high-gloss, graduated paper moving at 20 mm/sec.
2. A CEC, 26-channel, direct-reading oscillograph was used as backup for the Beckman 210 system for selected param [illegible].
3. Direct-inking graphic recorders (DIGR's), either Dynalog rotary chart or Esterline-Angus strip chart, were used to set prerun propellant tank and supply pressures, to monitor prerun chilldown, to provide "Quick-look" information, and as secondary backup to the Beckman and oscillograph recorders.

4. An Esterline-Angus 20-channel event recorder was used for direct inking recording of propellant valve signals and travel, as well as chart drive on-off signal.

Firing Procedures

(U) Fluorine System Passivation. Prior to assembly, fluorine system components were carefully and thoroughly cleaned in accordance with standard prescribed procedures (Ref. 11). Passivation of the assembled system (to main oxidizer valve), by provision of protective fluoride films on exposed surface, was carried out as follows: low-pressure gaseous fluorine was introduced into the system and maintained for successive 15-minute periods at 5, 10 and 15 psi; finally, 20 psi was maintained for several hours.

(U) The feed line-thrust chamber system downstream of the main valve was passivated immediately before each set of firings by flowing gaseous fluorine through the system for short intervals of time.

(U) Run Procedure. Before each firing, liquid nitrogen was bled through the main oxidizer valve to chill the fluorine inlet line to the thrust chamber to reduce gasification during the start transient. The chamber coolant valves were operated, manually and coolant flows were verified prior to start signal. The firing itself was sequenced through an automatic timer which controlled operation of the main propellant valves. A fuel lead and fuel-rich cutoff was maintained for every test.

TEST RESULTS

(U) This section presents the results of the Phase III hot firing effort. These tests successfully demonstrated the thermal performance and structural integrity of the three fabrication concepts in the combustion environment. Included in this test series were bell and segment injector checkout tests in solid wall chambers. Test results are presented in Tables XXI and XXII and discussed in the following paragraphs.

Bell Injector Checkout Tests

(U) The initial hot firings were conducted to checkout the LF_2/GH_2 triplet/doublet bell injector in a solid wall copper "heat sink" thrust chamber. A total of three short duration tests (001-003) to a maximum chamber pressure of 686 psia were successfully completed demonstrating the structural integrity, face cooling characteristics and performance of the injector.

(U) Subsequent inspection of the solid wall copper chamber revealed slight erosion at the throat plane in one location located directly in line with one of the elements in the center row of the injector. As discussed later, based upon the predicted time to reach the melting point of copper at the throat, the resultant heat flux at the throat was calculated to be quite close to the predicted value.

Spun INCO 625 Bell Chamber

(U) A total of four tests (004-007) for an accumulated test duration of 19 seconds were conducted over a chamber pressure range of 308-382 psia using water as the chamber coolant. Final post test inspection revealed

TABLE XXI

PHASE III HOT FIRING TEST

TEST NUMBER	TEST OBJECTIVES	INJECTOR	CHAMBER	MAINSTAGE DURATION (sec)	P_c (psia)	$\dot{W}_t$ (lb/sec)	M.R. (o/F)	η_{c*} (%)	TYPE	$\dot{W}$ (lb/
001	Ignition Transient	Triplet/ Doublet	Copper Solid Wall	0.0	—	2.460	9.6	—	—	—
002	Bell Injector Checkout			0.5	419	4.066	11.9	97	—	—
003	Bell Injector Performance			0.8	686	6.470	11.4	99	—	—
004	Hardware Checkout		Spun INCO 625	0.6	308	3.104	13.5	96	H_2O	10.7
005	Structural & Thermal Integrity			2.7	316	3.182	12.7	96		10.[illegible]
006				13.5	377	3.798	14.4	96		10.8
007	2000 F Wall Temp. Demonstration			2.2	382	3.798	11.3	96		10.9
008	Hardware Checkout		Powder Metal Nickel	0.6	296	3.050	11.2	96	GH_2	0.7
009	Structural & Thermal Integrity			4.8	300	2.994	12.1	96		0.[illegible]
010				4.8	343	3.411	11.6	96		0.8
011				5.2	374	3.670	12.3	97		0.9
012	1600 F Wall Temp. Demonstration			10.4	432	4.355	12.8	96		0.8
013				5.2	499	4.921	12.1	97		1.0
014				10.6	528	5.208	12.8	97		1.0
015	Segment Injector Checkout	Canted Fan	Calorimeter Chamber	0.6	290	0.566	16.3	100	H_2O	1.4
016	Heat Transfer & Performance			5.6	455	0.861	14.3	100		1.4
017				2.6	657	1.242	14.4	98		1.4
018	Cast Segment Checkout		Cast BeCu-10C Segment	0.6	414	0.567	12.1	100		
019	Structural & Thermal Integrity			5.0	406	0.564	12.2	100		
020	1000 F Wall Temp. Demonstration			5.6	455	0.533	12.1	100		
021	LF_2 Heat Exchange			2.2	460	0.652	15.1	100		

NOTES: ① Based on injector end chamber pressure.

② Calculated from bulk temperature rise applicable to throat of INCO 625 bell chamber and cast segment. Powder metal nickel bell chamber temperatures are for the combustion zone.

③ Throat values.

TABLE XXI

III HOT FIRING TEST RESULTS (U)

.../F)	η_{C^*} ① (%)	COOLANT PARAMETERS TYPE	$\dot{W}$ (lb/sec)	P_{in} (psia)	T_{in} (°F)	ΔT (°F)	$T_{wg\ max}$ ② (°F)	RESULTS
.6	—	—	—	—	—	—	—	Compatibility of facility/injector/chamber verified Facility operational procedures established. Injector structural integrity verified.
.9	97	—	—	—	—	—	—	Injector face cooling, structural integrity and performance demonstrated.
.4	99	—	—	—	—	—	—	Injector face cooling, structural integrity and performance verified. Local scarfing of solid wall copper chamber in throat region verified predicted throat heat flux values.
.5	96	H_2O	10.7	1152	72	35	—	Compatibility of injector/chamber verified. Fabrication concept structural integrity verified. Localized erosion of INCO 625 hot gas wall in combustion zone, located between doublets indicated higher than predicted chamber heat flux values.
.7	96		10.8	1172	68	43	1700	Structural integrity and thermal performance of fabrication concept demonstrated.
.4	96		10.8	1176	67	50	1850	Demonstration test of fabrication concept for long duration and near design wall temperatures in the throat. No further localized burning in chamber. Demonstrated localized burning was due to transient conditions.
.3	96		10.9	1180	66	49	1860	Demonstration test of fabrication concept to design hot gas wall temperature of ~2000 F in throat and exceeded locally in chamber.
.2	96	GH_2	0.70	1470	78	168	—	Compatibility of injector/chamber verified. Structural integrity of fabrication concept demonstrated.
.1	96		0.30	1622	77	188	980	Demonstration of structural integrity and thermal performance of fabrication concept.
.6	96		0.80	1634	72	209	1220	Demonstration of structural integrity and thermal performance of fabrication concept.
.3	97		0.81	1600	88	232	1370	Demonstration of structural integrity and thermal performance of fabrication concept.
.8	96		0.81	1611	85	261	1570	Further demonstration of structural integrity and thermal performance at design wall temperature of 1600 F or greater.
.1	97		1.04	1999	81	226	1600	Further demonstration of structural integrity and thermal performance at design wall temperature of 1600 F or greater.
.8	97		1.04	2006	77	234	1670	Further demonstration of structural integrity and thermal performance at design wall temperature of 1600 F or greater.
.3	100	H_2O	1.450 ③	1013	57	15	—	Injector checkout test for structural integrity and facility/injector/chamber compatibility.
.3	100		1.450	1013	58	26	—	Injector face cooling, structural integrity and performance demonstrated.
.4	98		1.450	1015	59	31	—	Injector face cooling, structural integrity and performance demonstrated.
.1	100	See Table XXII for COOLANT AND HEAT EXCHANGE DATA						Injector/segment/facility compatibility verified. Facility operational parameters established.
2	100							Demonstration of structural integrity and thermal performance of fabrication concept. Also demonstrated was heat exchange principle through use of multiple layers of coolant passages.
1	100							Fabrication concept demonstration at design hot gas wall temperature. Heat exchange benefits demonstrated.
1	100							Demonstration of fabrication concept and heat exchange principle with propellants of interest.

zone.

TABLE XXII

GH_2 COOLANT AND OXIDIZER HEAT EXCHANGE TEST RESULTS - BeCu-10C SEGMENT (U)

			GH_2 COOLANT PARAMETERS										HEAT EXCHANGE PANEL				
			SIDE PLATES				CONTOURED WALLS										
							LOWER			UPPER							
TEST NO.	P_c psia	M.R.	LOC	$\dot{W}$ #/sec	ΔT_B F	Q (2)	$\dot{W}$ #/sec	ΔT_B F	Q (2)	$\dot{W}$ #/sec	ΔT_B F	Q (2)	TYPE	$\dot{W}$ #/sec	ΔT_B F	P_{out}	$T_{wg_{max}}$ (1) (^oF)
018	414	12.1	R	.075	77.3	5.8	.400	58.4	23.3	.390	62.4	24.3	LN_2	.13	67	590	900
			L	.068	76.3	5.2											
019	406	12.2	R	.072	94	6.8	.385	76.9	29.6	.375	65.9	24.7		.26	89.4	967	900
			L	.067	103	6.9											
020	455	12.1	R	.068	106	7.2	.368	89	32.8	.358	64	22.9		.61	88	1093	1000
			L	.063	117	7.4				.356	85	30.2	---	---	---	---	
021	460	15.1	R	.080	86.5	6.9	.430	68	29.2	.410	72	29.5	LF_2	.25	36	107	960
			L	.074	97	7.2											

(1) Calculated maximum gas-side wall temperature (based on coolant bulk temperature increase)

(2) Product of flowrate and bulk temperature increase, lbm-F/sec

The throat, nozzle and most of the chamber to be in excellent condition. However, there was some localized chamber erosion approximately 0.020 deep just downstream of the injector face, located between the fluorine-hydrogen doublets. Post test photographs of this chamber are shown in Figs. 95 and 96.

(C) Review of the hardware, test records and movies taken during the tests showed this erosion to be associated with the start and cutoff transients. The start procedure was such that full fuel flow was established prior to opening of the main oxidizer valve. As the oxidizer valve opened and the lines and injector dome were primed, the fluorine flow through the injector orifices into the chamber was such that a low momentum ratio existed between the two propellants. As a result, in the doublet, the fluorine, instead of penetrating the hydrogen stream, was deflected and fanned out around the hydrogen stream, resulting in an extremely high heat flux region between the doublets. This was evident in examining the hardware which showed the wall erosion to be located over the lands, between the doublets with no erosion on the land located directly behind the doublet (Fig. 97). Also, movies taken during the test confirmed there was no erosion during steady state operation, evident from the fact that the third test on this chamber (test number 006) was for an extended duration of 13.5 seconds at a chamber pressure of 377 psia. However, during this long run stabilized coolant bulk temperature data showed a higher-than-predicted rise indicating a higher-than-calculated heat flux. An analysis of the test data is presented in a later section. Post test helium leak check showed no leaks through the INCO 625 or the electroformed nickel and post test throat area measurement was identical to the pre-test value.

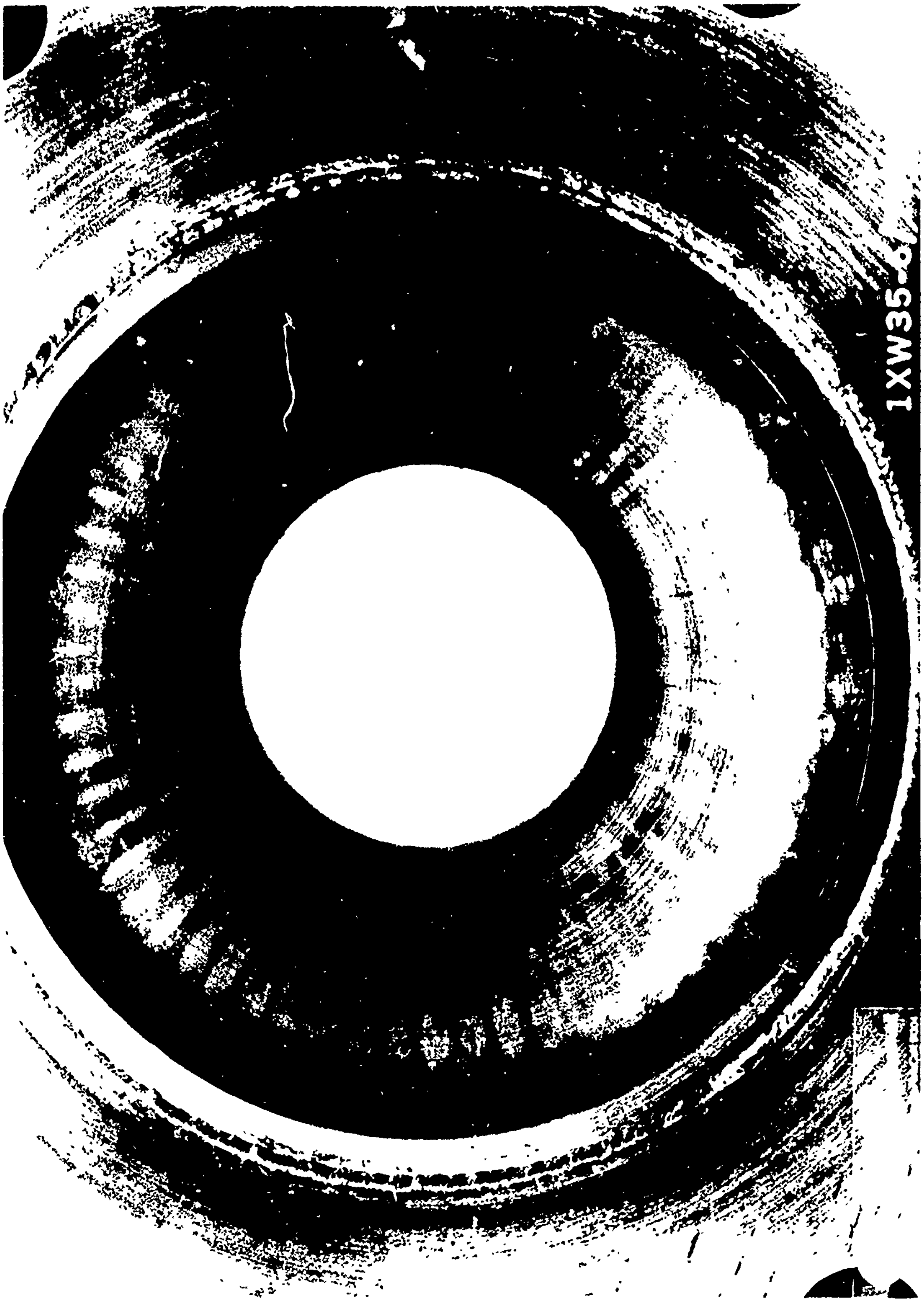

CONFIDENTIAL


Rocketdyne
North American Ro

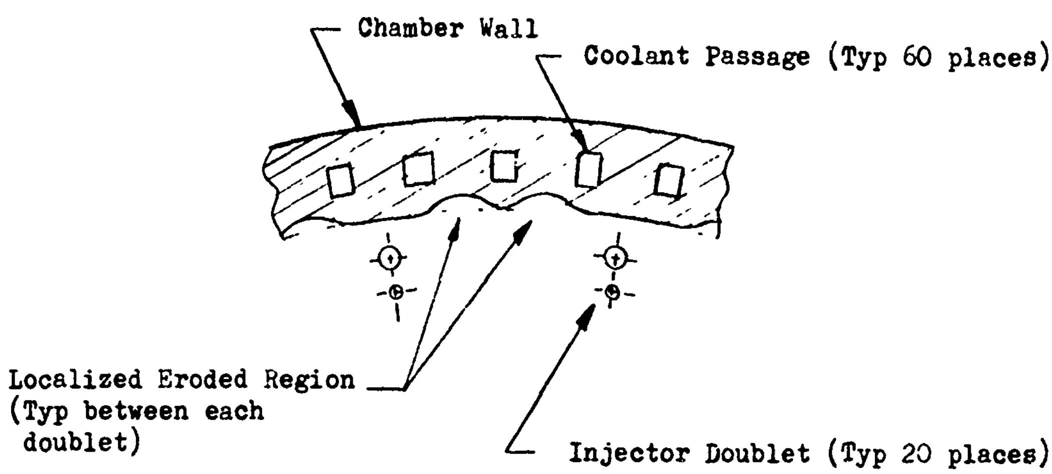

Figure 97. Sketch Showing Relationship Between Injector Doublet and Localized Eroded Regions on Spun INCO 625 Bell Chamber. (U)

(C) These tests demonstrated the structural integrity and thermal performance of this fabrication concept under even more severe conditions than required by the design. A hot gas wall temperature of $\sim$ 1900 F was achieved in the throat and exceeded locally in the chamber (where localized melting of the INCO 625 occurred). These temperatures were attained with relatively high coolant jacket pressures ($\sim$ 1100 psig) and moderate chamber pressures verifying structural integrity of the hot INCO 625 wall and the electroformed nickel shell. These tests demonstrated the feasibility of using the INCO 625 and this fabrication concept to extend the limits of regenerative cooling of bulk temperature limited storable propellants.

Powder Metal Nickel Bell Chamber

(C) The powder metal nickel bell chamber was successfully hot fire tested seven times (008-014) over a chamber pressure range of 296 to 528 psia with GH_2 (ambient) coolant. Accumulated test duration was 41.6 seconds over a mixture ratio range of 11.2 to 12.8. Calculated maximum hot gas wall temperature on these tests equaled or exceeded the 1600 F design value on the last three tests totaling 26.2 seconds. The detailed heat transfer analysis of the test results is presented in a later section.

(U) The test plan stipulated demonstration of thermal performance and structural integrity by operating at a 1600 F gas side wall temperature. Design analysis of this chamber, based on the test results on the spun INCO 625 bell chamber indicated this temperature was attained in the combustion zone at a chamber pressure of 465 psia, with the GH_2 coolant flowrate of 1.0 lb/sec (in a downpass system) and bulk temperature rise of 230 F. Hot gas wall temperatures in the combustion zone exceed throat values due to the very high combustion zone heat flux generated by the triplet/doublet injector.

(C) Post test inspection revealed no signs of chamber overheating or erosion; however, a post test coolant circuit helium leak check showed one crack in the hot gas wall. This axial crack, located just downstream of the injector, was approximately 3/8 of an inch long and was located between injector doublets (test results on the spun INCO 625 bell chamber showed this region to be extremely hot) and over the center of a coolant passage. Indications are that this was a thermal fatigue crack, resulting from the operation of the chamber at a greater than design hot gas wall temperature during the tests. This temperature reached a calculated maximum value of approximately 2500 F during the start transient and steady state values as high as 1915 F. Post test photographs of this chamber are shown in Figs. 98 and 99. Post test throat area measurement equaled the pre-test value.

(U) These tests demonstrated the structural integrity and thermal performance of regeneratively cooled powder metal nickel bell chambers under conditions even more severe than planned, resulting from the fact that the triplet/doublet injector produces an extremely high combustion zone heat flux as compared to predicted values.

Segment Injector Checkout Tests

(C) Three tests (015-017) were conducted in a water-cooled calorimeter chamber to checkout the canted fan injector. The tests were conducted to a maximum chamber pressure of 657 psia, successfully demonstrating the structural integrity, face cooling characteristics, performance, and heat transfer profile of the injector. A maximum throat heat flux value of 26 Btu/in^{-2}-sec was attained at 657 psia chamber pressure; quite close to the predicted design value.

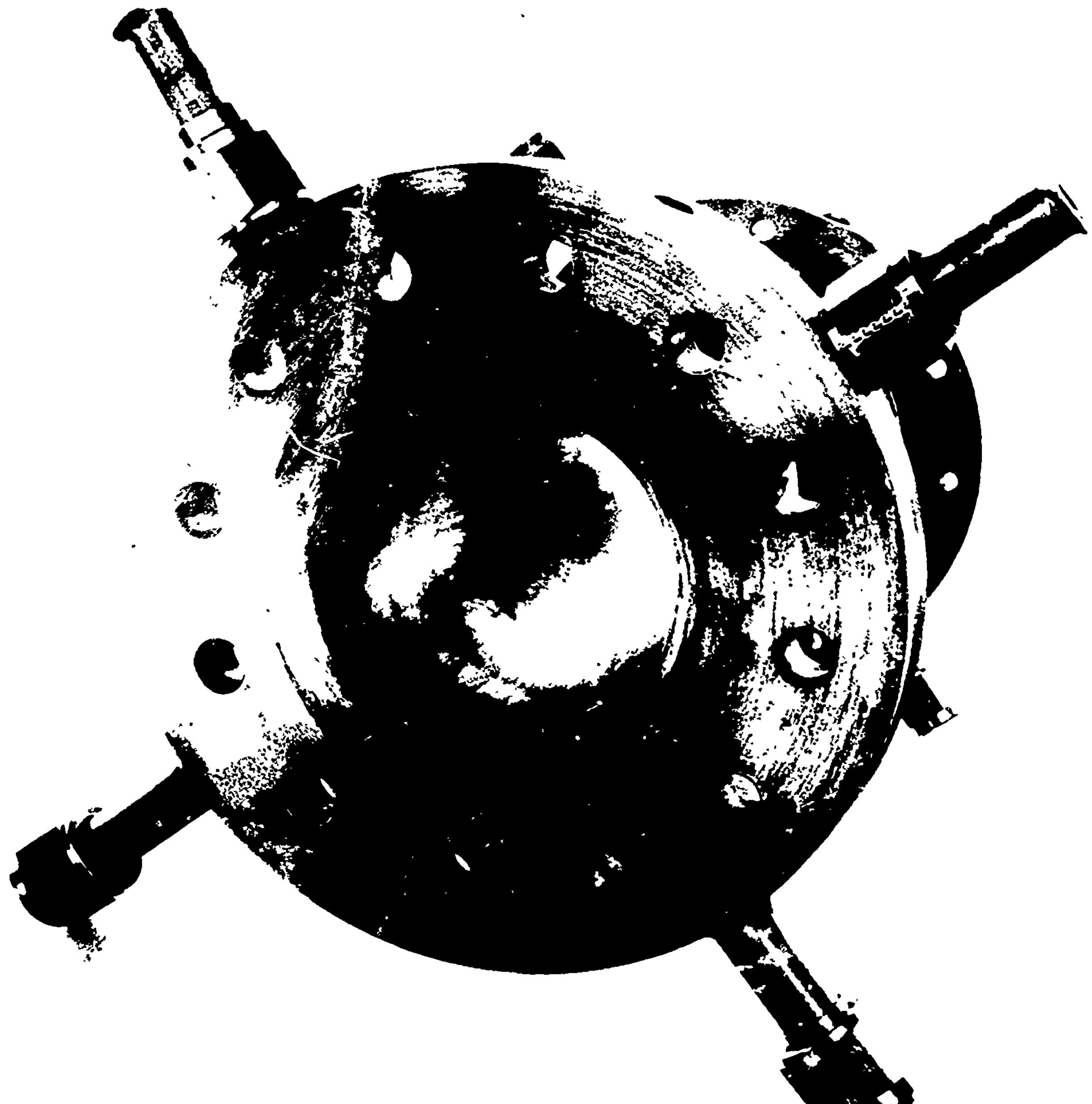

Fig. 98. Post Test Photograph of the Powder Metal Nickel Bell Chamber Showing the Combustion Zone (U)

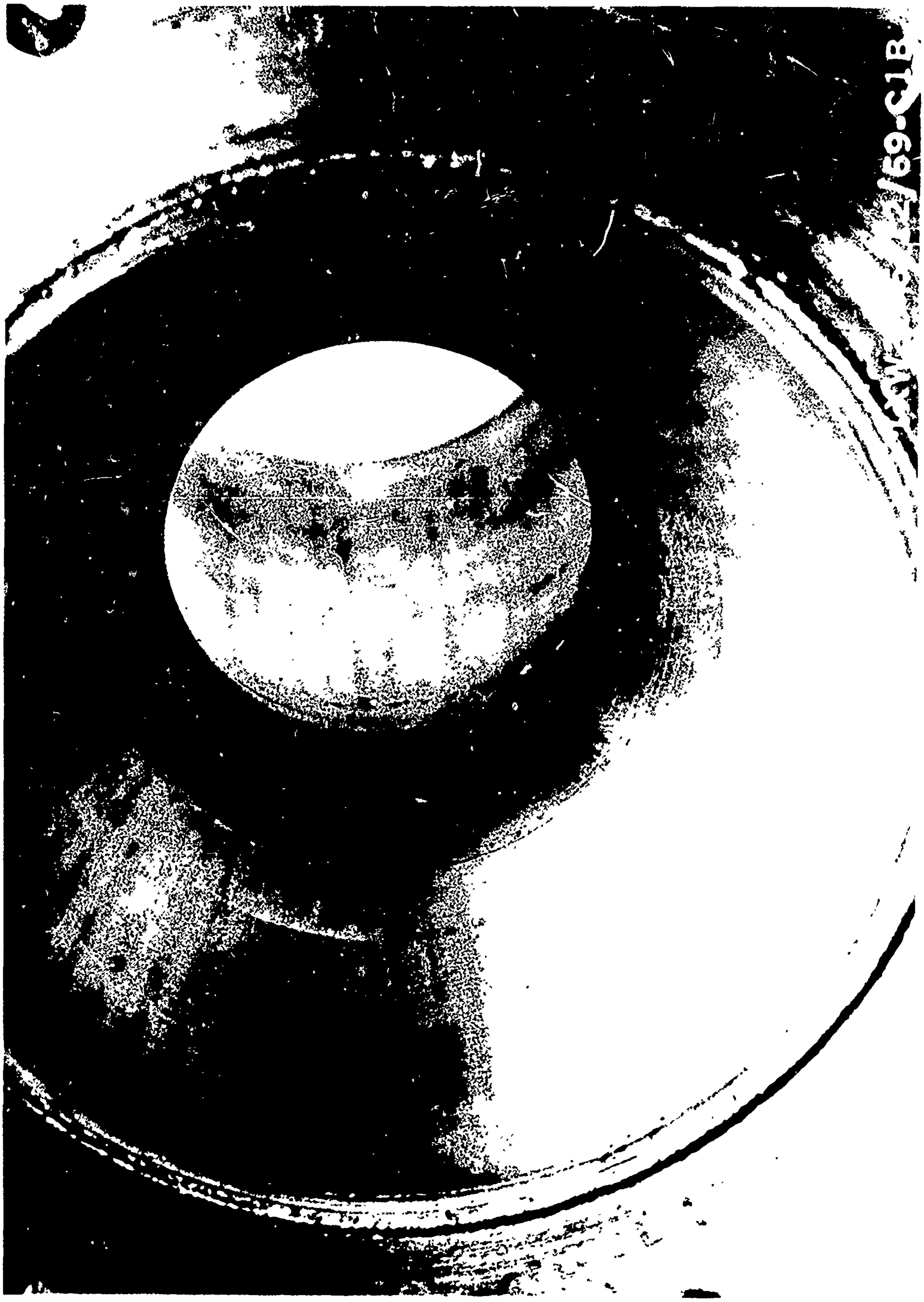

/69-C1B

Cast BeCu-10C Segment

(C) The cast segment was successfully hot fire tested four times (018-021) over a chamber pressure range of 406-460 psia. Accumulated test duration was 13.4 seconds with a mixture ratio range of 12.1 to 15.1. Primary coolant was GH_2 with LN_2 and subsequently LF_2 successfully used as the oxidizer heat exchange coolant. The test plan stipulated demonstration of structural integrity and thermal performance by operating at a 1000 F gas side wall temperature. Design analysis of the chamber had indicated that this 1000 F temperature would be attained at a chamber pressure of 455 psia with a corresponding GH_2 coolant flowrate of 0.36 lb/sec per contour panel.

(C) Test 020 demonstrated operation at the design conditions; 1000 F hot gas wall temperature (P_c = 455 psia) for 5.6 seconds. After 3.6 seconds of mainstage, the LN_2 flow (0.61 lb/sec) in the heat exchange panel was terminated to experimentally determine heat exchange values. Results showed a 30 percent increase in fuel bulk temperature for the upper contour panel corresponding to the "no oxidizer" flow condition at the time of cutoff. However, the 2.0 seconds of operation without LN_2 flow was not sufficient to stabilize the fuel bulk temperature. It is projected that the temperature increase would be another 4-6 degrees which would then result in a temperature rise similar to the lower panel for equal coolant flowrates.

(C) Test 021 was a demonstration test of the fabrication concept using GH_2 as the primary coolant and LF_2 as the coolant in the heat exchange panel. The test was conducted for 2.2 seconds at a chamber pressure of 460 psia and a calculated hot gas wall temperature of 960 F. This test successfully demonstrated the structural integrity and thermal performance of multiple layers of coolant passages with the propellants of interest.

(U) Post test inspection of the hardware revealed the chamber, nozzle and most of the throat to be in excellent condition. However, there was some localized erosion in one region on the upper contoured panel. The eroded area was approximately 0.020 deep (wall thickness was 0.060) and one half inch in diameter (Fig. 100).

(U) This erosion was attributed to one or more of the following; (1) localized coolant passage restriction, (2) abnormally high localized heat flux caused by some anomaly in the injector, (3) some inconsistency in the beryllium copper material properties, (4) some anomaly in the test operation or (5) some totally undefined adverse influence from the fluorine in the heat exchange panel.

(U) Review of the test records did not disclose any abnormal operating conditions. The overall bulk temperature rise and heat input to the eroded coolant panel agreed with predicted values. However, it should be noted that a very localized hot spot would not appreciably effect the overall heat transfer parameters.

(U) Subsequent review of the test movies (FASTAX camera - 400 FPS) showed that burning commenced at chamber pressure prime and continued until cutoff. Of significance is that the movies of the previous test (020) showed indications of burning starting $3\frac{1}{2}$ seconds after P_c prime and continuing until cutoff. The timing correlates with the termination of the LN_2 flow through the heat exchange panel. However, no hardware damage was noted during the post test inspection which implies very minor surface scarfing. This finding verified that the burning was not related to the fact that there was fluorine in the heat exchange panel.

(U) Subsequent water flow calibration of each coolant passage in the upper contoured panel showed no restriction in the passages. All passages flowed within 5 percent of the average and the passages located directly

Fig. 130. Post Test Photograph of ... Throat and Nozzle Showing Localized ...

under the eroded area were within 3 percent of the average. Further verification that there was no passage restriction was obtained by sectioning the segment at various locations.

(U) Metallurgical analysis of the casting revealed that material properties were consistent over the entire throat region and were within BeCu-10C specifications.

(U) Finally, the injector was water flowed with no indications of orifice restriction, misimpingement, or fan misalignment detected. However, it is recognized that this type of check would only pick up gross discrepancies.

(U) Orientation of the chamber eroded area with the injector showed that the burned zone was directly in line with the second set of orifice elements in the middle row of the injector (3 row injector -14 total sets of elements). As noted previously, the erosion in the throat of the water cooled hardware was also on the upper panel side, directly in line with one of the orifice elements in the middle row of the injector.

(U) Based on this investigation, it was concluded that this localized erosion was caused by a very high localized heat flux on the upper contoured panel.

(U) These tests demonstrated the structural integrity and thermal performance of this fabrication concept in that (1) the investment cast beryllium copper segment was tested to the design hot gas wall temperature of 1000 F with coolant pressures as high as 2400 psia, (2) the beneficial effort of multiple layers of coolant passages was demonstrated, and

(3) the integrity of the fabrication concept to retain the two propellants within close proximity of each other was demonstrated in the last test where GH_2 was used as the primary coolant and LF_2 was used as the heat exchange coolant.

(U) The coolant bulk temperature increase for the fuel and oxidizer coolant circuit on the contoured walls is shown in Fig. 101, 102 and 103. Results agreed quite closely with predicted values. The beneficial effect of the heat exchange panel is shown in Fig. 104. In this test, the LN_2 coolant in the heat exchange panel was terminated during the test, resulting in a significant increase in the GH_2 bulk temperature. The data show the heat exchange panel coolant had reduced the GH_2 bulk temperature approximately 25 percent. A detailed heat transfer analysis of the test results is presented in the following section.

Heat Transfer Analysis

(U) Results of the heat transfer analysis, as updated by the Phase III test results, are presented in the following paragraphs for each of the three fabrication concepts.

(U) Solid Wall Bell Chamber. As discussed previously, verification of the throat hot gas film coefficient prediction was obtained by testing the triplet/doublet injector in the solid wall copper thrust chamber with the same internal contour as the spun INCO 625 and powder metal bell chambers.

(U) A transient conduction analysis of the throat region was conducted with variable hot gas film coefficients, using the standard Heisler charts. A film coefficient was chosen to raise the surface temperature to the melting point within a time that just exceeded the test duration, Fig. 105.

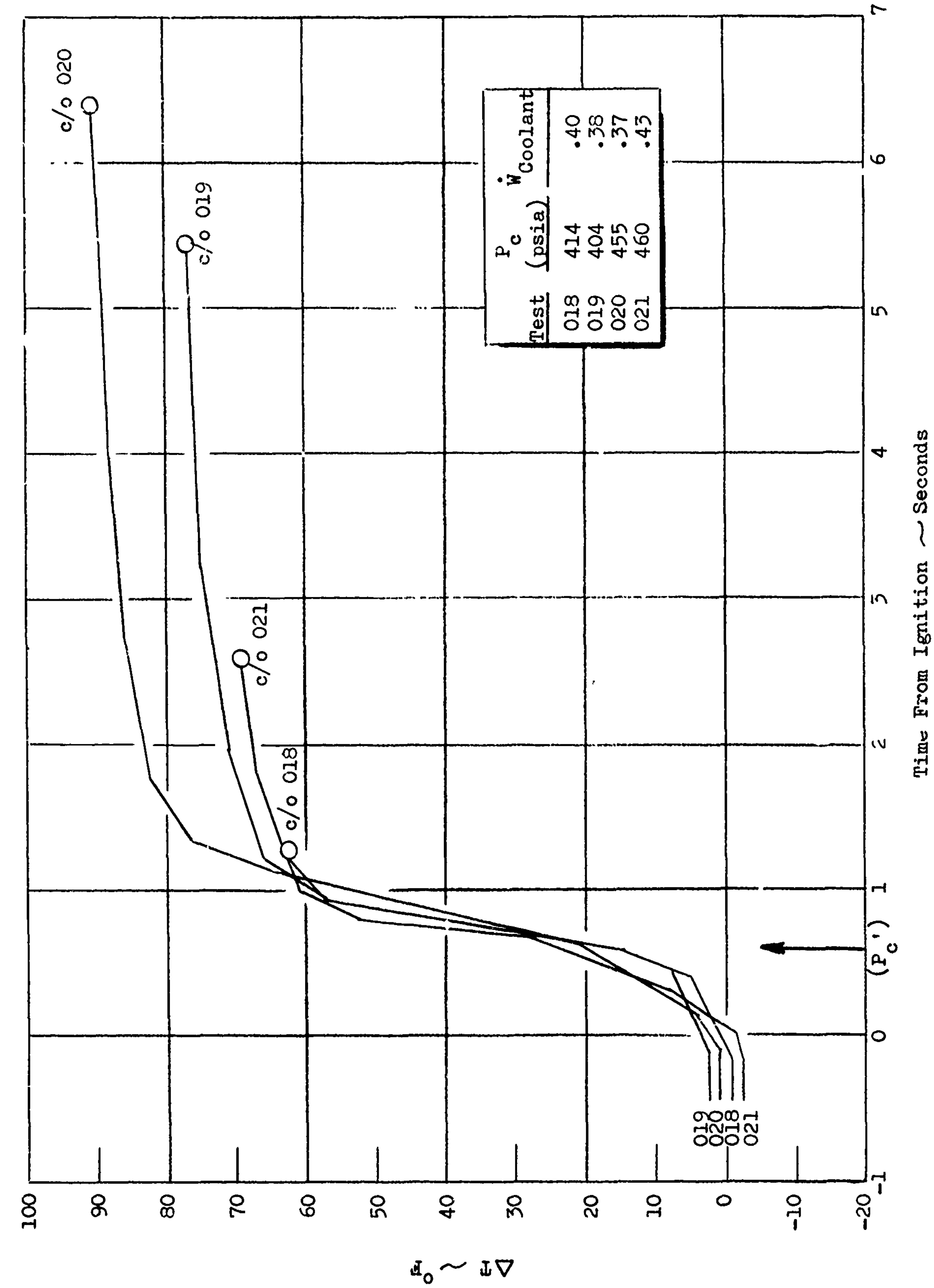

Figure 101.Cast Segment Lower Contour Panel Fuel Coolant Bulk Temperature Rise. (U)

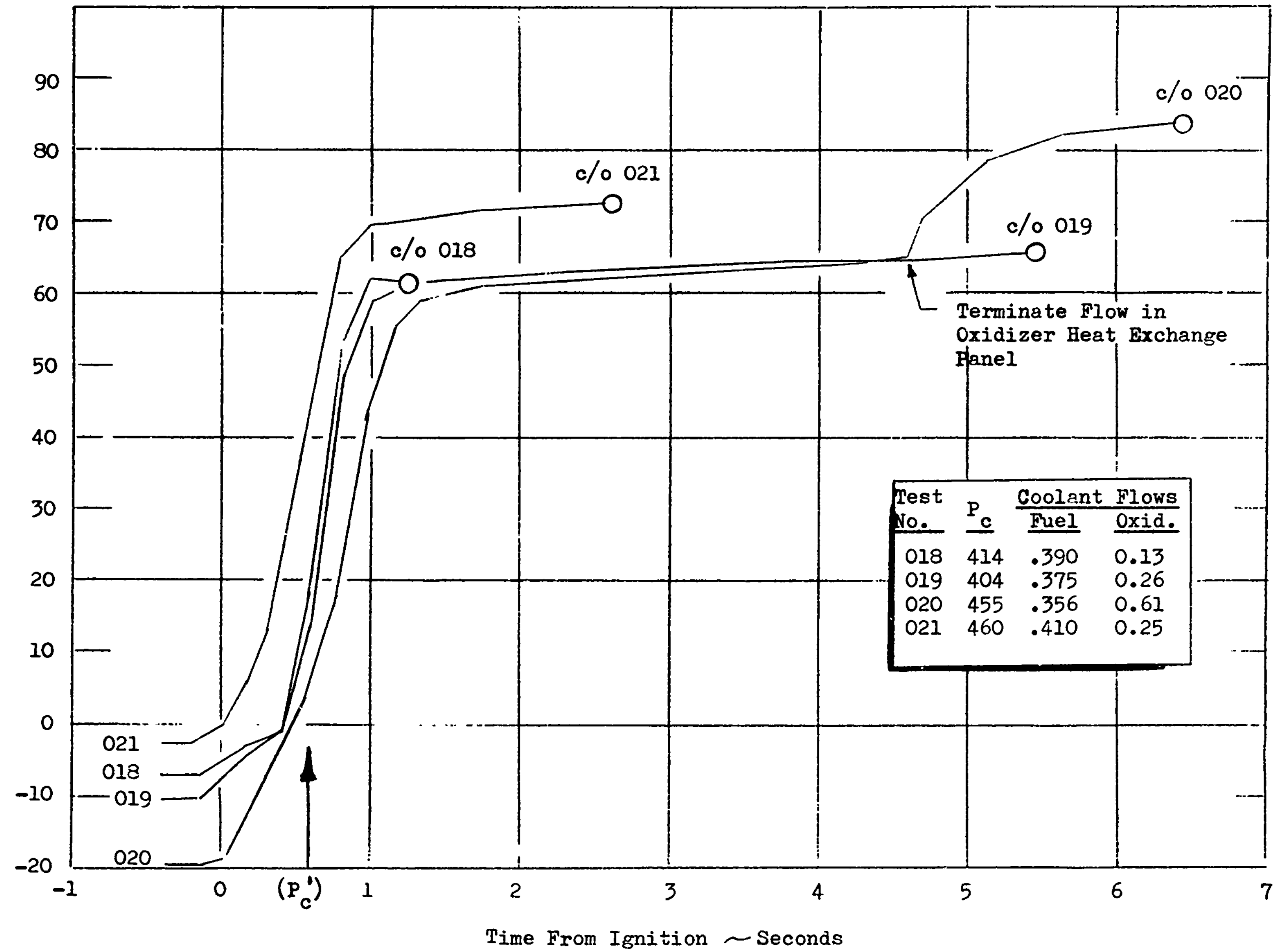

Figure 102. Cast Segment Upper Contour Panel Fuel Coolant Bulk Temperature Rise (Heat Exchange Side).(U)

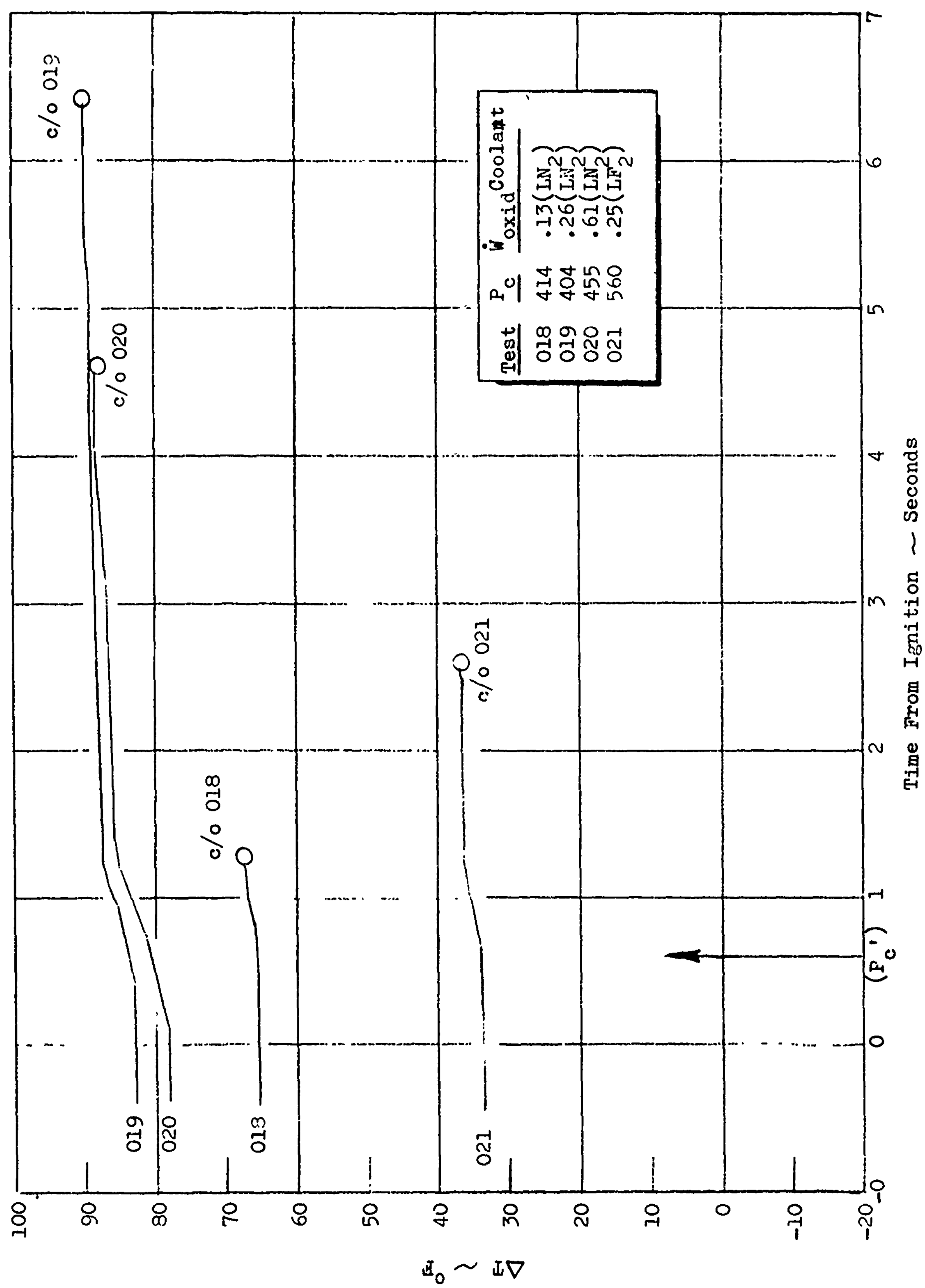

Figure 103. Cast Segment Oxidizer Heat Exchange Bulk Temperature Rise. (U)

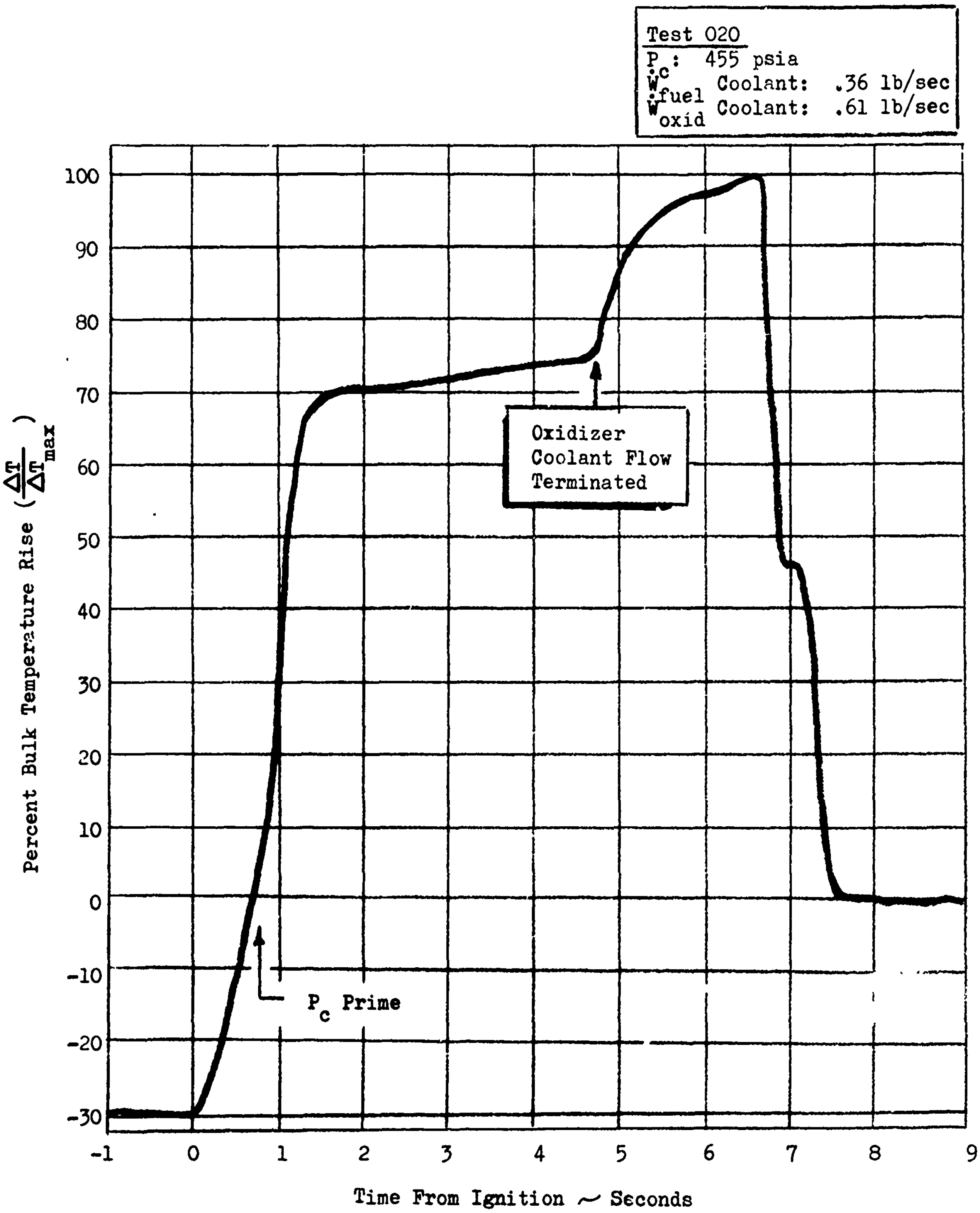

Figure 104. Cast Segment GH_2 Bulk Temperature Rise as Function of Oxidizer Heat Exchange Flow. (U)

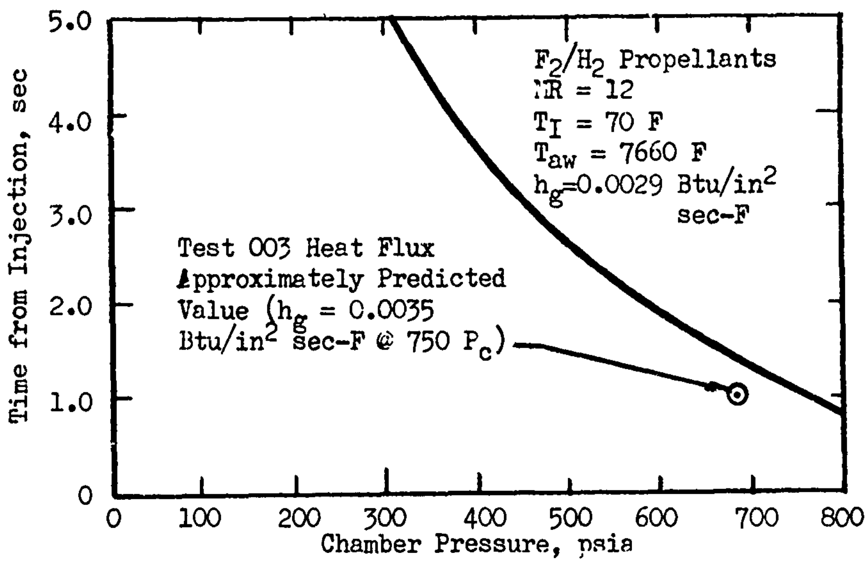

Fig. 105. Time Required to Reach Melting Point of Copper (U)

(C) The transient analysis predicts slightly low heating times, since a step function in the hot gas film coefficient is not actually experienced under test conditions. Hence, the hot gas film coefficient necessary to cause the surface to melt in Fig. 105 is slightly higher than 0.0029 and approaching that of 0.0035 Btu/in^2-sec, the predicted value. Based on this, it was concluded that the experimental throat heat flux values were quite close to those predicted.

(U) <u>INCO 625 Bell Chamber</u>. The INCO 625 chamber liner, operating at a hot gas wall temperature of 2000 F, had been selected as an attractive fabrication [illegible]ique for extending the limits of regeneratively cooled CPF/N_2H_4 [illegible]hambers,using N_2H_4 as the coolant and operating at a chamber pressure [illegible]sia. In the interest of economics, this chamber employed the F_2/H_2 [illegible]or which was designed to be used with the powder metal nickel

bell chamber. Consequently, demonstration of the 2000 F hot gas wall temperature was to be achieved at a chamber pressure of 480 psia due to the higher energy associated with the F_2/H_2 propellants (Fig. 4).

(U) The chamber contour shown previously in Fig. 76 was analyzed using the Integral Method, as applied to the energy equation, to obtain a hot gas film coefficient distribution as a function of chamber pressure. These results were then used to predict heat fluxes with the regenerative cooling computer program. Resulting coolant channel dimensions were also shown in Fig. 76. A 2-dimensional plot of the throat temperature is shown in Fig. 106.

(U) As the INCO 625 bell chamber test program progressed, it became apparent that, based on coolant bulk temperature measurements, the steady state combustion zone heat fluxes were higher than expected from the theoretical analysis. Also, during the start transient local erosion occurred in the combustion zone just downstream of the injector. Subsequent analysis of the eroded channel geometry provided the maximum possible heat flux experienced during the test (Fig. 107) to achieve this erosion. The hot gas convection coefficient necessary to just reach the melting point at the heated surface is given in Fig. 107 for comparison.

(U) These film coefficients are delineated in Fig. 108 relative to the theoretical profile. It is evident that the maximum combustion zone heat flux during the start transient was well above the throat value.

(U) Abnormally high combustion zone heat flux values were also experienced during steady chamber conditions, as indicated by the film coefficient profile estimated from experimental coolant heat absorption rates. The estimated combustion zone profile of Fig. 108 was determined by integration of the heat input over the entire thrust chamber, considering the

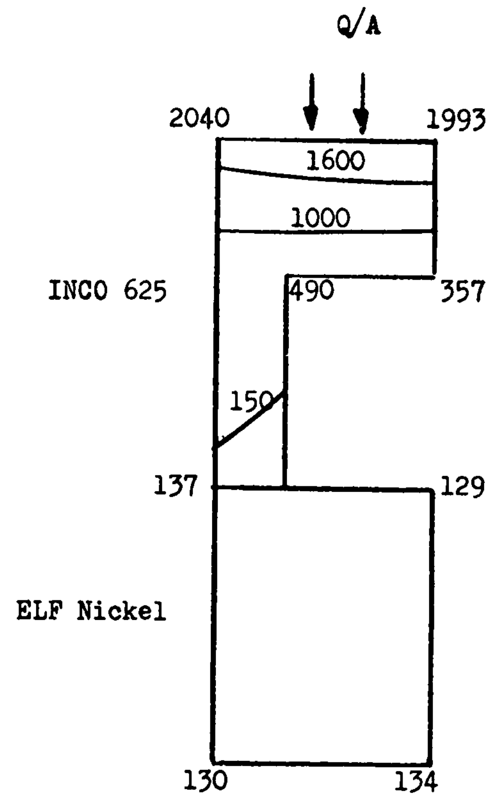

F_2/H_2 Propellants
P_c = 480 psia
Coolant: H_2O
$\dot{W}$ = 10.5 lb/sec

Figure 106. Temperature Distribution - Throat Channel of INCO 625 Bell Chamber - Design Point. (U)

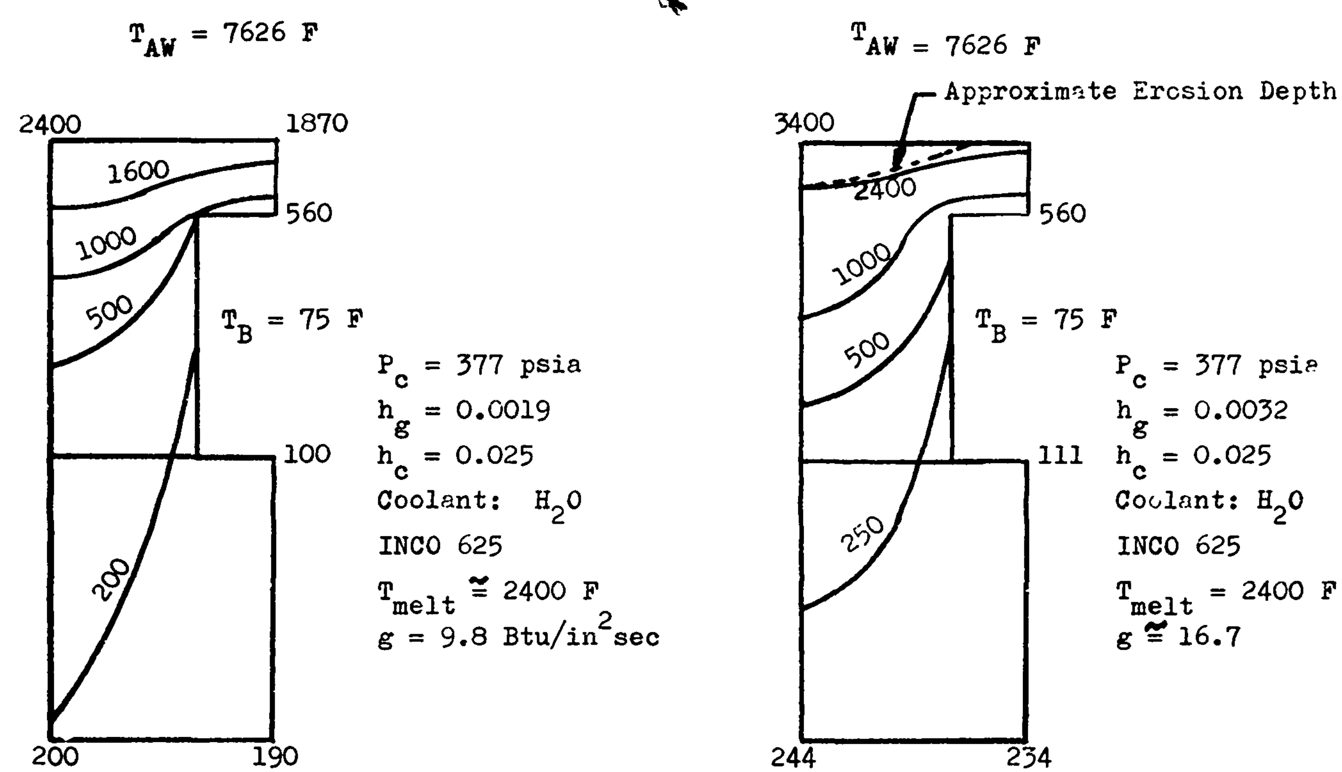

(a) Minimum Combustion Zone Heat Flux to Obtain Measured Heat Input to Coolant

(b) Maximum Combustion Zone Heat Flux to Locally Erode Chamber During Start Transient

Figure 107. INCO 625 Bell Chamber Isotherm Plots. (U)

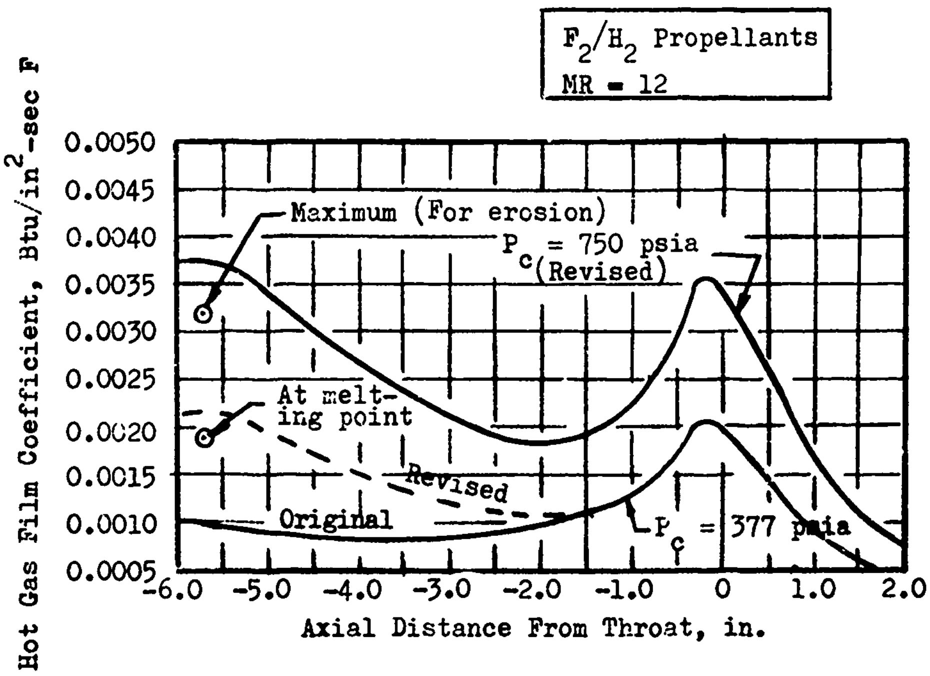

Figure 108. Comparison of Originally Predicted and Revised Hot Gas Film Coefficient Based on INCO 625 Test Results. (U)

nozzle and throat region to be accurately predicted theoretically. This new hot gas film coefficient distribution was then projected to other chamber pressures for subsequent analyses of the spun bell and powder metal thrust chambers (Fig. 108), continually cognizant of the extreme heat flux present during transient operation.

(U) As a result of the higher than predicted combustion zone heat fluxes, the maximum chamber pressure attained during the test series was 382 psia.

(U) Subsequently an analysis was completed to parametrically evaluate wall temperatures and coolant parameters using the revised film coefficient profile for comparison to experimental data. Results of this analysis showed that throat hot gas wall temperatures of approximately 1860 F were reached during the test. Combustion zone wall temperatures exceeded this temperature during the start transient when localized erosion occurred. Steady state temperatures were quite close to the 2000 F design value.

(U) One and two dimensional wall temperatures at the hot gas surface appear in Fig. 109 for the throat and combustion zone. The two dimensional temperature is in proximity of and below the one dimensional value in the throat, however, in the case of the combustion zone, they are widely divergent with the two dimensional value considerably higher. The agreement between one and two dimensional hot gas surface temperatures depends upon the relative resistance to heat transfer presented by the convection at the horizontal cooling surface, and the land conduction and subsequent convection at the sides of the channel. Operation of the thrust chamber at the design chamber pressure is not limited by the throat, but by the excessive wall temperatures in the combustion zone, especially the levels

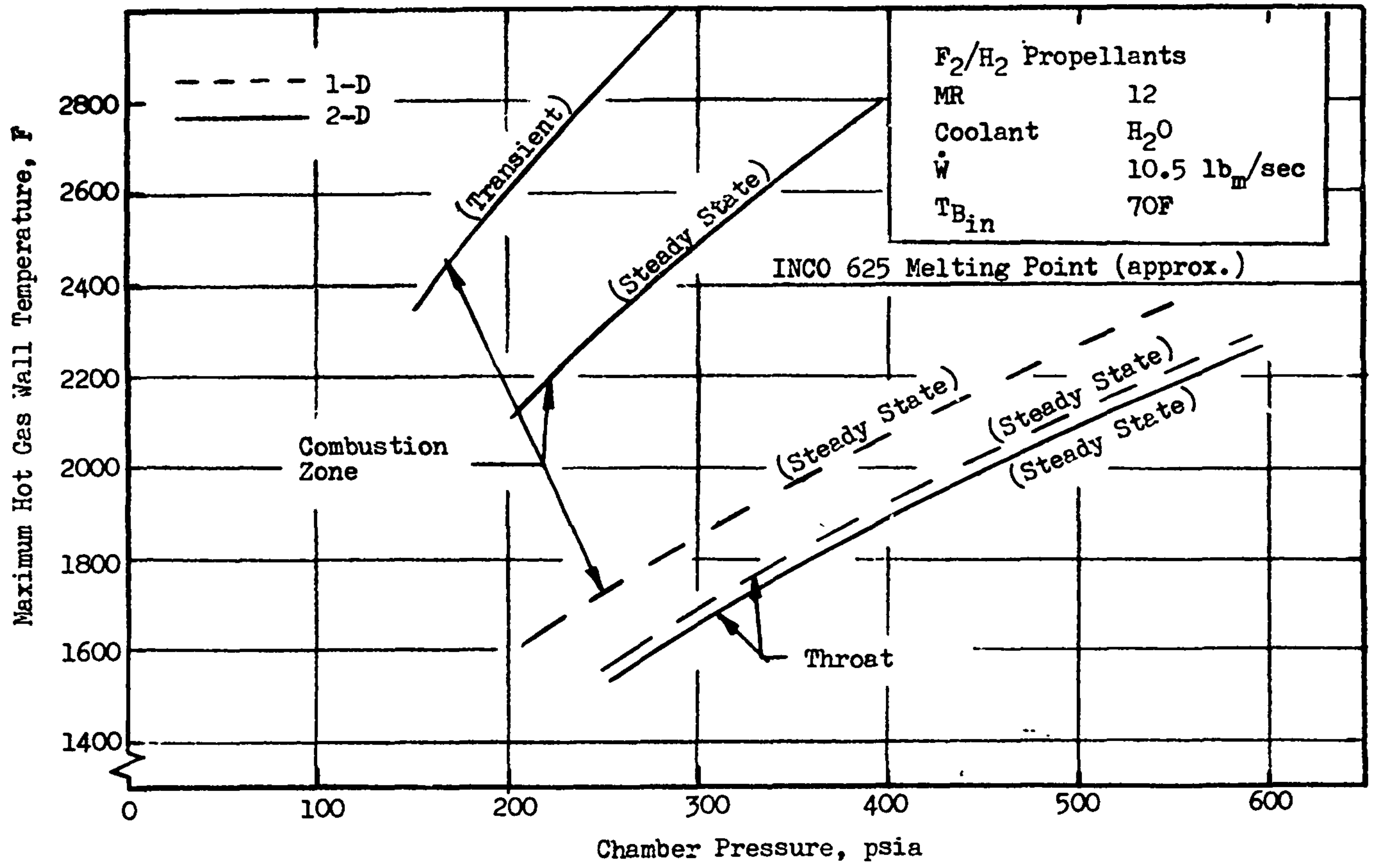

Fig. 109. Comparison of 1-D and 2-D Hot Gas Wall Temperatures for the INCO 625 Bell Chamber (U)

experienced during the start transient as seen in Fig. 109. If the combustion zone heat fluxes had been as originally calculated, the thrust chamber would have experienced wall temperatures equivalent to those in the throat.

(U) A comparison of measured coolant bulk temperature rises with the predicted values (using the experimentally determined hot gas film coefficient profile) is shown in Fig. 110. The deviation between the predicted and experimental values is within 5 percent, based on two dimensional wall temperature computations.

(C) Powder Metal Nickel Bell Chamber. Demonstration of the structural integrity and thermal performance of the powder metal nickel bell chamber fabrication technique was accomplished in a F_2/H_2 combustion environment. Coolant was ambient temperature hydrogen and the design point was a chamber pressure of 750 psia and a thrust level of 3300 pounds. Chamber geometry was presented earlier in Fig. 72 and operating parameters in Table XVIII.

(U) Based on this data and the originally predicted hot gas film coefficient profile (Fig. 108), the chamber was analyzed using the same theoretical approach as that used on the INCO 625 bell chamber (Appendix C).

(U) Use of GH_2 as the coolant, which is above supercritical temperature and pressure, involves only forced convection heat transfer at the cooling surface. Results of the convective cooling analysis on the powder metal nickel bell chamber established the coolant channel dimensions shown previously in Fig. 72. A 2-dimensional analysis of the throat region gave a temperature distribution as shown in Fig. 111 with coolant flowrate equal to injector fuel flowrate.

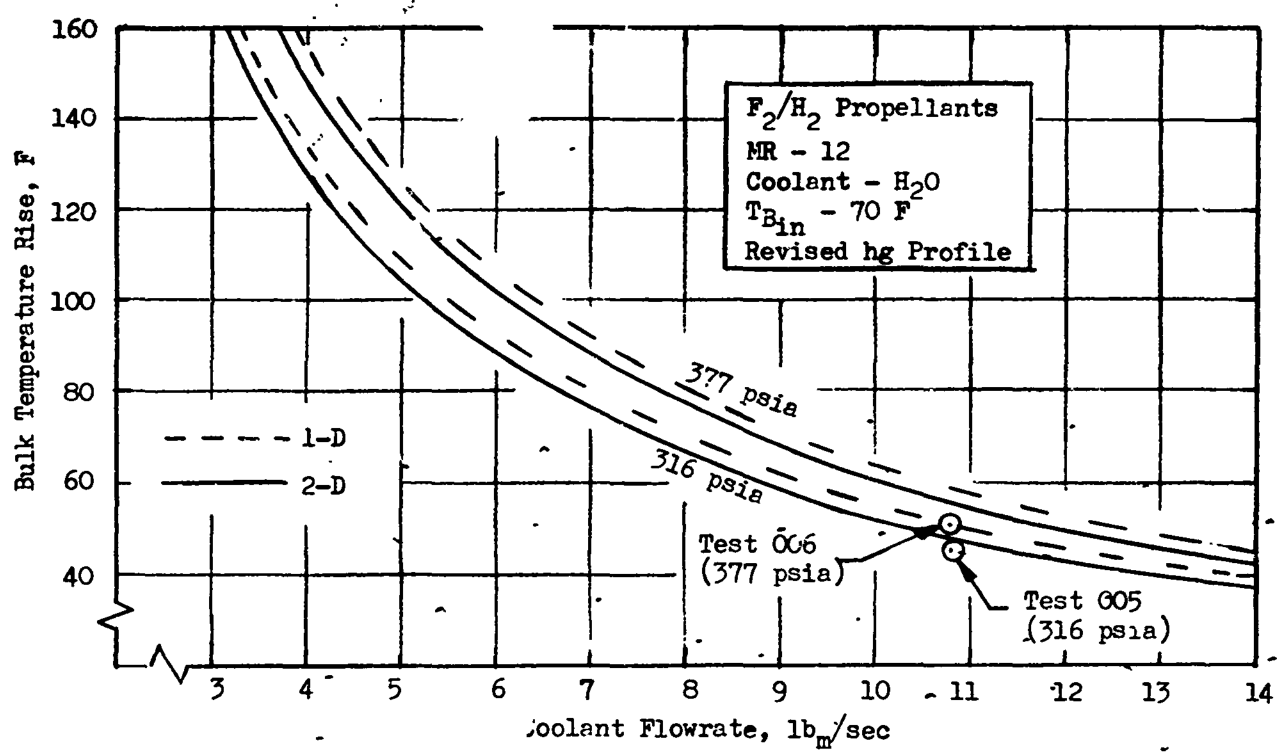

Fig. 110. Comparison of Predicted and Measured Coolant Bulk Temperature Rises for INCO 625 Bell Chamber (U)

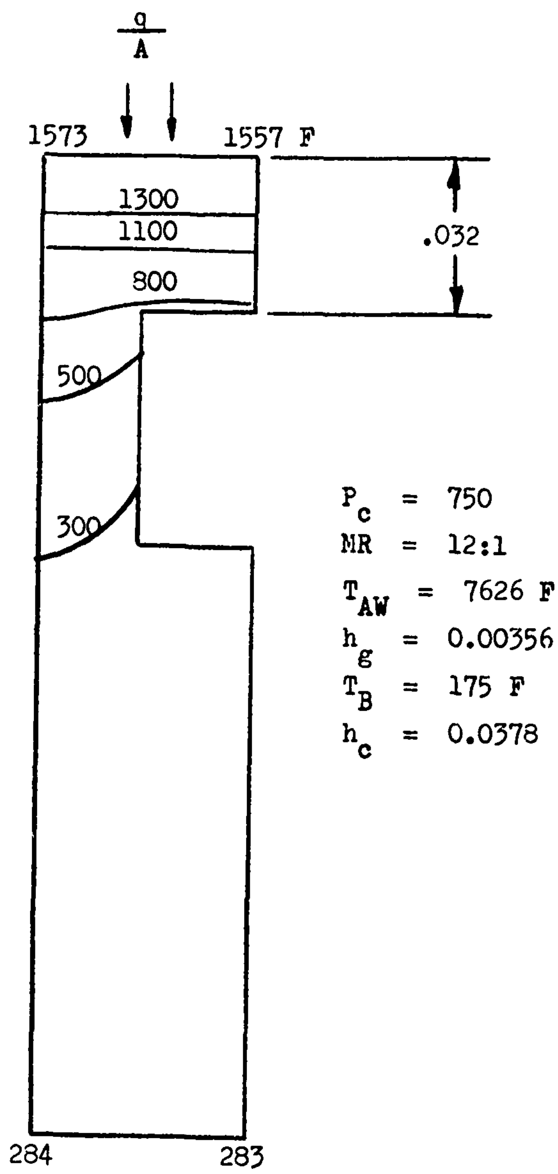

Figure 111. Point Design Temperatures - Throat Channel of Powder Metal Nickel Bell Chamber (U)

(U) However, the test series on the INCO 625 bell chamber and subsequent analysis of the test data showed a higher than predicted combustion zone heat flux. Consequently, the powder metal nickel bell chamber was reanalyzed to determine appropriate operating conditions for demonstration of the 1600 F design hot gas wall temperature.

(U) One and two dimensional parametric analyses (Fig. 112) of this chamber using the revised hot gas film coefficient profile showed that the 1600 F design wall temperature would be reached in the combustion zone at a chamber pressure lower than the original design point. Further, as a result of this higher combustion zone heat flux and based on the better cooling capability of ambient temperature hydrogen as compared to heated hydrogen, a downpass coolant flow path was selected for this chamber. A choked flow coolant flowrate of approximately 1.0 lb/sec and a coolant supply pressure of 2000 psig, reduces the combustion zone hot gas wall temperature approximately 200 degrees at 500 psia chamber pressure as compared to an uppass coolant circuit.

(U) The GH_2 coolant is in the forced convection regime in the powder metal nickel bell chamber and the wall temperatures are a direct function of the coolant flow. In particular, Fig. 112 shows that the low coolant flowrates force heat to be conducted by the lands to the channel sides resulting in two dimensional temperatures that are lower than the corresponding one dimensional values, while the opposite is true at high coolant flows.

(U) A total of seven tests were completed on this chamber over a chamber pressure range of 296 to 528 psia. The measured and predicted heat input and coolant flowrates are compared in Fig. 113 and 114 (measured values were within 3 percent of predicted values).

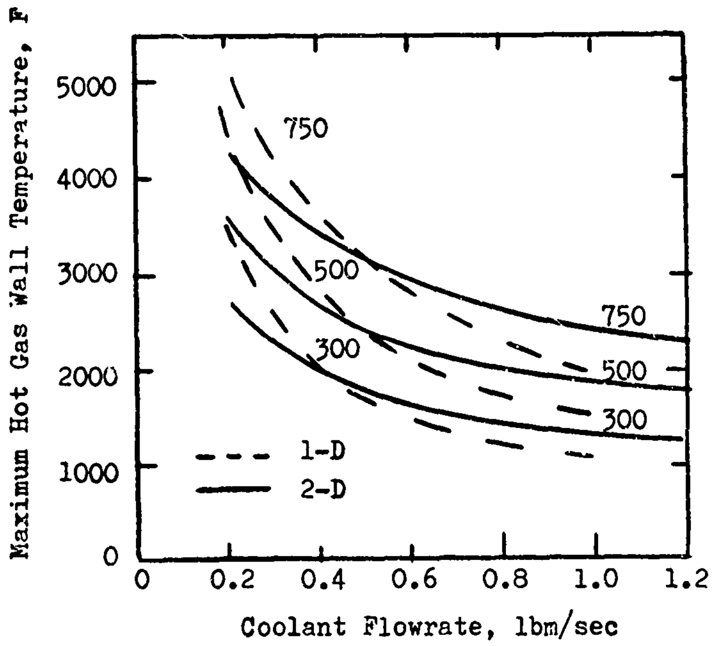

A) Combustion Zone

F_2/H_2 Propellants
MR = 12.0
Coolant - GH_2
Downpass Coolant Circuit

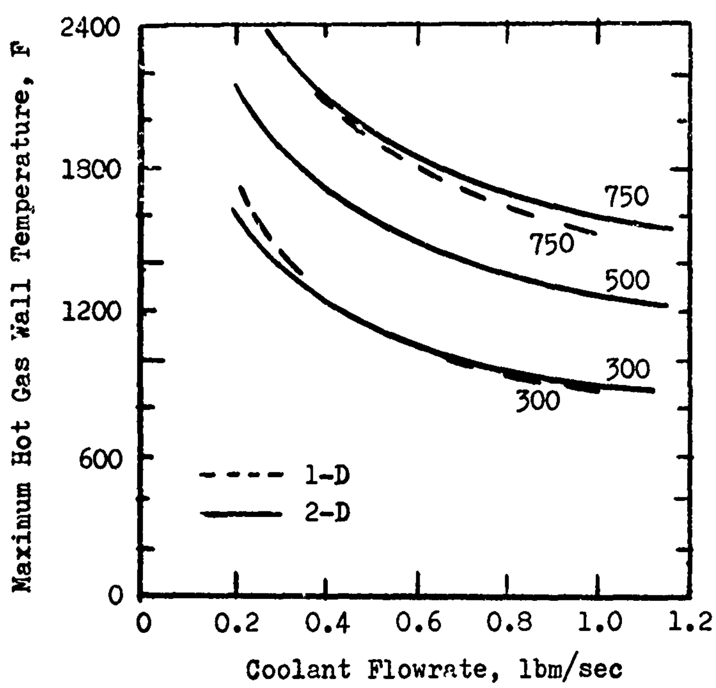

B) Throat

Figure 112. Peak Hot Gas Wall Temperatures for Powder Metal Nickel Bell Chamber - Revised Heat Flux Profile. (U)

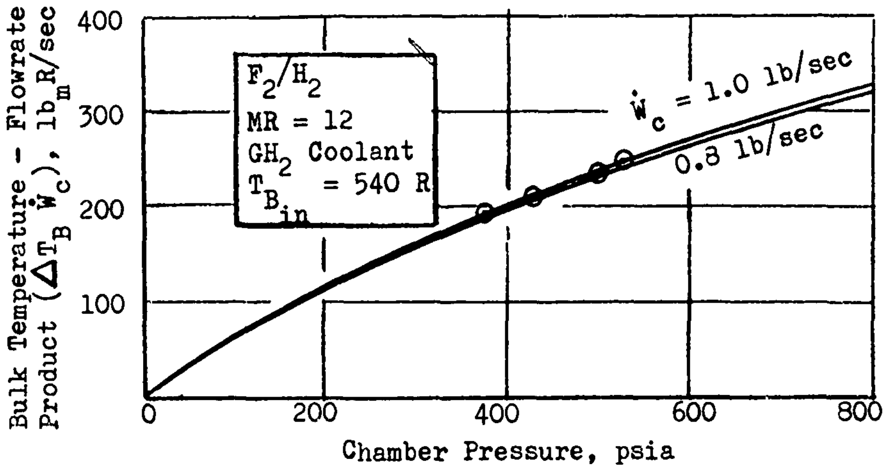

Figure 113. Predicted and Measured Heat Input Values for Powder Metal Nickel Bell Chamber.

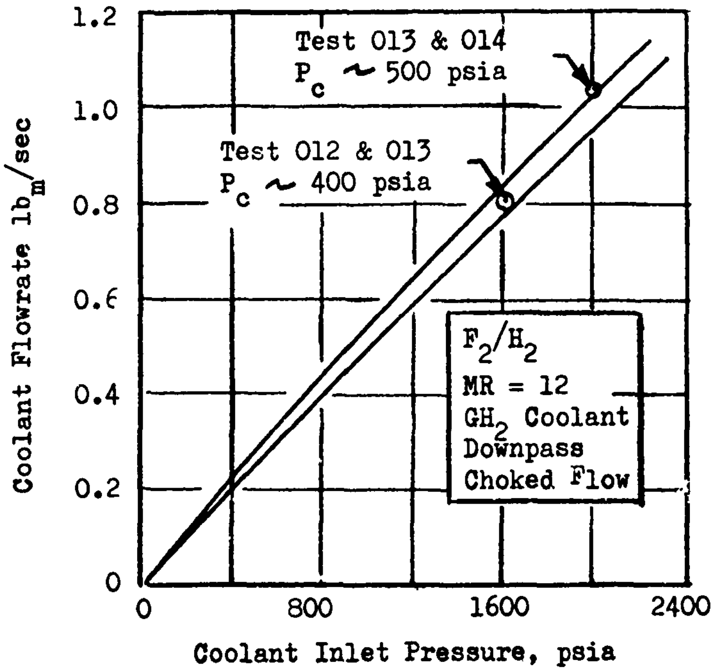

Figure 114. Predicted and Measured Coolant Flowrates for Powder Metal Nickel Bell Chamber. (U)

(U) Two dimensional wall temperatures of the combustion zone hot gas surface for the 528 psia chamber pressure test (Test 014) are presented in Fig. 115 for the steady state and transient chamber pressure cases. It is evident in examining the data of Fig. 115 that the structural integrity and thermal performance of the powder metal nickel fabrication concept was demonstrated under even more severe conditions than originally planned. The hot gas wall temperature in the combustion zone exceeded 2500 F during the start transient and equaled 1915 F during steady state operation. Steady state temperatures in the throat were in excess of 1300 F on the last test (Fig. 112).

(C) Cast BeCu Segment. As was discussed in the Phase II section, the coolant passages and as-cast hot gas wall thickness dimensions of the cast beryllium copper segment were established based on recommendations of the foundry and Rocketdyne Materials and Processes personnel. Further, the combustion zone contour and operating parameters (F_2/H_2 propellants, GH_2 cooled in the primary circuit and LF_2 cooled in the heat exchange circuit) were consistent with the annular chamber of contract F04611-67-C-0116. The coolant passage dimensions, constant width (.060) variable height (.040 to .080), and combustor contour were shown previously in Figs. 34 and 61. The corresponding dimensional requirements for the oxidizer heat exchange panel, constant width (.058) constant height (.040), were also shown in Fig. 34.

(U) Initial heat transfer analysis was concerned with the determination of the chamber pressure at which the design hot gas wall temperature of 1000 F was attained. Each circuit was fed independently with GH_2 "choked flow" coolant with variable coolant inlet pressures. Also, the experimentally determined thermal conductivity of overaged BeCu-10C was used. Results are plotted in Fig. 116.

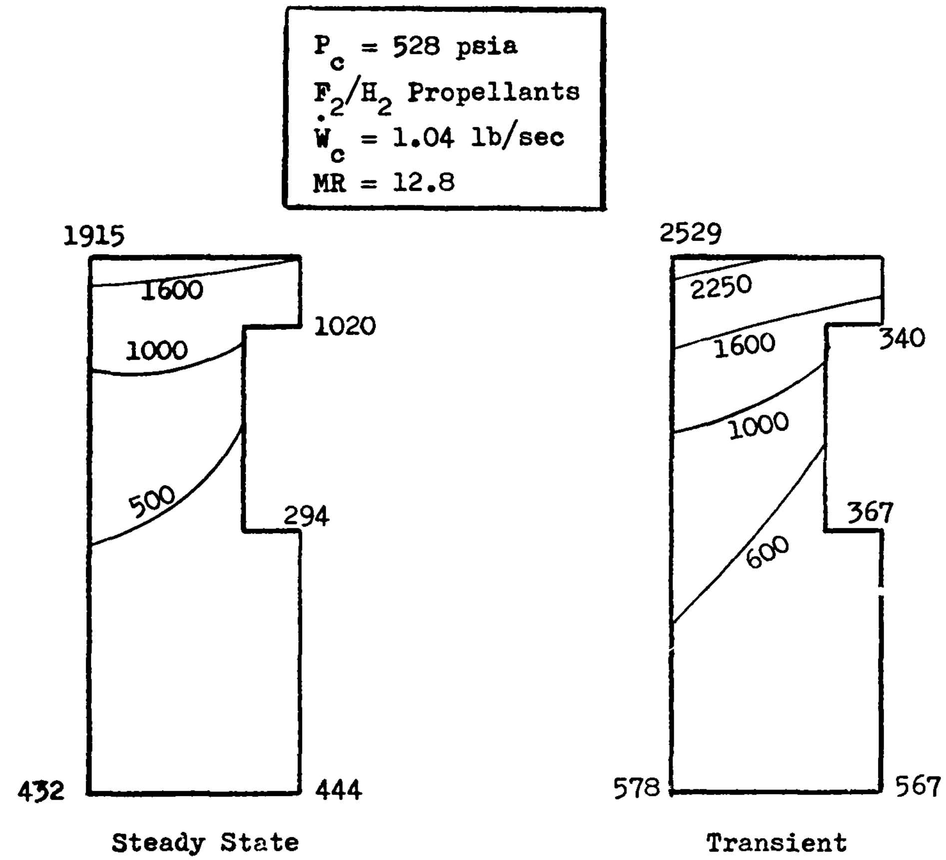

Figure 115. Combustion Zone Transient and Steady State Temperature. (U)

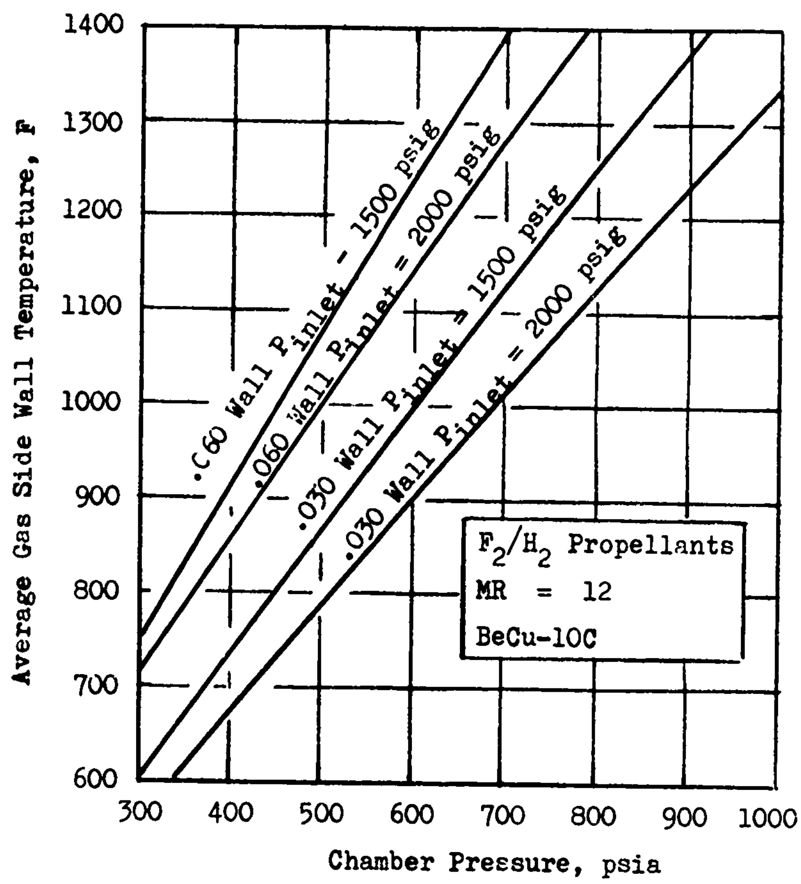

Figure 116. Cast BeCu-10C Segment Gas Side Wall Temperature. (U)

(U) As discussed previously, the Phase III castings were to be tested with an as-cast hot gas wall thickness of 0.060 inches; establishing a design point of 480 psia chamber pressure with GH_2 choked flow at a coolant inlet pressure of 2000 psig.

(U) A detailed analysis of the end plates was not completed since the wall-chamber geometry was similar to the contoured panels and all testing was to be conducted at maximum coolant flow conditions.

(U) Based on these criteria the segment was successfully hot fire tested four times to a maximum chamber pressure of 460 psia. Primary coolant was GH_2 and heat exchange coolant was LN_2 and subsequently LF_2.

(U) The thermal analysis of the contoured walls of the casting and heat exchange panel can be separated, to a certain extent, since the lower wall does not incorporate a heat exchange panel and the upper wall was cooled for a short period without the benefit of heat exchange coolant flow during the test program. The measured H_2 coolant bulk temperature rise was presented in Figs. 101 and 102 for the test series. The data of test 020 show the significant increase in GH_2 bulk temperature on the upper contoured wall when the LN_2 coolant flow was terminated during the test. Some extrapolation of the data was necessary in specific instances since the bulk temperatures were not completely stabilized. Liquid fluorine was utilized as a coolant in the heat exchange panel during test 021 with LN_2 as the coolant for the earlier tests.

(U) The coolant bulk temperature rise-flowrate product is directly proportional to the heat input to the coolant, at constant specific heat, and is quite accurate in the case of H_2 for the temperature range

considered here. This parameter is effectively used to compare the predicted and measured heat input to the contoured walls of the segment (Fig. 117). The results showed very good agreement between measured and predicted data.

(U) The LN_2 and LF_2 coolant bulk temperature rises are plotted in Fig. 103, as a function of time from ignition. These data are completely stabilized early in the run. The heating path taken by the LN_2 coolant as it progressed through the heat exchanger panel is shown on the temperature-entropy diagram in Fig. 118 for the two long duration tests. The heating path is always above the two phase region, indicated by the saturation line forming the dome, since the pressure was greater than the critical pressure for LN_2. Testing at supercritical, rather than subcritical, LN_2 pressures is desirable, because the measured bulk temperature rise is directly related to the heat input.

(U) On the last test, the fluorine in the heat exchange panel was at subcritical pressures, as indicated by the heating path in Fig. 119. The location in the dome was estimated from the LN_2 enthalpy rise data, utilizing the shift in film coefficients indicated by cooling correlations for supercritical and subcritical pressures. In addition, the measured outlet pressure corresponds to the outlet temperature, which was apparently constant over half the heat exchanger length where the flow was two phase. A theoretical calculation was performed for the LN_2 cooled cases only, due to the uncertainties involved with the two phase F_2 enthalpy rise data.

(U) The conduction problem of the counter flow double panel section is a highly two dimensional one, involving both H_2 and LN_2 convection. Convective cooling with LN_2 is extremely dependent upon the cooling surface temperature, which is observed by examining the cooling correlation in Appendix C.

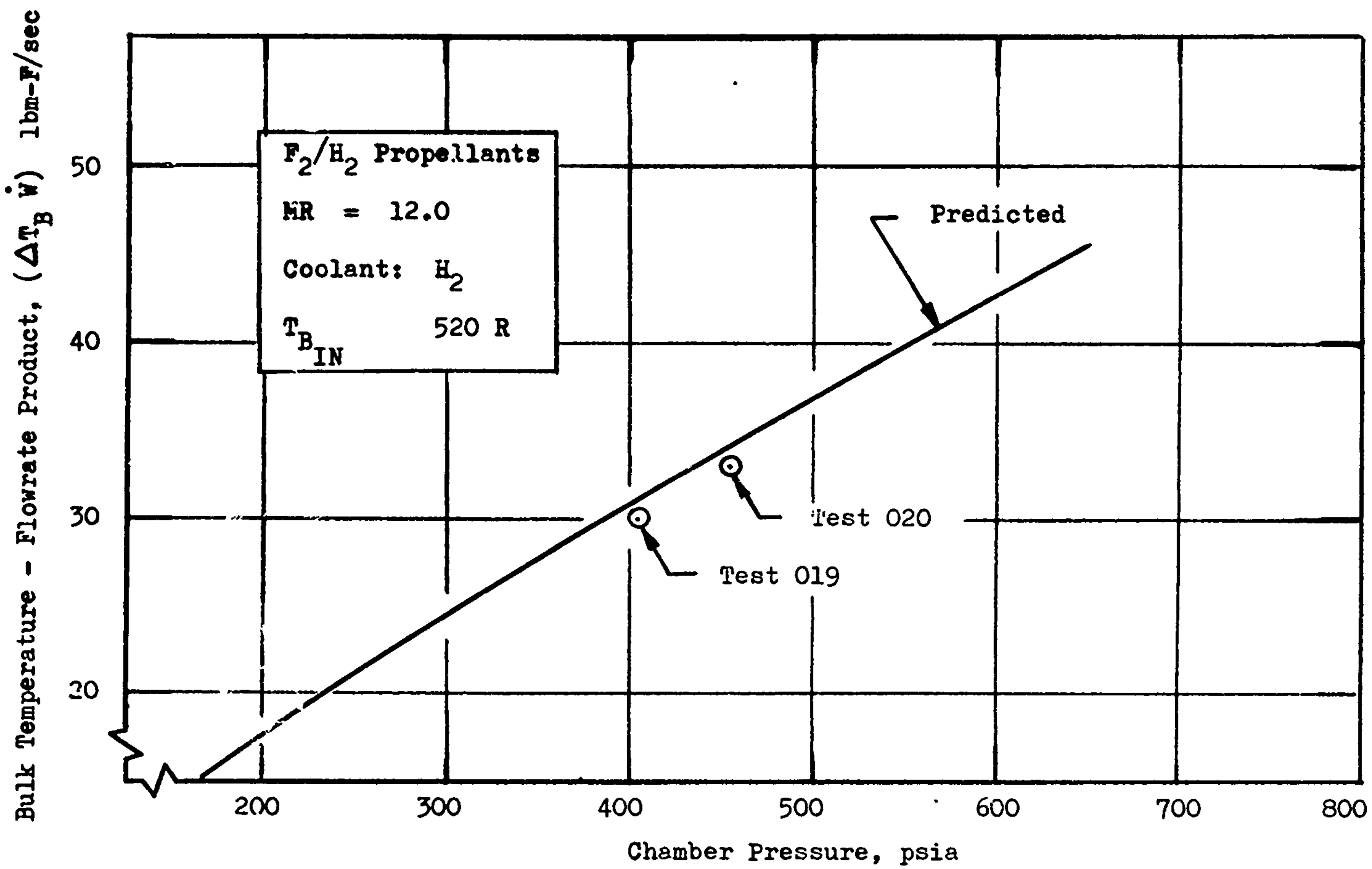

Figure 117. Predicted and Measured Heat Input to H_2 Coolant of Cast BeCu-10C Segment Contoured Walls. (U)

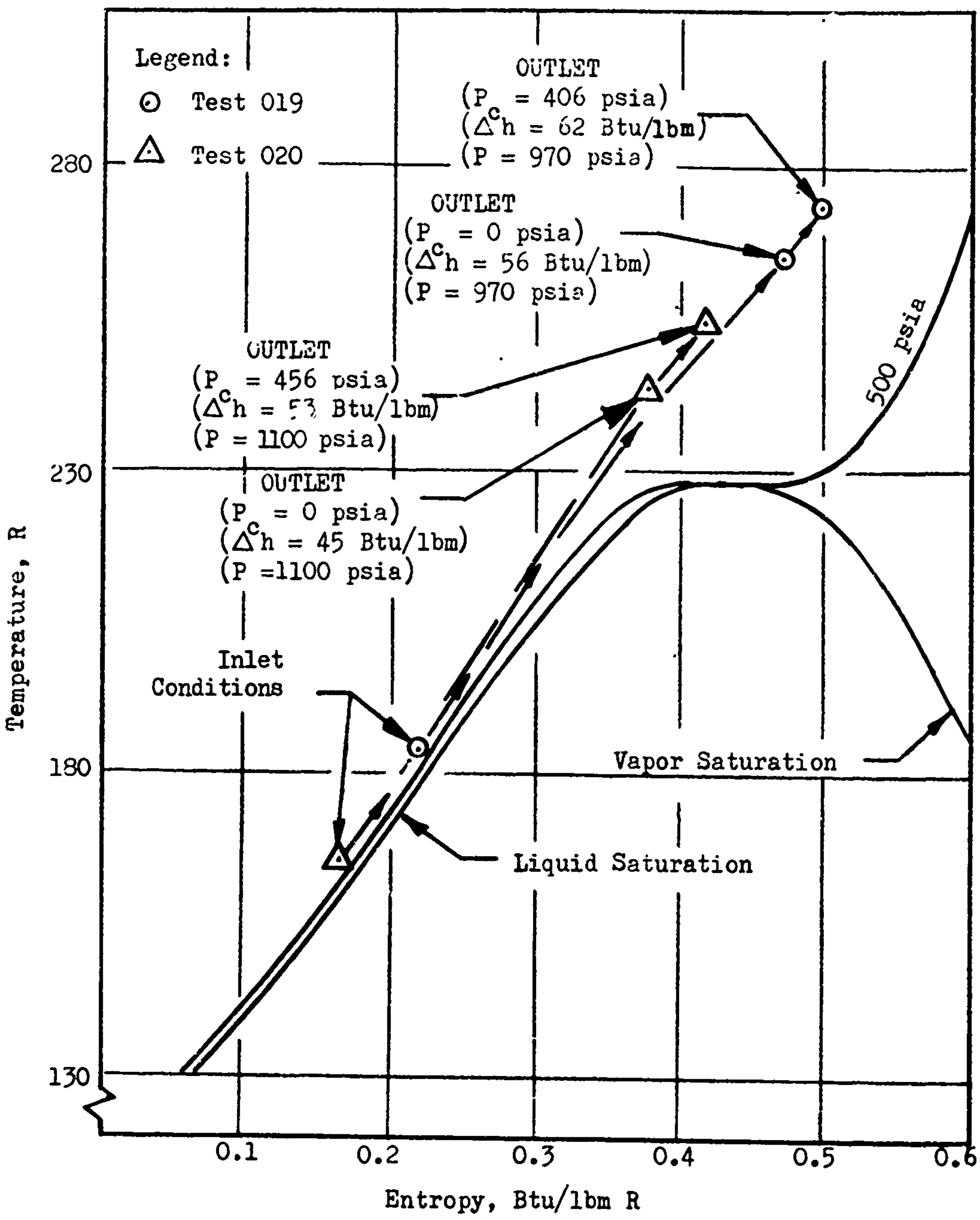

Figure 118. LN_2 Temperature Entropy Plot, LN_2 Panel Heating Paths. (U)

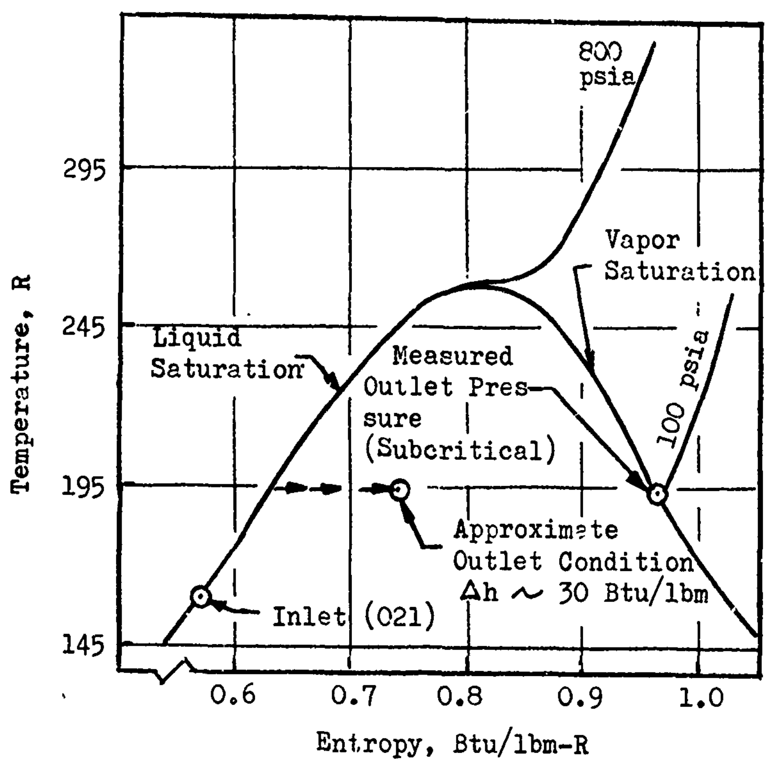

Figure 119. F_2 Temperature Entropy Plot - F_2 Panel Heating Path. (U)

(U) The two dimensional solutions to the throat heat exchanger cross sections shown in Fig. 120 are iterative, due to the wall temperature sensitivity of the LN_2 cooling equation.

(U) Enthalpy rises were calculated by summing the heat inputs from each surface of the LN_2 channel, based on the average film coefficient-wall temperature difference products for the throat and combustion zone. The theoretical LN_2 enthalpy rise through the heat exchanger is plotted in Fig. 121 as a function of LN_2 flowrate, along with the experimental data. The prediction is quite accurate; the data is within 5 percent of the values calculated for the cases with and without hot gas heating. A summary of the experimental and theoretical enthalpy rises for the LN_2 and H_2 contoured panels are presented in Table XXIII for convenience.

(U) An indication of the accuracy of the data was determined by noting that the heat input to the H_2 increased when the LN_2 flow was shut down, by the same amount the LN_2 absorbed (32 Btu/sec) during operation of the LN_2 panel, based on the enthalpy rises in the previous tabulation.

(U) The structural integrity and thermal performance of this fabrication concept was successfully demonstrated by attaining a maximum hot gas wall temperature of 960 F at the throat. The minor erosion in one region of the throat was attributed to an injector peculiarity. The chamber was successfully operated with the heat exchanger panel in operation flowing LN_2 and subsequently LF_2 as the heat exchange coolant. Excellent consistency was observed between theoretical predictions and test data.

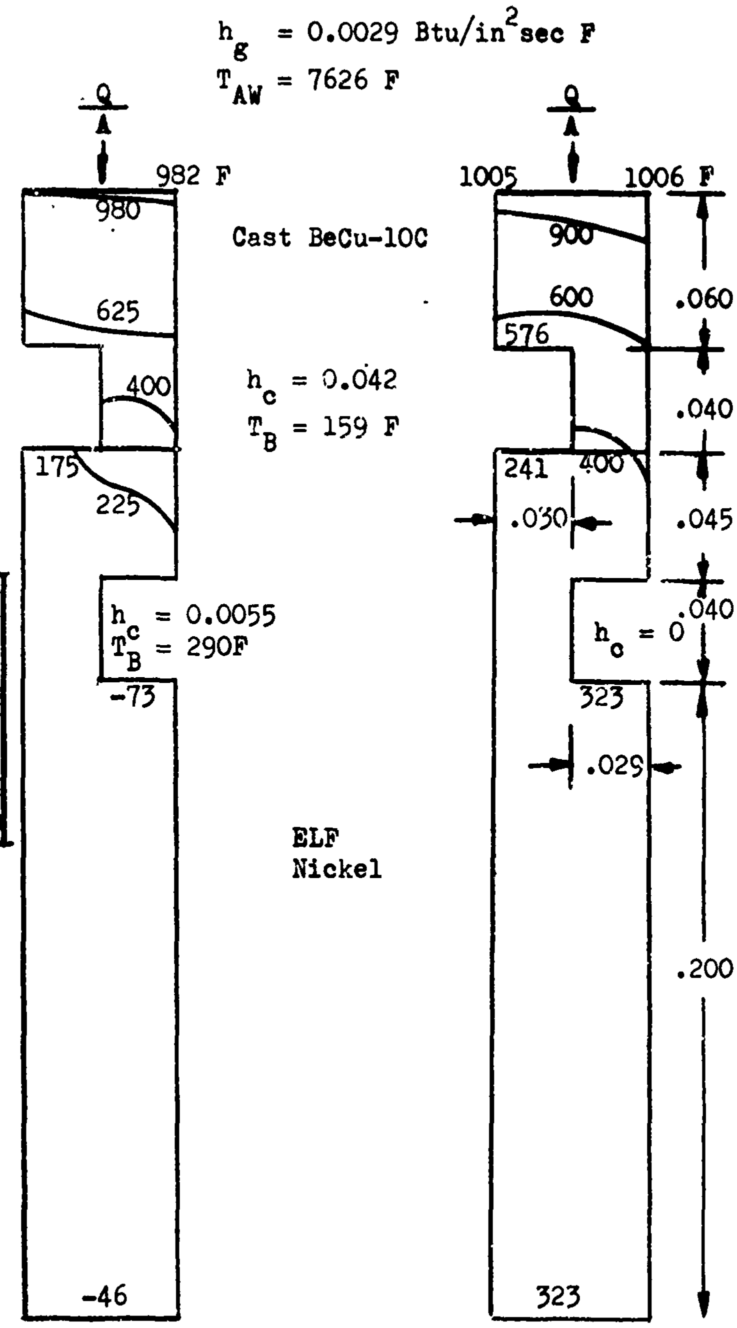

P_c = 455 psia
F_2/H_2 Propellant
MR = 12.1
Coolant: GH_2 (Primary)
LN_2 (Heat Exchange)

Figure 120. Two-Dimensional Temperature Plot - Cast BeCu-10C Segment With and Without Heat Exchange Flow. (U)

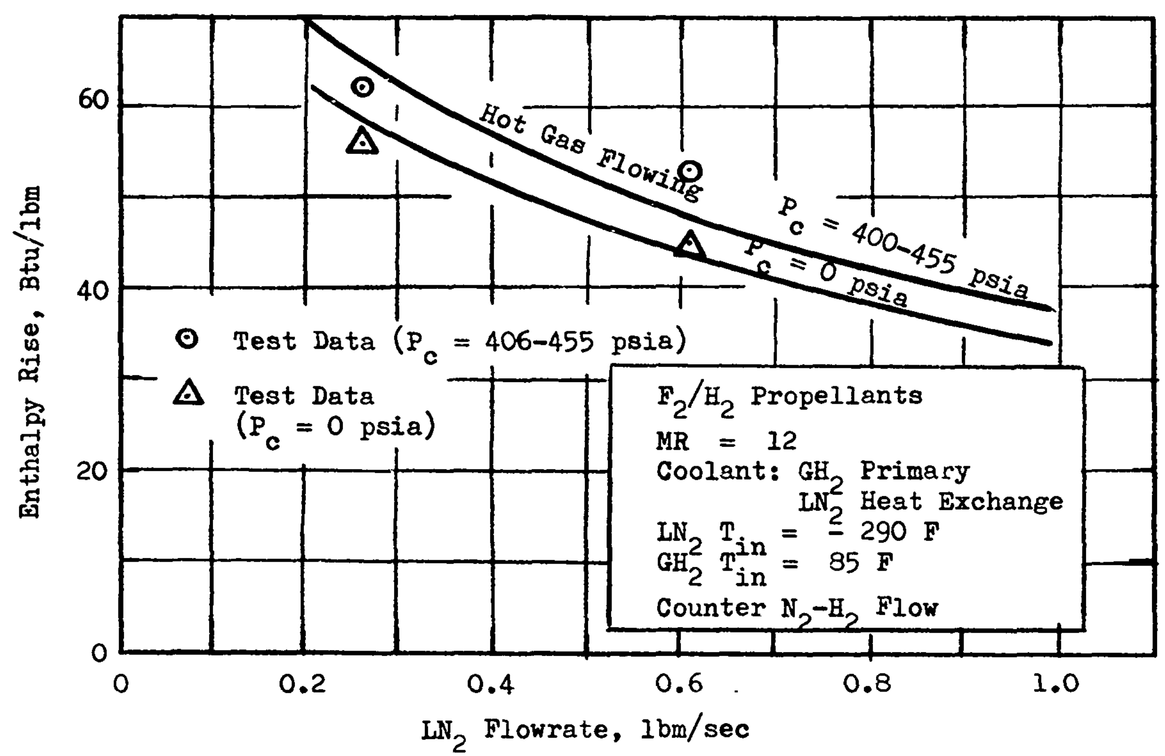

Figure 121. Comparison of Theoretical and Experimental N_2 Enthalpy Rises for the Cast Segment. (U)

TABLE XXIII

COOLANT ENTHALPY RISE FOR CAST SEGMENT AND HEAT EXCHANGE PANEL (U)

TEST ID	COOLANT	PANEL	P_c (psia)	$\triangle h$ (EXP.) (Btu/lbm)	$\triangle h$ (THEOR.) (Btu/lbm)
019	H_2	Lower	405	273	---
019	H_2	Upper	406	228	---
019	N_2	Heat Exchange	406	62	65
019	N_2	Heat Exchange	0	56	58
020	H_2	Lower	455	315	---
020	H_2	Upper	455	228*	---
020	N_2	Heat Exchange	455	53	48
020	N_2	Heat Exchange	0	45	43
021	H_2	Lower	460	252	---
021	H_2	Upper	460	259	---
021	F_2	Heat Exchange	460	(2 phase)	---

* This $\triangle h$ increased to 315 Btu/lbm when the N_2 flow was cut off.

CONCLUSIONS

(U) The three fabrication concepts which were experimentally evaluated during Phases II and III were selected on the basis of the parametric studies and the fabrication concept ranking study of Phase I.

(U) As a result of the experimental effort on the three selected fabrication concepts, conclusions reached during the Phase I study have been reviewed and updated. A discussion on each is presented in the following paragraphs.

POWDER METAL NICKEL BELL CHAMBER

(U) The parametric heat transfer studies of Phase I showed nickel bell thrust chambers to have a good range of regenerative cooling capability with both F_2/H_2 and CPF/Amine propellants.

(U) The fabrication ranking studies of Phase I showed the powder metal fabrication concept to offer the potential of very low fabrication cost in production. Conversely, the concept was considered to have high development risk and somewhat restricted range of application, due to the unknowns associated with structural integrity, dimensional repeatability and limit of minimum wall thickness.

(U) The fabrication development effort of Phase II demonstrated that the use of the Rocketdyne powder metal process to fabricate regeneratively cooled thrust chambers produced hardware with good structural integrity and dimensional repeatability. This development also established confidence that the range of application of this fabrication concept could be

extended to include chambers of larger size, smaller coolant passages and/or a thinner hot gas wall. Further, this development effort verified the Phase I cost studies and demonstrated that, in production, this process should be very low cost compared to conventional tubular chambers; offering the potential of fabricating complete chambers, including flanges and manifolds, by this process.

(U) The hot firing test effort of Phase III further substantiated the Phase II results and demonstrated the structural integrity of the fabrication concept under actual hot firing conditions.

(U) This program has shown the powder metal process can be used to produce internally cored hardware with good structural integrity and dimensional repeatability, making the process amenable to the fabrication of regeneratively cooled bell thrust chambers. This fabrication concept has a very extended range of application in that alternate materials or material combinations may be used and the coolant passage geometry may be varied as required.

(U) However, before this fabrication concept can be incorporated into a production thrust chamber, further development and refinement of the process parameters are required to assure repeatability during fabrication. In addition, to realize the full fabrication cost savings potential of the concept, further fabrication development is required to establish parameters for pressing the manifolds and flanges as an integral part of the chamber body.

SPUN BELL WITH MACHINED PASSAGES AND ELECTROFORMED NICKEL CLOSURE

(U) The fabrication concept ranking studies of Phase I showed this concept to offer the potential for low cost in production relative to a tubular chamber, to have a good range of application and to have minimal development risk.

(U) These conclusions were verified during the Phase II fabrication development effort where INCO 625 liners were spun and machined with good dimensional repeatability. This fabrication concept has a good range of application as a result of the flexibility in material selection, size, etc. Further, the electroforming of a nickel closure onto the slotted INCO 625 liners was demonstrated to repeatably produce a structural bond. Fabrication technology was substantiated during the Phase III hot firing test effort lending confidence that this fabrication concept requires a minimum amount of development prior to its use on production thrust chambers. The application of this concept is virtually unlimited, with liner material selected based on specific system requirements and propellant combination.

CAST SEGMENT WITH ELECTROFORMED NICKEL CLOSURE AND OXIDIZER HEAT EXCHANGE PANEL

(U) The Phase I Fabrication Concept Ranking Studies showed the potential of this fabrication concept to be quite low cost in production relative to a tubular chamber and to have a very good range of application. Conversely, this concept was moderately ranked in development risk, due to the unknowns associated with structural integrity and dimensional repeatability of investment cast segment liners.

(U) The fabrication development tasks undertaken in Phase II and related company funded efforts verified the prediction of low production cost potential and demonstrated good structural integrity and dimensional repeatability of the cast segment liners.

(U) Fabrication technology was further verified during the Phase III hot firing test program. Also, the hot firing tests of Phase III substantiated the predicted system advantages of the heat exchange panel concept, by significantly reducing the bulk temperature rise of the primary (H_2) coolant.

(U) Desirable development prior to incorporation of this fabrication concept into a production system includes additional effort on the castings to demonstrate repeatability (dimensional and hot gas wall quality) on larger size segments. Also, in-depth system studies are required to define system advantages and potential areas of application of the heat exchange principle.

REFERENCES

1) "Investigation of Non-Tubular Wall Regeneratively Cooled Thrust Chamber Concepts " (F04611-68-C-0061), Phase I Report, AFRPL-TR-68-112, June 1968 (C).

2) "Ultimate Heat Flux Limits of Storable Propellants", N. E. VanHuff and D. C. Rousar, Aerojet-General Corp., 8th Liquid Propulsion Symposium, CPIA Publication No. 121, Vol. II, October 1966.

3) "Experimental Investigation of Heat Transfer Characteristics of Hydrazine and a Mixture of 90% Hydrazine and 10% Ethylenediamine", M. B. Noel, Jet Propulsion Laboratory, Tech. Rep. No. 32-109, 27 June 196.

4) "Heat Transfer Study of MHF-5 and MMH", D. C. Rousar, N. E. VanHuff, R. E. Anderson, A. Fink, Aerojet-General Corp., Tech. Rep. AFRPL-TR-67-208, August 1967.

5) "Forced Convection and Peak Nucleate Boiling Heat Transfer Characteristics for Hydrazine Flowing Turbulently in a Round Tube at Pressures to 1000 psia", W. S. Hines, Rocketdyne Report R-2059, August 1959.

6) "Heat Transfer Study of Compound A", D. C. Rousar, N. E. VanHuff, and A. Fink, Aerojet-General Corp., Tech. Report AFRPL-TR-67-275, 31 October 1967.

7) "Heat Transfer Analysis of RS-17 Water-Cooled Segment Tests", J. M. Shoji, Rocketdyne LAP 68-331, 10 August 1968.

8) "The Heating Program", R. R. Liguori and J. W. Stephenson, Report No. 417-5.0, Astra, Inc., Raleigh, North Carolina.

9) "Experimental Heat Transfer Rates in Advanced Oxygen/Hydrogen Toroidal Thrust Chambers", R. B. Landis, W. R. Wagner and W. R. Studhalter, paper presented at the 9th Liquid Propulsion Symposium, St. Louis, Missouri, 25 October 1967.

10) "Final Report, AEA Heat Exchange Injector Study (Phase III), D. Trebes and J. Gerstley, Rocketdyne Report HTM68-8, 10 April 1968.

11) Design Handbook for Liquid Fluorine Ground Handling Equipment, Technical Report No. AFRPL-TR-65-123, Second Edition, Air Force Rocket Propulsion Laboratory, Edwards Air Force Base, California, August 1965.

APPENDIX A

PRODUCTION COST STUDIES

(U) The major goal of the Phase I, Task III study was to evaluate candidate thrust chamber fabrication techniques that offered the potential of lower production costs as compared to tubular wall chambers.

(U) To accomplish this, candidate fabrication concepts were evaluated for both bell and annular thrust chambers. Production quantities were 2, 20 and 250 units over a delivery time span of 5 years (the major effect of delivery rate is the number of sets of tooling required since inflation costs were not considered, i.e. current dollars were used). Additionally the study assumed adequate facilities were available to handle any production rate and/or quantitv.

(U) To conduct the production cost study bell and annular thrust chambers which developed 30,000 pounds of thrust were selected as the point designs. It was felt that chambers of this thrust level were of sufficient size to establish meaningful results and were within the range of interest of current and/or near future engine systems.

(U) Additionally, the bell thrust chambers, which utilized high area ratio nozzles, were considered to terminate at a low area ratio ($\epsilon = 4$), at which point a nozzle extension would be added. The cost studies, however, did not include the nozzles from $\epsilon = 4$ to $\epsilon = 100$, since the type of nozzle cooling used (regenerative, ablative, dump and/or radiation cooled)

is highly dependent upon the system and mission requirements. Furthermore, the annular chambers, depending again on mission and system requirements, may be either segmented or nonsegmented and may employ various types of backup structure.

(U) The annular chamber cost studies excluded the backup structure, since its requirements are so specifically tied to the complete system requirements and operating conditions (coolant bulk temperature and flow circuit, segmented vs nonsegmented, etc.).

(U) In summation, the production cost studies were performed on (1) bell thrust chamber coolant circuits which terminated at $\epsilon = 4$, (2) backup structures for the bell coolant circuits, (3) non-tubular cooling panels for nonsegmented annular thrust chambers, and (4) complete coolant circuit segments (inner body, outer body and supersonic baffles or end plates).

(U) Definition of the manufacturing learning curve to be used for each configuration was based upon a cost study of Rocketdyne fabricated thrust chambers. The historical cost data used in this study included only the actual labor and material dollars of five different production engine systems adjusted to current dollars, and included appropriate factors for purchased labor, quality control, etc. As a result, learning curves of 89 to 99 percent were realized. To relate the different learning curves so that a comparison curve could be generated as a guide in predicting costs the ratio of "labor dollars/material dollars" for each chamber configuration was determined using the initial production costs as the standard. This ratio was compared with the learning curve percentages and resulted in the curve shown in Fig. A-1.

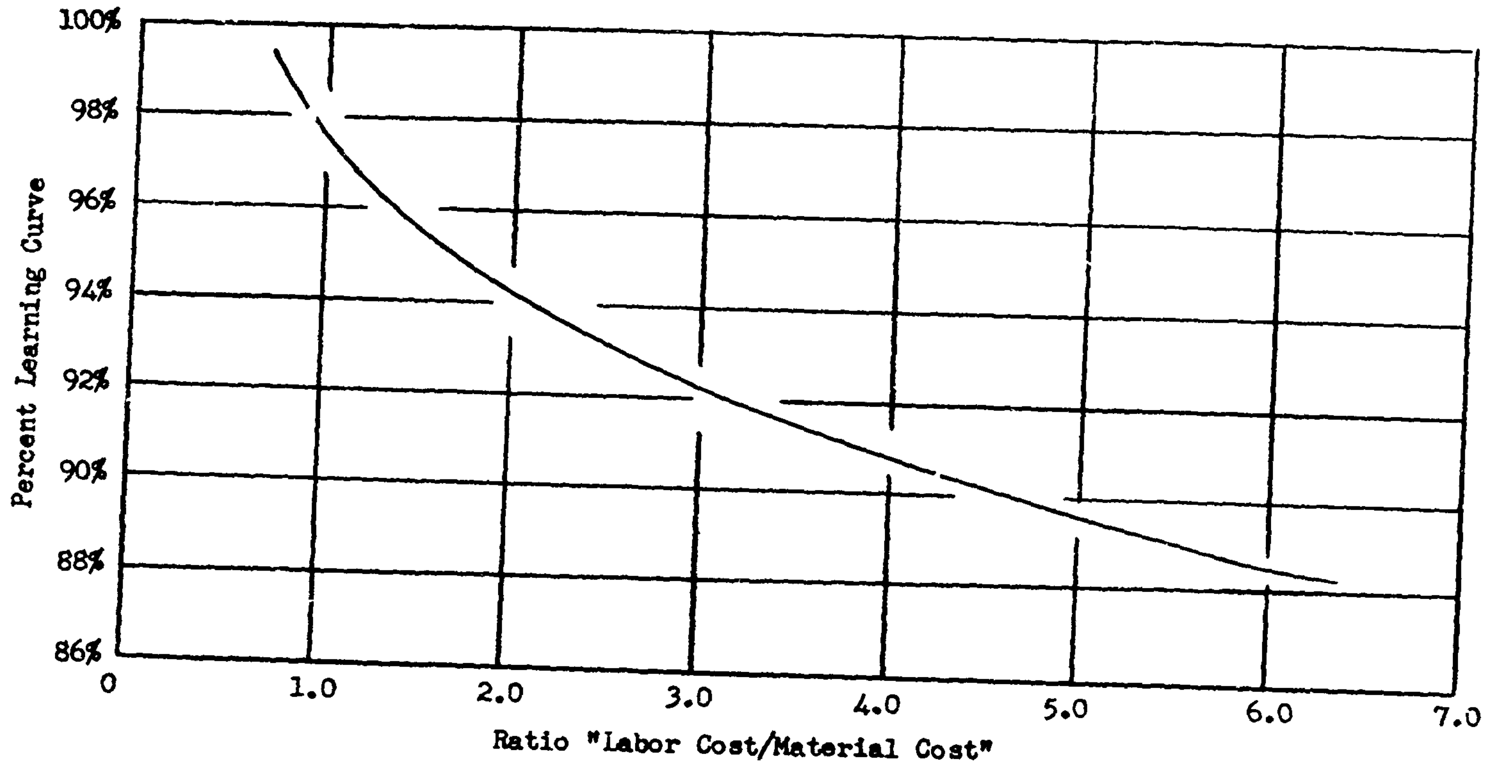

Figure A-1. Prediction of Manufacturing Learning Curve for Thrust Chamber Fabrication (U)

(U) A "labor dollar/material dollar" ratio was derived for each of the candidate fabrication concepts analyzed, based upon the estimated initial production cost, and this ratio was used to define each individual learning curve. The production costs as a function of the proper learning curve plus the amortized tooling costs were summarized to determine the costs per number of units fabricated for each fabrication concept.

(U) The fabrication concepts considered in the cost study are schematically represented in Fig. A-2 through A-4. These fabrication concepts were selected based on an initial screening and survey of all the potential concepts under consideration in Task III and were considered to offer the greatest potential for low cost in production.

(U) The cost data generated for the various bell chamber coolant circuits and backup structure is shown in Fig. A-5. The data are presented relative to the cost of a tubular-wall, furnace brazed thrust chamber which includes both coolant circuit and backup structure inherent in the design. In actual operation, the backup structure for the bell chambers would be a function of the specific coolant circuit and system requirements, but for the purpose of this study they were considered interchangeable.

(U) The cost data were generated on the basis that sufficient fabrication development had been completed on each concept to allow for confident entry into the manufacture of production chambers.

(U) The powder metal chamber and the cast chamber with electroform nickel closure showed the lowest production cost, since the processes (in production) are amenable to fabricating flanges and manifolds as an integral part of the chamber body. Conversely, the fabrication concepts which

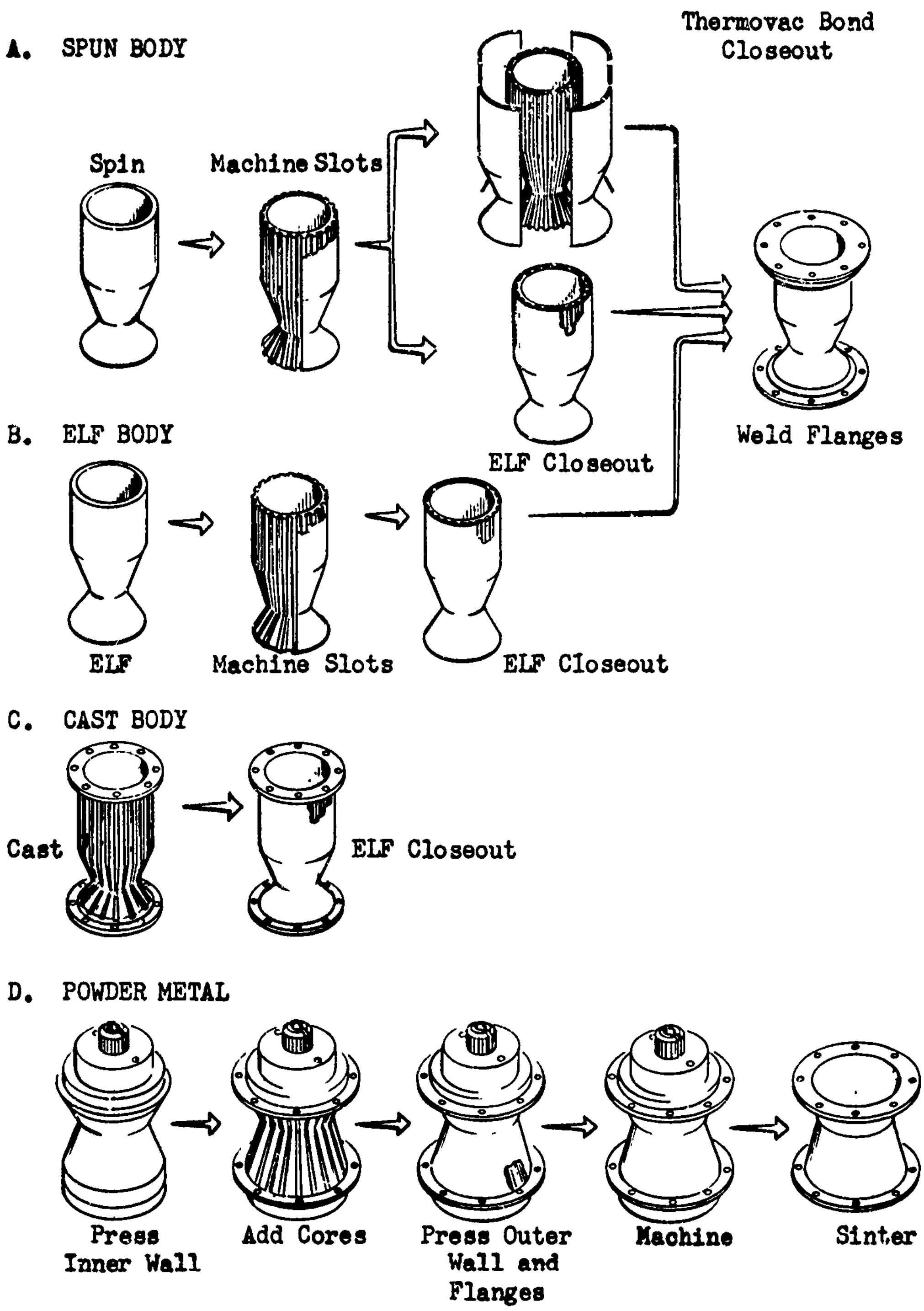

Fig. A-2. Candidate Fabrication Concepts - Bell Thrust Chambers (U)

A. FORMED AND MACHINED PANELS

B. CAST PANELS

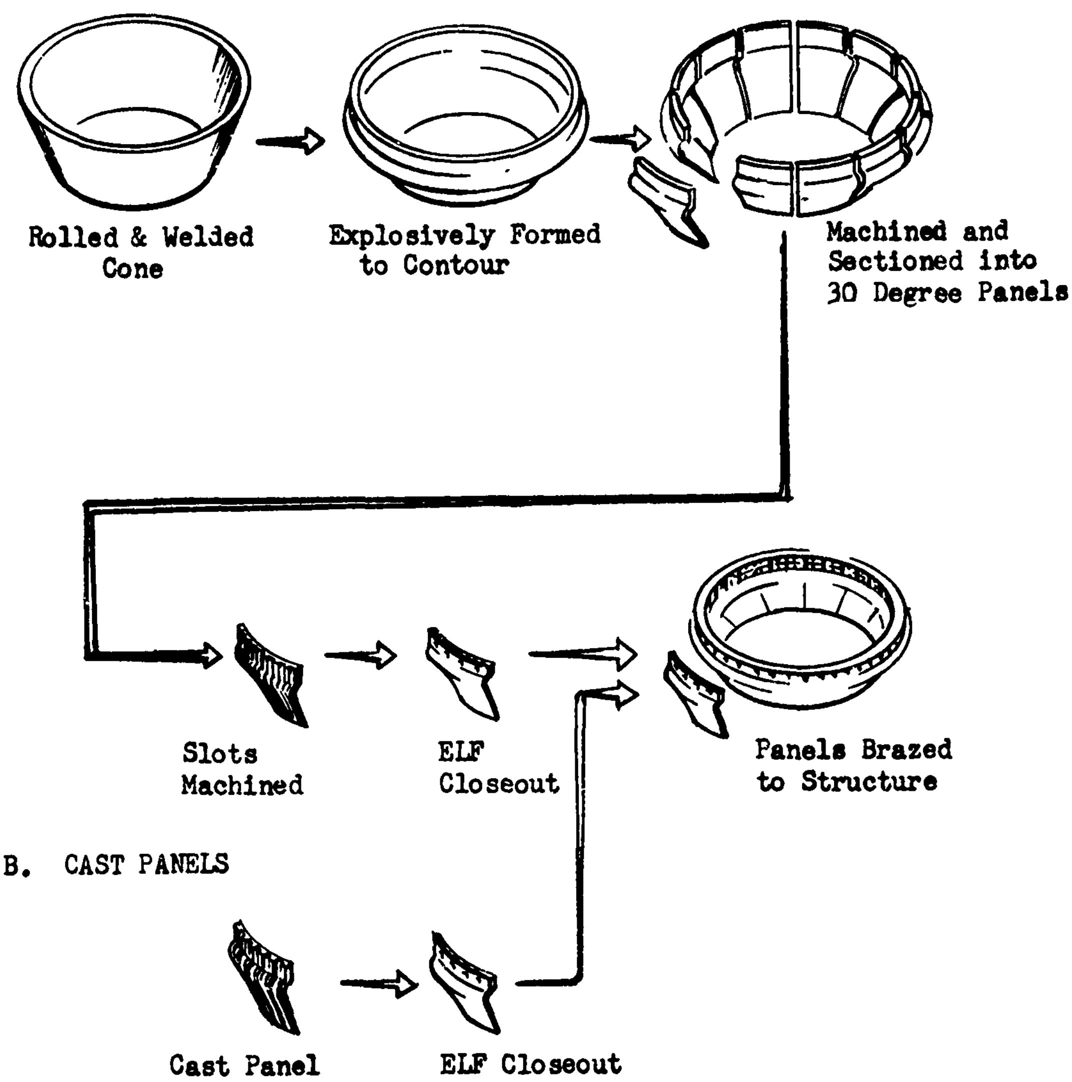

Fig. A-3. Candidate Fabrication Concepts - Nonsegmented Annular Thrust Chamber (U)

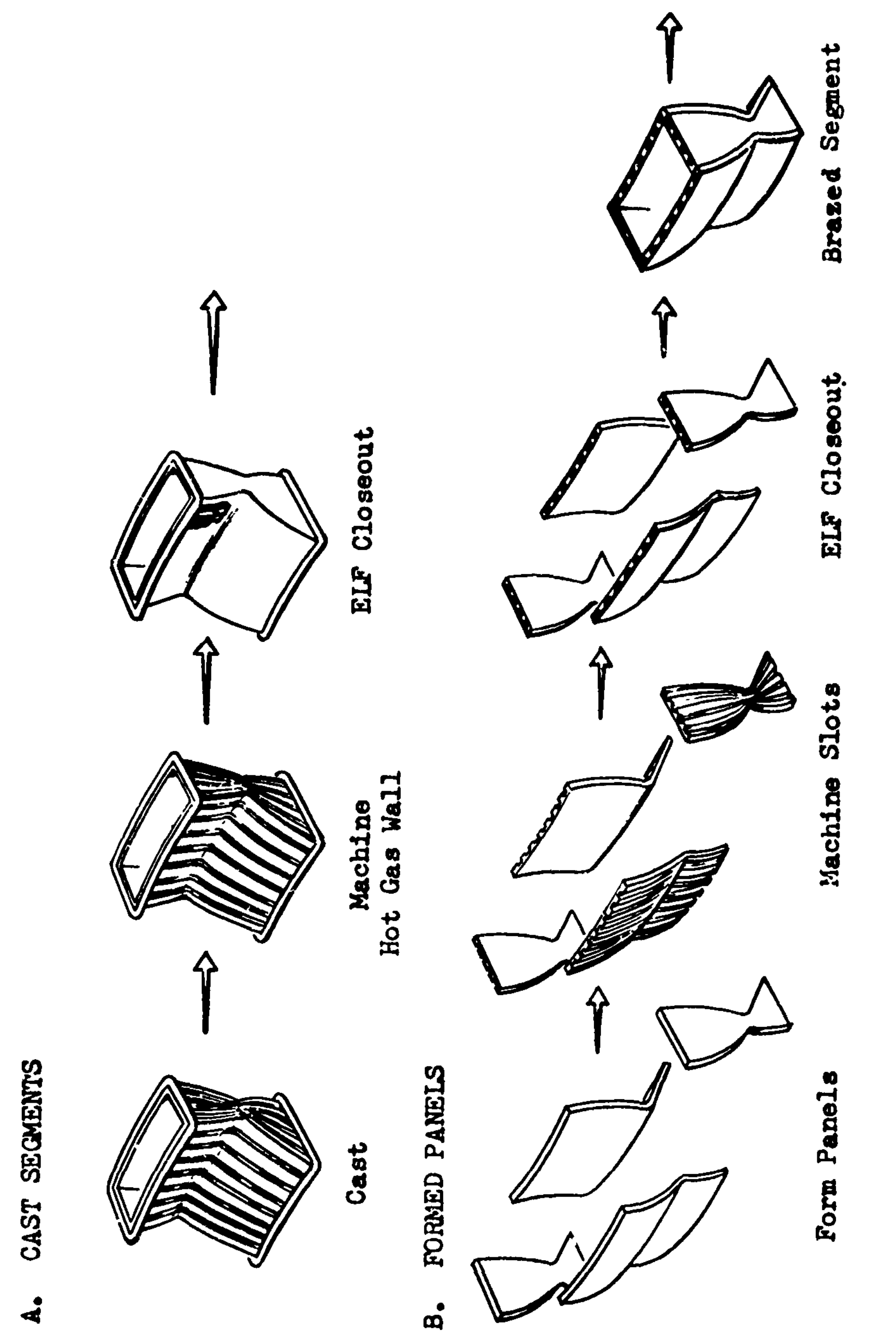

Fig. A-4. Candidate Fabrication Concepts - Segmented Annular Thrust Chambers (U)

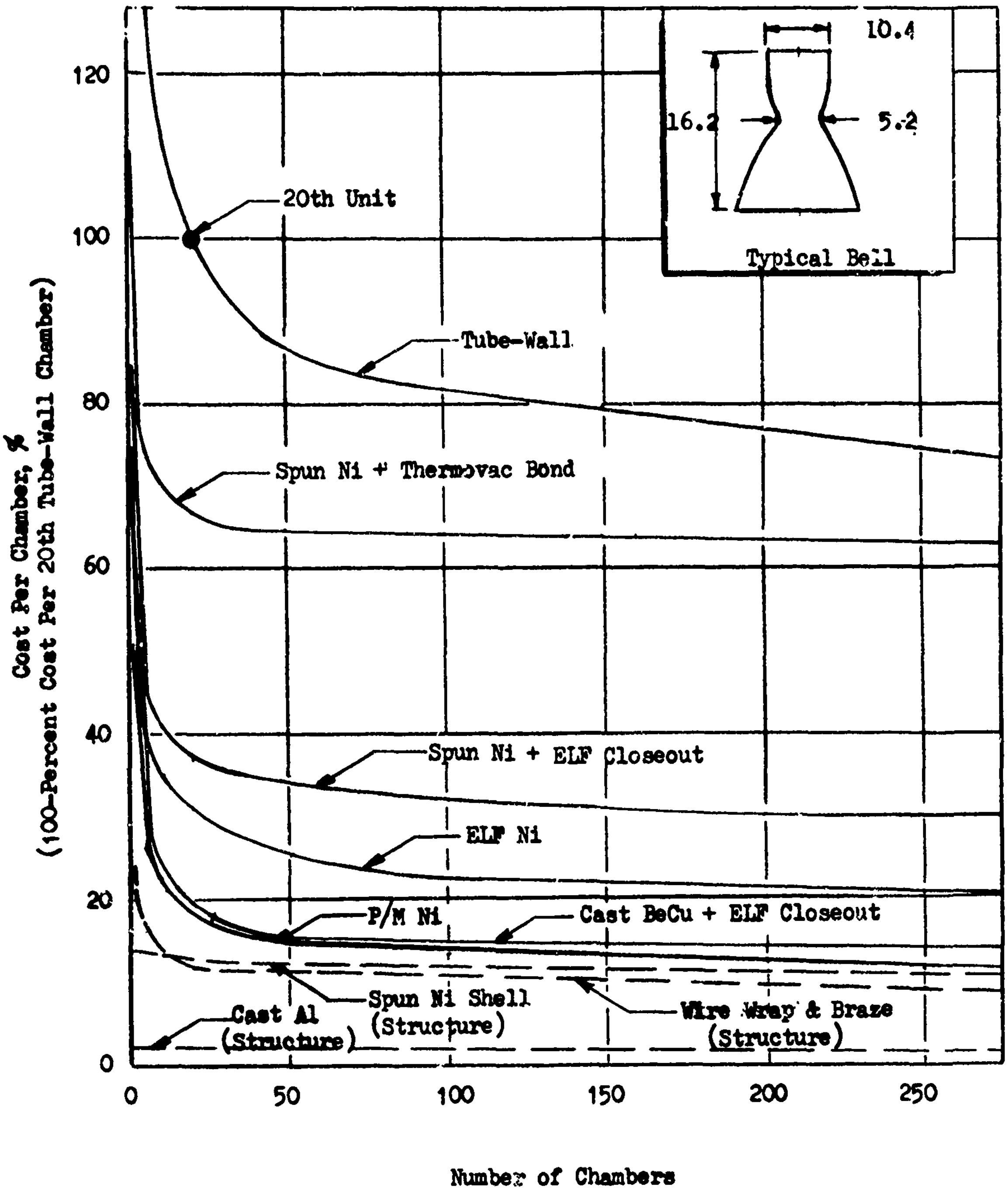

Figure A-5. 30K Bell Chamber Estimated Production Costs (U)

employ all electroformed chambers and the spun liner with electroformed or Thermovac Bond closures require that flanges and manifolds be welded or brazed in place after completion of the chamber body.

(U) It is significant that the cost of any of these advanced non-tubular fabrication concepts is considerably lower than the cost of a conventional tubular wall chamber.

(U) The cost data generated for the nonsegmented annular chamber coolant circuit subassembly are shown in Fig. A-6, related to the costs of a comparable conventionally brazed tubular wall coolant circuit subassembly. The relative costs of a segmented annular chamber coolant circuit subassembly is shown in Fig. A-7. Here also the cost data considered that sufficient fabrication development had been completed to establish a high confidence factor in producing production quantities of chambers.

(U) For the annular chamber, as with the bell chambers, it is obvious in reviewing the data presented in the appropriate tables and figures that the most promising non-tubular fabrication concepts offer the potential of significant production cost savings over the conventional tubular wall construction techniques. Also, it is apparent that casting offers the greatest potential of reducing the production costs of such thrust chambers.

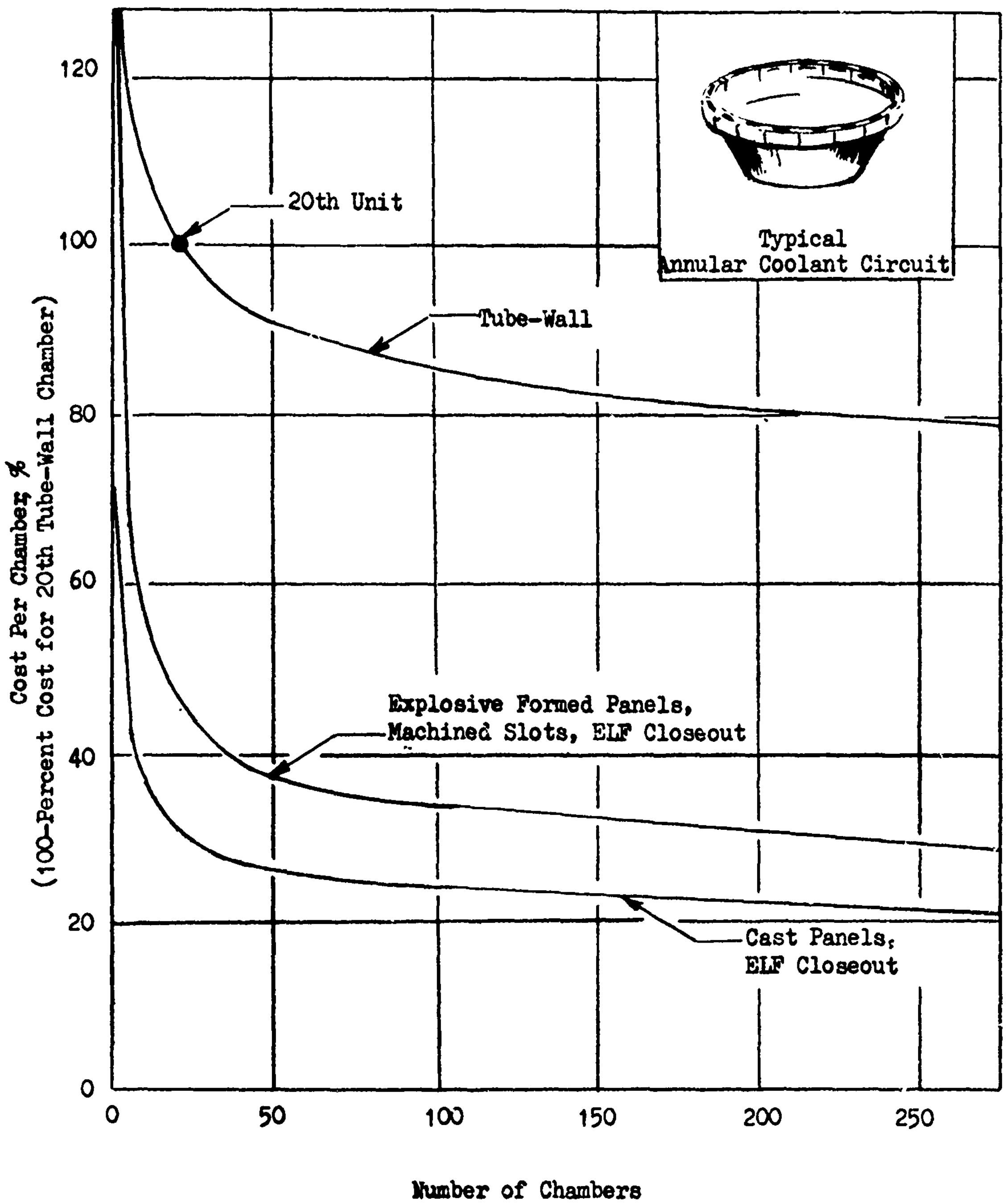

Figure A-6. 30K Annular Chamber Coolant Circuit Estimated Production Costs (U)

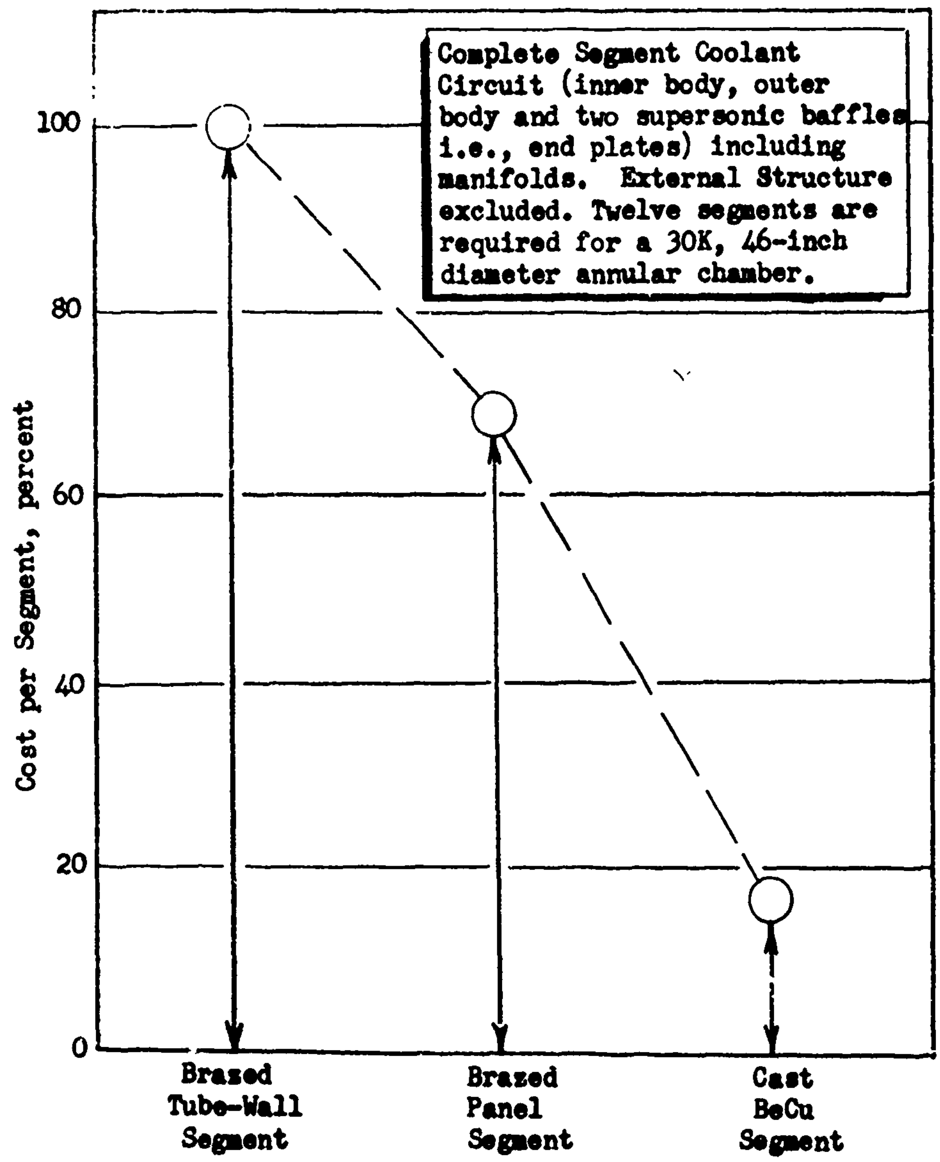

Figure A-7. Annular Segment Coolant Circuit Estimated Production Costs (U)

APPENDIX B

MATERIALS EVALUATION

(U) Complementary materials evaluation effort conducted in support of the three fabrication concepts included overaging studies for cast beryllium copper-10C and -50C and relative life ($\alpha \Delta T$) data for the candidate materials and processes.

Overaging Studies - Beryllium Copper-10C and -50C

(U) Elevated temperature tests on as-cast bars had shown low ductility values at approximately 900 F. Consequently, heat studies were initiated on the BeCu-10C to determine if these values could be improved.

(U) Initially, 10C specimens were exposed to various time temperature cycles to determine the trends of ductility, conductivity and strength. The objective was to determine an overage (or stabilizing) heat treatment to provide best ductility and conductivity from cryogenic to an elevated temperature above the predicted maximum operating temperature (selected temperature range was -320 F to 1350 F).

(U) Time-temperature parameters were established at 2 to 12 hours and 750 to 1500 F. Evaluation of the data included ductility (bend angle), conductivity (electrical) and strength (hardness). Typical results are presented in Fig. B-1.

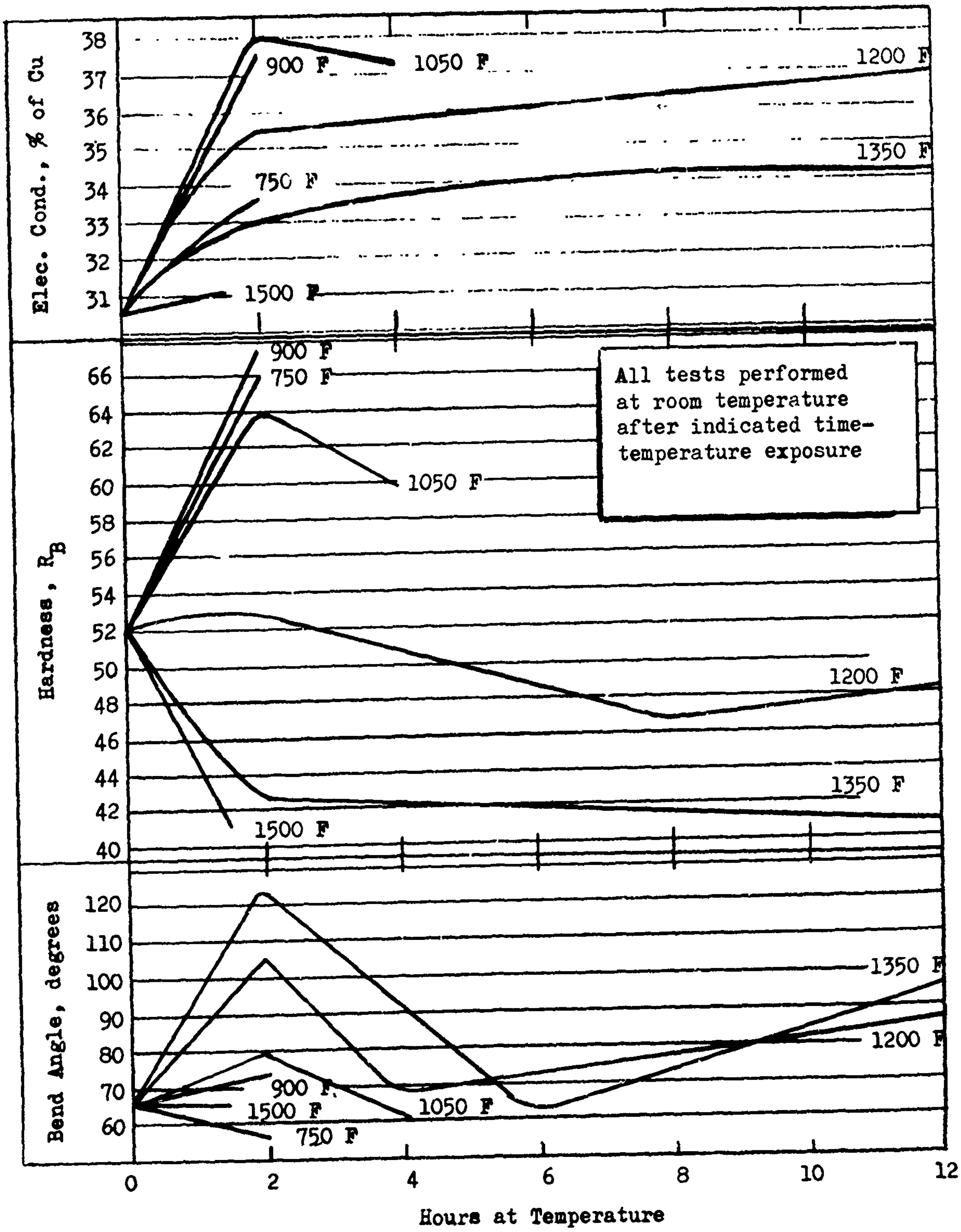

Figure B-1. BeCu-10C - Room Temperature Properties vs Time-Temperature Exposures. (U)

(U) The hardness data is considered to be quite accurate; however, the bend test results (ductility) depend on operator judgment and cannot be accepted with the same degree of credence. The electrical conductivity data represent what is assumed to be a proportional indication of thermal conductivity.

(U) The hardness data followed the expected hardness drop-off indicating progressive overaging (agglomeration of the gamma beryllium-copper precipitate) at successively higher temperatures and increasing time above 900 F. The increasing electrical conductivity with increasing time at temperature confirmed the gamma precipitate reaction; however, the establishment of lower conductivity ranges with successively high temperatures above 900 F demonstrated that additional elemental transfer was taking place. The probable reaction was a solutioning of a high cobalt phase(s) resulting from casting segregation. The limits of the planned study allowed only simple metallographic studies be performed. The study did confirm the elemental transfer by the solutioning of a script formation and a resulting Kirkendall Effect* at temperatures from 1050 to 1500 F. The morphology of the script phase was such that it was the first solid formed during solidification again indicating it to be a cobalt phase. A review of heat treat studies and metallographic examinations performed on wrought Berylco 10 by both Rocketdyne and the Beryllium Corporation provide no evidence of similar behavior by the wrought product. The discovery of the Kirkendall Effect provided an explanation for the higher temperature bend test results. The peaking of ductility at short times would have resulted from the gamma overaging reaction being predominant during the first 1-2 hours of exposure. Subsequently, the drastic reduction and partial recovery of ductility would have been due to the cobalt phase dissolving and accompanied Kirkendall Effect becoming predominant with increasing exposure time.

---

* Kirkendall Effect denotes an inbalance in the diffusion of elements within a metal resulting in internal voids and high internal stress concentration.

(U) Metallographic evidence of the Kirkendall reaction was found in that the as-cast structure showed only a very small amount of micro-shrinkage. Occurrences of needle and plate shaped Kirkendall voids showed after 2 hours at 1350 F. Progressing to 4 and 6 hours at 1350 F, the amount and size of voids increases. Though not confirmed metallographically, the recovery in ductility shown by longer time exposure bend tests would seem to result from spheroidizing of the voids and relaxation of the internal stresses as matric saturation causes a reduction in diffusion rates slowing down the Kirkendall reaction.

(U) A second heat treat experiment was performed to determine if a high temperature stabilization treatment (overaging) could inhibit the reported 900 F ductility minimum as well as changes in thermal conductivity and structure that would result from service temperature exposure. Specimens like those used in the first experiment were stabilized for 4 hours at 1350 F and then given additional 2 hour exposures at temperatures from 750 to 1350 F. Room temperature electrical conductivity, hardness, and bend angle results were then compared to earlier experimental data for as-cast specimens given the same 2 hour exposures. Both the bend angle and hardness data showed strong stabilizing tendency. The electrical conductivity, though not responding with the same degree to the stabilization treatment, showed a significant increase in conductivity base line after heat treatment.

(U) The third and final heat treat experiment was performed to determine if high temperature solution annealing would avoid the Kirkendall Effect. For this study small sections of cast tensile bars were given 1650 and 1800 F solution anneals for up to 48 hours. Metallographic examination showed secondary phase solution without void formation. Overaging of

the 1650 F, 48 hour specimen at 1350 F for 8 hours produced a metallographic structure free of voids. The high temperature anneal was successful in avoiding the Kirkendall Effect.

(U) Tensile tests were then performed on bars in the as-cast condition, in four overaged conditions, and overaged after solution anneal. The data are presented in Figs. B-2 and B-3.

(U) The analysis of the as-cast data was keynoted by the reduced ductility as the materials were tested in their aging temperature range. A comparison increase in yield strength was measured. All overaging treatments tested gave improved aging range ductility and lower yield strength than as-cast. The best of these treatments was the as-cast 1.5 hours at 1350 F. This condition gave ductility minimums at 900 F of 14 percent Elongation and 18 percent Reduction of Areas as compared to the as-cast minimums of 5 percent at 1050 F and minimums of 9 to 13 percent for the other overaging treatments tested. Very limited data on 48 hour 1650 F solution treated plus 1350 F overaging shows good ductility increase but insufficient test data were obtained to verify the magnitude of the trend.

(U) It was concluded from these tests that

1. BeCu-10C responds to overaging in the range of 1200 to 1500 F to provide increased ductility and electrical conductivity and decreased yield strength as compared to the as-cast properties.
2. Overaging for more than 2 hours can result in a severe drop in ductility due to a Kirkendall Effect. The Kirkendall Effect can be avoided by high temperature solution annealing prior to overaging.

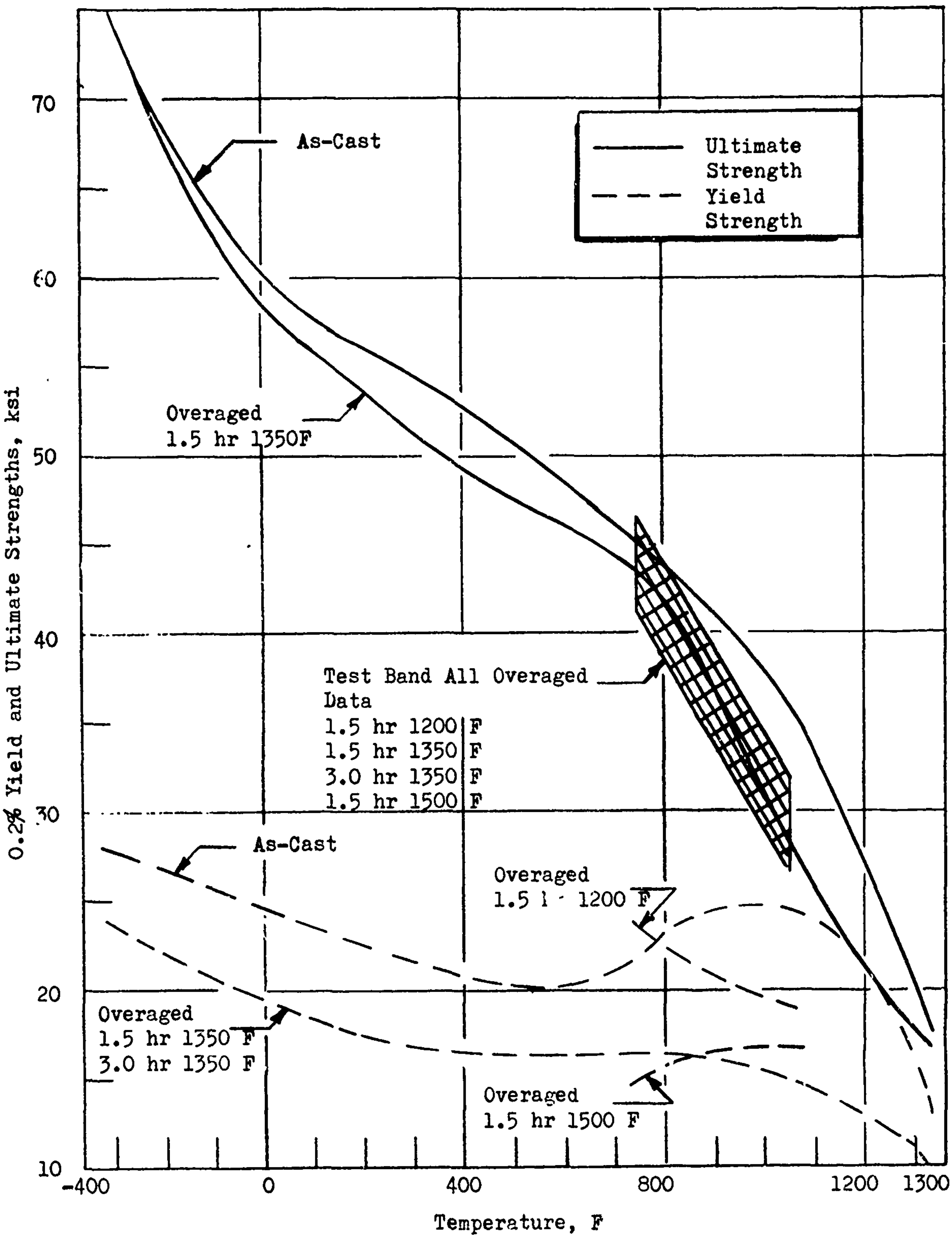

Figure B-2. BeCu-10C - Average Tensile Test Properties. (U)

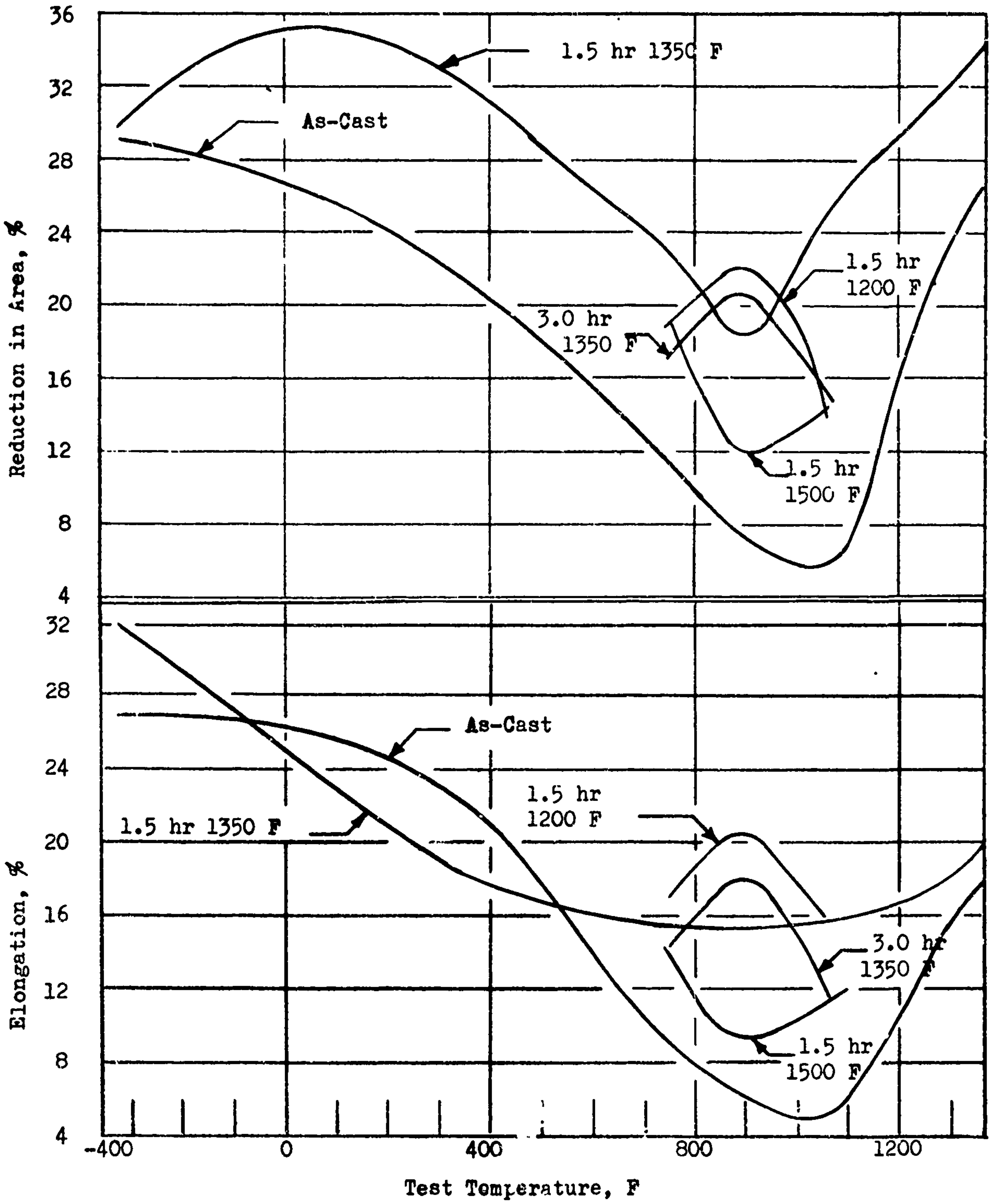

Figure B-3. BeCu-10C - Average Tensile Test Properties. (U)

3. Overaging at 1350 F for four hours reduces greatly the effect on properties by subsequent lower temperature exposures.

4. All Phase II and III BeCu-10C segments should be overaged at 1350 F for 1.5 hours in a purified argon atmosphere prior to electroforming.

5. The -50C segments should use the same overaging cycle or the -10C.

Relative Life ($\alpha\Delta T$) Tests

(U) In an effort to determine the relative thermal fatigue characteristics of candidate materials and fabrication process in more depth than the relative ductility (Reduction of Area) measurements, tubular specimens fabricated from the candidate fabrication sources (sintered nickel, electroformed nickel, wrought nickel and cast beryllium copper) were tested in the fixture shown in Fig. B-4 . The test sections of the specimens were 2 inch long, 3/8 inch diameter tubes with a 0.020 inch wall thickness. Maximum temperatures were 1350 F for the cast beryllium copper and 1600 F for the nickel specimens.

(U) The tube specimens were constrained in the test fixture and then resistance heated during the heat-up cycle to the desired temperature at midlength. The tube temperature was then reduced during the cool-down cycle by flowing argon gas through it. An argon atmosphere was furnished around the tube to prevent oxidation. A thermocouple placed at midlength of each tube specimen measured its temperature during the heat-up and cool-down cycles. Due to the constraint of the test fixture, the tubes were in compression during the heat-up cycle.

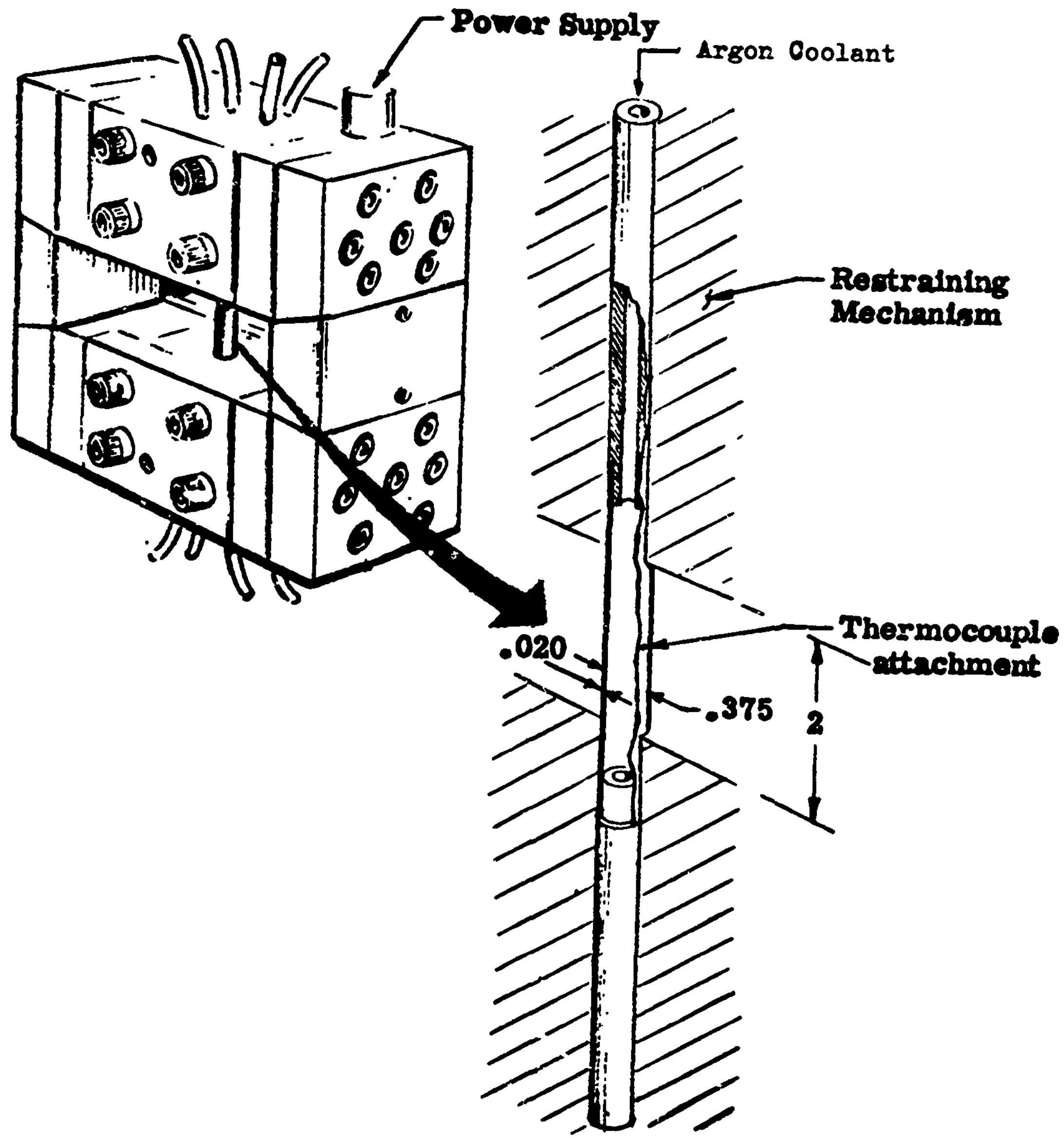

PROCEDURE

Resistance heat at rate of 160F/second to desired temperature

Argon cool to ambient

Cycle at 34 second increments until failure

RESULTS

Demonstrate relative fatigue life of various materials through series of tensile and compressive loading

Figure B-4. ELEVATED TEMPERATURE ($\alpha \Delta T$) FATIGUE TESTS (U)

(U) The magnitude of the compressive strain acting on the tubes is dependent upon the temperature distribution acting along the entire length of the tube and the rigidity of the test fixture. If the entire tube length were subjected to the same temperature and if the fixture were rigid, then the compressive strain would equal the $\alpha \Delta T$ associated with the change in temperature of the tube. However, temperature measurements indicated a non-uniform distribution with the tube temperature decreasing adjacent to the test fixture. A typical temperature distribution curve is shown on Fig. B-5 below.

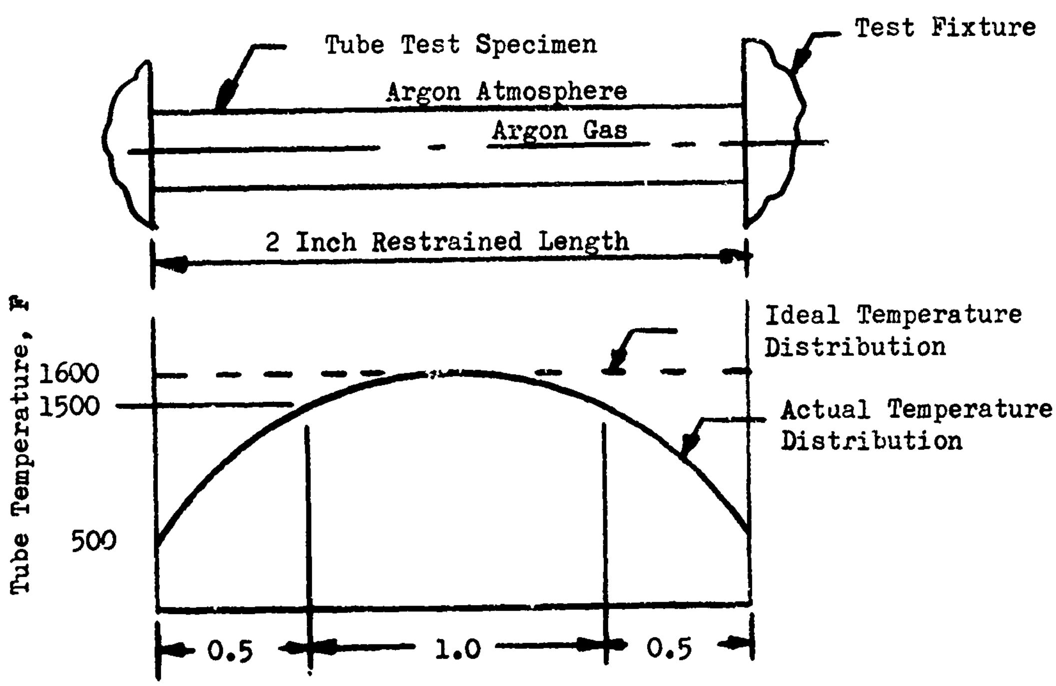

Figure B-5. Temperature Distribution for Nickel Tubes. (U)

(U) Analysis and test measurements indicated that the magnitude of the strains acting on the tubes is extremely sensitive to the temperature distribution and that the stiffer cooler tube material adjacent to the fixture tended to redistribute the strains along the length of the tube and increase the strain at the weaker hot material near the middle of the tube. Maximum compressive strains at the middle of the tubes were calculated for maximum test temperatures using available stress-strain data and a non-uniform temperature distribution along the tubes. These values are tabulated in Table B-I. Note that the calculated strains for non-uniform temperature distribution exceeded the $\alpha\Delta T$ values for a tube with a uniform temperature distribution.

(U) Calculations and test measurements also indicated that the specimens had a permanent compressive strain after the tubes cooled to room temperature. This permanent contraction is progressive for each cycle and resulted in thermal ratcheting until the tubes buckled. The tubes then continued to thermally cycle after buckling until rupture occurred. The number of cycles to failure recorded from the tests are not valid since the tubes buckled at a low number of cycles and once buckling has occurred, the maximum strain will vary.

(U) To obtain meaningful data a more uniform temperature distribution is required along the length of the tube to minimize thermal ratcheting: however, care must be taken in determining the specimen length. Increasing the length without changing the diameter to thickness ratio (D/t) of the tube will make column buckling more prevalent (column buckling of the specimen will make test results invalid). Therefore, future investigations should include analysis to obtain a more optimum specimen geometry before the tests begin. More temperature measurements should also be made on future tests to determine the actual temperature gradients.

TABLE B-I

THERMAL STRAINS (U)

Specimens *	Maximum Test Temp. (^{o}F)	$\alpha \Delta T$ (•) (in./in.)	Maximum (●) 1st Cycle Strain (in./in.)
347 CRES	1600	0.0157	0.0226
Brazed Wrought Nickel 200	1600	0.0137	0.0157
Beryllium Copper-10C (As-Cast)	1200	0.0111	0.0145

* Two-inch long tubes with 0.020-inch wall thickness

(•) Free thermal strains based on maximum test temperature

(●) Maximum calculated 1st cycle thermal strains at middle of tube

APPENDIX C

HEAT TRANSFER EQUATIONS

(U) This appendix presents the equations used to conduct the heat transfer analysis of Phase I and III.

I. Regenerative Cooling Relations

A. Convective Hot Gas Heating

$$q = h_g (T_{AW} - T_{wg})$$

B. One Dimensional Wall Conduction

$$q = \frac{1}{X_W} \int_{T_{wc}}^{T_{wg}} K \, d\,T$$

(U) Two dimensional wall conduction is calculated numerically by the computer program described in Ref. 8.

C. Forced Convection Cooling

$$q = h_c (T_{wc} - T_B)$$

D. Boiling Convection Cooling

$$T_{wc} \cong T_{sat} + 25 \text{ F}$$

(U) This is very nearly true over the entire nucleate boiling regime, where the wall temperature only varies by some 50 F from initiation to the film boiling transition point ("Burnout"). Therefore, the heat flux is controlled by resistances A and B above for nucleate boiling conditions.

E. Coolant Heat Absorption

$$q \, dA_s = \dot{W}_c \int C_p \, d \, T_B$$

F. Coolant Pressure Loss

$$\Delta P_T = \int_o^{L_P} \frac{f}{d} \frac{G_c^{\,2}}{2 \rho g} \, ds + \int_{G_{c1}}^{G_c} \frac{1}{2 \rho g} (d \, G_c)^2$$

$$+ \sum_n \left[K \frac{G_c^{\,2}}{2 \rho g} \right]_n$$

(U) These equations are calculated incrementally by the regenerative cooling program.

II. Hot Gas Film Coefficient Calculation (h_g)

$$\frac{d}{ds} \left[\phi r \; \rho \; M^* \, (H_s - H_w) \right] = r \, \rho \; M^* \; (H_{AW} - H_W) \, C_H$$

$$C_H = \frac{h_g}{\rho U_s C_p}$$

$$C_H = \frac{0.012}{(R_{e\phi})^{0.25}} \left(\frac{T_s}{T_r}\right) \left(\frac{\rho_s}{\rho_r}\right)^{0.25} \left(\frac{\mu r}{\mu s}\right)^{0.25} \frac{1}{P_r^{\;.067}}$$

(U) The differential equation in ϕ (energy thickness) is obtained upon applying the Integral Method to the energy equation for compressible axisymmetric boundary layer flows. The expression for C_H is applicable to turbulent flows and is empirically derived assuming similarity between enthalpy and velocity profiles (Ref. 9).

III. Forced Convection Cooling Correlations (h_c)

A. Hydrogen (H_2)

$$\frac{h_c}{G_c C_p} = \frac{f/8}{1T\ (f/8)^{0.5}\ \left[g(\epsilon^*,\ P_r) - 9.48\right]}\ \phi_c$$

where: $\epsilon^* = \frac{G_c\,\epsilon}{\mu}\ (f/8)^{0.5}$

$$g(\epsilon^*, P_r) = 4.5 + 0.57\ (\epsilon^*)^{0.75} \qquad (0 \leq \epsilon^* \leq 7)$$

$$g(\epsilon^*, P_r) = 4.7\ (\epsilon^*)^{0.2} \qquad (\epsilon^* > 7)$$

B. Oxygen (O_2), Nitrogen (N_2), and Fluorine (F_2)

$$h_c = 6.1 \times 10^{-4}\ \frac{G_c^{\ 0.8}}{d^{0.2}} \left(\frac{T_{wc}}{500\ R}\right)^{-1.2} \quad \text{(Supercritical pressure)}$$

(U) Physical properties of these fluids are similar enough to allow the same cooling correlation for all three over the temperature range considered here (Ref. 10).

C. Water (H_2O)

$$h_c = 0.023\ \frac{K}{d} \left(\frac{G_c d}{\mu}\right)^{0.8} \left(\frac{\mu C_p}{K}\right)^{0.4}$$

D. Hydrazine (N_2H_4)

$$h_c = 0.0054 \frac{K}{d} \left(\frac{G_c d}{\mu}\right)^{0.95} \left(\frac{\mu C_p}{K}\right)^{0.4}$$

IV. Film Boiling Transition Correlations

A. Water (H_2O)

$$q_{BO} = 0.01 \quad V_c^{0.5} \quad (T_{sat} - T_B)$$

B. Hydrazine (N_2H_4)

$$q_{BO} = 0.0031 \quad V_c^{0.615} \quad (T_{sat} - T_B)$$

Unclassified
Security Classification

DOCUMENT CONTROL DATA - R & D

(Security classification of title, body of abstract and indexing annotation must be entered when the overall report is classified)

1. ORIGINATING ACTIVITY (Corporate author) Rockwell Corporation, 6633 Canoga Avenue, Canoga Park, California 91304 — Rocketdyne, a Division of North American Rockwell	2a. REPORT SECURITY CLASSIFICATION CONFIDENTIAL
	2b. GROUP 4

3. REPORT TITLE

Investigation of Non-Tubular Wall Regeneratively Cooled Thrust Chamber Concepts - Final Report

4. DESCRIPTIVE NOTES (Type of report and inclusive dates)

5. AUTHOR(S) (First name, middle initial, last name)

Rocketdyne Engineering

6. REPORT DATE	7a. TOTAL NO. OF PAGES	7b. NO. OF REFS
December 1969		

8a. CONTRACT OR GRANT NO. F04611-68-C-0061	9a. ORIGINATOR'S REPORT NUMBER(S) R-7910
b. PROJECT NO.	
c.	9b. OTHER REPORT NO(S) (Any other numbers that may be assigned this report) AFRPL-TR-69-164
d.	

10. DISTRIBUTION STATEMENT

11. SUPPLEMENTARY NOTES	12. SPONSORING MILITARY ACTIVITY

13. ABSTRACT

This report presents the results of a three-phase program for the "Investigation of Non-Tubular Wall Regeneratively Cooled Thrust Chamber Concepts" (F04611-68-C-0061) contracted with the AFRPL at Edwards, California.

During Phase I, parametric analyses, materials evaluation and thrust chamber ranking studies provided the basis for the selection of three fabrication concepts for experimental evaluation.

In Phase II, test panels and full-size chambers of the three concepts were fabricated and laboratory tested to establish process parameters, structural limits, dimensional repeatability and non-destructive inspection techniques for subsequent hot firing hardware.

In Phase III, thrust chambers representing each of the three concepts were successfully fabricated and hot fire tested demonstrating the structural integrity and thermal performance of the three fabrication concepts when exposed to the combustion environment.

DD FORM 1 NOV 65 1473

Unclassified
Security Classification

Unclassified
Security Classification

14. KEY WORDS	LINK A ROLE	LINK A WT	LINK B ROLE	LINK B WT	LINK C ROLE	LINK C WT
Annular Thrust Chamber, Cast Beryllium Copper Segment						
Bell Thrust Chamber, Powder Metal Nickel						
Bell Thrust Chamber, Spun Wall						
Electroforming						
Thrust Chamber Fabrication Methods Ranking						
Parametric Heat Transfer and Stress Analyses						
Structural Integrity and Thermal Performance						
Non-Destructive Testing						
F_2/H_2 Combustion Environment						
Multiple Layers of Coolant Passages						

Unclassified
Security Classification